NASA CONTRACTOR REPORT

NASA CR-2320

NASA CR-2320

THE INFLUENCE OF WING LOADING ON TURBOFAN POWERED STOL TRANSPORTS WITH AND WITHOUT EXTERNALLY BLOWN FLAPS

by R. L. Morris, C. R. Hanke, L. H. Pasley, and W. J. Rohling

Prepared by
THE BOEING COMPANY
WICHITA DIVISION
Wichita, Kans. 67210
for Langley Research Center

NATIONAL AERONAUTICS AND SPACE ADMINISTRATION • WASHINGTON, D. C. • NOVEMBER 1973

1. Report No. NASA CR-2320	2. Government Accession No.	3. Recipient's Catalog No.
4. Title and Subtitle The Influence of Wing Loading on Turbofan Powered STOL Transports With and Without Externally Blown Flaps		5. Report Date November 1973
		6. Performing Organization Code -
7. Author(s) R. L. Morris, C. R. Hanke, L. H. Pasley, and W. J. Rohling		8. Performing Organization Report No. D3-8514-7
9. Performing Organization Name and Address The Boeing Company Wichita Division Wichita, KS		10. Work Unit No. 741-86-03-03
		11. Contract or Grant No. NAS1-11370
12. Sponsoring Agency Name and Address National Aeronautics and Space Administration Washington, D.C. 20546		13. Type of Report and Period Covered Contractor Report
		14. Sponsoring Agency Code

15. Supplementary Notes

This is a final report.

16. Abstract

The effects of wing loading on the design of short takeoff and landing (STOL) transports using (1) mechanical flap systems, and (2) externally blown flap systems are determined. Aircraft incorporating each high-lift method are sized for Federal Aviation Regulation (F.A.R.) field lengths of 2,000 feet, 2,500 feet, and 3,500 feet, and for payloads of 40, 150, and 300 passengers, for a total of 18 point-design aircraft. An assumed 1975 level of technology is applied to both concepts in terms of propulsion, weights, active controls, supercritical wing methodology, and acoustics. Low-wing-loading STOL configurations with mechanical flaps are found to be competitive with externally blown flap STOL configurations over wide ranges of payload and field length for the airworthiness rules and technology improvements assumed. Because the results of design studies like this one are sensitive to the ground rules assumed, careful attention is paid to describing the assumptions. These assumptions must be understood before the results are compared with other STOL airplane studies.

17. Key Words (Suggested by Author(s))	18. Distribution Statement
STOL, Low Wing Loading	Unclassified - Unlimited

19. Security Classif. (of this report)	20. Security Classif. (of this page)	21. No. of Pages	22. Price*
Unclassified	Unclassified	164	Domestic, $4.75 Foreign, $7.25

*For sale by the National Technical Information Service, Springfield, Virginia 22151

TABLE OF CONTENTS

TABLE OF CONTENTS (CONT'D)

THE INFLUENCE OF WING LOADING
ON TURBOFAN POWERED STOL TRANSPORTS
WITH AND WITHOUT
EXTERNALLY BLOWN FLAPS – FINAL REPORT

BY
R. L. MORRIS
C. R. HANKE
L. H. PASLEY
W. J. ROHLING

1.0 SUMMARY

The objective of this study was to determine the effects of wing loading on the design of short takeoff and landing (STOL) transports using (1) mechanical flap systems, and (2) externally blown flap systems. Aircraft incorporating each high-lift method were sized for Federal Aviation Regulation (F.A.R.) field lengths of 2,000 feet, 2,500 feet, and 3,500 feet, and for payloads of 40, 150, and 300 passengers, for a total of 18 point-design aircraft. An assumed 1975 level of technology was applied to both concepts in terms of propulsion, weights, active controls, supercritical wing methodology, and acoustics.

The objective of this study was to determine if low-wing-loading short takeoff and landing (STOL) transports with mechanical flaps (MF) are competitive with externally blown flap (EBF) configurations. Aircraft incorporating each high lift method were sized for Federal Aviation Regulation (F.A.R.) field lengths of 2,000 feet, 2,500 feet and 3,500 feet, and for payloads of 40, 150 and 300 passengers for a total of 18 point design aircraft.

Throughout the study every effort was made to evaluate the two concepts on a common basis, so that a true comparison would emerge. An assumed 1975 level of technology was applied to both concepts in terms of propulsion, weights, supercritical wing methodology and acoustics.

All airplanes were sized for the same mission (.8 Mach cruise speed) using the same engine technology. Weight estimating methods were identical except for weight scaling of the flaps and flap tracks for the EBF configurations.

An important factor in this study was the assumption that an active gust load alleviation (GLA) system was incorporated on all airplanes. The benefits of such a system are structural weight reduction due to limitation of design gust loads to 2.5 g's and ride smoothing.

In the absence of F.A.R.'s for powered lift configurations a set of takeoff, approach and go-around safety margins were developed so that the EBF airplane takeoff and landing performance would be comparable to the MF airplane. Low speed aerodynamic characteristics for the MF configurations were developed from empirical and theoretical high lift data. Low speed aerodynamic characteristics for the EBF airplanes were based on NASA wind tunnel data.

Supercritical wing technology was assumed for both concepts. Wing thickness was determined so both MF and EBF configurations would have the same wing drag divergence Mach number.

A specific noise criteria was not a constraint of the study. However, an equivalent level of noise attenuation was applied to both concepts, except that a 10 dB noise increase was assigned to the EBF configurations due to the under wing blowing.

The two concepts were compared primarily on a gross weight basis. In addition, a noise and direct operating cost (DOC) comparison was made for selected design point airplanes. For the range of field lengths and payloads investigated the MF configurations were lighter, quieter and more economical than the EBF configurations. Gust load alleviation provides a large weight savings for airplanes with field lengths shorter than 2,500 feet. This improvement is greater for the MF configurations.

Because the results of design studies like this one are sensitive to the ground rules assumed, careful attention has been paid to describing the assumptions. These assumptions must be understood before the results are compared with other STOL airplane studies.

2.0 INTRODUCTION

A large number of STOL airplane aerodynamic configuration studies have been performed to examine various powered lift concepts. Most of these studies indicated that wing loadings in the neighborhood of 100 lbs/ft^2 were desired to provide high speed cruise performance and acceptable ride. A study was completed in 1971 for NASA by Boeing-Wichita, Reference 1, on a 130 passenger, 2,000 foot F.A.R. field length configuration. Results of the study are also presented in Reference 2. This study showed that by utilizing modern control system technology to provide ride smoothing, a low-wing-loading (50 lbs/ft^2) 2,000 foot field length STOL airplane appeared competitive with a high-wing-loading powered lift design, (airplane model 751 of Reference 1). Because powered lift was not relied upon, the configuration which resulted offered advantages in system simplicity, reliability and safety.

The objective of the current study was to:

- Determine the effects of wing loading on the design of larger and smaller airplanes than the referenced configuration.
- Compare the mechanical flap and externally blown flap concepts as field length and payload vary.

STOL transports were sized for payloads of 40, 150 and 300 passengers for F.A.R. field lengths of 2,000 feet, 2,500 feet and 3,500 feet. The airplanes were sized for a mission consisting of three unrefueled 250 nautical mile hops plus reserves, the cruise portion of which was flown at M = .8 at 35,000 feet. The airplanes were first sized considering low-wing-loading, which for the purpose of this study is defined as achieving STOL performance from mechanical flaps (MF). Airplanes were then sized with externally blown flaps (EBF) resulting in a total of 18 point design aircraft. To assist in evaluating the merits of each configuration, the direct operating costs and noise aspects of selected point design airplanes were determined.

Initially the ground rules and assumptions for a 1975 level of technology were established followed by the development of the wing planform for the MF configuration. Takeoff and landing design constraints were determined and tail sizing criteria were established prior to sizing of the 18 point design airplanes. Finally, a comparison of the 18 airplanes was made on a gross weight basis without the weight penalties associated with noise attenuation. One iteration was made on selected design point aircraft to determine the gross weight penalty which would result from noise suppression. Direct operating costs (DOC) were determined and DOC sensitivity trade studies were accomplished.

Page intentionally left blank

3.0 SYMBOLS

AP_I	—	Change in functional area for a particular fuselage segment
AR	—	Aspect ratio
A_{WET}	—	Wetted area, m^2 (ft^2)
a_H	—	Horizontal tail lift curve slope, per deg.
a_V	—	Vertical tail life curve slope, per deg.
a_{WB}	—	Wing-body lift curve slope, per deg.
BPR	—	Engine by-pass ratio
b	—	Wing span, m (ft)
C_{AF}	—	Aft flap chord, percent local chord
C_D	—	Airplane drag coefficient
$C_{D_{FLAPS\ DOWN}}$	—	Airplane flaps-down drag coefficient
C_{D_i}	—	Induced drag coefficient
C_{D_f}	—	Skin friction drag coefficient based on wing reference area
C_{D_0}	—	Zero lift or parasite drag coefficient with no compressibility
$C_{D_{P_{MIN\ CRUISE}}}$	—	Cruise configuration minimum parasite drag coefficient
C_f	—	Skin friction drag coefficient based on wetted area
CG	—	Airplane center of gravity as a fraction of wing aerodynamic center
C_L	—	Airplane lift coefficient
C_{LE}	—	Leading edge flap chord, percent local chord
$C_{L_{APP}}$	—	Airplane approach lift coefficient

C_{L_α} — Airplane lift curve slope, per deg

C_{L_H} — Horizontal tail lift coefficient

C_{L_δ} — Lift coefficient for minimum wing twist factor

$C_{L_{MAX}}$ — Maximum lift coefficient

C_{L_V} — Vertical tail lift coefficient

$C_{L_{V_{MIN}}}$ — Airplane lift coefficient corresponding to minimum flight speed

C_{L_S} — Airplane lift coefficient corresponding to stall speed

$C_{L_{WB}}$ — Wing-body lift coefficient

C_{ℓ_β} — Rolling moment coefficient due to sideslip, per deg.

C_{MF} — Main flap chord, percent local chord

C_M — Pitching moment coefficient

$C_{M_{0_{WB}}}$ — Wing-body pitching moment coefficient at zero lift

C_{n_β} — Yawing moment coefficient due to sideslip, per deg.

$C_{n_{\beta V}}$ — Vertical tail yawing moment coefficient due to sideslip, per deg.

$C_{n_{\beta WB}}$ — Wing-body yawing moment coefficient due to sideslip, per deg.

C_P — Pressure coefficient, $\frac{\Delta P}{q}$

C_T — Thrust coefficient, $\frac{T}{qS}$

$C_{T_{MAX.}}$ — Maximum thrust coefficient, $\frac{T_{MAX}}{qS}$

c	–	Chord, m (in)
c_d	–	Two dimensional drag coefficient
c_l	–	Two dimensional lift coefficient
$\bar{c}$	–	Wing mean aerodynamic chord, m (in)
D	–	Drag and diameter, newtons (lb), m (ft)
DL_I	–	Change in fuselage diameter over the change in length of each fuselage segment
D_{RAM}	–	Engine ram drag, newtons (lb)
dB	–	Decibel
EBF	–	Externally blown flap
F_N	–	Scaled engine sea level static thrust, newtons (lb)
$F_{N_{REF}}$	–	Reference engine sea level static thrust, newtons (lb)
f	–	Frequency, Hz
GLA	–	Gust load alleviation
g	–	Acceleration of gravity, $^{m}/sec^2$ ($^{ft}/sec^2$)
I_{ZZ}	–	Airplane yaw moment of inertia, $kg - m^2$ ($slug - ft^2$)
i_T	–	Horizontal tail incidence, deg.
KB_I	–	Fuselage wave drag factor
K_f	–	Interference and tolerence factor for adjustment of skin friction drag
$(L/D)_{EQUIV}$	–	Equivalent lift-to-drag ratio
l_B	–	Fuselage length, m (ft)
ℓ_H	–	Horizontal tail arm measured from the wing aerodynamic center to the horizontal tail aerodynamic center, m (in)
ℓ_V	–	Vertical tail arm measured from the wing aerodynamic center to the vertical tail aerodynamic center, m (in)
M	–	Free stream Mach number

M_{2D}	–	Two dimensional Mach number
M_{3D}	–	Three dimensional Mach number
M_{DD}	–	Airplane drag divergence Mach number
M_{DD_c}	–	Drag divergence Mach number of a 1969 technology wing
$M_{DD_{WING}}$	–	Wing drag divergence Mach number
M_L	–	Local Mach number
M_O	–	Free stream Mach number for which compressibility drag begins to develop on the body
M_P	–	Free stream Mach number for which maximum compressibility drag has developed on the body
MF	–	Mechanical flap
N	–	Number of engines
NOY	–	Unit of perceived noisiness
n	–	Load factor
OWE	–	Operating weight empty, newtons (lb)
PNL	–	Perceived noise level
q	–	Dynamic pressure $^{kg}/_{m^2}$ ($^{lb}/_{ft^2}$)
S	–	Wing area, m^2 (ft^2)
S_B	–	Body cross sectional area, m^2 (ft^2)
SFC	–	Engine specific fuel consumption
SPL	–	Sound pressure level
S_H	–	Horizontal tail area, m^2 (ft^2)
S_{REF}	–	Reference area, m^2 (ft^2)
S_V	–	Vertical tail area, m^2 (ft^2)
T	–	Thrust, newtons (lb)

T_{BL}	—	Blowing thrust, newtons (lb)
T_{PRIM}	—	Direct thrust which does not interact with lift and drag, newtons (lb)
T_{REF}	—	Reference thrust, newtons (lb)
T_{STATIC}	—	Static thrust, newtons (lb)
t/c	—	Wing thickness ratio, factional part of local chord
V_{APP}	—	Aircraft approach speed, knots
V_{CW}	—	Cross wind component perpendicular to aircraft flight path, knots
V_e	—	Equivalent airspeed, knots
$\overline{V}_H$	—	Horizontal tail volume coefficient
V_{JET}	—	Jet velocity, $^m/sec$ ($^{ft}/sec$)
V_{LOF}	—	Airplane lift off speed, knots
V_{MC}	—	Airplane engine out minimum control speed, knots
V_{MCG}	—	Airplane engine out ground minimum control speed knots
V_{MU}	—	Airplane minimum unstick speed, knots
V_{MO}	—	Airplane maximum operational speed, knots
V_R	—	Airplane takeoff rotation speed, knots
V_S	—	Airplane stall speed, knots
$\overline{V}_V$	—	Vertical tail volume coefficient
V_1	—	Critical engine failure speed, knots
V_2	—	Takeoff climb speed, knots
$V_{2_{OEI}}$	—	Takeoff climb speed with one engine inoperative, knots
W	—	Gross weight, newton (lb)

$X_{AC_{WB}}$	–	Wing body aerodynamic center measured relative to the mean aerodynamic chord, m (in)
X_{CG}	–	Center of gravity measured relative to the mean aerodynamic chord, m (in)
X/C	–	Fractional percent of local chord measured along the chord
X_{MG}	–	Main landing gear location measured relative to the mean aerodynamic chord, m (in)
y_e	–	Critical engine moment arm, m (in)
Z_T	–	Engine pitching moment arm, m (in)
α_{APP}	–	Angle of attack at approach lift coefficient, deg.
α_S	–	Stall angle of attack, deg.
γ	–	Flight path angle, deg.
$\Delta\alpha$	–	Incremental angle of attack, deg.
$\Delta C_{D_{i_{TE}}}$	–	Induced drag of leading edge flaps
ΔC_{D_M}	–	Drag rise due to compressibility
$\Delta C_{D_{M_B}}$	–	Fuselage drag rise due to compressibility
ΔC_{D_P}	–	Drag correction for variation from parabolic polar, clean wing
$\Delta C_{D_{P_{MIN_{LE}}}}$	–	Parasite drag of leading edge flap
$\Delta C_{D_{P_{MIN_{TE}}}}$	–	Parasite drag of trailing edge flap
Δg	–	Change in load factor
ΔM_{TECH}	–	Mach number technology correction for wing design technology other than M_{DD_C}

Δ_{M_t}	–	Mach number thickness correction
Δ_{M_Λ}	–	Mach number sweep correction
$\delta_{C_{D_P}}$	–	Drag correction for variation from parabolic polar with leading and trailing edge flaps down
δ_{CRAB}	–	Crab angle of landing gear relative to the ground velocity vector at touchdown, deg.
δ_F	–	Wing flap angle, deg.
δ_O	–	Nonelliptic factor for untwisted wings
δ / δ_O	–	Twist factor
η	–	Percent semispan
Θ_{AEO}	–	Pitch attitude with all engines operating, deg.
Θ_{OEI}	–	Pitch attitude with outboard engine inoperative, deg.
Λ	–	Sweep angle, deg.
Λ c/4	–	Sweep of quarter chord, deg.
Λ_{EFF}	–	Effective wing sweep angle, deg.
λ	–	Wing taper ratio
ρ	–	Atmospheric density, kg/m^3 ($slugs/ft^3$)
$\omega_{n_{DR}}$	–	Dutch roll natural frequency, 1/sec
$\frac{d\sigma}{d\beta}$	–	Change in sidewash with respect to sideslip

Page intentionally left blank

4.0 1975 TECHNOLOGY ASSUMPTIONS

This section discusses the background and details of assumed 1975 technology in terms of propulsion, weights, gust load alleviation (GLA) system weight, supercritical wing methodology, lift and drag.

Propulsion system improvements anticipated for 1975 technology advancement were applied to both the MF and EBF configurations. Both the MF and the EBF configurations were found to be gust load critical because of low-wing-loadings. GLA was required and applied to both configurations.

Through the use of supercritical wing technology, it was possible to develop a wing for the MF configurations which was capable of a .8 Mach cruise speed. Since only 10 degrees sweep was required, maximum low speed lift was attained. The EBF configuration wing geometry was specified by NASA. The thickness distribution for the EBF configuration wing, which had a 30 degree sweep, was developed so it would have the same drag divergence Mach number as the MF configuration wing.

4.1 PROPULSION SYSTEM

The powerplants for this study were synthesized using the following ground rules and engine characteristics.

- Installation losses were assumed to be the same as those developed for installing a TF39-1A engine. The installation effects amount to four percent takeoff rated thrust loss and seven percent increase in SFC at cruise (M = .8 at 35,000 feet).

- Nacelle dimensions were scaled using the CF6-6D engine as the baseline (two-thirds length fan duct cowl).

$$\text{Fan Duct Diameter} = .0441 \sqrt{\left(F_N^*/F_{N_{Ref}}^*\right)\left(F_{N_{Ref}}^*\right)} \text{ , Ft.}$$

$$\text{Fan Duct Length} = 0.676 \sqrt{\left(F_N^*/F_{N_{Ref}}^*\right)\left(F_{N_{Ref}}^*\right)} \text{ , Ft.}$$

where

$$F_{N_{Ref}^*} = 39{,}400 \text{ lbs.}$$

- Basic acoustic characteristics were assumed to be equivalent to those of the CF6-6D engine.

- 1975 engine technology is a basic assumption of the study, therefore a two percent fuel flow improvement over installed TF39-1A performance at cruise was used. This amounts to a seven percent improvement over installed CF6-6D performance at cruise. Takeoff thrust lapse rate (thrust decay with velocity) was assumed to be the same as the lapse rate on the TF39-1A engine and is shown in Figure 1. TF39-1A lapse rate (F_N/F_{N^*}) is about two percent worse at takeoff speed than the CF6-6D. Installed thrust specific fuel consumption (TSFC) curves are shown in Figure 2.

- Weight scaling is commensurate with the GE-13/F6 engine.

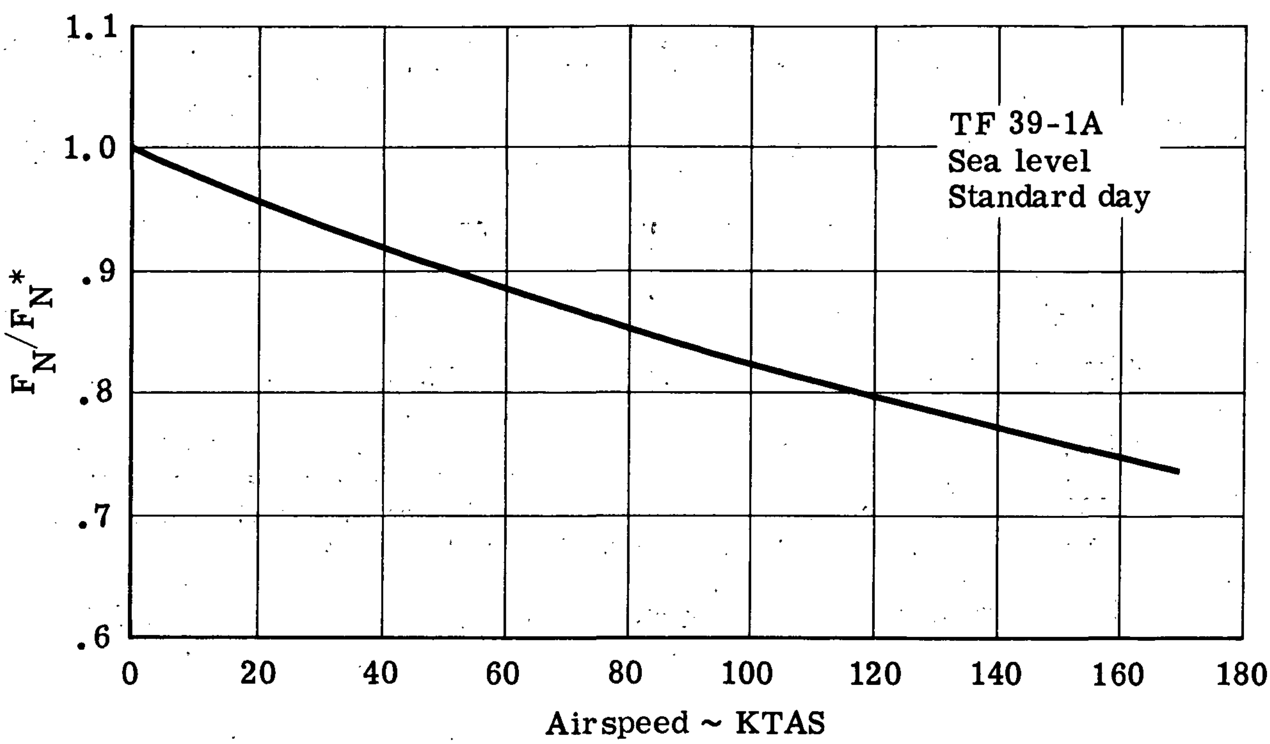

Figure 1 Takeoff thrust lapse rate

4.2 WEIGHTS METHODOLOGY

The Airplane Sizing and Mission Performance (ASAMP) computer program (Reference 3) contains a Class I weight prediction subroutine. Class I weight predictions are developed parametrically based on preliminary configuration data. These methods were intended primarily for commercial subsonic transports, but have been expanded to cover STOL types, as discussed below. Class I weight prediction methods are expected to yield relative weight accuracies between 5% and 10% when comparing several aircraft designed to do similar transport tasks.

Emphasis has been placed on weight prediction improvements for MF and EBF STOL

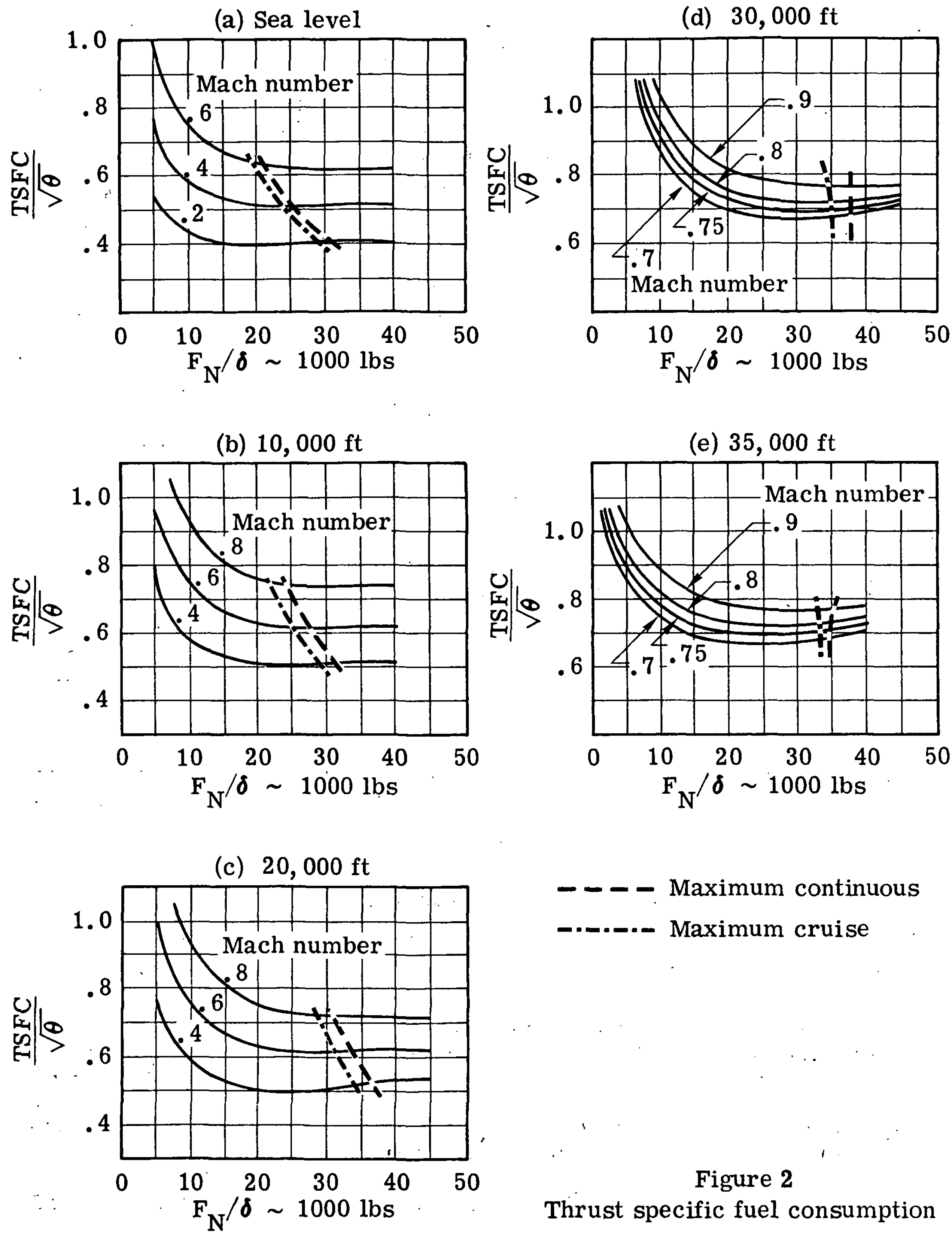

Figure 2
Thrust specific fuel consumption

configurations. Since the Reference 1 study was completed, the weights module of the ASAMP computer program has been updated by the methods of Reference 4. The wing weight portion of this revision of the computer program has subsequently been updated by the methods of Reference 5. Adjustments to the methods of Reference 4, which is Conventional Takeoff and Landing (CTOL) oriented, to account for STOL weight trends are as follows:

Item	Weight Multipliers
Fuselage	1.15
Landing Gear	1.25
Passenger Accommodations	.86
Cargo Accommodations	.67
Emergency Equipment	1.12
Air Conditioning	1.05
EBF Configurations Only (See Flow Chart, Figure 3).	
Trailing Edge Flap	
Area Factor	1.47
Fowler Motion Factor	1.57

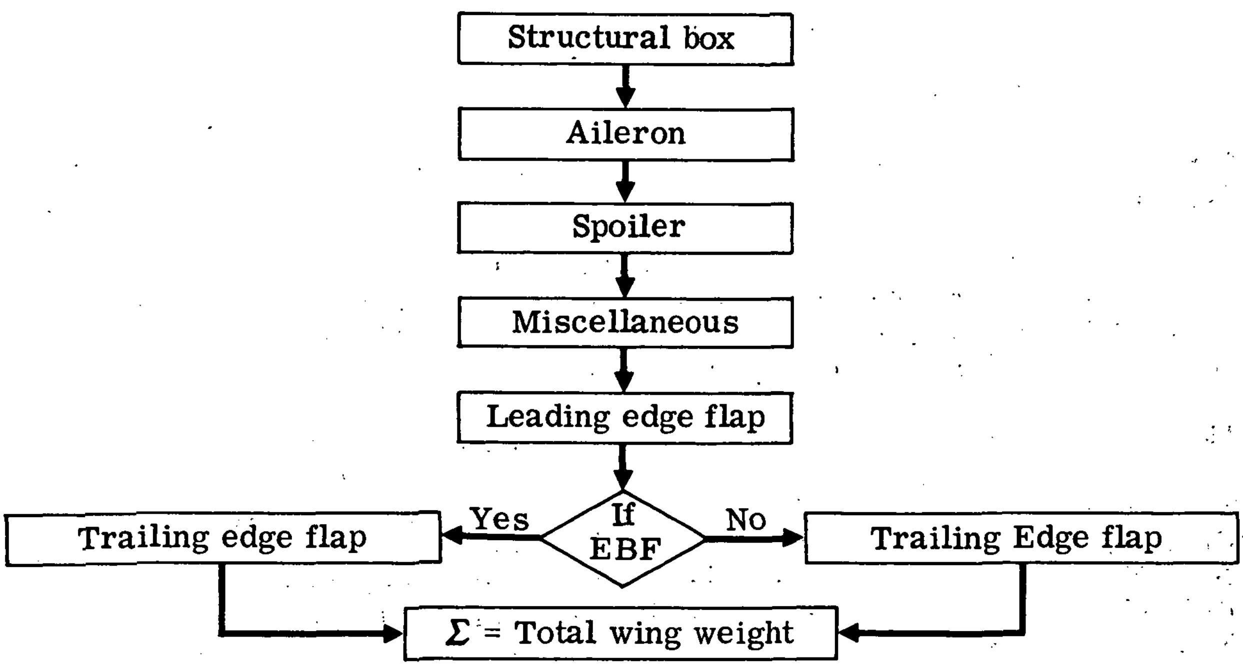

Figure 3 ASAMP wing weight flow chart

Weight multipliers are used in the following manner:

$$\begin{pmatrix}\text{ASAMP PREDICTED}\\ \text{COMPONENT WEIGHT}\end{pmatrix}_{\text{STOL}} = \begin{pmatrix}\text{WEIGHT}\\ \text{MULTIPLIER}\end{pmatrix}\begin{pmatrix}\text{ASAMP PREDICTED}\\ \text{COMPONENT WEIGHT}\end{pmatrix}_{\text{CTOL}}$$

Background data and justification for the primary engine weight scaling factor are shown on Figure 4. The slope of the line through the data point labeled GE-13/F6 is .152 lbs/lbs. The scaling relationship for primary engine weight is:

$$\text{Primary Engine Weight} = .152 \left(F_N^*/F_{N_{Ref}}^*\right) \left(F_{N_{Ref}}^*\right), \text{ lbs.}$$

where:

$$F_{N_{Ref}}^* = 39{,}400 \text{ lbs.}$$

4.2.1 GUST LOAD ALLEVIATION SYSTEM WEIGHTS

An assumption of this study is that the airplane structure would be designed to 2.5 g's limit load factor. If the design load factor had to be increased due to gust loads, then a gust load alleviation (GLA) system would be incorporated, which would insure that the airframe would not be exposed to "g" loads higher than 2.5.

The systems involved in achieving GLA are:
- Hydraulics and Pneumatics
- Electronics
- Surface Controls

Figure 5(a) illustrates the method for increasing the weight of these systems for design load factors higher than 2.5 due to gust load criticality.

The critical gust load factors are shown on Figure 5(b). The critical load factors for the wings of both the MF and EBF configurations occur at 360 KEAS (assumed V_{MO}) at 20,000 ft. in a 50 ft/sec (EAS) vertical gust. The two wings have a different gust load factor at the same wing loading because they have different wing planforms, and hence different lift curve slopes.

Figure 5(a) was derived from experience gained from the programs of References 1, 6, 7 and 8.

A more detailed weight investigation was made to check the validity of the hydraulic and pneumatic GLA weight multiplier shown in Figure 5(a). The 150 passenger 2,000 ft. MF configuration (lowest wing loading) was used for the investigation. At 360 KEAS four degrees of aft flap deflection is required to limit the airframe response to a 50 ft/sec vertical gust to 2.5 g's, (see Section 8.7.1). Total unbalanced surface hinge moments for this flight condition are shown in Table 1. The actuators would be housed inside the flap track fairings. The weight per unit force output compatible with 1970 actuator technology is .0023 lb/lb force for a 3000 psi hydraulic system. The resulting weights of the actuators required to deflect the GLA flap four degrees are also shown in Table 1.

An actuator rate requirement of 60 degree/sec will require the volumetric flow rates shown in Table 1. Based on current equipment, hydraulic pumps capable of supplying these flow rates will weigh

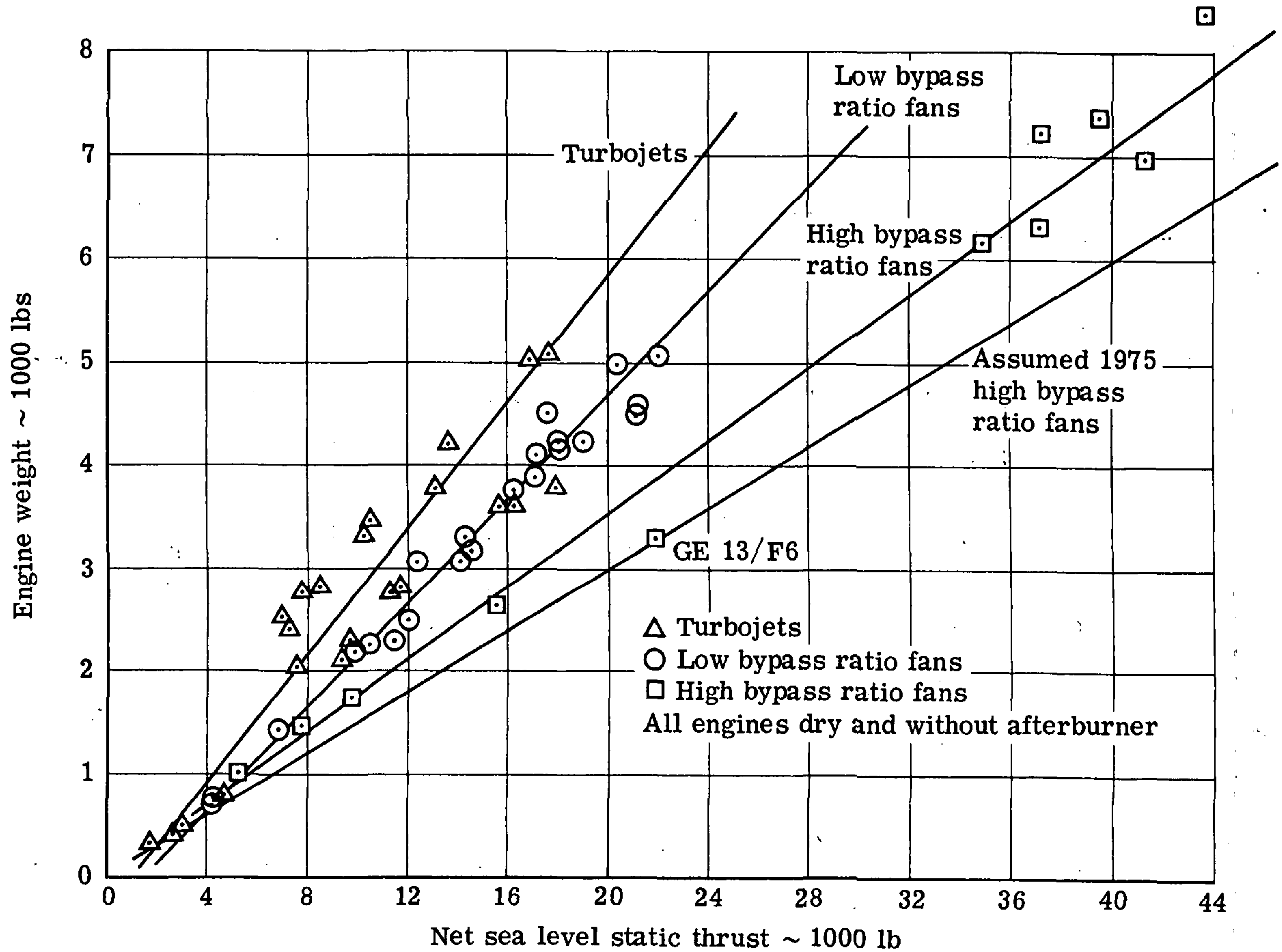

Figure 4 Dry engine weight

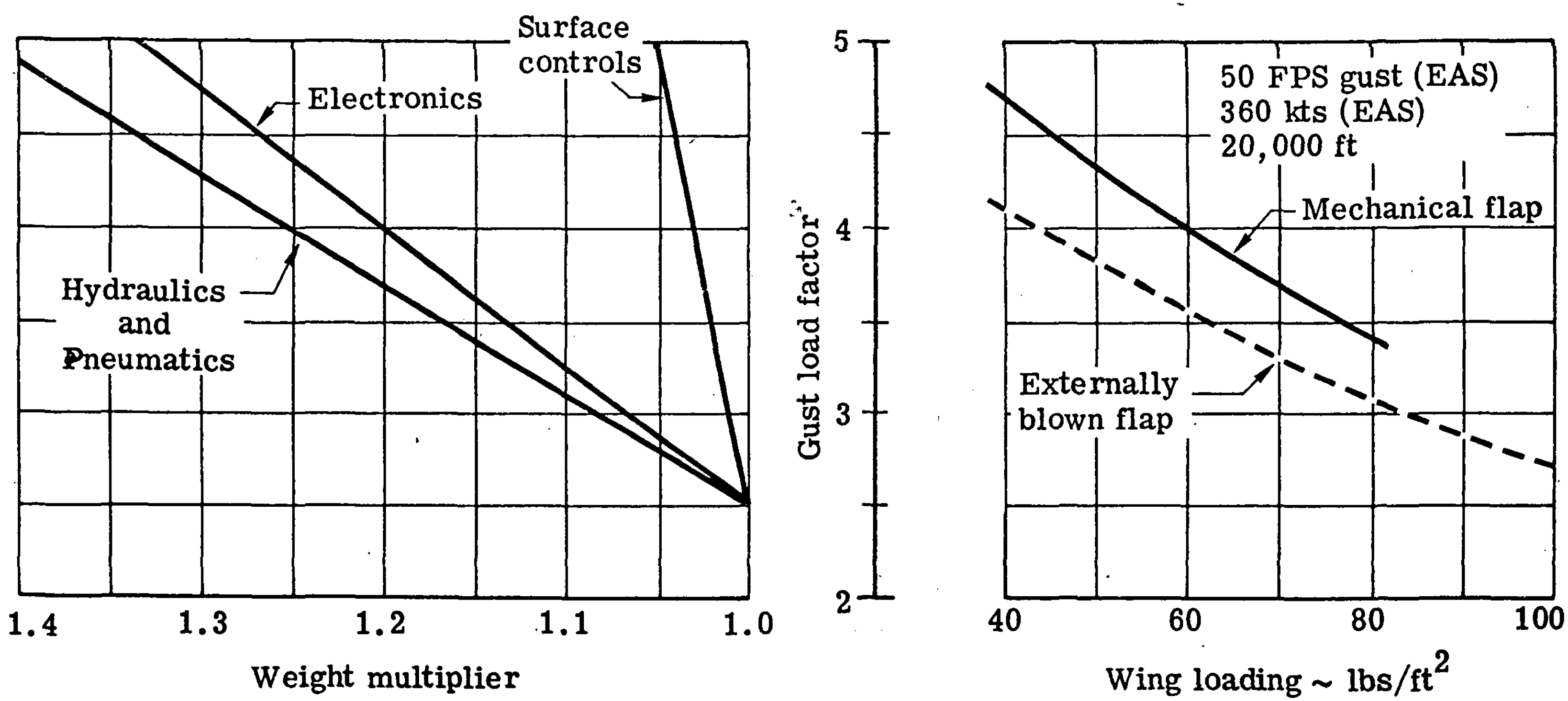

(a) Gust load alleviation
System weight penalties

(b) Design gust load factor
(Ref F.A.R. Part 25, Par. 25.341)

Figure 5 Gust load alleviation

approximately .8 lb/gpm flow rate. Hydraulic pump weights are also shown in Table 1. The last entry in Table 1 is the computed GLA weight multiplier which is derived from the combination of hydraulic pump and actuator weights. From Figure 5(a) the GLA weight multiplier used in this study is 1.36 for a wing loading of 42 psf.

TABLE 1 DETAILED GLA HYDRAULIC SYSTEM REQUIREMENTS

No. Passengers	Moment (Ft-Lb)	Actuator Weight (Lb)	Hydraulic Flow Rate (gpm)	Hydraulic Pump Weight (Lb)	GLA Computed Weight Multiplier
40	14,700	40	16	13	1.07
150	83,600	127	91	73	1.21
300	306,000	302	333	266	1.43

4.2.2 GROUP WEIGHT STATEMENT

Structures Group

The Structures Group is made up of the following items:

- Wing
- Horizontal Tail
- Vertical Tail
- Fuselage
- Landing Gear
- Engine Struts
- Engine Nacelles
- Engine Duct
- Engine Mount

Figure 6 is a correlation of actual versus ASAMP predicted wing weight for a wide range of airplanes using the method of Reference 5. A correlation of the total actual Structures Group weights compared to the ASAMP predicted summation is shown on Figure 7. The ± 10 percent accuracy lines are included.

Propulsion Group

The Propulsion Group contains the following items:

- Primary Engines
- Engine Accessories
- Engine Controls
- Engine Starting System
- Thrust Reversers
- Fuel System

Reference Figure 4 for primary engine weight. The total Propulsion Group weight correlation by ASAMP is shown on Figure 8.

Fixed Equipment Group

The Fixed Equipment Group contains the following items:

- Instruments
- Surface Controls
- Hydraulics
- Pneumatics
- Electricals
- Electronics
- Flight Desk Accommodations
- Passenger Accommodations
- Cargo Accommodation
- Emergency Equipment
- Air Conditioning
- Anti-Icing
- APU

The ASAMP predicted correlation with actual total Fixed Equipment is shown on Figure 9.

Standard And Operational Items

Standard Items

Standard items are equipment and fluids not an integral part of a particular aircraft and not a variation for the same type of aircraft. These items may include, but are not limited to the following:

- Unusable fuel and other unusable fluids
- Engine oil
- Toilet fluid and chemical
- Fire extinguishers, pyrotechnics, emergency oxygen equipment
- Structure in galley, buffet and bar
- Supplementary electronic equipment

Operational Items

Operational items are personnel, equipment and supplies necessary for a particular operation but not included in basic empty weight. These items may vary for a particular aircraft and may include, but are not limited to the following:

- Crew and baggage
- Manuals and navigational equipment
- Removable service equipment for cabin, galley and bar
- Food and beverages, including liquor
- Usable fluids other than those in useful load
- Life rafts, life vests and emergency transmitters
- Aircraft cargo handling system and cargo container

The correlation is shown on Figure 10.

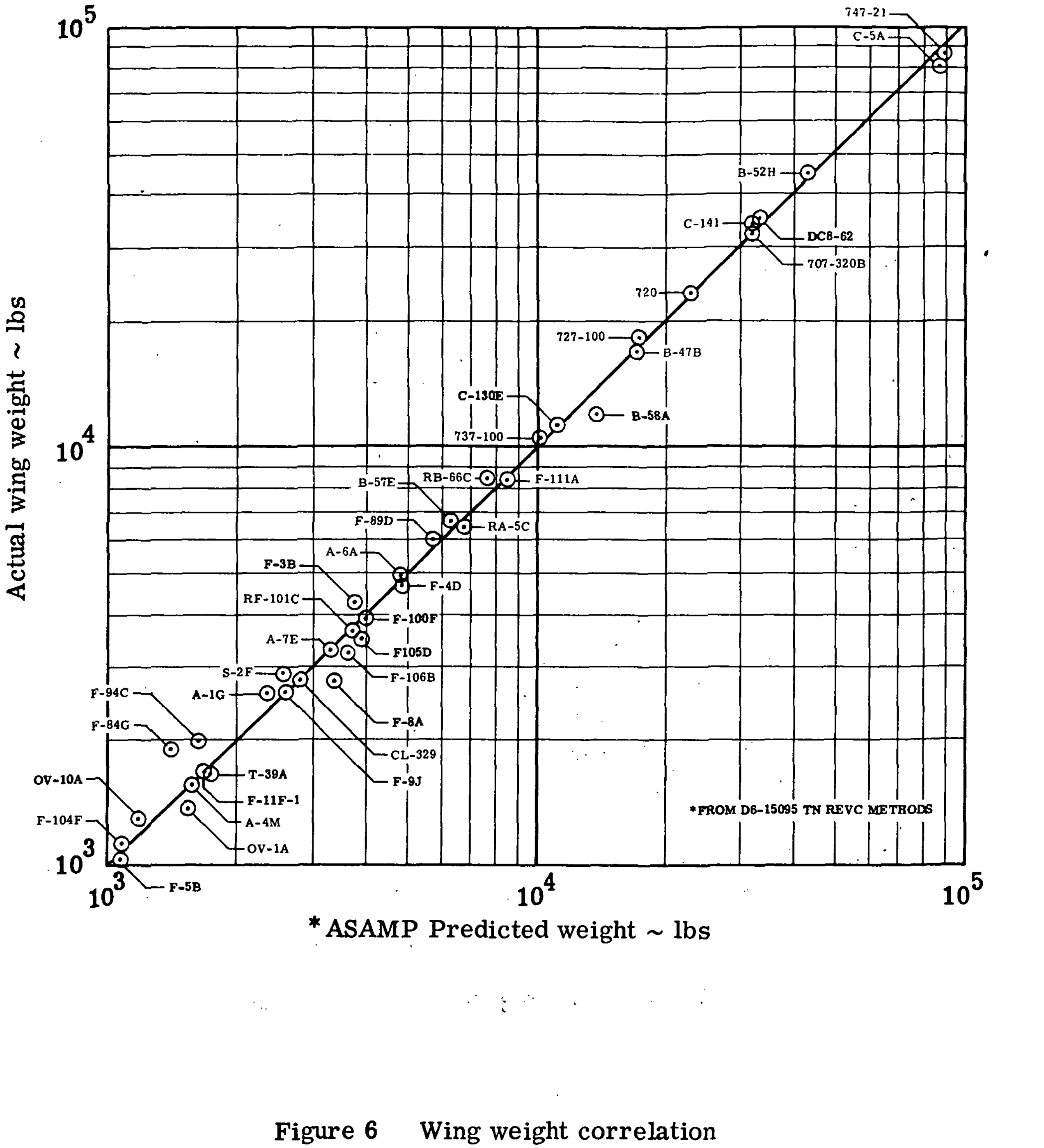

Figure 6 Wing weight correlation

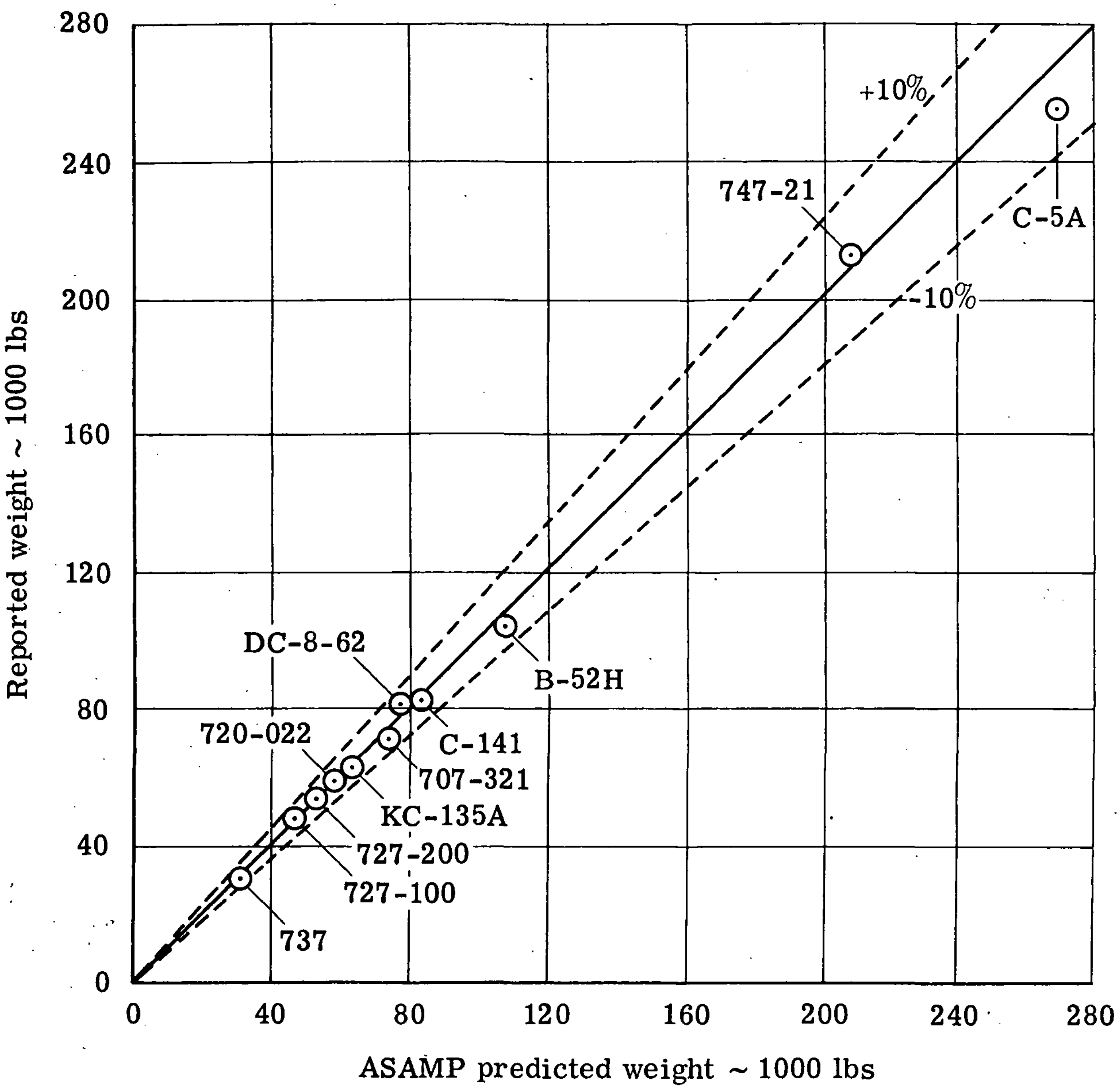

Figure 7   Structures group prediction accuracy

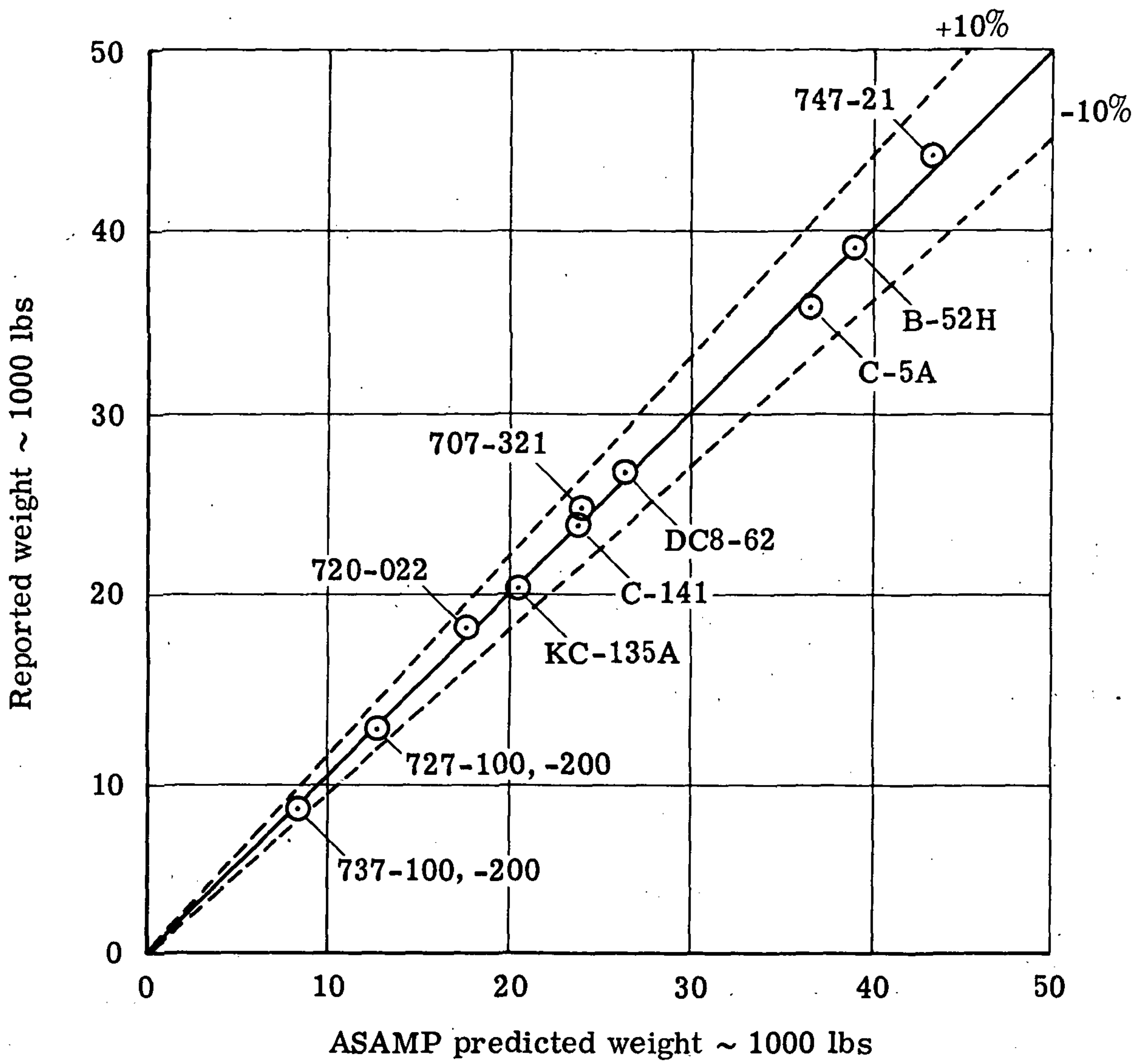

Figure 8 Propulsion group prediction accuracy

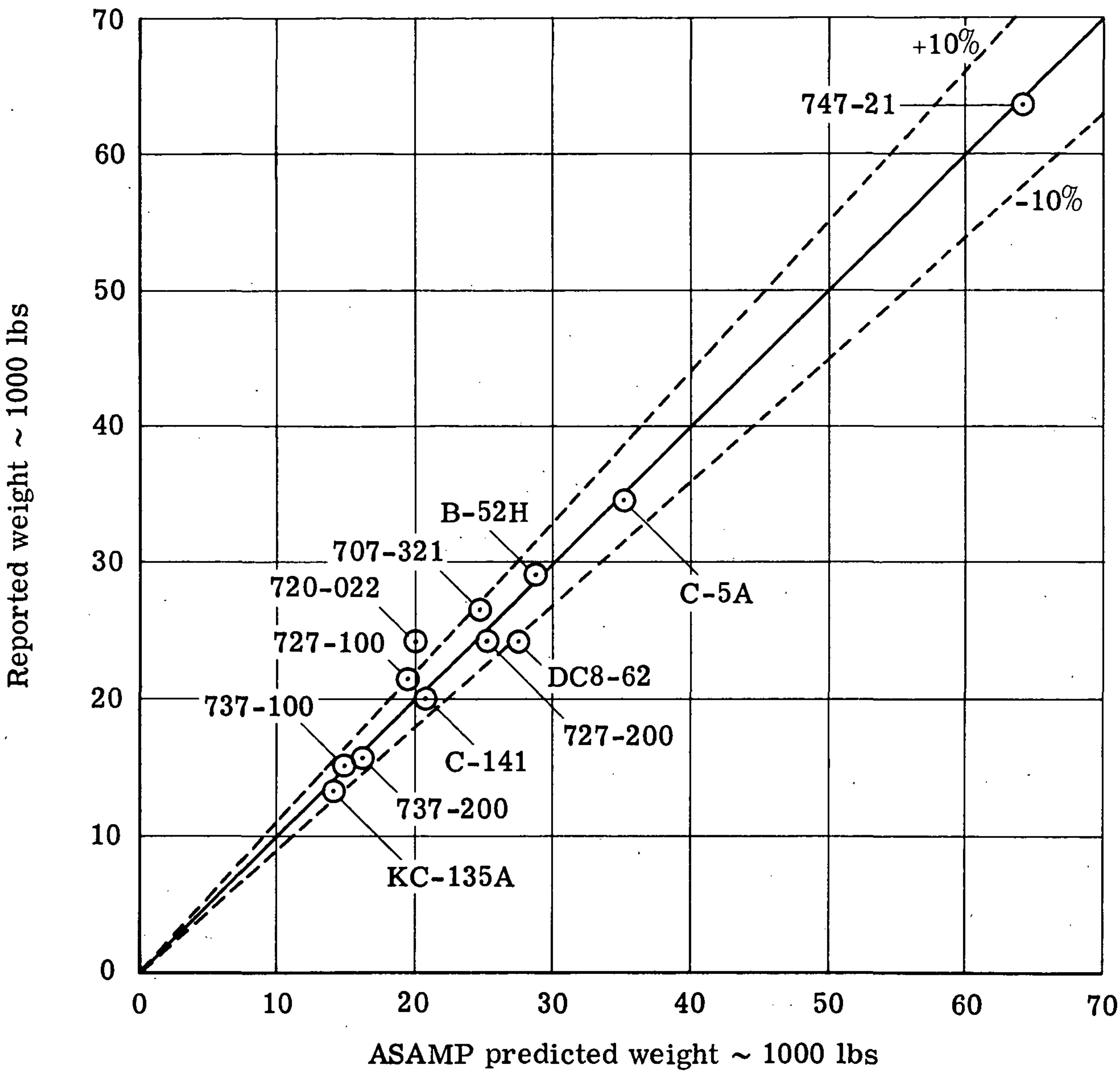

Figure 9 Fixed equipment group prediction accuracy

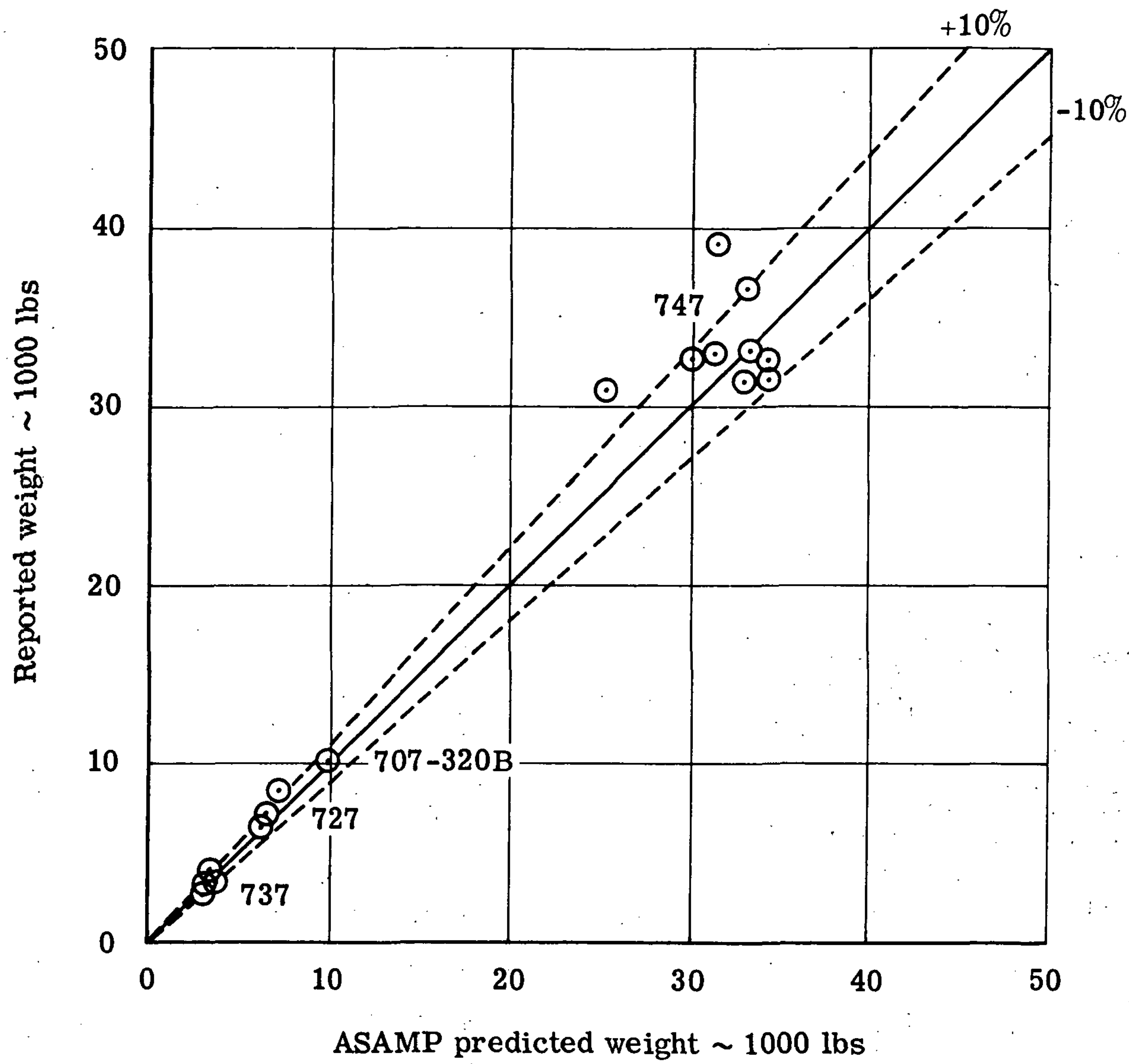

Figure 10 Standard and operational items prediction accuracy

4.2.3 FINAL WEIGHT STATEMENTS

Final weight statements for the 18 point design airplanes of this study are contained in Appendix A.

4.3 AERODYNAMICS

4.3.1 SUPERCRITICAL WING METHODOLOGY

The method used for this study enables the designer to choose the wing section required to satisfy a given design mission. The critical assumption is that the performance of a three-dimensional wing can be predicted from its two-dimensional section characteristics. Consequently, if the two-dimensional characteristics of a family of airfoil sections of current technology can be predicted, then a series of wings using these sections can be matched to the design mission and the optimum wing section selected. The problem to solve is: given the technology level and the three-dimensional drag divergence Mach number, how does one make the transformations to section drag divergence and lift and the corresponding section thickness ratio back out again to a wing thickness distribution that will in fact demonstrate the proper drag divergence and drag rise. A discussion of two-dimensional to three-dimensional correlation is required before this solution can be explained.

Two-Dimensional Generalization

Data from several two-dimensional wind tunnel tests have been generalized and used to predict the performance of a complete family of airfoil sections. Ordinarily the analysis is accomplished in two parts; first, polar shape is determined and second, drag rise and critical Mach number obtained. However, in this study the order of events in the use of this method was modified slightly. A cruise Mach number of .8 was a goal of the study. Based on previous experience the corresponding wing drag divergence Mach number was .81. Therefore, rather than solving for the drag divergence Mach number knowing thickness distribution, the reverse was done. Drag rise and polar shape are handled in ASAMP in the drag routine. This will be discussed in Paragraph 4.3.2

Drag Rise and Drag Divergence Mach Number

The key assumptions related to drag rise, drag divergence and the associated section thickness ratios are discussed below.

An idealized chordwise pressure distribution was devised as illustrated in the following sketch:

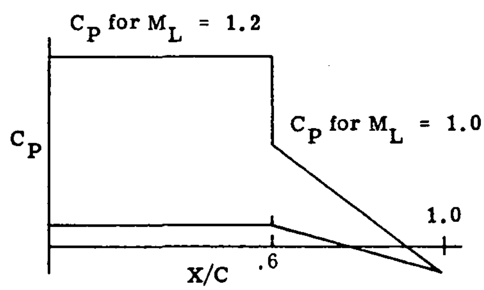

The upper surface c_p corresponds to a local Mach number of 1.2 (and extends from the leading edge) back to the pressure recovery point. At the recovery point (60 percent chord point) the c_p drops to a local Mach number of 1.0 with a linear recovery to the trailing edge. Assuming the thickness pressures from Reference 9, this c_p distribution will give various c_l capabilities as a function of free stream Mach number, thickness ratio and recovery point. An example of this process is shown on Figure 11 for a recovery point at .6 chord. This drag divergence Mach number curve represents the envelope of a family of airfoils designed to the above specified pressure distribution with different camber and thickness ratios. The level of technology represented by these data have been verified by personnel in the 8-Foot Tunnels Branch at NASA Langley.

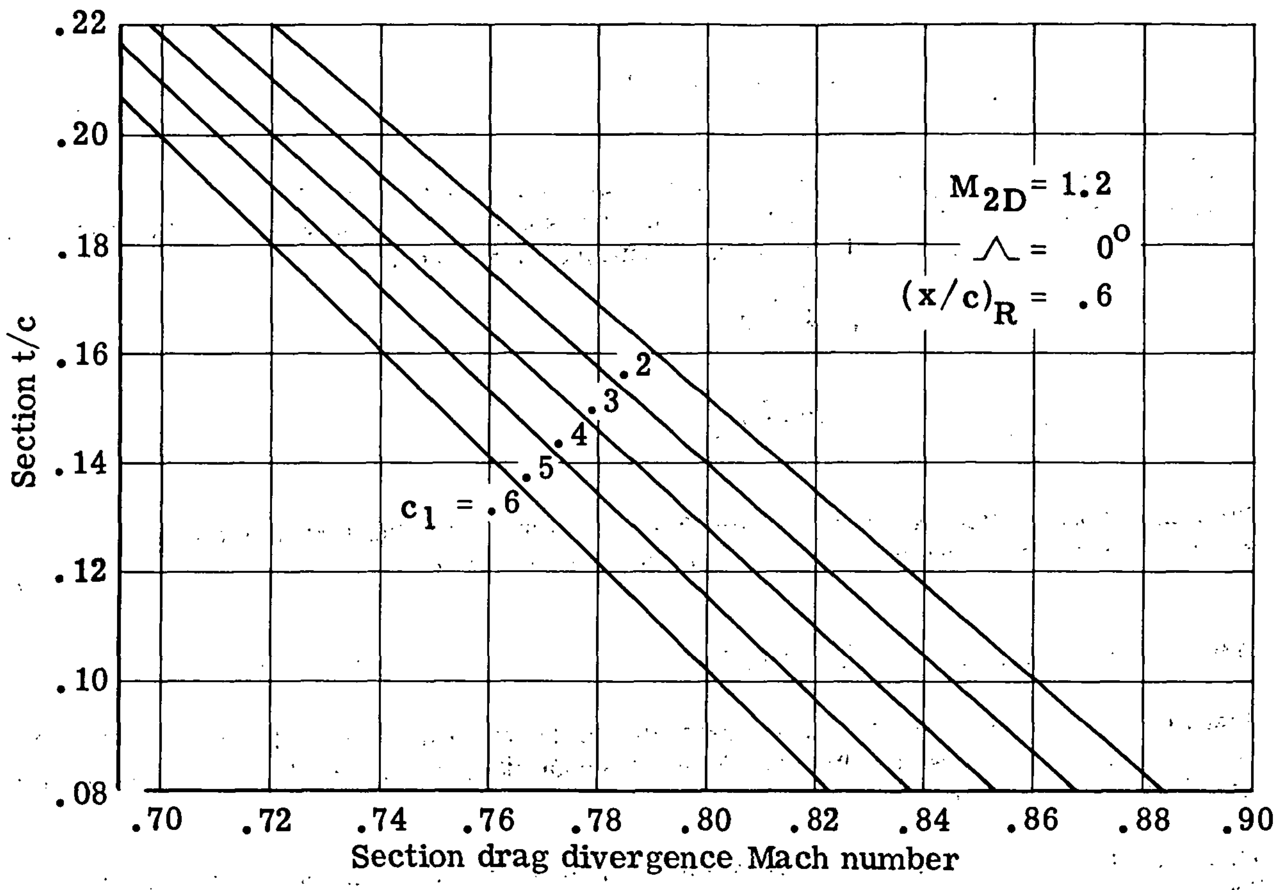

Figure 11 Technology level

Two-Dimensional to Three-Dimensional Correlation

In order to use the generalized two-dimensional data, a procedure must be developed to convert the two-dimensional (2D) to three-dimensional (3D) characteristics. The obvious point of departure is simple sweep theory, which gives the following relationships:

$$M_{3D} = M_{2D} (\text{Sec } \Lambda)$$
$$C_L = c_l (\text{Cos}^2 \Lambda)$$
$$C_D = c_d (\text{Cos}^3 \Lambda)$$

This theory has been applied with two slight modifications. First, the sweep of the recovery point is used as the effective sweep angle when calculating the drag divergence boundary. This can be justified by noting it is the shock sweep that determines drag divergence, not the quarter chord sweep, and the shock is generally located at the section pressure recovery point. In addition, a .90 factor should be applied to the three-dimensional lift coefficient to allow for the decrease in lift at the root and tip. Therefore, the following expressions should be used for the three-dimensional drag rise derivation:

$$M_{3D_{DR}} = M_{2D} (\mathrm{Sec}\ \Lambda_{EFF})$$

$$C_{L_{DR}} = .9\, c_l (\mathrm{Cos}^2\ \Lambda_{EFF})$$

Second, a $\cos^2 \Lambda$ correction to the drag coefficient gives a much better correlation. It was found experimentally that the $\cos^3 \Lambda$ effect could not be justified. Consequently, the following expressions were used to calculate the three-dimensional polar shape:

$$C_{L_{PS}} = c_l (\mathrm{Cos}^2\ \Lambda_{c/4})$$

$$C_{D_{PS}} = c_d (\mathrm{Cos}^2\ \Lambda_{c/4})$$

Note the quarter chord sweep is recommended for use in the polar shape derivation because experimental results indicate that this relationship yields a valid correlation.

4.3.2 HIGH SPEED DRAG ESTIMATION

Prediction of subsonic airplane drag in the cruise configuration is an internal routine in ASAMP. The prediction methods are used when wind tunnel data is not available for the specific configuration of interest.

The drag estimation method used in this study is based on theoretical and experimental data which have been accumulated in recent years. Results from Boeing research programs and airplane development efforts, such as 737 and 747 are included.

The total subsonic drag is made up of three general terms:

$$C_D = C_{D_o} + C_{D_i} + \Delta C_{D_M}$$

TOTAL DRAG	PARASITE	INDUCED	DRAG RISE (COMPRESSIBLE)

Parasite Drag

Parasite drag includes the friction and pressure (separation, interference, profile) drag assuming no compressibility effects. All compressibility effects are accounted for in the ΔC_{D_M} term.

$$C_{D_o} = \frac{K_f}{S_{Ref}} \left[\sum (C_f \, A_{wet}) \quad \begin{matrix} \text{wing} \\ \text{horizontal tail} \\ \text{vertical tail} \\ \text{fuselage} \\ \text{nacelle} \end{matrix} \right]$$

where

K_f is an empirical factor for interference and construction tolerances representing C_{D_o}/C_{D_f} and is assumed to have the value of: $K_f = 1.26$

C_f is the friction drag coefficient for a fully turbulent boundary layer on a smooth flat plate corrected for temperature due to compressibility in the boundary layer by the mean enthalpy method. C_f is adjusted to account for friction drag increase due to overspeed. For this study C_f was assumed constant at a value of: $C_f = .0032$

Induced Drag

The major portion of the induced drag is caused by the wing lift. Several other airplane components can contribute also. The induced drag from these other components is included in the parasite drag. The drag method assumes that considerable tailoring and optimizing of the configuration has been accomplished. True elliptic loading is not anticipated due to the need for design compromise. The induced drag is estimated by the following equation:

$$C_{D_i} = \left[1.03 + \delta_o \, (\delta / \delta_o) + (D/b)^2 \right] \frac{C_L^2}{\pi AR}$$

where: $$\delta / \delta_o = \left(\frac{C_{L_\delta}}{C_L} - 1 \right)^2$$

The constant (1.03) in the equation is a factor included to reflect a probable minimum nonellipticity. Further, nonelliptic effects may be eliminated for one specific C_L by proper spanwise camber and twist distribution. Minimizing the nonelliptic induced drag near the $C_{L_{design}}$ is usually a design goal. This design approach would provide slightly improved off design drag for holding or endurance performance, while trading trim drag improvements for increases in induced drag at the cruise condition.

The term $(\frac{D}{b})^2$ provides for an effect of the body on the wing load distribution and therefore on the induced drag.

The δ_o (δ/δ_o) term was derived from References 10 and 11 and provides for wing planform characteristics which dictate particular span load distributions. The basic planform effects can then be modified by some spanwise variation of camber and twist to achieve elliptic or nearly elliptic load distribution at one desired C_L.

Drag Rise

Drag rise includes all the additional drag occuring at Mach numbers greater than the incompressible Mach number. The drag rise includes the many drag increments from airplane components in the following equation:

$$\text{Total } \Delta C_{D_{M_{\substack{Drag\\Rise}}}} = \Delta C_{D_{M_{Wing}}} + \Delta C_{D_{M_{Body}}} + \Delta C_{D_{M_{Tail}}} + \Delta C_{D_{M_{Nacelle}}} + \Delta C_{D_{M_{Misc}}}$$

The drag rise region occurs at Mach numbers greater than the incompressible Mach number. This is an arbitrary definition, since compressibility effects occur at all Mach numbers greater than zero. Any of the airplane components can contribute to the drag rise. However, the wing usually has the largest effect.

Wing

Determination of the wing drag rise characteristics are required first because other components are related to the wing (e.g., wing mounted nacelles, trim, wing mounted miscellaneous items, etc.). The first step of this procedure is to find the drag divergence Mach number (M_{DD}) for each of the selected C_L values. For this document, M_{DD} is defined as the Mach number at which the drag coefficient has increased by .0020 over the incompressible C_D. M_{DD} is determined by using the following equation:

$$M_{DD_{WING}} = M_{DD_c} + \Delta M_{TECH} + \Delta M_{\Lambda} + \Delta M_t$$

The M_{DD_c} term represents achievable values for a 30° sweep, 10% t/c, 1969 technology wing with various cambers and C_L. When the analysis involves other wing technology, the appropriate technology correction (ΔM_{TECH}) should be made. The ΔM_{TECH} correction for this study was derived from the data of Figure 11 and the methods of Section 4.3.1 for developing three-dimensional data from two-dimensional supercritical wind tunnel data.

After M_{DD} has been determined, the drag rise shape (ΔC_{D_M}) may be fitted through it. The drag rise shape is shown on Figure 12.

The effects of wing-body interference are an integral part of the wing data presented in this section. It is assumed that the configuration is well tailored. Untailored configurations can easily have a critical Mach number degradation of .02 or more.

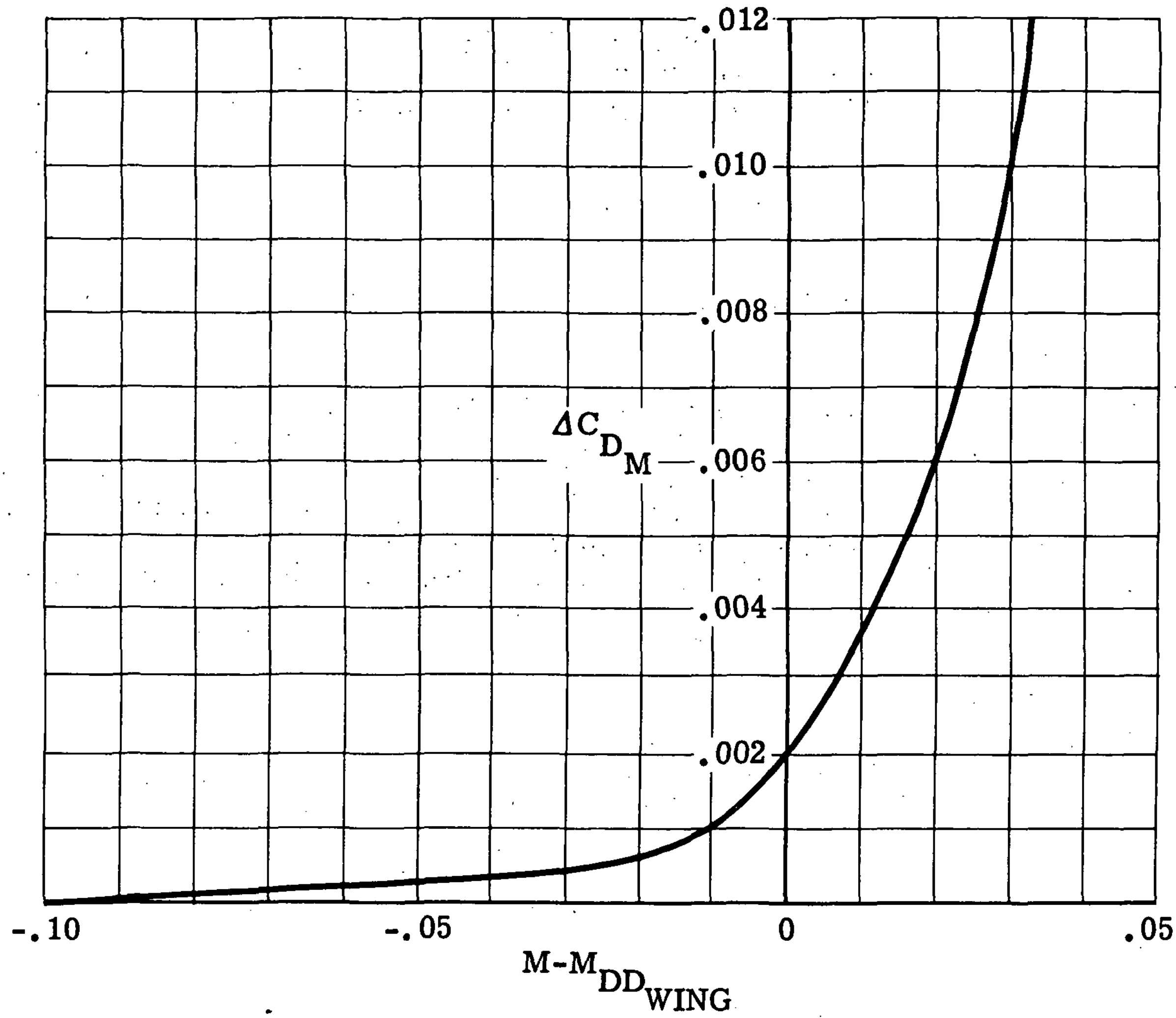

Figure 12 Drag rise shape

Vertical and Horizontal Tails

The method just described for the wing is also used for the tail surfaces.

Body

The nose shape of the fuselages used for this study produce .0001 rise in drag due to compressibility at M = .8. The body drag rise equation is:

$$\Delta C_{D_{M_B}} = \frac{.7}{S} \quad \Sigma\,(KB_I)\,(AP_I)\,(DL_I)^{5/3}$$

If M $\leq$ M_o then KB_I = 0. If $M_o < M < M_p$ then:

$$KB_I = \frac{1}{2} + \frac{\sin}{2}\left[\left(\frac{M - M_o}{M_p - M_o}\right)\pi - \frac{\pi}{2}\right]$$

M_o and M_p are determined from Figure 13.

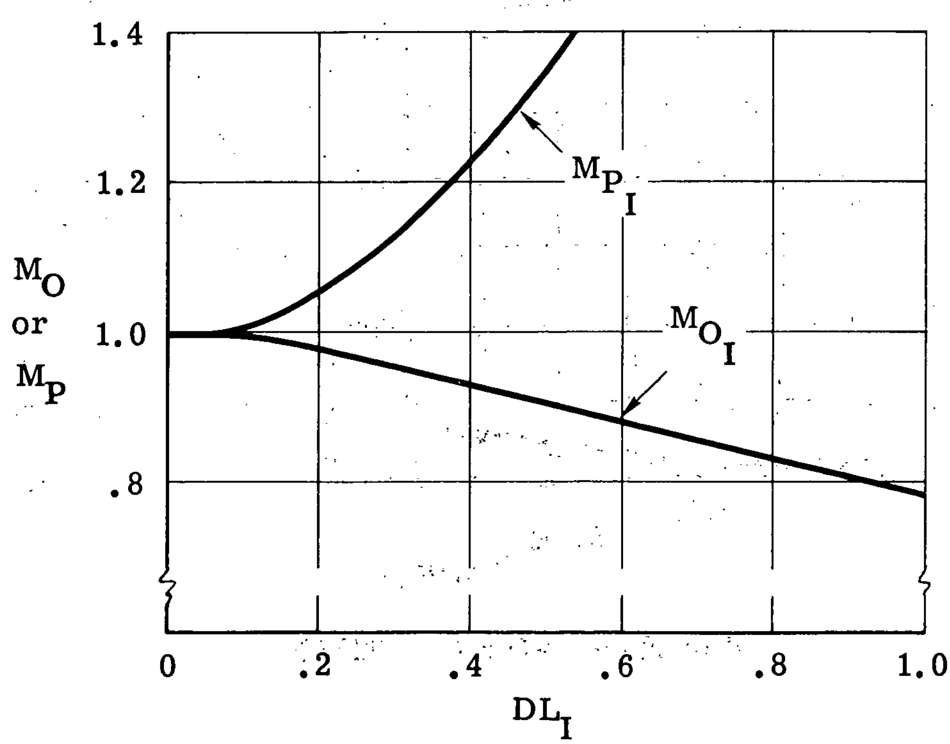

Figure 13 Fuselage wave drag shape

Nacelles and Miscellaneous

Nacelle and other miscellaneous protuberance drag increases due to compressibility were accounted for in the interference conservatisms of the parasite drag buildup.

4.3.3 HIGH SPEED AERODYNAMIC CHARACTERISTICS

Final ASAMP predicted high speed drag polars are contained in Appendix B.

Flaps up aerodynamic characteristics of the MF configuration are shown on Figure 14. Lift curve slope and downwash data were estimated using the methods of Reference 12. Neutral point was estimated from Reference 13.

Flaps up aerodynamic data for the EBF configuration were developed from unpublished NASA wind tunnel data. A three-view of the EBF configuration wind tunnel model is shown in Figure 15.

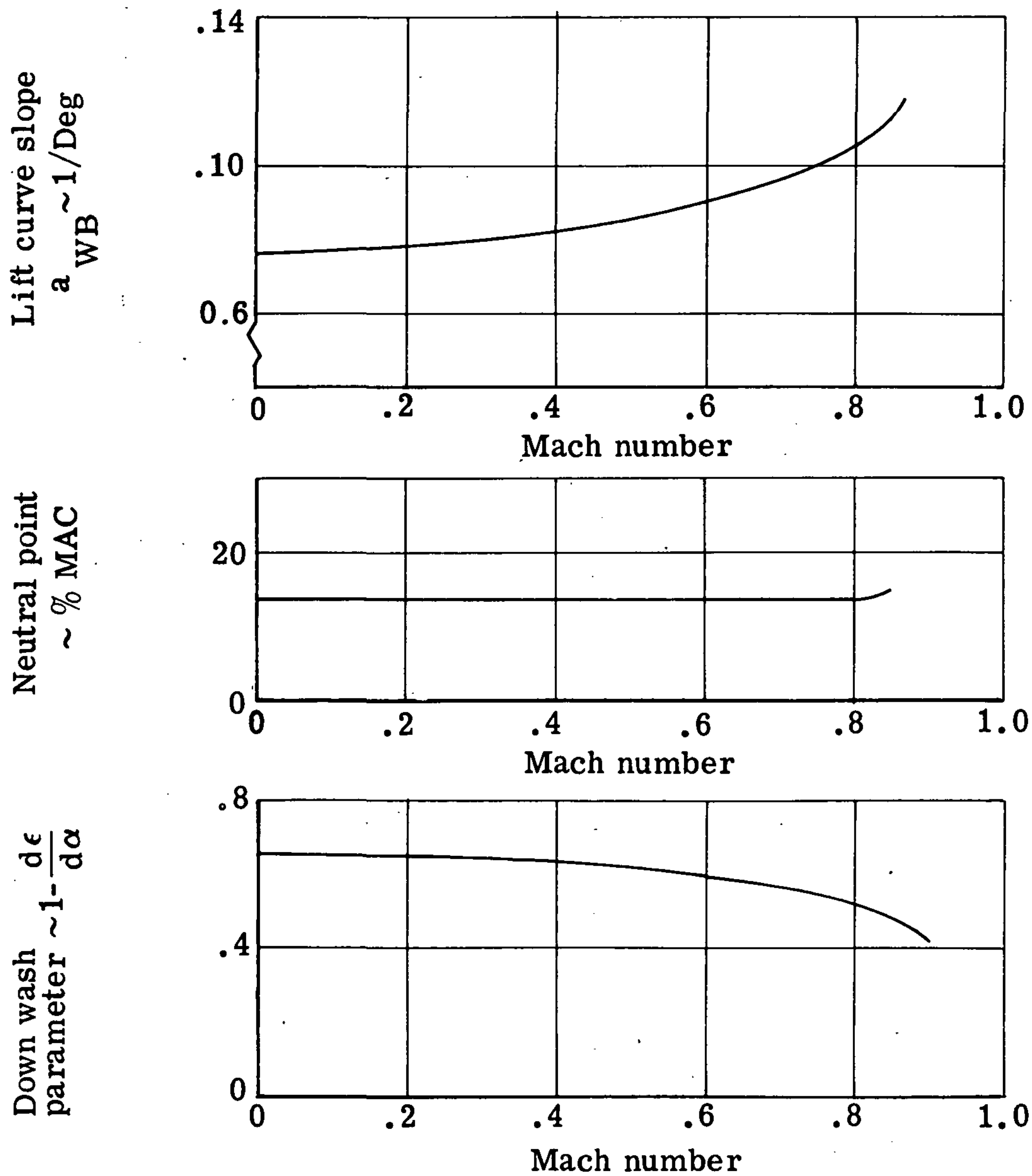

Figure 14 Flaps up aerodynamic data for the MF configurations

WING:	
Area, Sq. Ft.	5.202
Mean aerodynamic chord, Ft.	.885
Span, Ft.	6.240
Aspect ratio	7.48
HORIZONTAL TAIL:	
Area, Sq. Ft.	1.551
Mean aerodynamic chord, Ft.	.699
Span, Ft.	2.613
Aspect ratio	4.40
VERTICAL TAIL:	
Area, Sq. Ft.	1.488
Mean aerodynamic chord, Ft.	.964
Span, Ft.	1.600

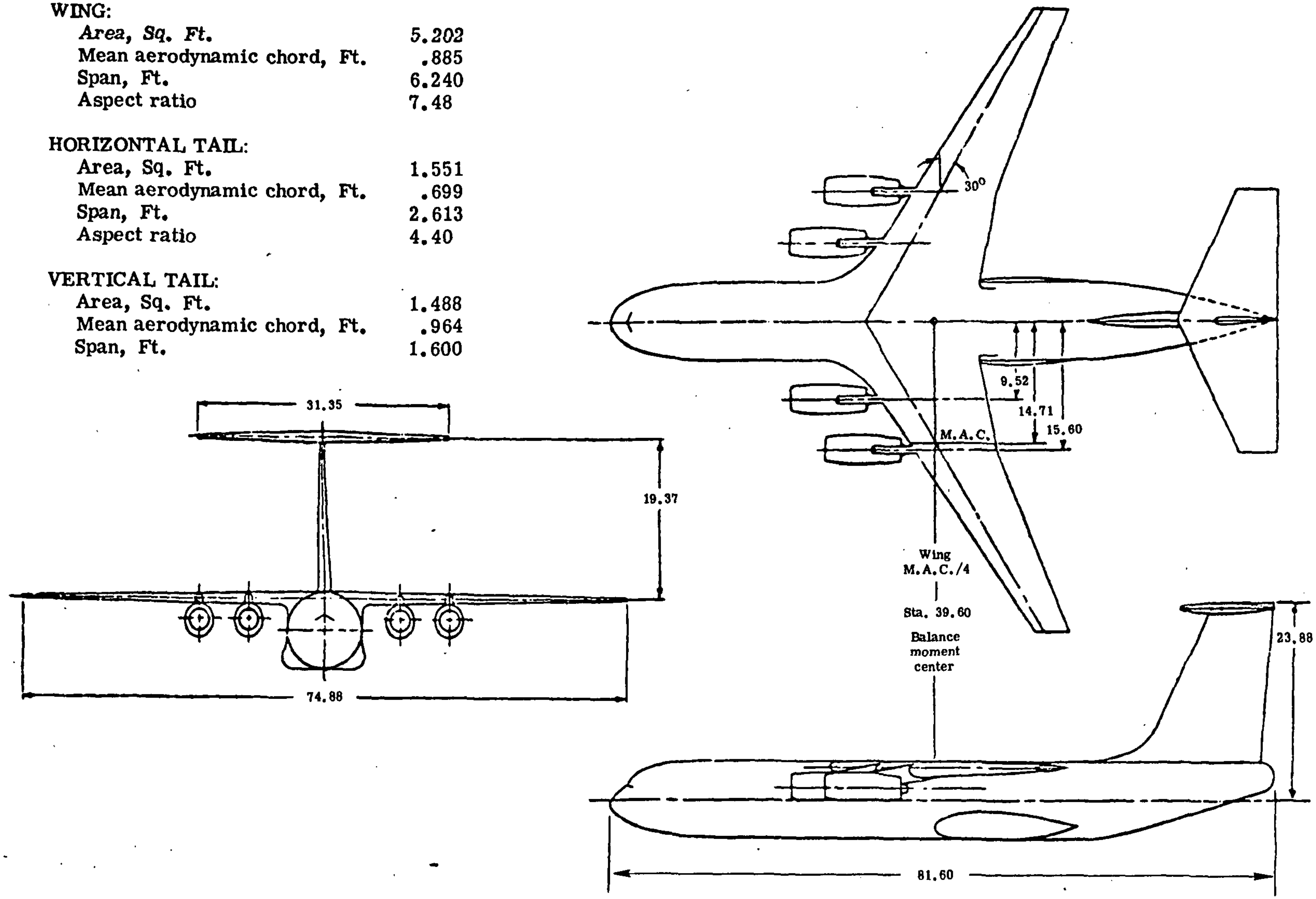

Figure 15 EBF configuration wind tunnel model

Page intentionally left blank

4.3.4 LOW SPEED AERODYNAMIC CHARACTERISTICS

Low speed drag polars were estimated for the MF configurations using the methods of Reference 14. The wing flap system is shown on Figure 16. The method assumes the following buildup of the untrimmed drag polar:

$$C_{D_{\substack{FLAPS\\DOWN}}} = C_{D_{P_{\substack{MIN\\CRUISE}}}} + \frac{C_L^{\,2}}{\pi AR} + \Delta C_{D_{P_{MIN_{LE}}}} + \Delta C_{D_{P_{MIN_{TE}}}} + \Delta C_{D_{i_{TE}}} + \delta C_{D_P} + \Delta C_{D_P}$$

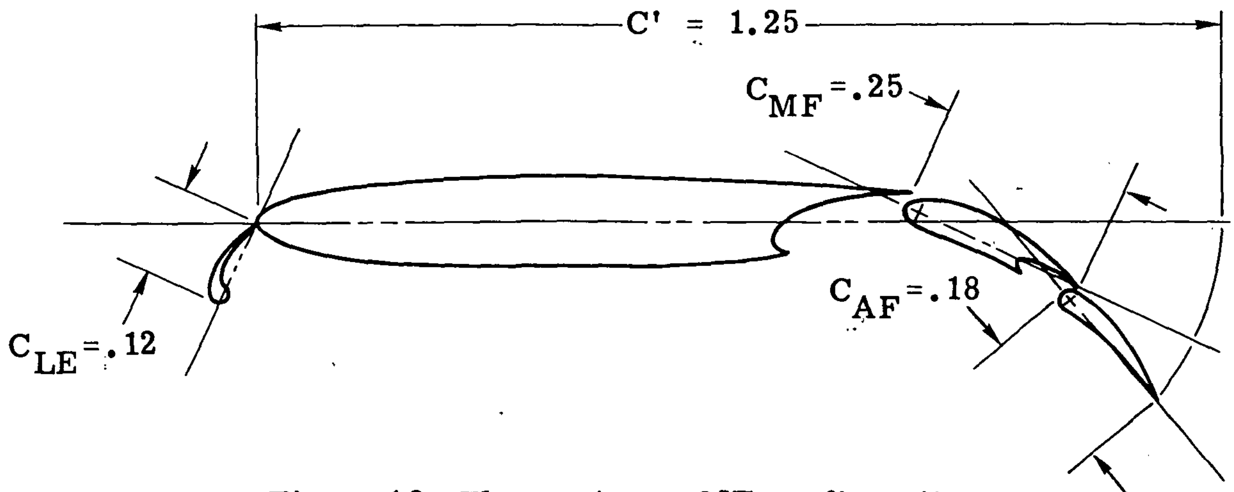

Figure 16 Flap system - MF configuration

The low speed lift curves were also predicted by the methods of Reference 14, however, maximum lift values were improved by 5 percent to account for 1975 capabilities. Estimated drag values were used. Flaps down pitching moment characteristics were estimated by the methods of Reference 14. The MF configuration low speed aerodynamic characteristics, out of ground effect, are shown on Figure 17.

The low speed aerodynamic characteristics for the EBF configuration were obtained from unpublished NASA wind tunnel data. A three-view of the EBF configuration wind tunnel model is shown in Figure 15. Lateral, directional and engine out data were provided by NASA Langley in a preliminary, unchecked preworking paper. The wind tunnel model configuration chosen for use in this study is as follows:

Bypass ratio	=	6.2
High horizontal tail location (T-tail)		
Horizontal tail incidence angle	=	5^{o}
Leading edge slat chord (%C)	=	25%
Leading edge slat deflection	=	50^{o}
Part span flaps		
Engine out rolling moment trimmed with ailerons		

(a) Lift

(b) Pitching moment

(c) Drag

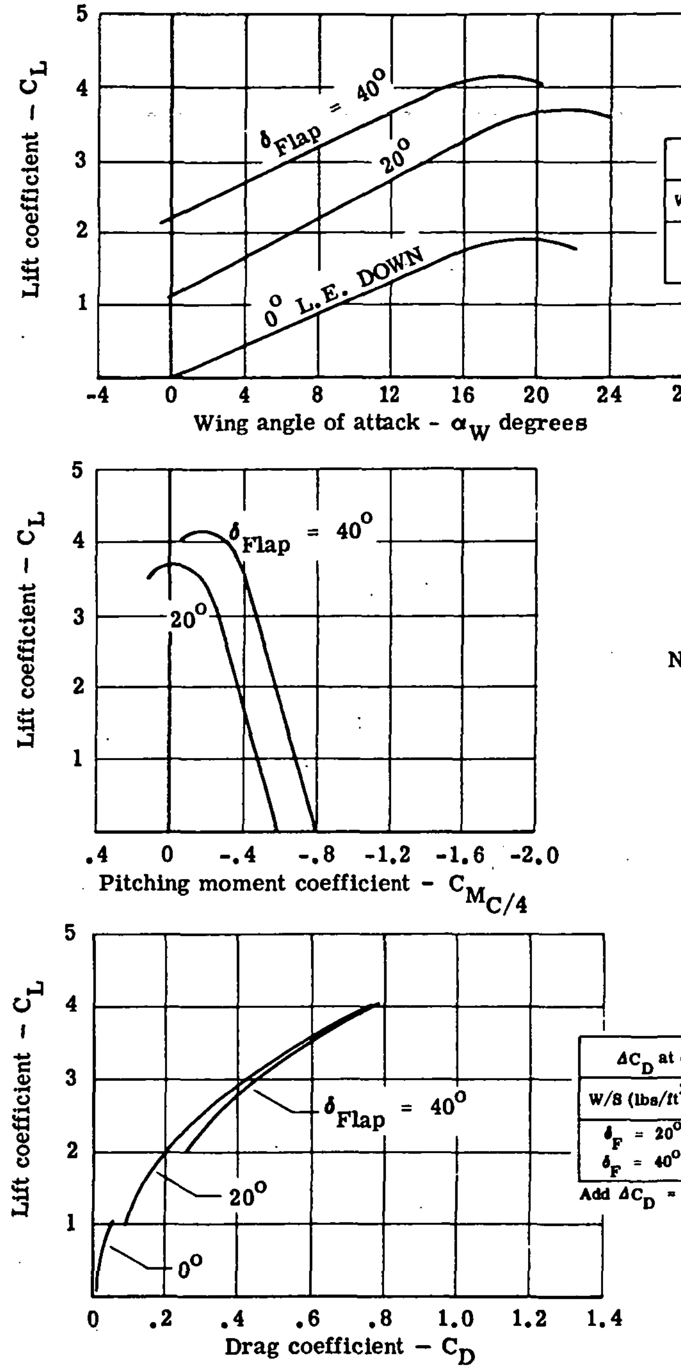

ΔC_L at constant α_{wing}

W/S (lbs/ft²)	40	80
δ_F = 20°	.04	-.04
δ_F = 40°	.12	-.10

Note: W/S = 60 lbs/ft²

ΔC_D at constant C_L

W/S (lbs/ft²)	40	80
δ_F = 20°	-.002	.002
δ_F = 40°	-.006	.006

Add ΔC_D = .01 for landing gear

Figure 17 Estimated tail off low-speed aerodynamic characteristics - MF configuration

Wind tunnel data were taken for three flap settings; 0°, 35° and 65°, and three values of C_T; 0, 2 and 4. To facilitate the estimation of airplane performance from this data, cross plots were made which describe force polars for intermediate flap settings and C_t's, i.e., 15°, 25°, 45° and C_T = .5 and 1.0.

5.0 TAKEOFF AND LANDING

Takeoff and landing performance was calculated using a computer program which has a ground effect subroutine. This subroutine calculates the changes in lift and drag over a specified range of ground heights. The method was used for both MF and EBF configurations.

5.1 TAKEOFF RULES AND PROCEDURE

Takeoff performance is calculated by numerical integration of the longitudinal and vertical equations of motion, based on inputs of aerodynamic, propulsion and geometric information for an airplane.

The takeoff calculation procedure is carried out within the bounds of specified margin and gradient criteria. These criteria are:

- $V_{LOF} \geqslant 1.05\ V_{MU}$ O.E.I. (One Engine Inoperative)
- $V_{LOF} \geqslant 1.08\ V_{MU}$ A.E.O. (All Engines Operating)

  If Airplane is Geometry Limited
- $V_{LOF} \geqslant 1.1\ V_{MC}$
- $V_R \geqslant 1.05\ V_{MC}$
- $V_{2_{O.E.I.}} \geqslant 1.2\ V_S$
- 2nd segment climb gradient (one engine inoperative)

  $\geqslant$ .030 (4 engine airplane)

  $\geqslant$ .027 (3 engine airplane)
- $V_1 \leqslant V_R$

The minimum unstick speed is calculated according to Reference 15. An optimization routine allows the best flare profile to be calculated for minimum flare distance. A matrix of gradient and margin data for the configuration is generated automatically as a function of T/W and C_L for both the all engines operating and one engine inoperative conditions.

The takeoff calculation is initiated by the determination of V_{MU}. Using the maximum attitude (geometry limit) at lift-off, the minimum lift-off speed is computed. If insufficient gradient capability is available, the speed is increased systematically until either sufficient gradient is available, or the gradient capability fails to increase with increasing speed, in which case the calculation is terminated. This procedure is completed for all engines operating and one engine inoperative. Following the computation, an estimate of rotation speed is made based on a specified maximum pitch rate and acceleration. V_1 is then set equal to V_R, and the ground run, flare and stopping time histories are calculated by numerical integration of the equations of motion. The relevant margins and gradient criteria at V_R, V_{LOF} and V_2 are then checked for both all engines operating and one engine inoperative. If any criteria is not satisfied, the rotation speed is increased systematically. After all criteria are satisfied, the optimum rotation speed to minimize the field length is determined, whether it be limited by all engine or engine out criteria. Following this optimization, the stopping distance is calculated. If the airplane is stopping distance limited, V_1 is reduced until the distance to continue takeoff with an engine out and the distance to stop with an engine out are within a specified tolerance.

Takeoff Input Data

Aerodynamic data are input in the form of a matrix of free air trimmed data versus angle of attack and C_T (for powered lift airplanes), for all engines operating and one engine inoperative. The data is repeated for up to five flap angles. The flap angle selected for takeoff need not correspond to one of those input, since the program interpolates between the data sets. The ground effect on lift and drag may be calculated by a subroutine in the program, or if desired, may be input for each takeoff flap angle in the form of a matrix of lift ratios and drag increments versus angle of attack, C_T and ground height. For conventional airplanes the reference C_T is set to zero and this specific dimension in both free air and ground effect matrices reduces to a one element array.

The propulsion data are input as three arrays of thrust component ratios versus speed. The three arrays are the blowing thrust on a powered lift airplane, $({}^{T}BL/{T_{REF}})$, the ram drag of the engine $({}^{D}RAM/{T_{REF}})$, and the direct thrust from the engine which does not interact with lift and drag $({}^{T}PRIM/{T_{REF}})$. The term ${}^{T}REF$ is the reference engine size which corresponds to the selected $({}^{T}REF/{W})$ for a particular case. For a conventional airplane the thrust is input the same way except $({}^{T}BL/{T_{REF}})$ is set to zero.

Various geometric properties of the airplane are required such as M.A.C., gear stroke, and maximum pitch attitude at lift-off and during climbout.

Maneuver margin and climb gradient requirements at V_2 must be input for the takeoff calculation. The resulting takeoff speed schedule will attempt to satisfy these requirements by overspeeding if necessary.

Various constants for the calculation of refused takeoff (R.T.O.) stopping distance must be input. These consist of items such as braking coefficient, transition time, reverser effectiveness, etc.

Ground Run Calculation Method

For conventional airplanes where lift and drag are not strong functions of engine thrust, the ground run calculation is a simple integration of the acceleration from zero speed to V_R. The terms accounted for in the equation of motion are fan thrust, primary thrust, ram drag, aerodynamic drag, and ground roll friction based on gear reaction. The calculation is made for all engines operating up to V_R, then for all engines operating up to V_1 followed by one engine out up to V_R.

The calculation becomes somewhat more complex for a powered lift airplane since both lift and drag are expressed as functions of C_T. At low speeds this quantity becomes very large and exceeds the maximum value for which aerodynamic data is input. It is therefore necessary to change the calculation procedure below a speed corresponding to $C_{T_{MAX}}$. The method used is to interpolate linearly between a specified static acceleration computed using $\left(\frac{T_{STATIC}}{T_{REF}}\right)$ and $\left(\frac{T_{PRIM}}{T_{REF}}\right)$, and the acceleration at $C_{T_{MAX}}$. Clearly, the error in the procedure is minimized if $C_{T_{MAX}}$ is large. In practice the sensitivity of the ground run distance to $\left(\frac{T_{STATIC}}{T_{REF}}\right)$ is quite low since the effect of acceleration changes over the first part of the ground run is also low.

Stopping Distance Calculation

The stopping calculation consists of two segments,

- The transition segment from a condition with all engines operating to a condition with reverse thrust, brakes on and spoilers up, and
- The stopping segment from the end of transition to full stop.

The deceleration during transition is based on a linear interpolation between the two end points. The values of lift and drag at the end of transition are evaluated at $C_T = 0$ for a powered lift airplane. These values are then used during the stopping segment. If thrust reversers are used, the reverser effectiveness and number of engines used are applied directly to the specified reference thrust-to-weight ratio to calculate the reverser retarding force, regardless of whether the airplane is conventional or of the powered lift type.

Flare Calculation Method

The flare calculation is basically the integration of the longitudinal and vertical equations of motion for a specified input pitch time history from the point of rotation to the clearance of a 35 foot obstacle. The gear representation is simple, consisting of a linear spring with specified stroke from taxi position, and specified preload at maximum extension. The point of lift-off occurs when the gear load becomes zero or equal to the preload.

Although the initial pitch history is specified, the computational routine has four optional features that essentially eliminate the sensitivity of the takeoff calculation to these specifications. These options are:

- A load factor limitation that enables the user to specify n_{max} during the flare; this value will not be exceeded.
- A velocity feedback system that either prevents the airplane from losing any significant amount of speed or allows a specified speed loss between lift-off and V_2. This is

accomplished by automatic modification of the pitch profile when low longitudinal accelerations are registered. The procedure is designed to simulate typical pilot reactions observed from flight testing, and appears to work quite well.

- The input pitch profile is used directly for the all engines operating flare calculation, however, for the engine out flare, a reduction factor may be input that results in a proportionate reduction in attitude versus time, i.e., $\theta_{OEI} = (1\text{-THK})\,\theta_{AEO}$ where THK is an empirical factor. Typical flight test data shows a conservatism on the part of the pilot when he encounters an engine failure condition. This generally results in a pitch rate reduction of 20 percent to 30 percent which may be simulated by the appropriate choice of THK.

- An optimizing routine is available that will generate the flare procedure that minimizes the flare distance within the constraints of a maximum pitch rate, acceleration, lift-off attitude and attitude at 35 feet.

Ground Effect Calculation

The program user has the option of either specifying the ground effect on lift and drag, or he may elect to use the ground effect subroutine. This routine calculates the changes in lift and drag over a specified range of ground heights. The theory is applicable to either conventional or powered lift airplanes.

The takeoff program was used on the 737-200 airplane to obtain comparison with flight test results. The agreement is quite close both in terms of general level and also variation in flare technique.

5.2 LANDING RULES AND PROCEDURE

Landing approach speeds are calculated using the following set of rules:

Sea Level, Standard Day

Dry Runway

35 Ft. Obstacle

1.10 Flare Load Factor

3 Ft/Sec. Touchdown Sink Rate

6° Glide Slope

.6 Field Length Safety Factor

1.0 Sec. Coast Time

.35 g Deceleration

The sensitivity to variations in flare load factor and coast time in terms of F.A.R. field length and approach speed is shown on Figure 18.

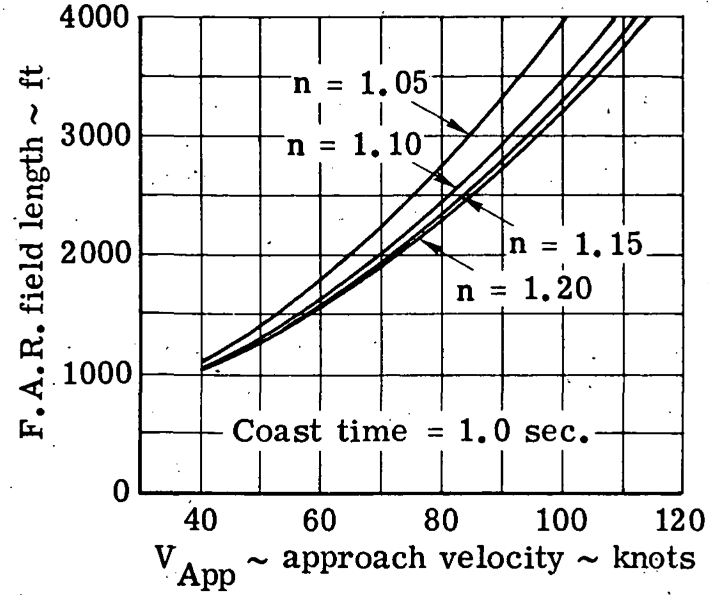

(a) Effect of flare load factor

Sea level, standard day
Obstacle = 35 feet
Ground roll deceleration = 0.35g
F.A.R. field length factor = 0.6
$\gamma = -6^{o}$
$(R/S)_{Touchdown}$ = 3 ft/sec

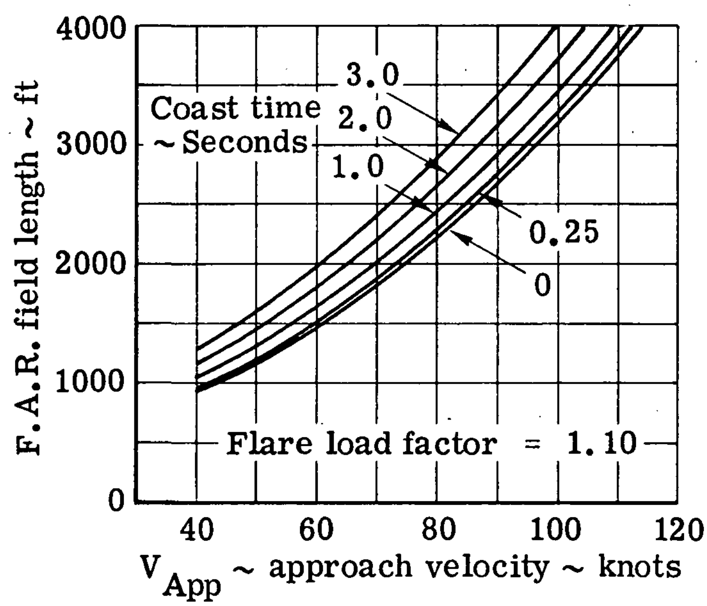

(b) Effect of coast time

Figure 18 Landing rules sensitivity

The MF configuration landing approach speed margin is 1.3 V_S. The EBF configuration landing approach margins and go-around procedures are discussed in the following paragraphs.

EBF configuration gradient and margin rules are listed in Table 2. Since wind tunnel data were used in the computer program, the lift margin rules are equivalent to a 1.3 V_S safety margin. In other words it is assumed that:

$$\left[\left(\frac{C_{L_{V_{MIN}}}}{C_{L_{APP}}} - 1\right) \geqslant .44\right]_{\substack{\text{Wind}\\\text{Tunnel}}} = \left[\left(\frac{C_{L_{V_{MIN}}}}{C_{L_{APP}}} - 1\right) \geqslant .69\right]_{\substack{\text{Full}\\\text{Scale}\\\text{F.A.R.}}}$$

TABLE 2 LANDING GRADIENT AND MARGIN RULES

Rule	Flap Setting	Flight Phase	Velocity	Power Setting	No. of Eng. Operating	Conditions to be met
1	Approach	Landing (Gear down)	V_{APP}	Approach	All	$[\alpha_s - \alpha_{App}] \geq 15°$
2	Approach	Landing (Gear down)	V_{APP}	Approach	One out	$[\alpha_s - \alpha_{App}] \geq 10°$
3	Approach	Balked landing (Gear down)	V_{APP}	Max	All	$[(C_{L_S}/C_{L_{APP}}) - 1] \geq .44$* Gradient $\geq .032$
4	Approach	Balked landing (Gear down)	V_{APP}	Max	One out	$[(C_{L_S}/C_{L_{APP}}) - 1] \geq .30$* $\gamma \geq 0°$
5	Go-around	Balked landing (Gear up)	V_{APP}	Max	One out	$[(C_{L_S}/C_{L_{APP}}) - 1] \geq .25$* or $[\alpha_s - \alpha_{APP}] \geq 10°$ Gradient $\geq .027$

*Based on wind tunnel data

This represents a 17 percent improvement in maximum lift capability from "1g" wind tunnel to flight test F.A.R. stall. The 17 percent is made up of an assumed seven percent improvement in "1g" stall $C_{L_{max}}$ wind tunnel to "1g" $C_{L_{max}}$ flight test and 10 percent improvement from "1g" flight test to F.A.R. stall. This reasoning also applies to the listed engine out "g" margins. The gradient rules are from Reference 16. As an additional check for safety, $\Delta\alpha$ margins are monitored in the gradient and margin computer program. The $\Delta\alpha$ margins (Rules 1 and 2) of Table 2 are intended to provide vertical gust protection equivalent to current commercial transports.

Reference 17 contains calibration information for the propulsion system simulators used on the EBF configuration wind tunnel model. Calibration results indicate that the secondary weight flow induced through the ejector inlet by the primary nozzles is only about one-half as high as a full scale engine with the same bypass ratio at a typical STOL takeoff airspeed. This means that the wind tunnel data contains only one-half the ram drag. Therefore, one-half the TF39-1A ram drag was added to account for this.

The gradient and margin computer program calculates the maximum allowable C_L's and the required approach T/W's to meet specified "g" margins from stall and climb gradient requirements, respectively. The allowable approach C_L is computed for the range of T/W's used in the margin and gradient calculation. For a conventional airplane these numbers would not be a function of T/W. The required approach T/W's are computed at C_L's used in the margin and gradient calculation.

The procedure for determining the approach speed and required T/W for each approach flap setting considered is shown on Figure 19. The limiting approach C_L is described by the most critical angle of attack margin ($\Delta\alpha$) or acceleration margin (Δg) between an approach flight path angle and a go-around climb gradient for all engines or engine out, at the approach flap setting (Rules 1, 3, 2 or 4, respectively, in Table 2). If the all engine condition is critical (which has been the case for all EBF configuration flap settings considered in this study), then the C_L which corresponds to the most critical margin between $\Delta\alpha$ and Δg (Rule 1 or 3) is the limiting approach C_L. For the EBF configuration the $\Delta\alpha = 15^\circ$ requirement at approach power setting (Rule 1) has consistently been more critical than Δg = .44 at maximum thrust, therefore, it has defined the approach speed.

The design thrust to weight ratio (T/W) could be defined by the greater of:

1)	gradient	=	.032 all engine	approach flap setting
2)	gradient	=	0 one engine out	approach flap setting
3)	gradient	=	.027 one engine out	approach flap setting
4)	gradient	=	.027 one engine out	go-around flap setting

at the limiting C_L defined above (shown as points A, B, C and D, respectively, on Figure 19). The design T/W is always critical for Condition 2 or 4.

During the initial phase of the study Rule 4 from Table 2 contained a requirement to meet Condition 3 from above. For the EBF configuration being studied the T/W required to climb with a gradient of .027, engine out, at the approach flap setting would always be critical. With this in mind, the decision was made to allow a configuration change to a lower flap setting in the event that an engine out go-around is necessary. This procedure resulted in Condition 2 from above being critical for assumed approach flap settings above 30 degrees. For assumed approach flap settings less than 30 degrees, Condition 4 was critical.

The calculations are made for various flap angles and wing loadings. The results identify the optimum flap angles and corresponding minimum operating speeds for a specified configuration.

The development of actual EBF configuration wing loadings and design T/W's are contained in Appendix C.

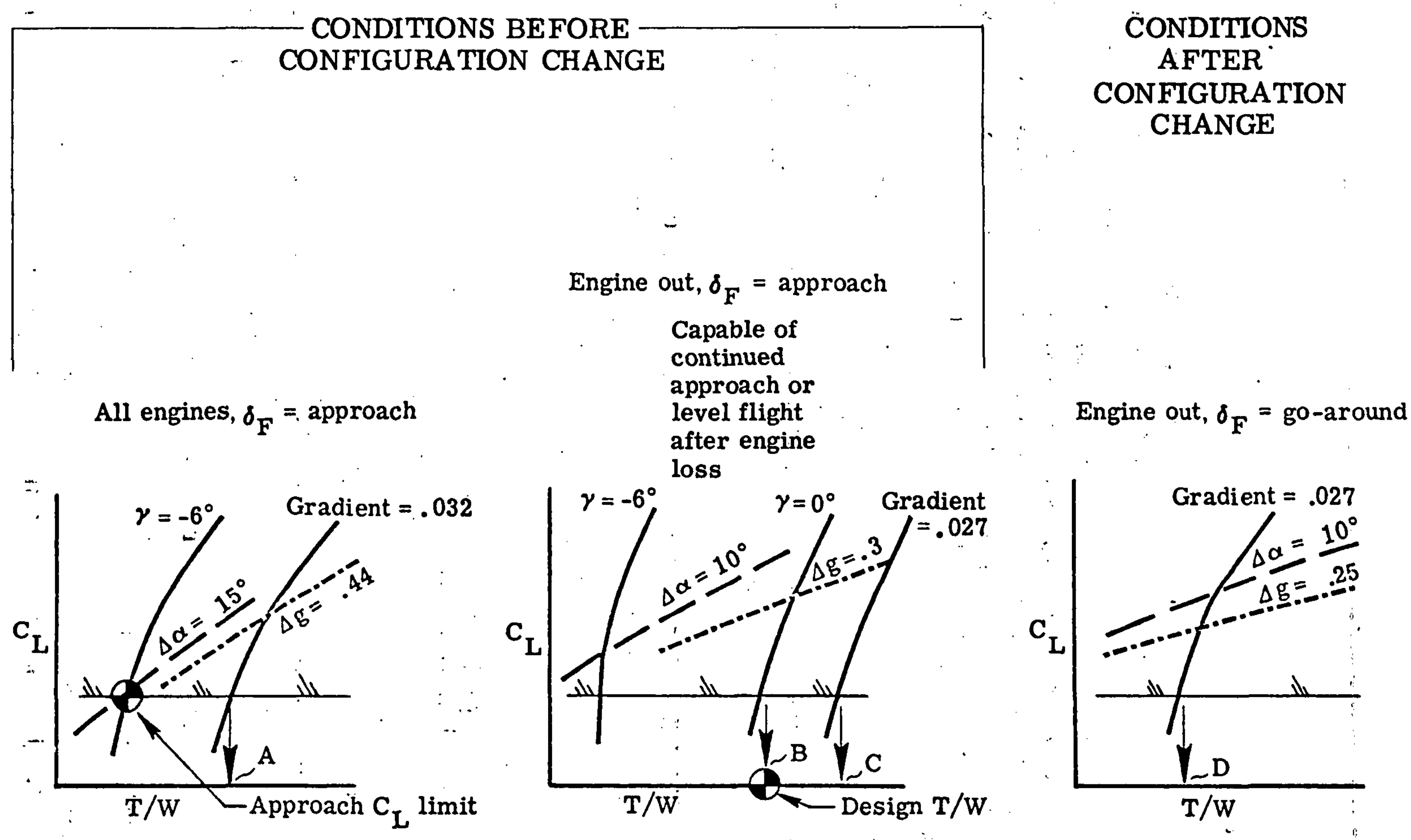

Figure 19 Powered lift approach analysis procedure

6.0 VERTICAL TAIL SIZING

Vertical tail sizes were determined considering:

(1) Ground minimum control speed requirement, (V_{MCG})
(2) Static and dynamic directional stability requirements
(3) Crosswind landing requirement

Figure 20 schematically illustrates the vertical tail area requirements as a function of the critical engine moment arm. For multi-engine aircraft with wing-mounted engines, the minimum critical engine moment arm is usually limited by providing adequate clearance between engines or between engine and fuselage to minimize interference effects which would penalize cruise performance. The maximum allowable vertical tail area is dictated by the crosswind requirement. A small vertical tail usually improves the crosswind landing capability because of the directionally unstable wing-body combination which provides a favorable yawing moment. The minimum vertical tail size is determined from the ground minimum control speed requirement and/or static and dynamic stability requirements.

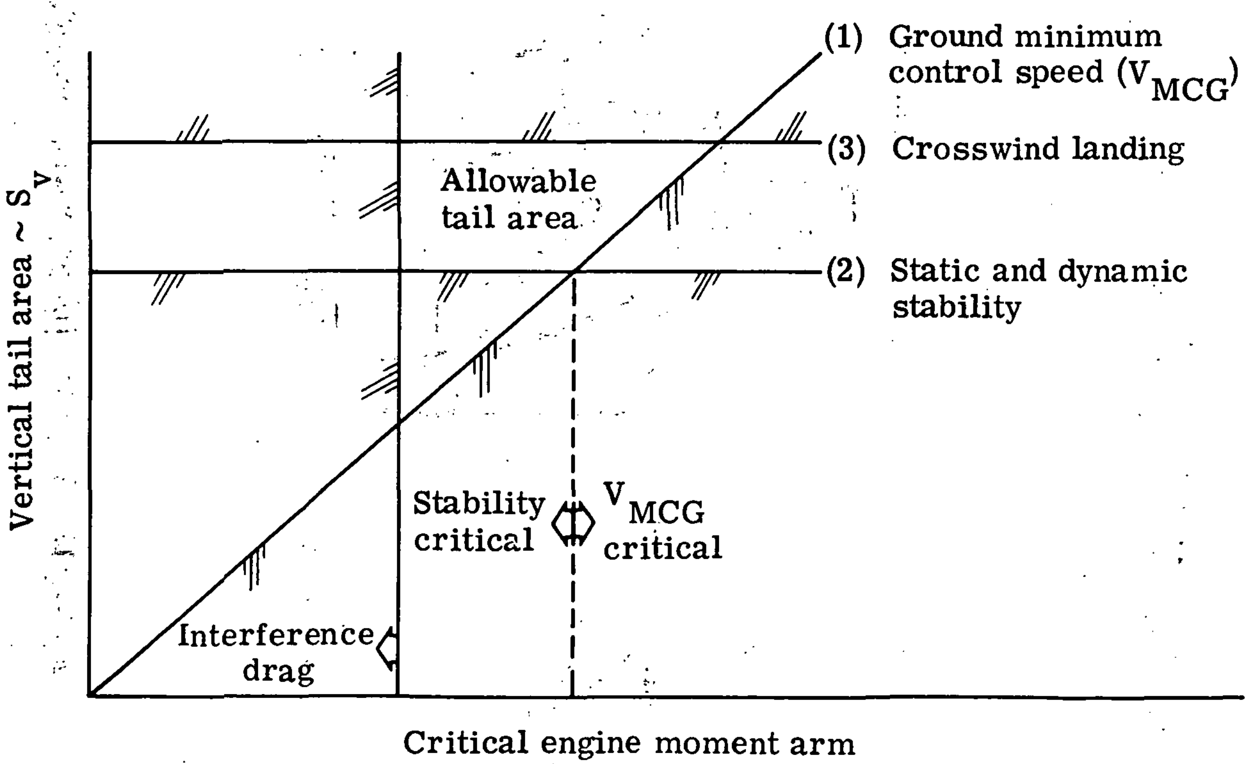

Figure 20 Vertical tail sizing

Ground Minimum Control Speed Requirement

During the takeoff run it must be possible to maintain control of the aircraft following a sudden loss of thrust on the most critical engine. If the critical engine fails prior to reaching the ground minimum control speed (V_{MCG}), the takeoff must be aborted. If the critical engine fails at or above V_{MCG}, the aircraft must have adequate aerodynamic control power to continue the ground roll with takeoff thrust on the remaining engines. A maximum deviation of 25 feet from the intended ground roll path is allowed following an engine failure. No credit is allowed for nose wheel steering.

Sizing the vertical tail to allow a 25 foot deviation from the runway centerline allows the most critical engine to fail prior to a speed at which the rudder controls can statically balance the engine out yawing moment. If the takeoff run is continued following an engine failure, the speed continues to increase as the aircraft departs from its originally intended flight path. Prior to reaching the maximum allowed 25 foot deviation from the intended ground path, the speed has increased and at this speed the rudder control must be able to overcome the engine out yawing moment. The aircraft is then able to return to its originally intended flight path without exceeding the 25 foot allowed deviation. This vertical tail sizing method (besides being cumbersome to solve because the airplane dynamics are involved) gives a V_{MCG} which is less than a static analysis in which the rudder yaw moment exactly balances the engine out yaw moment.

For this study the vertical tail area required to satisfy the ground minimum control speed requirement was determined from a static balance of engine out yaw moment and rudder yaw moment at the takeoff decision speed V_1. The V_1 speed is the maximum allowable V_{MCG} speed.

The ratio of vertical tail area to wing area required to statically balance the engine out yaw moment using only rudder control is given by:

$$\frac{S_V}{S} = \frac{295 \left(\frac{T}{NW}\right)\left(\frac{Ye}{\ell_V}\right) \frac{W}{S}}{C_{L_V} \; V_1^2}$$

Because of the low speeds at which STOL aircraft operate, the critical engine moment arm must be kept small if reasonable sized vertical tails with conventional aerodynamic controls are used.

Also of importance is the amount of usable vertical tail lift coefficient which can be generated by the rudder. The lift coefficient is determined primarily by the size of the rudder and the complexity of the rudder or a high lift system, i.e., simple flap control, double articulated flap control, blown surface, etc.

Static and Dynamic Directional Stability Requirements

The static directional stability derivative C_{n_β} (weathercock stability) does not have an explicit required value; however, when the aircraft is in a sideslip relative to its flight path, the yawing moment produced must tend to restore the aircraft to symmetric flight. In terms of rudder required to sideslip the aircraft, right rudder pedal deflection and force must produce left sideslip and left rudder pedal deflection and force must produce right sideslip.

The total airplane weathercock stability is composed of the wing-body contribution (usually unstable) and the vertical tail contribution (stable) or

$$C_{n_\beta} = C_{n_{\beta_{WB}}} + C_{n_{\beta_V}}$$

The wing-body contribution ($C_{n_{\beta_{WB}}}$) is primarily a function of the body volume coefficient $\frac{S_B \ell_B}{S\,b}$ and was estimated using data from the Boeing family of airplanes.

The vertical tail contribution ($C_{n_{\beta_V}}$) is estimated by

$$C_{n_{\beta_V}} = a_V \left(\frac{S_V}{S}\right)\left(\frac{\ell_V}{b}\right)\left(1 - \frac{d\sigma}{d\beta}\right)$$

The sidewash factor is difficult to estimate and wind tunnel tests are required to determine the value. In general, sidewash factors are favorable and tend to increase the level of directional stability above the value predicted if the effect is neglected.

For this study the sidewash factor was neglected, therefore, the static directional stability level should be conservative.

The complete three degree-of-freedom equations for determing the dynamic stability are complicated for the basic airframe and more complex when an automatic damping system is added. In order to determine the vertical tail area required to provide the aircraft with satisfactory dynamic stability characteristics (reasonable restoring accelerations) in this preliminary design study, a simplified approach was used. The Dutch roll natural frequency can be approximated by

$$\omega_{n\ DR}^{2} = \frac{C_{n_\beta}\, q\ S\ b}{I_{zz}}$$

If more than one aircraft is being studied or evaluated, all aircraft can be designed to have the same basic Dutch roll natural frequency if:

$$\frac{C_{n_{\beta x}}}{C_{n_{\beta o}}} = \left(\frac{I_{zz_x}}{I_{zz_o}}\right)\left(\frac{S_o}{S_x}\right)\left(\frac{b_o}{b_x}\right)\left(\frac{V_{e_o}}{V_{e_x}}\right)^2$$

The subscript "o" indicates the values of a baseline aircraft and the subscript "x" indicates the values of any other aircraft. The weathercock stability derivative C_{n_β} is a function of S_V/S. Therefore, the vertical tail area to wing area ratio $(S_V/S)_x$ required to give the aircraft in question the same Dutch roll natural frequency (same restoring acceleration due to sideslip) as the baseline aircraft can be determined.

The baseline aircraft used for this study was the 3,500 foot field length, 150 passenger aircraft, since it is a more conventional type aircraft. An estimate of the Dutch roll natural frequency at the maximum gross weight and lift-off speed gives $\omega_{n_{DR}}$ = .37 rad/sec with C_{n_β} = .001/deg. The

Reference 19 STOL study required $\omega_{n_{DR}}$ to be $\geq$ .4 rad/sec. A study comparing the validity of the approximation to the Dutch roll natural frequency was made (Reference 20) and showed that for small values of $\omega_{n_{DR}}$ the approximate solution could be anywhere from 12 percent to 25 percent below the exact solution. It is anticipated that C_{n_β} = .001/deg for the 3,500 foot field length aircraft will exceed the minimum Dutch roll natural frequency requirement of .4 rad/sec as specified in Reference 19.

Crosswind Landing Requirement

A requirement of this study was that the airplane must have sufficient directional control power to hold a constant ground track in a 25 knot 90 degree crosswind at the approach speed. If the yaw moment due to lateral control required to balance the roll moment is assumed to be zero, the rudder generated lift coefficient on the vertical tail required to exactly balance the weathercock yaw moment ($C_{n_\beta} \beta_{\text{cross wind}}$) can be expressed as:

$$C_{L_V} = \frac{\left[C_{n_{\beta\,\text{wing body}}} + a_V \dfrac{S_V \ell_V}{S b}\right] \left[\sin^{-1}\left(\dfrac{V_{cw}}{V_e}\right) - \delta_{crab}\right]}{\dfrac{S_V \ell_V}{S\ b}}$$

The procedure used in checking the crosswind landing capability was to use the vertical tail to wing area ratio (S_V/S) required to provide the aircraft with adequate engine out directional control and/or directional stability and see if the resulting tail lift coefficient required for crosswind landing is less than that required for engine out control.

The rudder directional control required for crosswind landing is significantly influenced by the type of lateral control used on the aircraft. Aircraft with large amounts of dihedral effect (negative C_{ℓ_β}) using spoiler lateral control devices require larger amounts of rudder control than aircraft with aileron controls. The drag associated with spoiler control requirements in a crosswind landing is in opposition to the aircraft yaw moment produced by the rudder. The vertical tail lift coefficient requirement for engine out control was compared to that required for the crosswind landing.

6.1 MECHANICAL FLAP CONFIGURATION VERTICAL TAIL SIZE

A trade study of the vertical tail area to wing area ratio for the 150 passenger aircraft was made as a function of the field length requirements for various levels of vertical tail lift coefficient (ground minimum control speed requirement) and weathercock stability (dynamic stability requirement). The data are shown in Figure 21. The vertical tail has been sized for dynamic stability. The amount of rudder generated vertical tail lift coefficient for the engine out control requirement with the vertical tail sized for dynamic stability is less than the design limit ($C_{L_V} \leq 1.0$).

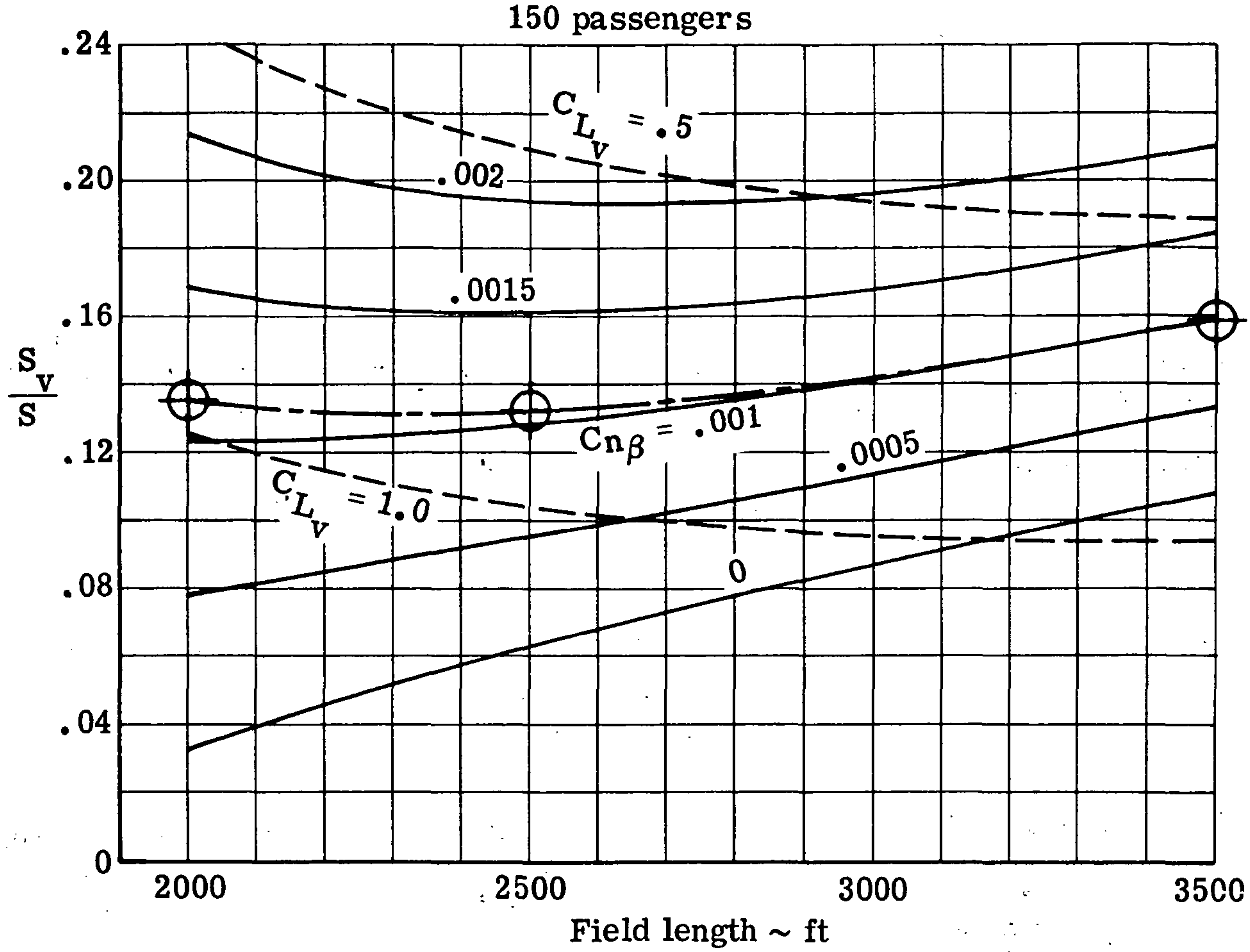

Note: Nominal vertical tail arm ℓ_V = 660 in.

– – – – Engine out control ~ V_{MCG}

——— Weathercock stability

—— - —— Dynamic stability

⊕ Required tail area ratio for nominal tail arm

Figure 21 MF configuration vertical tail sizing

Figure 22 shows the vertical tail lift coefficient which must be generated by the rudder to meet the engine out requirement or the 25 knot crosswind requirement. The engine out requirement is critical. The vertical tail lift coefficient required for the 25 knot crosswind capability (no lateral control yaw moment) is significantly less than the engine out requirement. Rudder authority is expected to be adequate for the crosswind landing with a spoiler type lateral control system used in conjunction with an aileron located in the "cut out" region behind the wing mounted nacelles. A summary of the vertical tail size requirements as a function of the field length for the 150 passenger airplane is shown in Table 3. A nominal vertical tail arm of 660 inches was assumed.

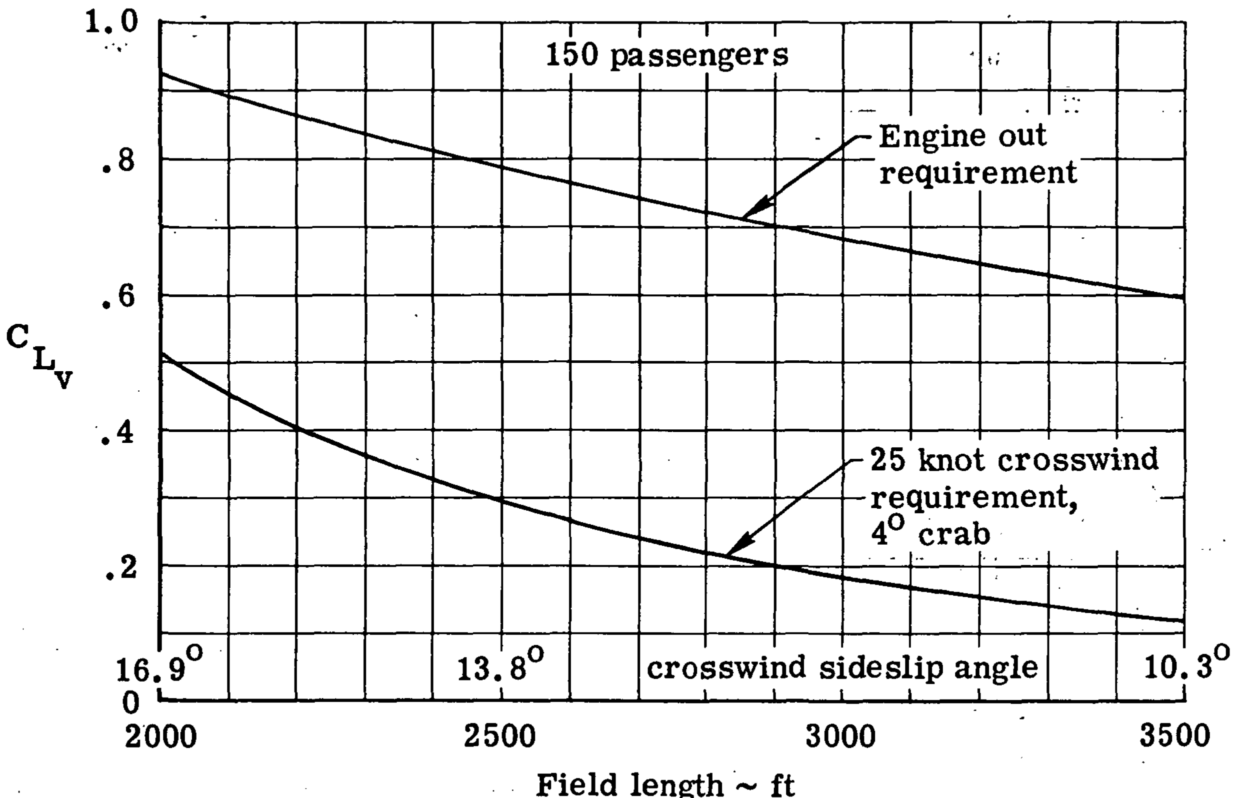

Notes:

C_{L_V} ~ vertical tail lift coefficient which must be generated by the rudder

Nominal vertical tail arm ℓ_V = 660 in.

Vertical tail sized for dynamic stability

Figure 22 MF configuration crosswind capability

The nominal tail arm used for the vertical tail sizing trade study (Figure 21) required adjustments for weight and balance considerations and scaling for the 40 and 300 passenger aircraft. Figure 23 shows the influence of changing the tail arm parameter $\frac{\ell_V}{b/2}$ on the vertical tail area ratio (S_V/S) for the stability critical mechanical flap configuration. Figure 23 was used to finalize the tail size for the 150 passenger aircraft and to size the vertical tails for the 40 and 300 passenger aircraft.

TABLE 3
NOMINAL VERTICAL TAIL SIZE, 150 PASSENGER, MF CONFIGURATION

Field Length Feet	2000	2500	3500
Vertical tail area ratio S_V/S	.136	.133	.158
Usable lift coefficient which must be generated by the rudder	.925	.79	.595

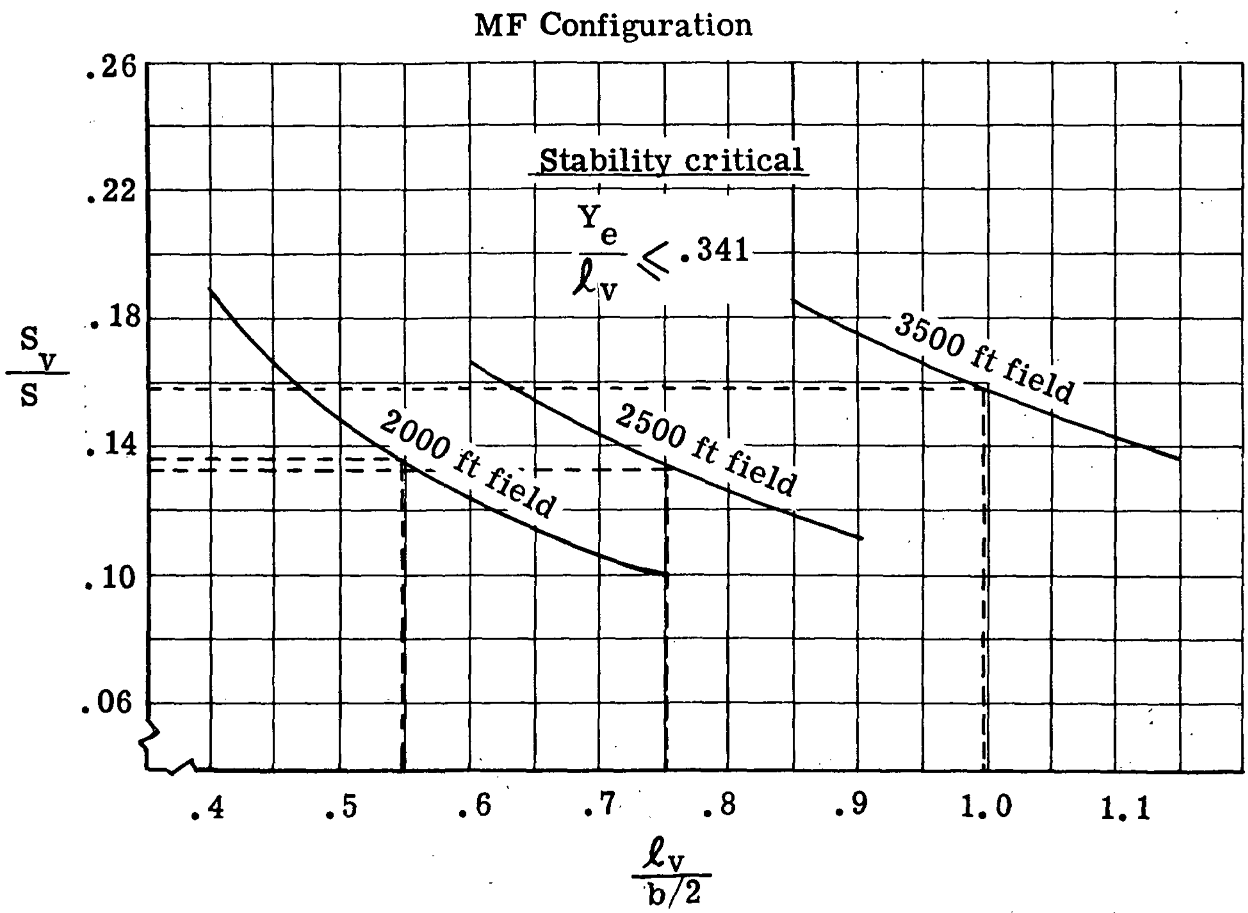

Note: Dashed lines represent basic 150 passenger airplane with nominal vertical tail arm 660 in.

Figure 23. Effect of vertical tail arm parameter $\frac{\ell_v}{b/2}$ on vertical tail size (Sv/S)

6.2 EXTERNALLY BLOWN FLAP CONFIGURATION VERTICAL TAIL SIZE

Figure 24 shows results of a trade study of the vertical tail area to wing area ratio for the 150 passenger aircraft. Vertical tail lift coefficient (ground minimum control speed requirement), weathercock stability and dynamic stability requirements were considered.

Two takeoff thrust-to-weight ratios were considered:

- *Design thrust-to-weight*
- Reduced thrust-to-weight to match takeoff field length requirements

The EBF configuration thrust required is critical for engine out go-around. If this design thrust is used for takeoff the resulting field length is less than the design field length. An excessive vertical tail size is required for engine out control on the 2,000 ft. and 2,500 ft. field length aircraft. The vertical tail area to wing area ratios for the 2,000 ft. and 2,500 ft. field length aircraft are .361 and .225 respectively for a usable vertical tail lift coefficient of 1.0. As a result, a partial power takeoff was considered with a thrust-to-weight ratio which would produce a field length equal to the design field length. The vertical tail size requirements for the 2,000 ft. and 2,500 ft. field length aircraft were significantly reduced (vertical tail area to wing area ratios of .222 and .158 respectively). The 3,500 ft. field length aircraft is stability critical for either thrust-to-weight ratio considered.

Figure 25 shows the vertical tail lift coefficient which must be generated by the rudder to meet the engine out requirement or the 25 knot crosswind requirement. These data assume the vertical tail has been sized for the reduced thrust takeoff. As for the MF configuration, the vertical tail lift coefficient required for the EBF configuration in a 25 knot crosswind (no lateral control yaw moment) is much less than the engine out requirement. Rudder authority is expected to be adequate for the crosswind landing with a spoiler type lateral control system used in conjunction with an aileron located outboard of the outer flap section. A summary of the vertical tail size requirements as a function of the field length for the 150 passenger airplane (nominal tail arm of 660 in.) is shown in Table 4.

TABLE 4

NOMINAL VERTICAL TAIL SIZE, 150 PASSENGER, EBF CONFIGURATION

Field length	2,000	2,500	3,500
Vertical tail area ratio S_V/S	.222	.158	.162
Usable lift coefficient which must be generated by the rudder	1.0	1.0	.732
	V_{MCG} Critical		Stability Critical

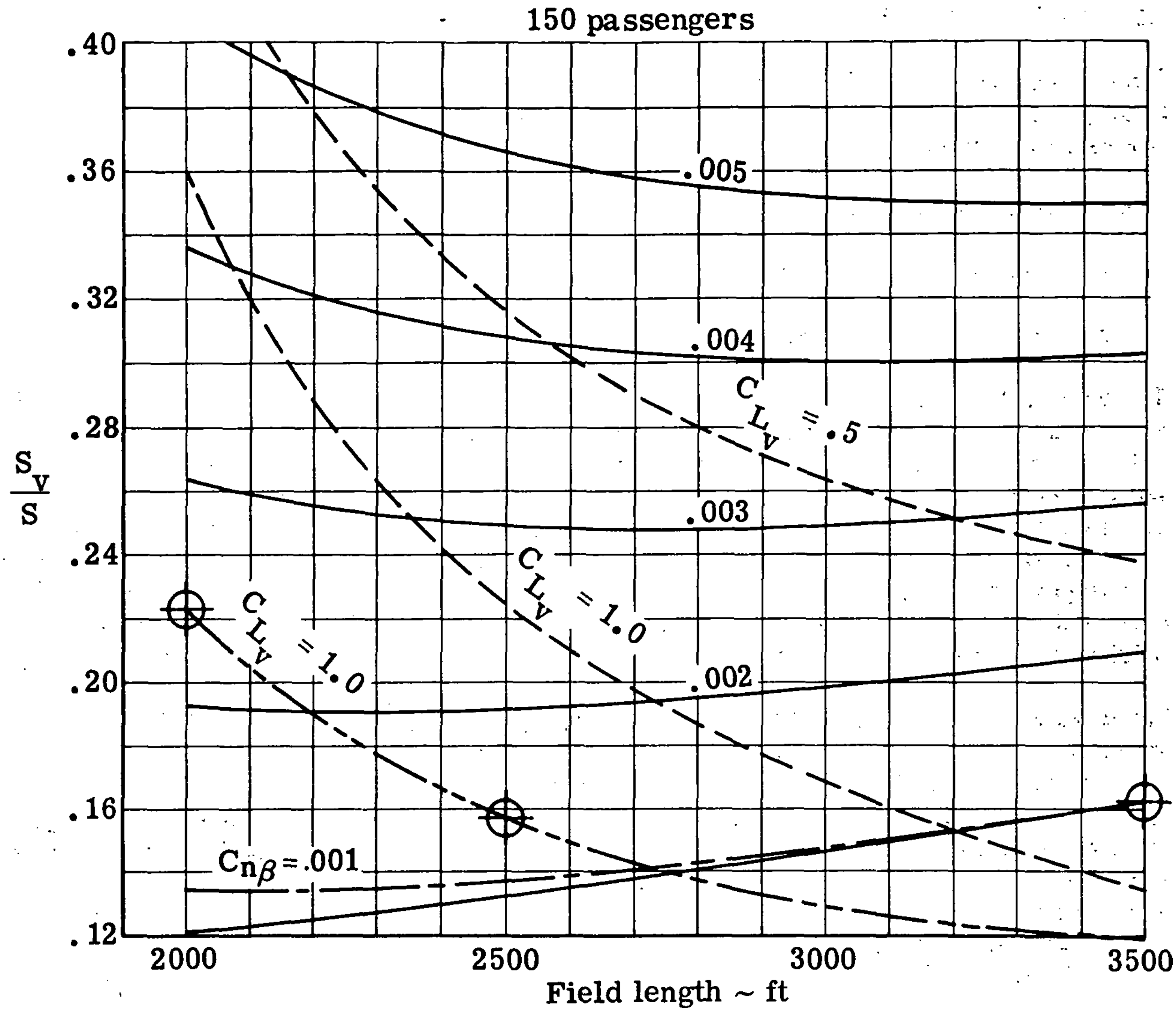

Note: Nominal vertical tail arm ℓ_v = 660 in.

— — — — Engine out control ~ V_{MCG}, max design T/W

———— Weathercock stability

—— - —— Dynamic stability

—— - - - —— Engine out control ~ V_{MCG}, design T/W reduced for design field length

⊕ Required tail area ratio for nominal tail arm

Figure 24 EBF configuration vertical tail sizing

150 passengers

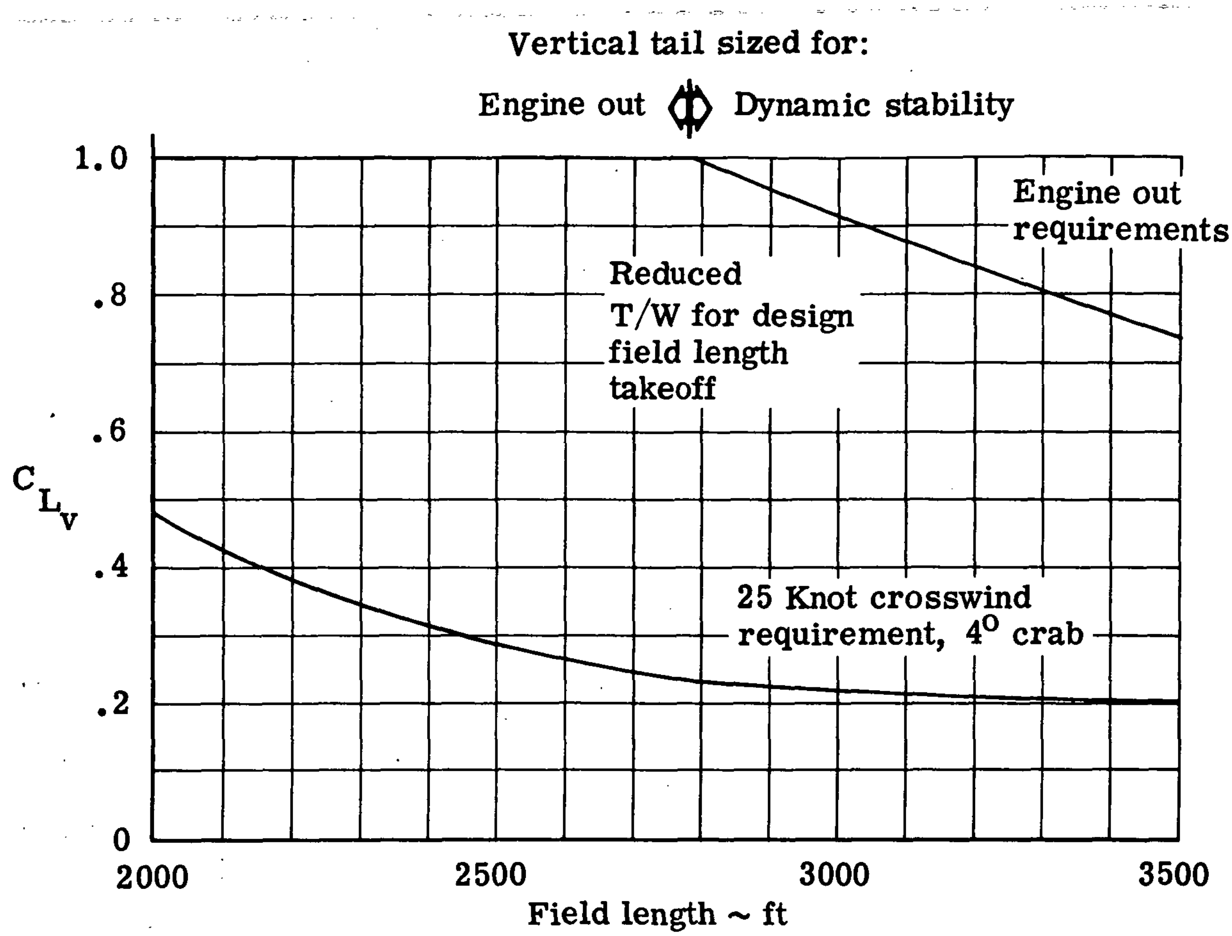

C_{L_V} ~ Vertical tail lift coefficient which must be generated by the rudder

Nominal vertical tail arm ℓ_V = 660 in.

Figure 25 EBF configuration crosswind capability

The nominal tail arm (ℓ_V = 660 in.) used for the vertical tail sizing trade study (Figure 24) required adjustments for weight and balance considerations and for the 40 and 300 passenger aircraft. Figure 26 shows the influence of changing the tail arm parameter $\frac{\ell_V}{b/2}$ on the vertical tail area ratio S_V/S for the engine out critical and stability critical EBF configurations. Figure 26 was used to finalize the tail size for the 150 passenger aircraft and to size the vertical tails for the 40 and 300 passenger aircraft.

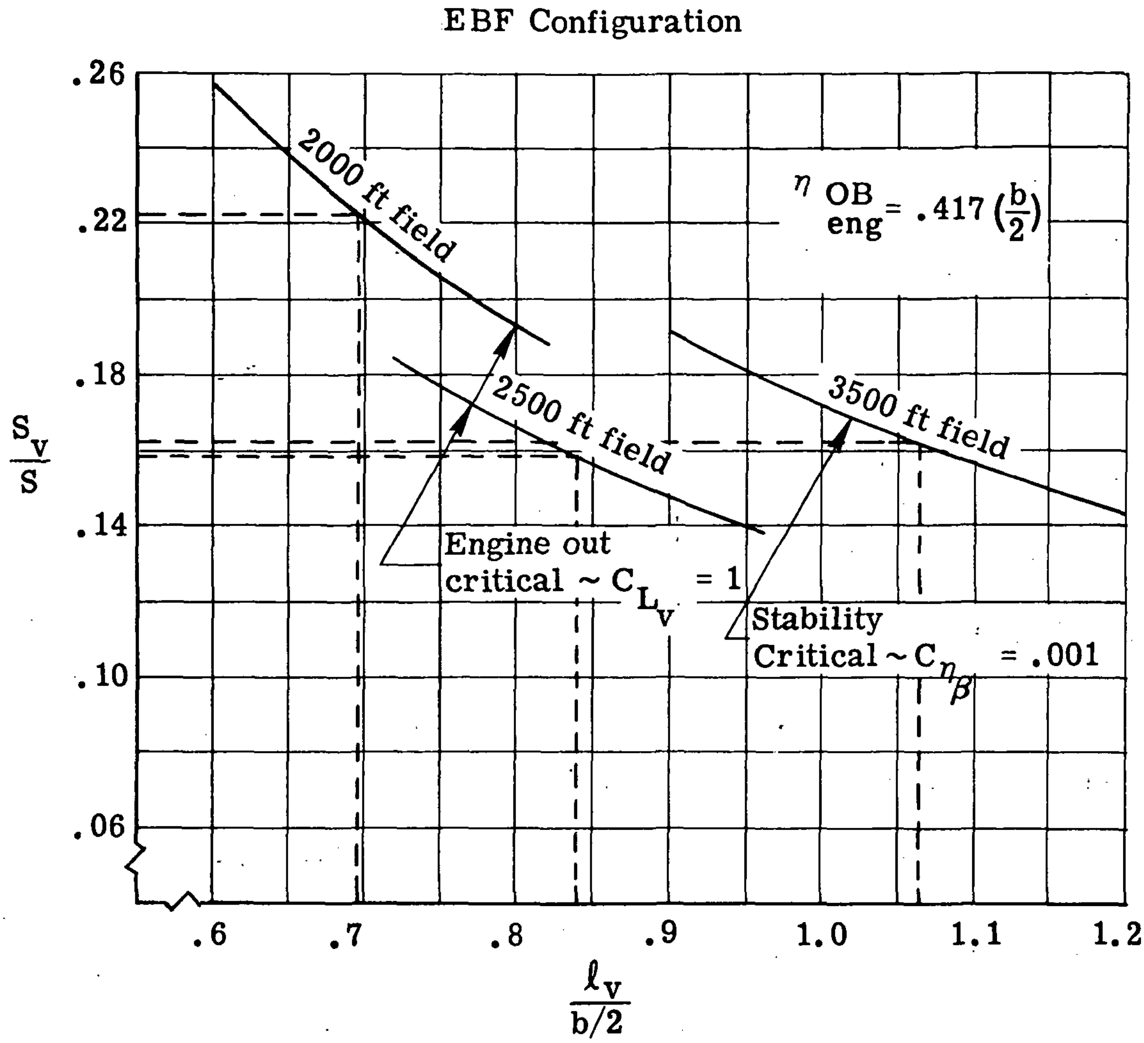

Note: Dashed lines represent basic 150 passenger airplane with nominal vertical tail arm 660 in.

Figure 26. Effect of vertical tail arm parameter $(\frac{\ell_v}{b/2})$ on vertical tail size (S_v/S)

Page intentionally left blank

7.0 HORIZONTAL TAIL SIZING

Horizontal tail sizes were determined by:

1. Sufficient static longitudinal stability.
2. Adequate nose wheel steering.
3. The ability to rotate the aircraft to takeoff attitude at the rotation speed.
4. The ability to trim the aircraft at the approach speed.
5. Usable CG range which encompasses the variations in CG which occur due to fuel usage or passenger loading.

Items 1 or 2 determine the aft CG limit while Items 3 or 4 determine the forward CG limit. Item 5 is the difference in the forward and aft CG limits as determined by the critical Items 1 through 4. Figure 27 schematically illustrates the horizontal tail area requirements as a function of CG position. The optimum tail area for a required CG range is achieved by varying the wing position until a location is found in which the forward and aft aerodynamic CG limits just encompass the forward and aft weight and balance loading limits.

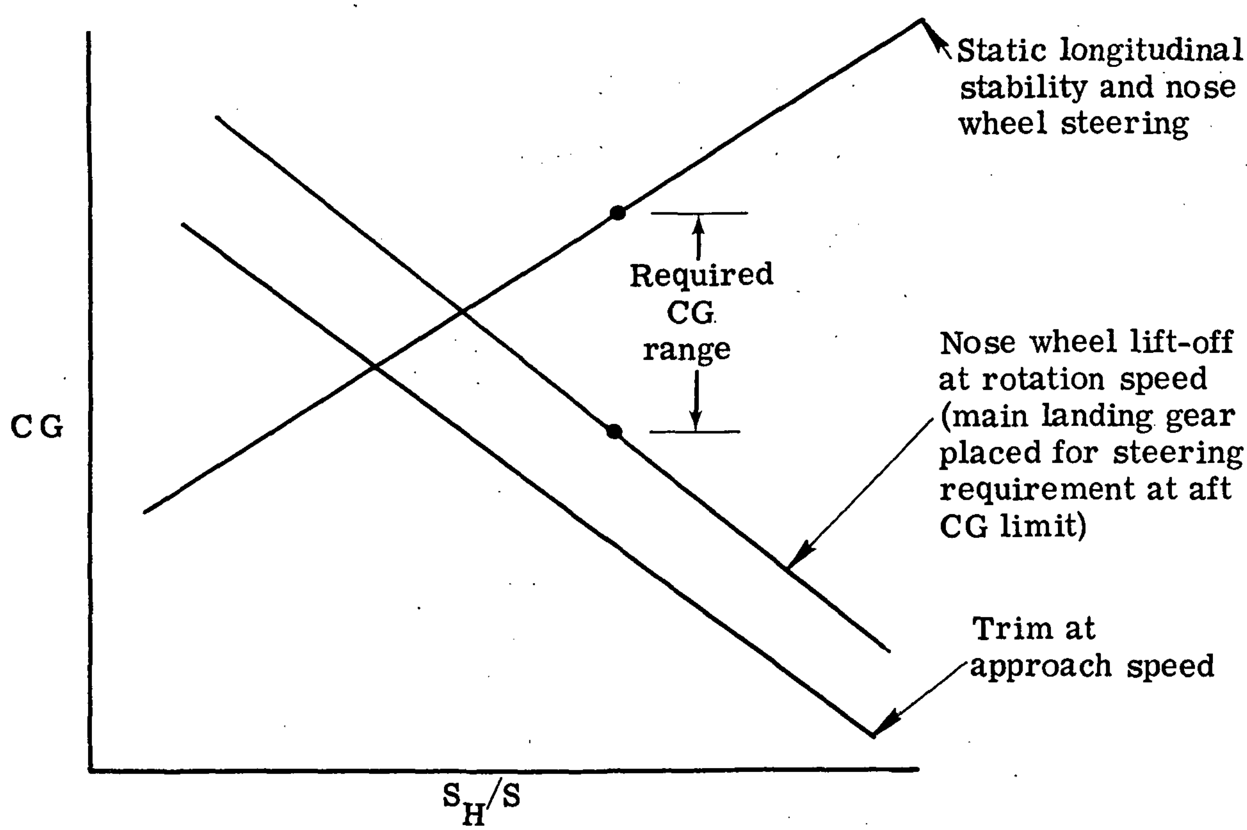

Figure 27 Horizontal tail sizing schematic

Static Longitudinal Stability

The static longitudinal stability criteria chosen for this study was to provide the aircraft with a three percent static stability margin when flying with the CG on the aft limit. The horizontal tail area to wing area ratio (S_H/S) required to provide the aircraft with neutral static stability ($dC_m/dC_L = 0$) was computed by:

$$\frac{S_H}{S} = \frac{\left(\frac{X_{CG}}{\bar{c}} - \frac{X_{AC_{WB}}}{\bar{c}}\right)}{\frac{a_H}{a_{WB}}\left(1 - \frac{d\epsilon}{d\alpha}\right)\left(\frac{\ell_H}{\bar{c}} + .25 - \frac{X_{CG}}{\bar{c}}\right)}$$

The horizontal tail area to wing area ratio required for a three percent static margin is then obtained by limiting the CG position three percent ahead of the values used in the equation above.

Nose Wheel Steering

When the aft CG limit as a function of the horizontal tail area to wing area ratio has been determined which will satisfy the static longitudinal requirements, the nose wheel steering requirement can be satisfied by proper placement of the main landing gear. With the CG at the aft limit for the static stability requirement, the main landing gear can be located so that adequate nose wheel steering is available for the aircraft considering power on and off effects. If the effective thrust line is located below the CG, nose wheel lightening can occur at low gross weights and high thrust applications. This type of design requires a larger margin between the aft CG and the main landing gear than a design with the thrust line located above the CG.

Using this technique forces the aft CG limit to simultaneously satisfy the static longitudinal stability requirement and the nose wheel steering requirement. The main landing gear were placed so the loading on the nose wheel was always greater or equal to five percent of the total zero velocity gear load. This is comparable to the gear load distribution on Boeing commercial aircraft. The horizontal tail area which will satisfy forward CG limit criteria can now be determined.

Nose Wheel Lift Off Requirement

When the rotation speed is reached during the takeoff ground roll it must be possible to rotate the aircraft to takeoff attitude at the most forward CG location and with the takeoff power setting. The horizontal tail area to wing area ratio (S_H/S) required to rotate the aircraft about the main gear was determined as follows:

$$\frac{S_H}{S} = \frac{\left(\frac{W/S}{q} - C_{L_{WB}}\right)\left(\frac{X_{MG}}{\bar{c}} - \frac{X_{CG}}{\bar{c}}\right) + C_{L_{WB}}\left(\frac{X_{AC_{WB}}}{\bar{c}} - \frac{X_{CG}}{\bar{c}}\right) - C_{m_{O_{WB}}} - \frac{1}{q}\left(\frac{T}{W}\right)\left(\frac{W}{S}\right)\frac{Z_T}{\bar{c}}}{C_{L_H}\left(\frac{X_{MG}}{\bar{c}} - \frac{\ell_H}{\bar{c}} - .25\right)}$$

Trim at the Approach Speed

At the landing approach speed and in the landing configuration it must be possible to trim the aircraft with the stabilizer only (no elevator control). The horizontal tail area to wing area ratio required to trim the landing approach was determined by the following equation:

$$\frac{S_H}{S} = \frac{C_{mo_{WB}} + \frac{W}{qS}\left(X_{CG} - X_{AC_{WB}}\right)}{C_{L_H}\left(\frac{\ell_H}{\bar{c}} + .25 - X_{AC_{WB}}\right)}$$

7.1 MECHANICAL FLAP CONFIGURATION HORIZONTAL TAIL SIZE

Horizontal tail sizing for the 150 passenger 2,500 foot field length airplane is shown in Figure 28. The CG travel from the aircraft fully loaded to empty varies from 32 percent MAC to 36.5 percent MAC respectively. The weight and balance analyses are shown in Appendix D. A 10 percent allowable CG range which will encompass the 4.5 percent CG variation requires a nominal horizontal tail to wing area ratio of .222. The aft CG limit (39 percent MAC) is high altitude cruise stability critical. The forward CG limit (29 percent MAC) is takeoff rotation critical. For the

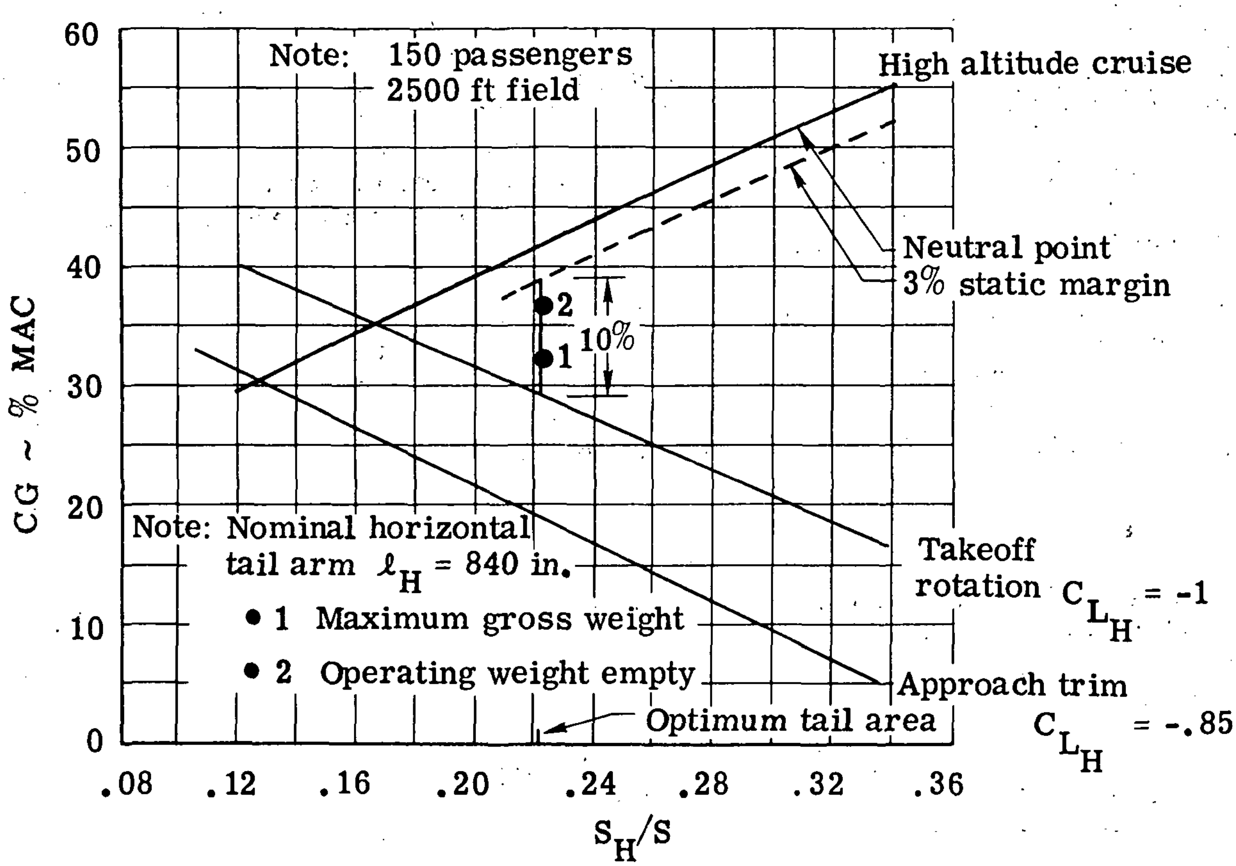

Figure 28 MF configuration horizontal tail sizing

takeoff rotation a usable horizontal tail lift coefficient of - 1.0 is required. This level of lift coefficient is easily obtainable with stabilizer trim plus full deflection of a conventional elevator control surface. The approach trim condition is not critical in determining the forward CG aerodynamic limit.

The nominal horizontal tail arm (ℓ_H = 840 in.) used for the horizontal tail sizing of the 150 passenger, 2,500 foot field length aircraft required adjustments for the 2,000 foot and 3,500 foot field length versions and required scaling for the 40 and 300 passenger versions.

Figure 29 shows the influence of changing the tail arm parameter $\left(\frac{\ell_H}{\bar{c}}\right)$ on the horizontal tail area ratio (S_H/S). Figure 29 was used to adjust the tail sizing for the 150 passenger, 2,000 foot and 3,500 foot field length versions and to size the horizontal tails for the 40 and 300 passenger versions.

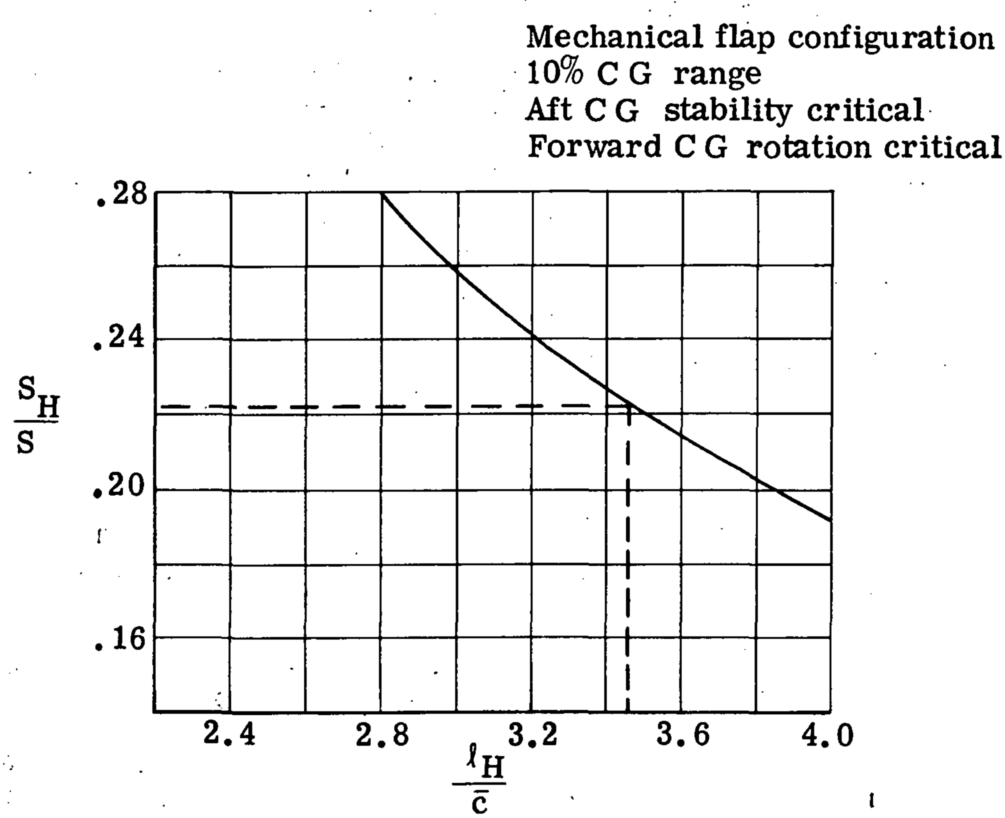

Note: Dashed line represents basic 150 passenger, 2,500 ft field length airplane tail size with nominal horizontal tail arm 840 in.

Figure 29 Effect of horizontal tail arm parameter ($\ell_H/\bar{c}$) on horizontal tail size (S_H/S)

7.2 EXTERNALLY BLOWN FLAP CONFIGURATION HORIZONTAL TAIL SIZE

Horizontal tail sizing for the EBF configuration involves solution of a unique problem not encountered in the conventional MF configuration design, that of extreme wing placement. If the EBF configuration wing is longitudinally placed in a mid-fuselage position similar to CTOL wing-mounted engine configuration, the EBF configuration will have a forward CG problem due to the relatively large engines. This problem is schematically shown in the horizontal tail sizing diagram in Figure 30. The extreme forward CG location requires an excessively large horizontal tail to meet the forward CG requirements (for this particular design, takeoff rotation). For the required CG range, the aircraft now has an excessive static stability margin as shown in Figure 30. Several methods or combinations of methods are available to solve the problem:

- Increasing the amount of horizontal tail lift coefficient which can be generated by the elevator
- Adding ballast in the aft fuselage
- Moving the wing forward

The required horizontal tail area to rotate the aircraft to takeoff attitude is inversely proportional to the amount of negative horizontal tail lift coefficient which can be generated by the elevator. For the EBF configuration a usagle horizontal tail lift coefficient (C_{L_H}) of −1.5 was assumed (C_{L_H} = - 1 for the MF configuration). This effect on the horizontal tail size required for nose wheel lift off is also schematically illustrated in Figure 30. To achieve a usable horizontal tail lift coefficient of 1.5 requires a more sophisticated elevator design than would be required for the MF configuration.

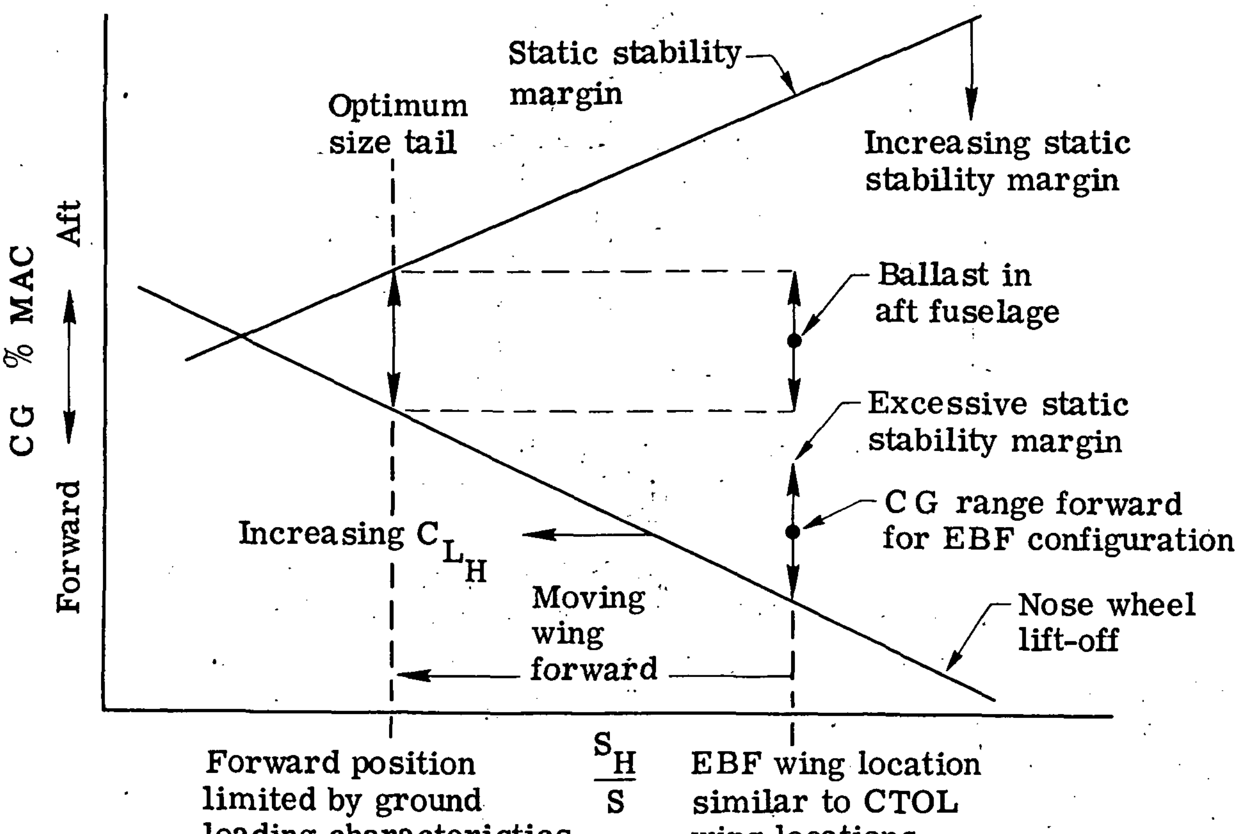

Figure 30 Schematic EBF configuration horizontal tail sizing

By adding the proper amount of ballast in the aft fuselage the EBF configuration with a longitudinal wing location similar to CTOL aircraft can be balanced. An optimum size tail can be selected which will allow the aerodynamic limit to coincide with the structural weight and balance limits as illustrated in Figure 30.

The wing placement technique was used in lieu of the ballast technique to balance the aircraft and obtain an optimum size tail. This method makes use of the existing structure behind the wing for ballast without having to add any "dead weight" ballast.

Increasing the horizontal tail usable lift coefficient from −1 to −1.5, and moving the wing to the most forward position relative to the fuselage without compromising good ground loading characteristics, allowed selection of an optimum size horizontal tail.

Figure 31 shows the EBF configuration horizontal tail sizing as a function of CG location for the wing located in a relative longitudinal position to the fuselage as the wind tunnel model, Figure 15. Figure 31 was constructed with a variable main landing gear position relative to the aft CG limit to maintain a constant percent of the total gross weight on the nose wheel for good nose wheel steering characteristics. For horizontal tail to wing area ratios between .199 and .246 a CG range varying from 0 percent to 10 percent becomes available which is based on a three percent static margin for the aft limit and takeoff rotation for the forward limit. The maximum required CG range was chosen to be 10 percent MAC. For horizontal tail area to wing area ratios greater than .246 the

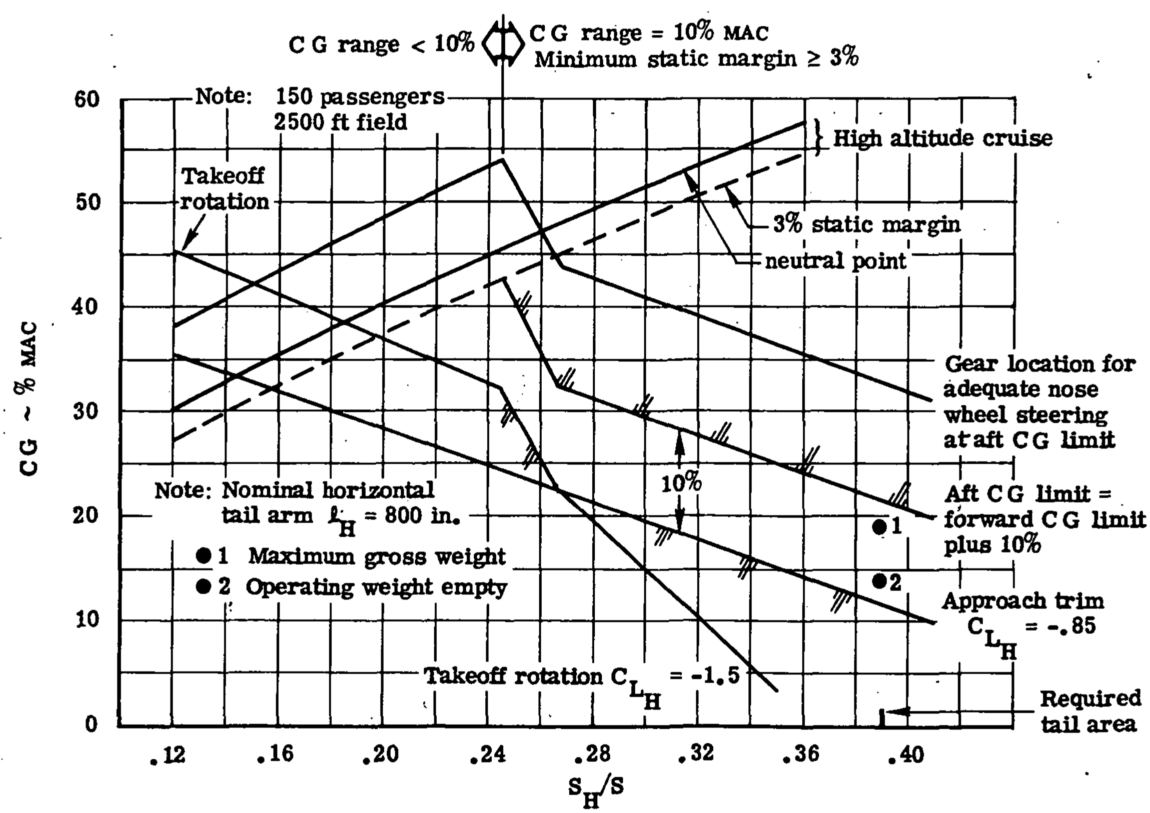

Figure 31 EBF configuration horizontal tail sizing ~ wing location of Figure 15

available CG range will exceed 10 percent if the same critical conditions (three percent static margin and takeoff rotation) are used to define the forward and aft CG limits. For horizontal tail area to wing area ratios between .246 and .267 the forward CG limit is takeoff rotation critical while the aft CG limit is maintained 10 percent aft. The main landing gear can now be moved forward with the increasing horizontal tail area to wing area ratios. The change in CG with respect to horizontal tail area ratio required to meet the takeoff rotation requirement is greatly increased. For horizontal tail area to wing area ratios greater than .267, the forward CG limit becomes approach trim critical and the aft CG limit is still 10 percent aft and nose wheel steering critical. Also shown in Figure 31 are the CG's corresponding to the maximum gross weight and operating weight empty for the 150 passenger, 2,500-foot field length EBF configuration with the wing located relative to the fuselage in a longitudinal position as shown in Figure 15. The weight and balance analyses are shown in Appendix D. The required horizontal tail area to wing area ratio is .390. The forward CG limit is approach trim critical and the aft CG limit is nose wheel steering critical. With this horizontal tail the static stability margin at the aft CG limit is 39 percent, far too large for good handling quality characteristics. An optimum size tail can be used if the wing is moved 89 inches forward as shown in Figure 32. The CG's corresponding to the maximum gross weight and operating weight empty are now 38.5 percent MAC and 33 percent MAC, respectively (see Appendix D). A horizontal tail area to wing area ratio of .222 is required to provide a 10 percent CG range. The forward CG limit is takeoff rotation critical and the aft CG limit is nose wheel steering critical with a static stability margin of four percent MAC.

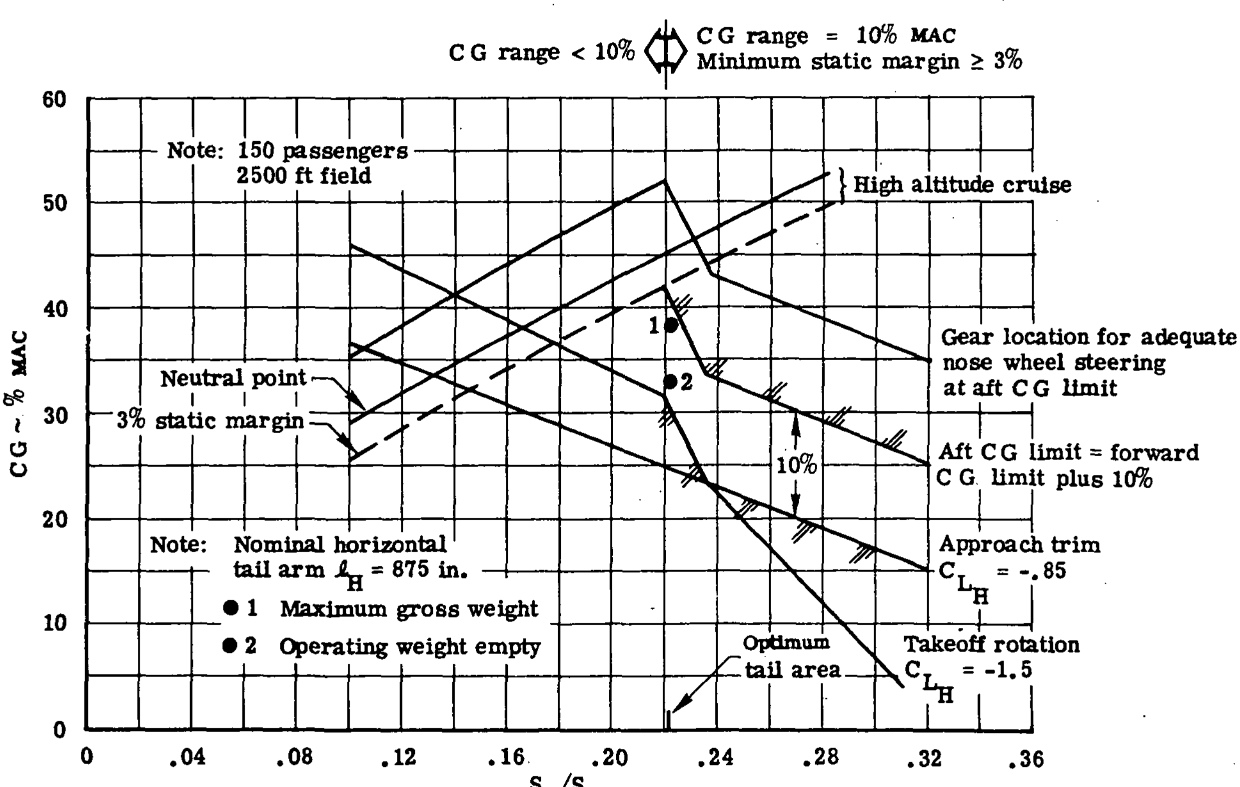

Figure 32 EBF configuration horizontal tail sizing ~ optimum wing location

The nominal horizontal tail arm (ℓ_H = 875 in.) used for the horizontal tail sizing of Figure 32 required adjustments for the 2,000 foot and 3,500 foot field length versions and required scaling for the 40 and 300 passenger versions. Figure 33 shows the influence of changing the tail arm parameter $\left(\frac{\ell_H}{\bar{c}}\right)$ on the horizontal tail area ratio (S_H/S). Figure 33 was used to adjust the tail sizing for the 150 passenger, 2,000 foot and 3,500 foot field length versions and to size the horizontal tails for the 40 and 300 passenger versions.

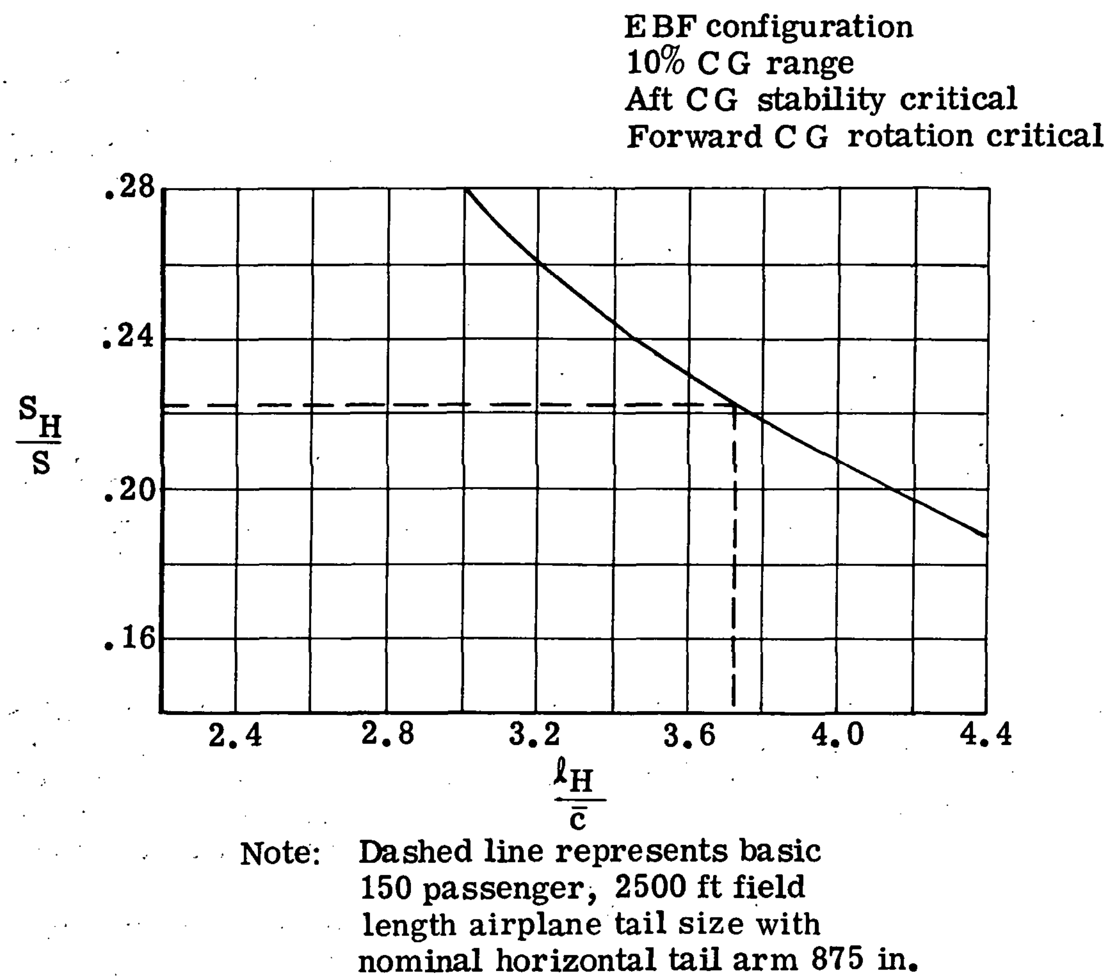

Figure 33 Effect of horizontal tail arm parameter ($\ell_H/\bar{c}$) on horizontal tail size (S_H/S)

8.0 CONFIGURATION DEVELOPMENT

This section contains the details of the development of the Mechanical Flap (MF) and the Externally Blown Flap (EBF) configurations. Information common to both concepts will be discussed first. This is followed by a development of the MF configuration wing geometry. The development of design constraints and sizing of the 18 airplanes in Table 5 are discussed.

TABLE 5 REQUIRED STOL AIRPLANES

		F.A.R. Field Length		
		2,000 Ft.	2,500 Ft.	3,500 Ft.
MF Configurations	Number of Passengers	40 150 300	40 150 300	40 150 300
EBF Configurations	Number of Passengers	40 150 300	40 150 300	40 150 300

Sensitivities to gust load alleviation (GLA) cruise altitude and cruise Mach number will be presented.

8.1 MISSION

All airplanes are sized for the same mission. This mission, shown in Figure 34, consists of three unrefueled 250 NM hops, the cruise portion of which is flown at M = .8 at 35,000 feet. Reserve fuel is provided for a climb, cruise and descent to an alternate field 100 NM away. The alternate field cruise is at best range speed at 15,000 feet. Additional reserve fuel is available for one-half hour loiter at 30,000 feet. For sizing purposes an air maneuver time of six minutes and a ground

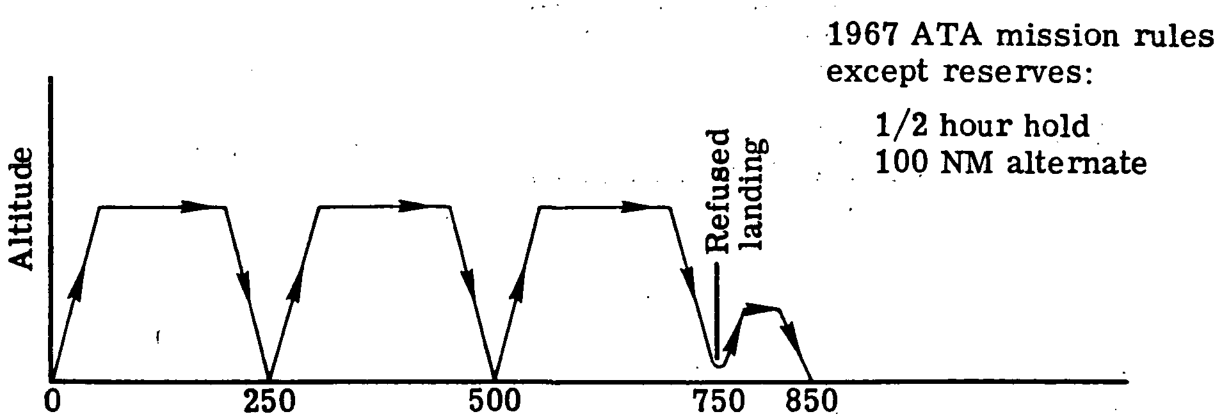

Figure 34 Mission

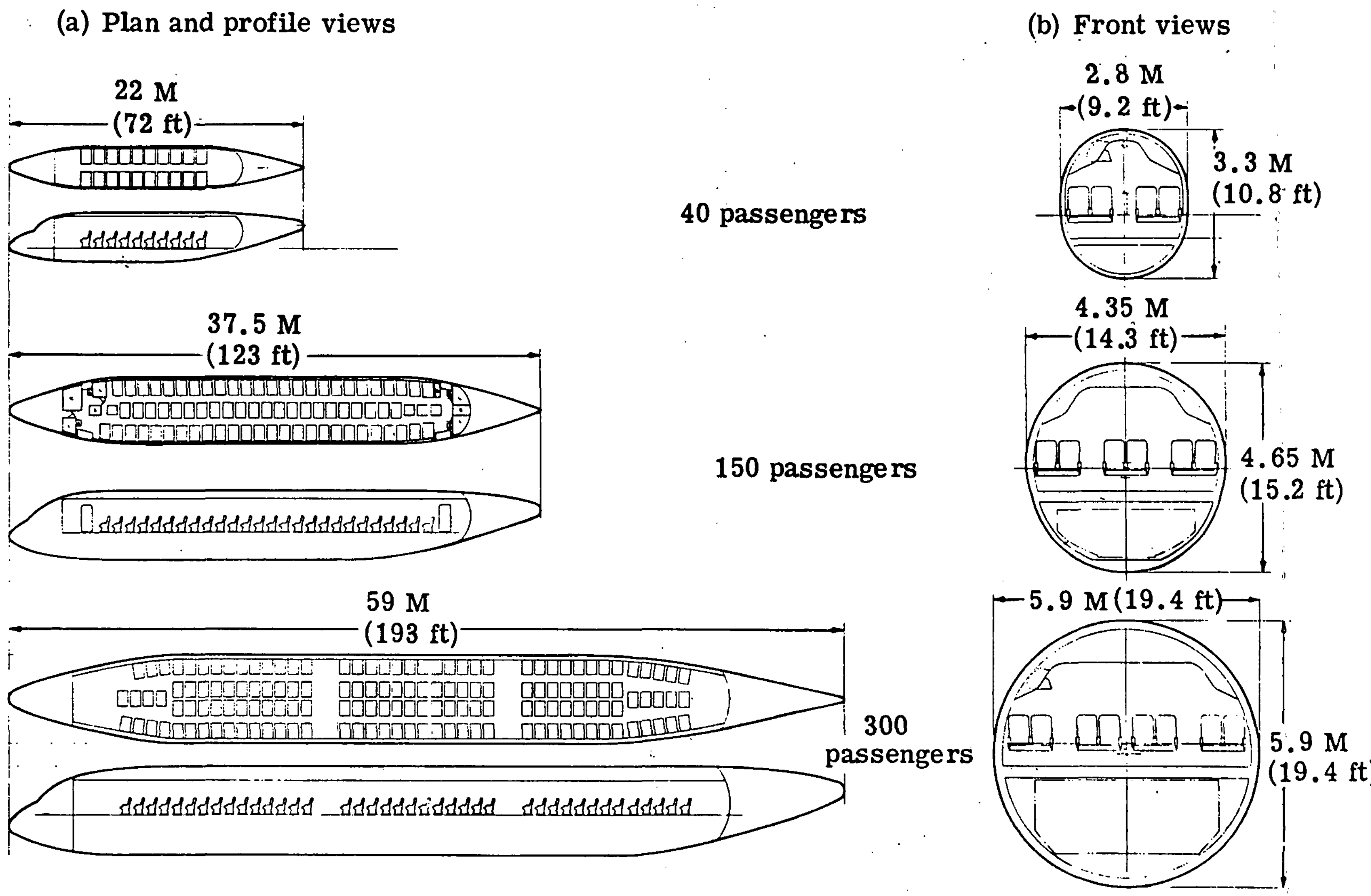

Figure 35 Fuselage arrangement

maneuver time of two minutes per leg was used. Time, fuel and distance to accelerate to start climb speed and from the end climb speed to M = .8 at 35,000 feet also influenced the sizing.

8.2 FUSELAGES

The interior arrangements are shown in Figure 35. Figure 35(a) are plan and profile views. Figure 35(b) are larger scale front views of each fuselage.

All-economy seating was assumed for all payloads on a 34 inch seat pitch. The 40 passenger seating arrangement is four abreast double seat with a single center aisle. The 150 passenger fuselage is a six abreast double seat arrangement separated by two aisles, while the 300 passenger airplanes have an eight abreast double seat configuration separated by two aisles and a large console type armrest down the centerline.

8.3 MECHANICAL FLAP CONFIGURATION WING DEVELOPMENT

A requirement of this study was to develop the wing geometry of the Mechanical Flap (MF) STOL airplane, that is, to optimize the geometry in terms of sweep, thickness, taper and aspect ratio to accomplish a .8 Mach cruise.

The fundamentals controlling the sweep and thickness trade are concerned with the level of supercritical wing technolgy. The basis for the level of technology assumed in this study is shown on Figure 11.

The wing geometry assumed at the time of the sweep/thickness trade was:

	MF	EBF (FIXED)
Aspect Ratio	6	7.48
Taper Ratio	.4	.29
$C_{L_{Design}}$	.2	.3
M_{DD}	.81	.81

The initial MF configuration wing geometry is from the feasibility study airplane of Reference 1. The EBF configuration wing geometry is fixed except for thickness.

The 2D to 3D correlating relationships referred to in Section 4.3.1 were used to determine the average chordwise thickness ratio for a series of sweep angles for the MF configuration and for a quarter chord sweep of 30° for the EBF configuration. The spanwise thickness ratio was assumed to be distributed according to Figure 36. In this Figure $(t/_c)_{av}$ is $(t/_c)_{2D}$ corrected for sweep. The results of this transformation are contained in Table 6.

TABLE 6 WING THICKNESS DISTRIBUTION

	MF				EBF
QUARTER CHORD SWEEP	10°	15°	20°	25°	30°
$(t/_c)_{2D}$	.146	.152	.164	.182	.189
$(t/_c)_{av}$ (Streamwise)	.148	.153	.163	.175	.175
$(t/_c)_{outbd.}$	.129	.133	.142	.152	.152
$(t/_c)_{root}$	.174	.180	.192	.205	.208

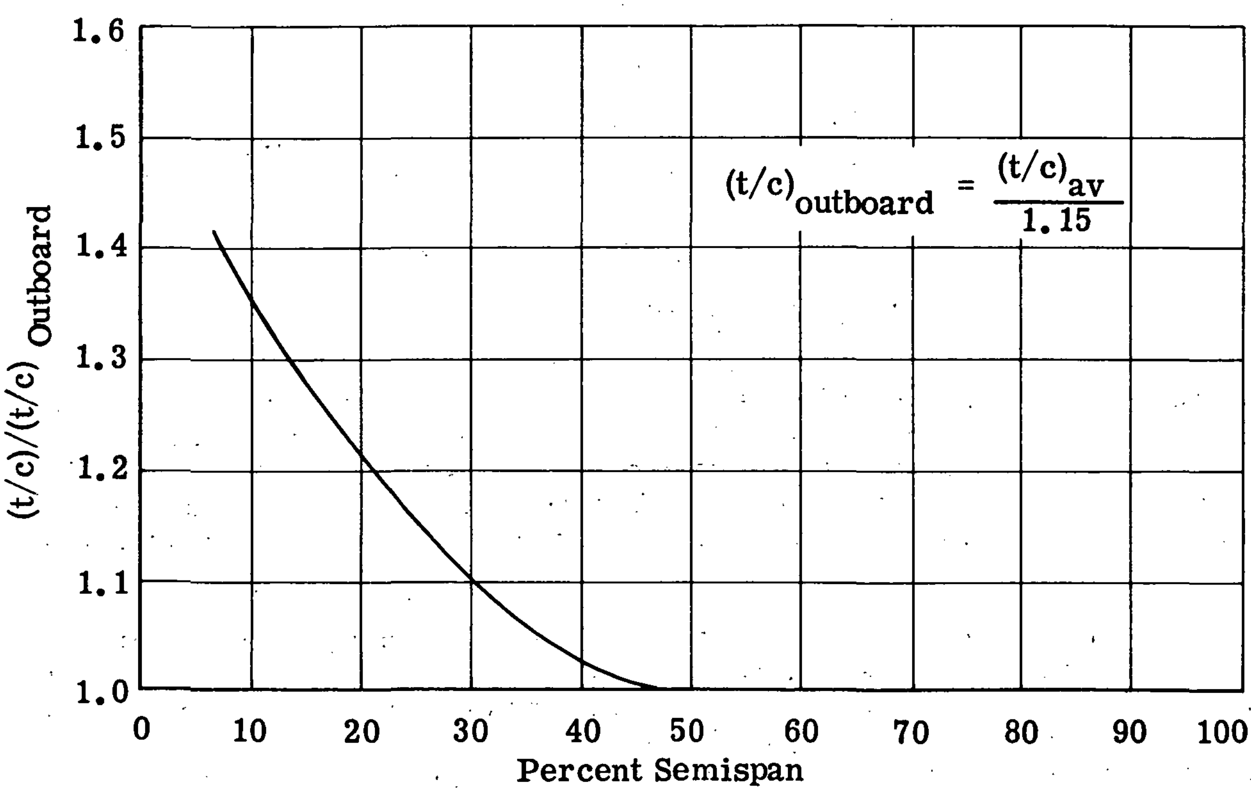

Figure 36 Spanwise thickness

The average thickness ratio is shown on Figure 37(a). The EBF configuration data point does not fit the trend because it has a different planform than the MF configuration.

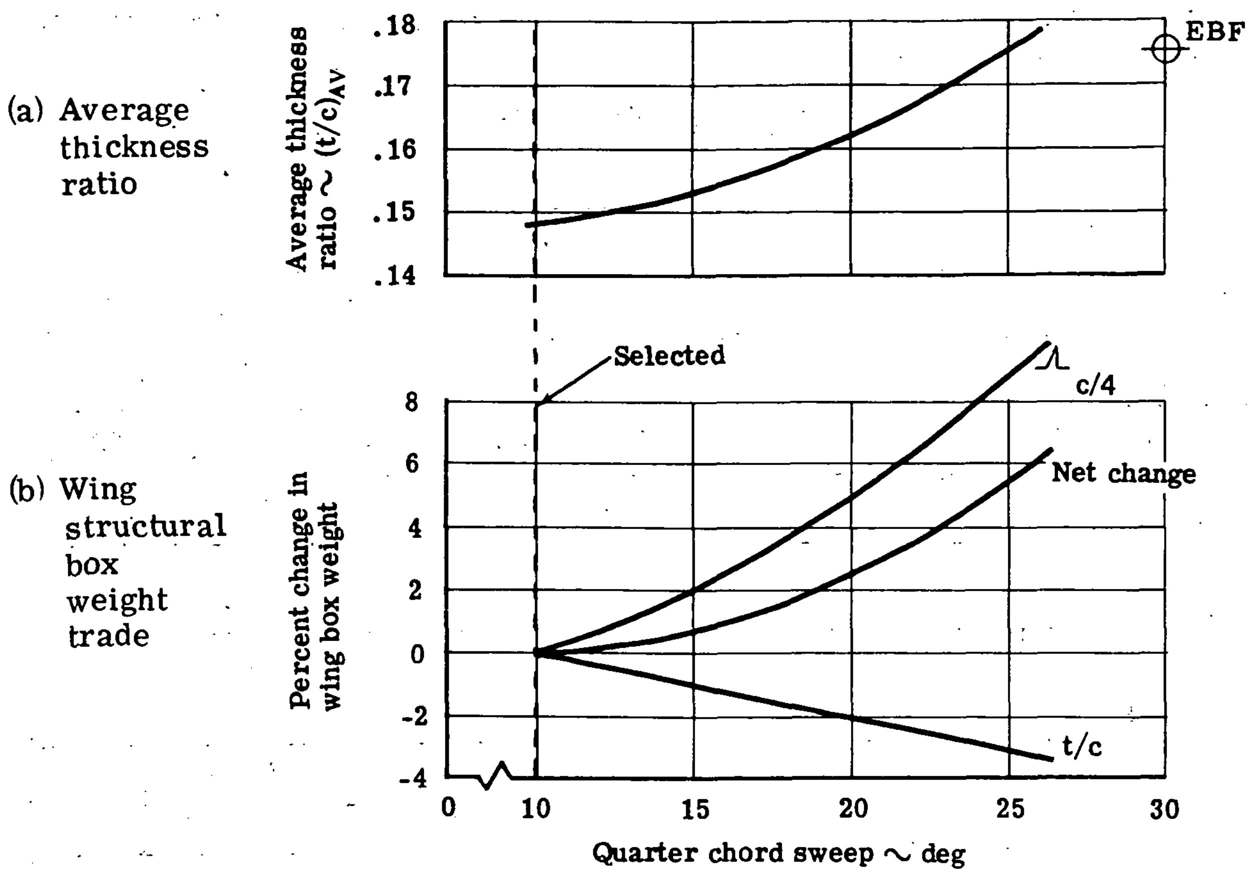

Figure 37 Sweep/thickness trade

The figure of merit used to determine the best wing geometry in terms of sweep and thickness was the wing structural box weight. Figure 37(b) contains the results of this study. Class I weight estimation methods were used to calculate the wing structural box trends with Λ $c/_4$ and $t/_c$. The net change is an increase in wing box weight with increasing sweep. Therefore, minimum sweep was chosen which not only provides the lightest wing box for .8 cruise Mach number but also provides higher lift at low speeds.

Optimum taper and aspect ratio were determined by sizing a 150 passenger airplane for a 2,500 foot F.A.R. field length assuming an unswept trailing edge flap hinge line and the proper wing loading, $\Lambda_{c/4}$, T/W, $\overline{V}_H$ and $t/_c$ as taper ratio was varied for constant values of aspect ratio. The results of this work are shown on Figure 38. These data indicate that the lightest airplane would have an aspect ratio of about 13 and taper ratio .1. However, aspect ratio 8 and taper ratio .275 were chosen for the study. There are several reasons for accepting a geometry which appears to be less than optimum.

- Structural box weight multiplier was extrapolated above aspect ratio 11.5 due to lack of empirical data for high speed wings with larger aspect ratios.
- The increase in aspect ratio from 8 to 13 is a 20 percent increase in span which impairs ground handling as well as roll response.

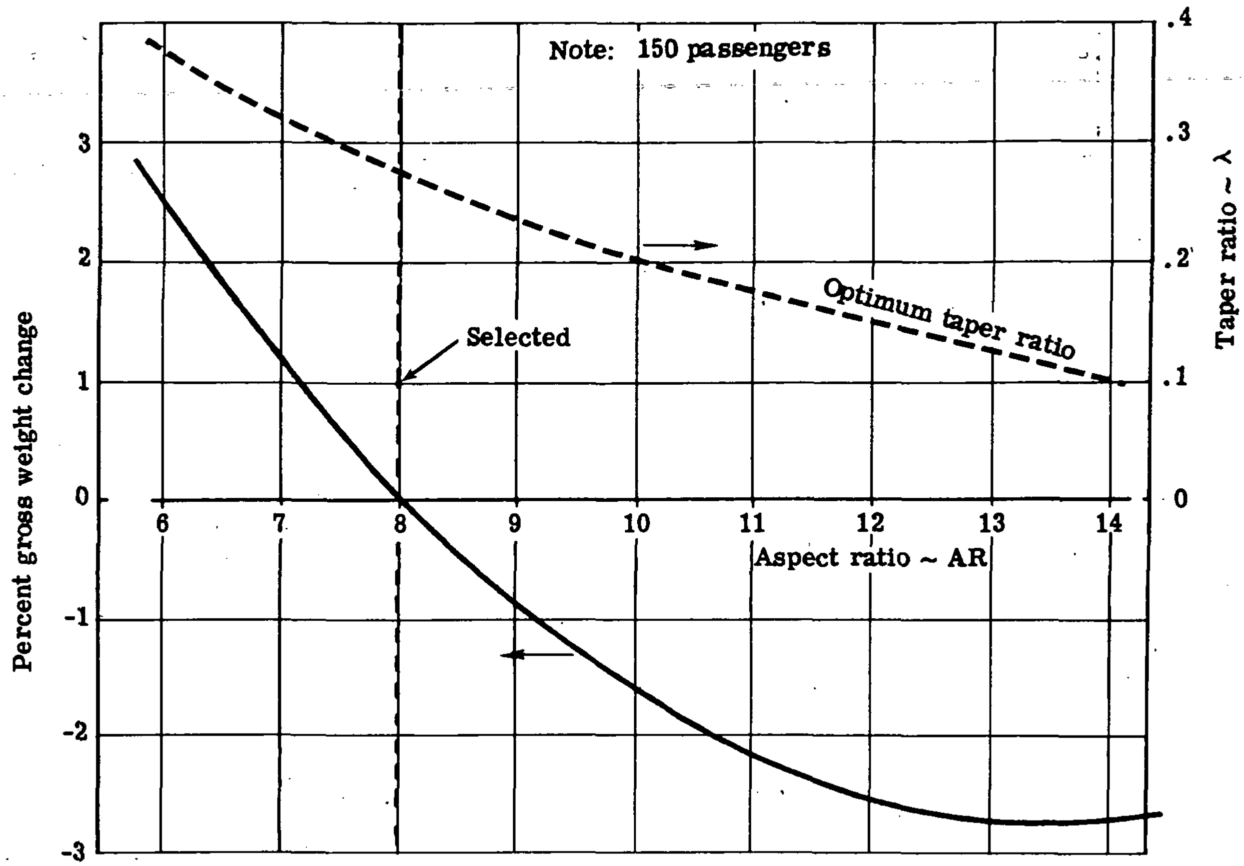

Figure 38 Wing planform optimization

- Wing weight actually increases above aspect ratio 7. This would imply a costlier wing especially when it is realized that the optimum taper ratio decreases with increasing aspect ratio resulting in short, thin wing tips.

The final geometry of the MF airplane wing is shown on Figure 39.

8.4 AIRPLANE PERFORMANCE AND SIZING

8.4.1 MECHANICAL FLAP CONFIGURATION DESIGN CONSTRAINTS

The design constraints for the MF configuration are shown on Figure 40. The minimum gross weight mechanical flap configuration results from the definition of maximum wing loading available and minimum installed thrust-to-weight/ratio required. Wing loading is defined by landing. Installed sea level static thrust-to-weight ratio is critical for the start cruise requirement of .8 Mach at 35,000 feet. Engine-out go-around climb limits and the landing constraint were analyzed using the low speed lift and drag polars and the installed engine data. The takeoff and start-cruise constraints were determined using computer programs. The takeoff program, described in Paragraph 5.1, requires

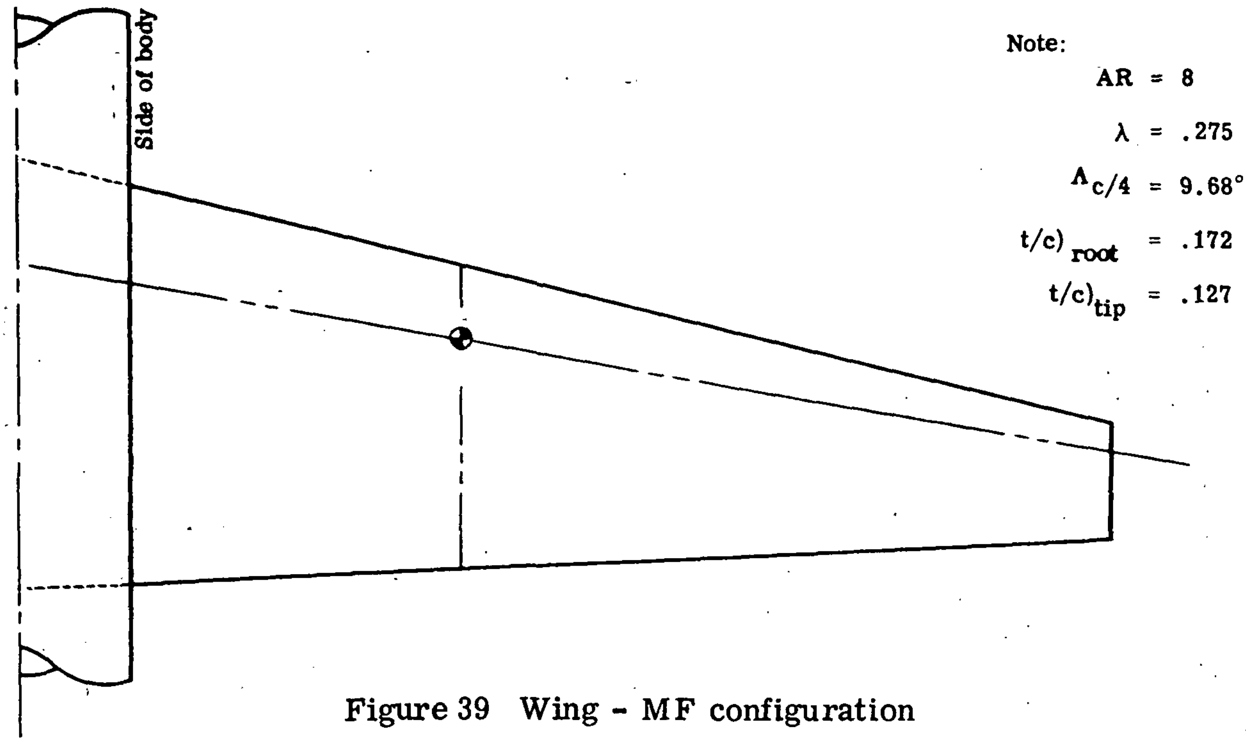

Figure 39 Wing - MF configuration

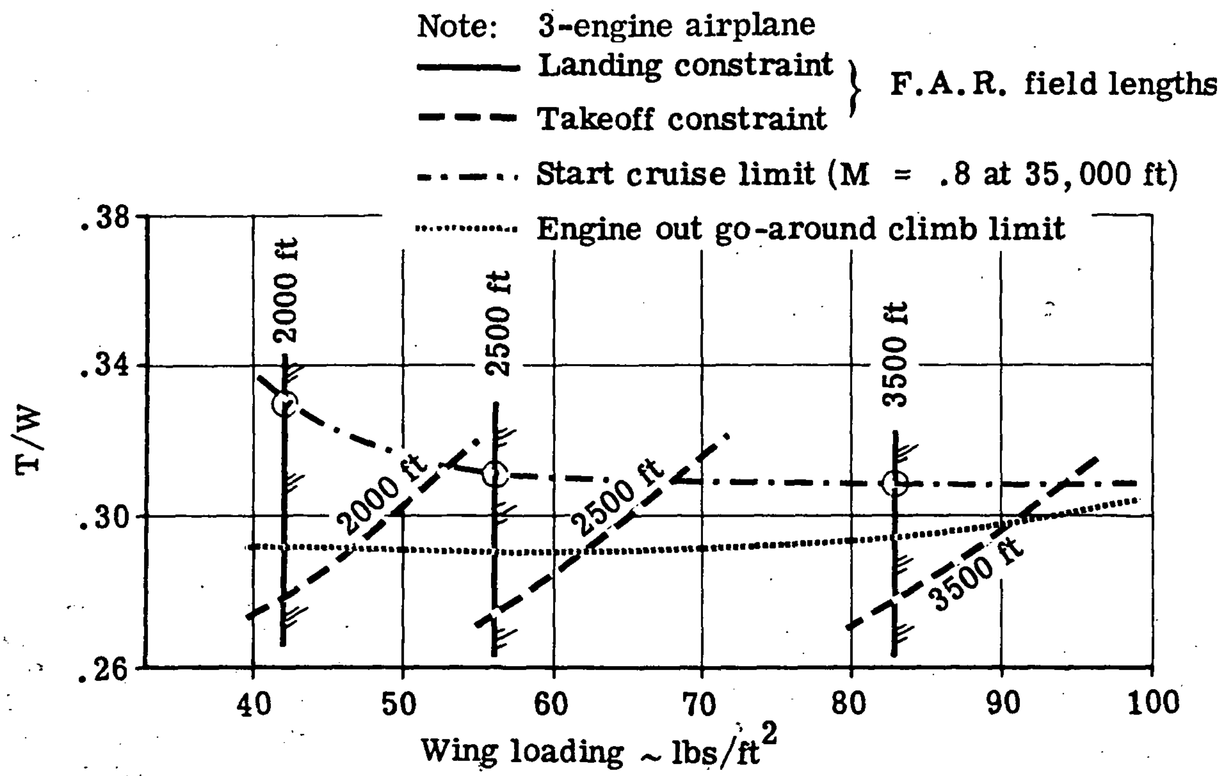

Figure 40 MF configuration design constraints

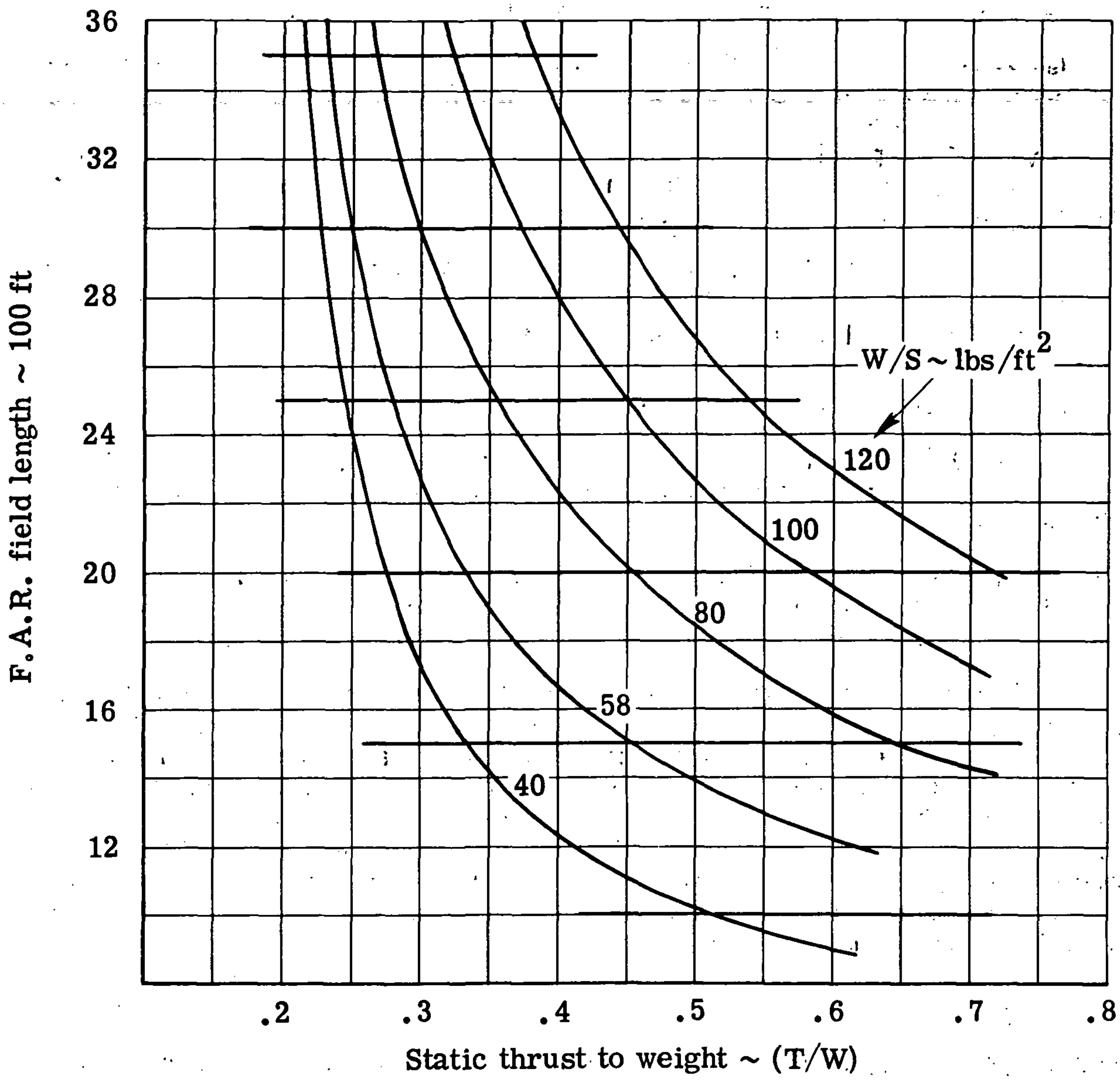

Figure 41 MF configuration takeoff design chart

that the low speed polars and engine data be input. The airplane sizing program (ASAMP) which determines the thrust required to cruise also estimates the high speed clean drag. Engine data as a function of altitude is input to this program.

Results from the takeoff computer program are plotted as shown on Figure 41. This curve is read at the field length of interest and that data is cross plotted on the design constraint chart of Figure 40.

8.4.2 EXTERNALLY BLOWN FLAP CONFIGURATION DESIGN CONSTRAINTS

The design constraints for the EBF configuration are shown on Figure 42. Takeoff and landing performance were analyzed by the computer programs referred to in the previous section. The takeoff and landing design curves for the EBF configuration are shown on Figures 43 and 44, respectively. The landing design curve is an outgrowth of the procedure described in Section 5.2 for the analysis of an approach and go-around with powered lift. The curves of C_L versus T/W for all engines and engine out are contained in Appendix C.

The landing performance is critical for all field lengths. Aircraft were sized for a set of wing loadings and their corresponding thrust-to-weight ratio along each landing constraint line. The locus of minimum gross weight airplanes from this analysis is noted in Figure 42.

8.5 STOL TRANSPORT SIZE COMPARISON

A summary of design constraints is shown on Figure 45. For the same field length the EBF configurations have higher wing loadings but also require higher installed thrust to weight ratio than the MF configurations.

Inputing these constraints and the horizontal and vertical tail volume coefficients derived from Sections 6.0 and 7.0 the transport size comparison of Figure 46 can be made. The EBF configurations are heavier than the MF configuration for all field lengths and payloads.

It should be pointed out that the EBF configurations are extremely sensitive to landing approach safety margins and go-around procedures. A rough indication of this is shown on Figure 47. Lines 1 and 3 correspond to the landing and takeoff constraints, respectively, shown previously on Figure 42. Line 2 is the location of the landing constraint if a combination of the approach safety margin for gusts and the go-around procedure is changed. This relaxation of rules results in a reduction of EBF airplane gross weight from 214,000 pounds to about 190,000 pounds. The MF configuration gross weight for the 2,000 foot field length is 184,000 pounds, however, this airplane approaches at $1.3V_s$ which allows about 16^o of α margin for gust protection and it can meet the engine out climb gradients without a configuration change.

8.6 3-VIEWS

Nine 3-views are shown including an alternate configuration for the 2,500 foot 150 passenger MF configuration. The airplanes for which a 3-view is presented and the figure number is shown in Table 7.

TABLE 7 LOCATION OF THREE-VIEWS

Number of Passengers	Mechanical Flap Configuration		Externally Blown Flap Configuration	
	F.A.R. Field Length		F.A.R. Field Length	
	2000 Feet	2500 Feet	2000 Feet	2500 Feet
40		Figure 52		Figure 53
150	Figure 50	Figure 48 Figure 56 (alternate)	Figure 51	Figure 49
300		Figure 54		Figure 55

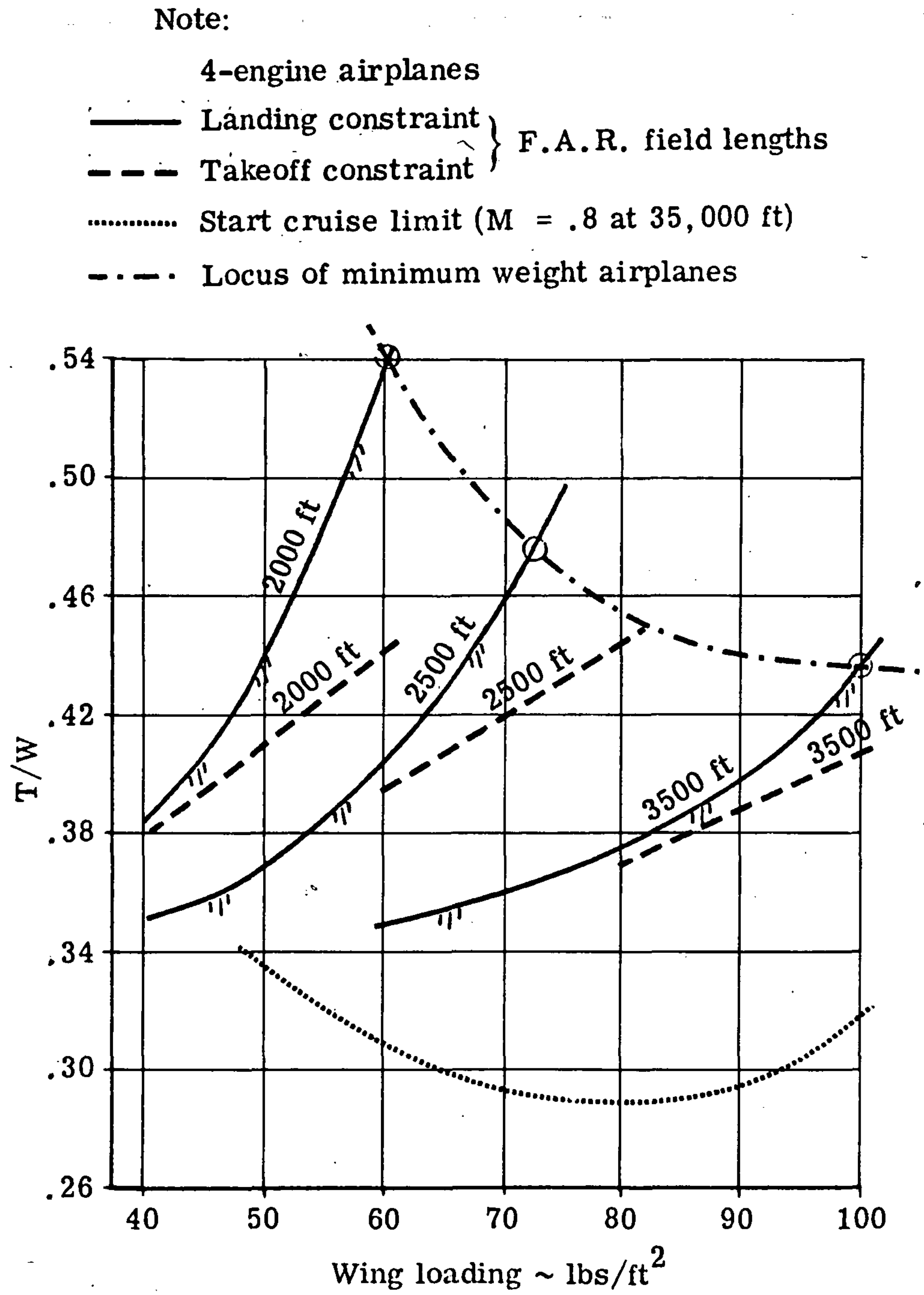

Figure 42 EBF Configuration design constraints

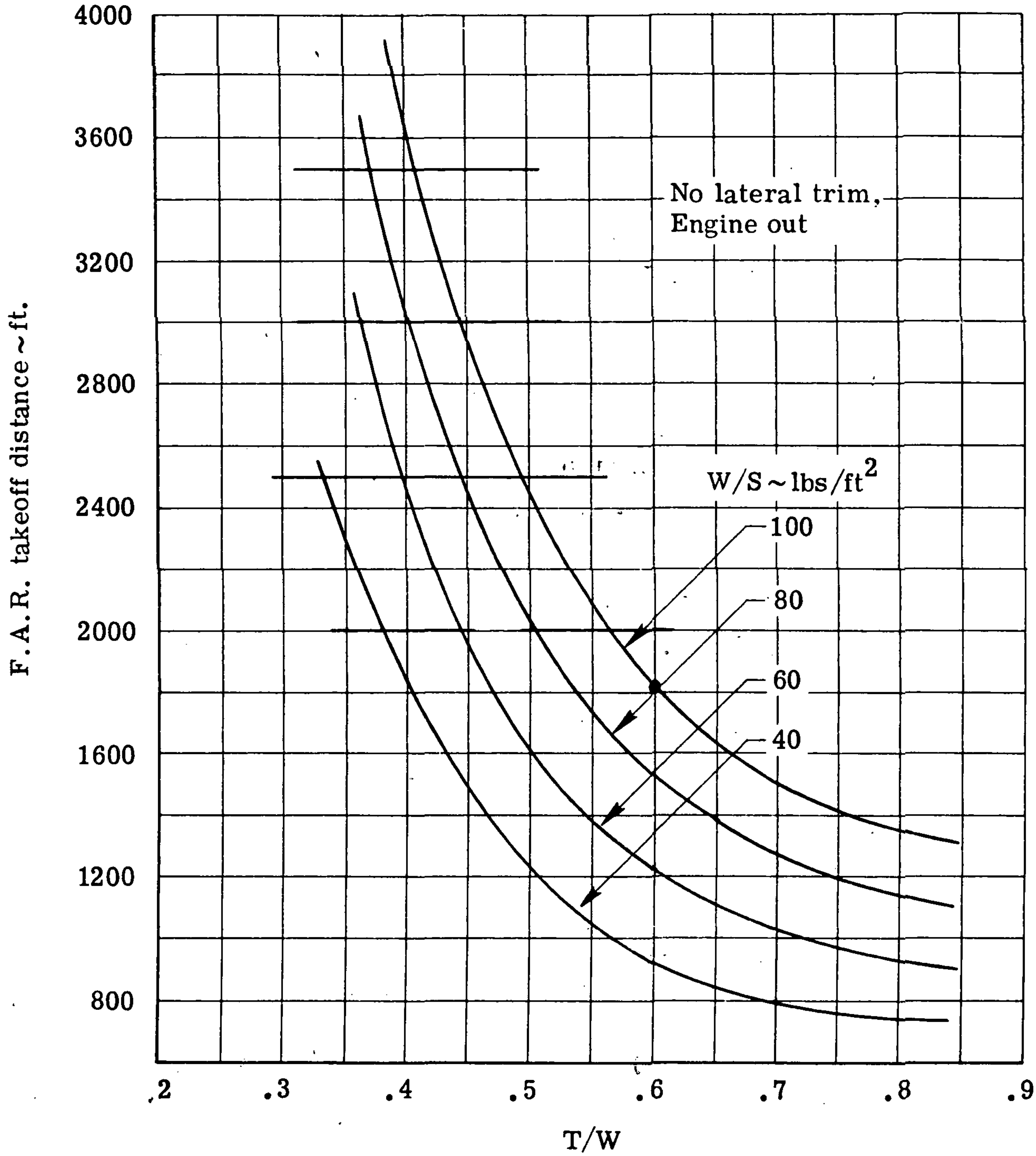

Figure 43 EBF configuration takeoff design chart

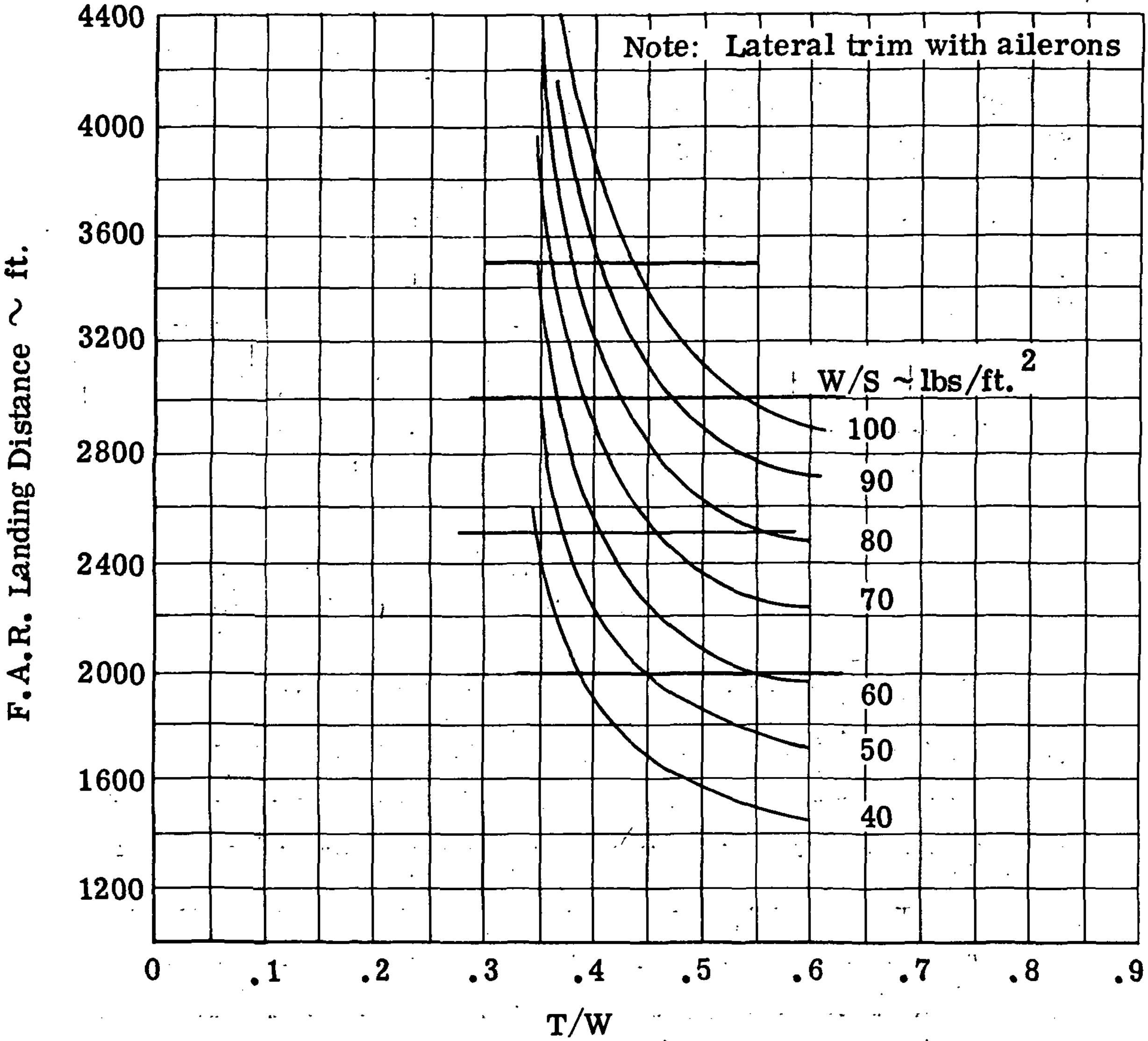

Figure 44 EBF configuration landing design chart

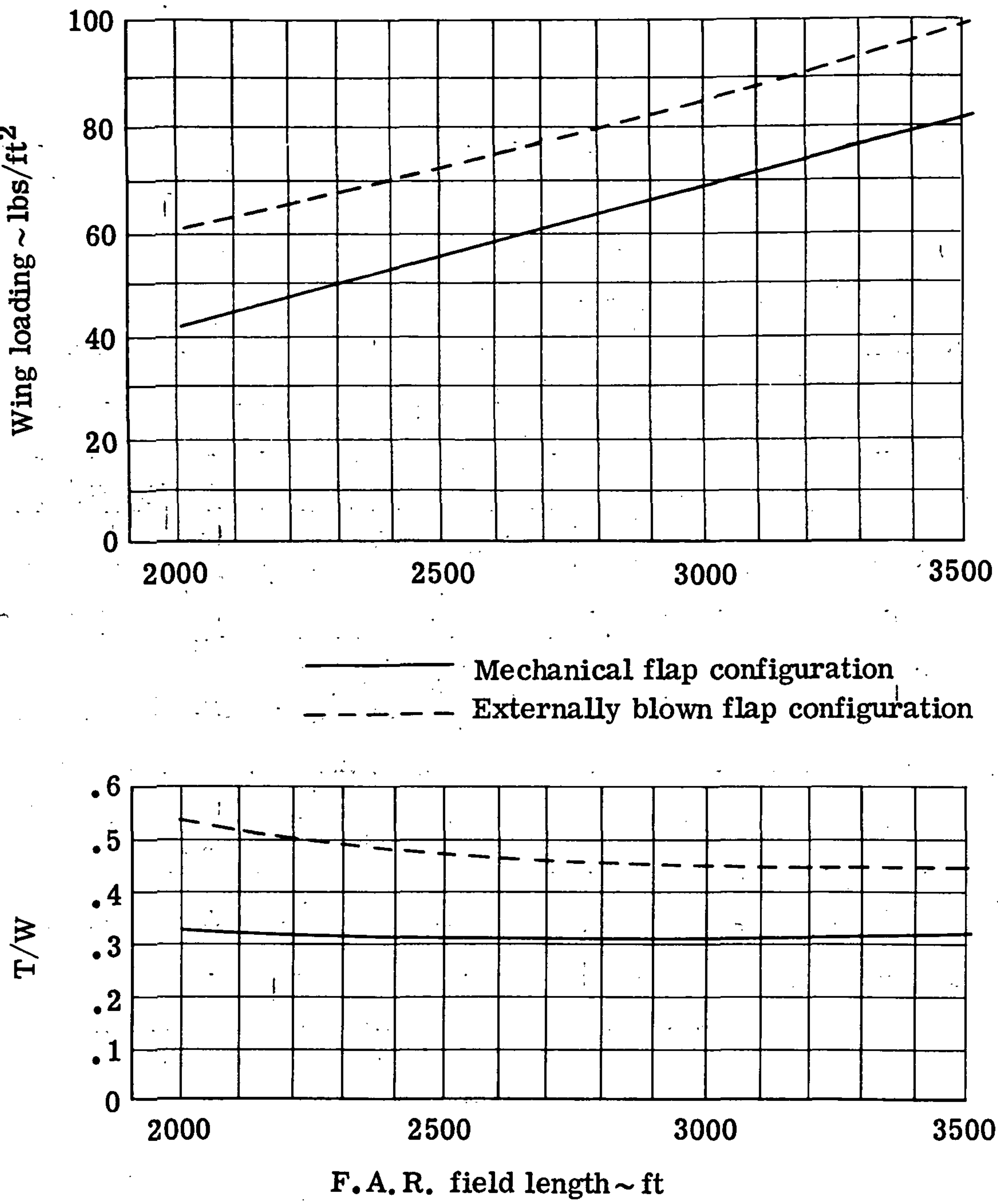

Figure 45 Stol transport design constraint summary

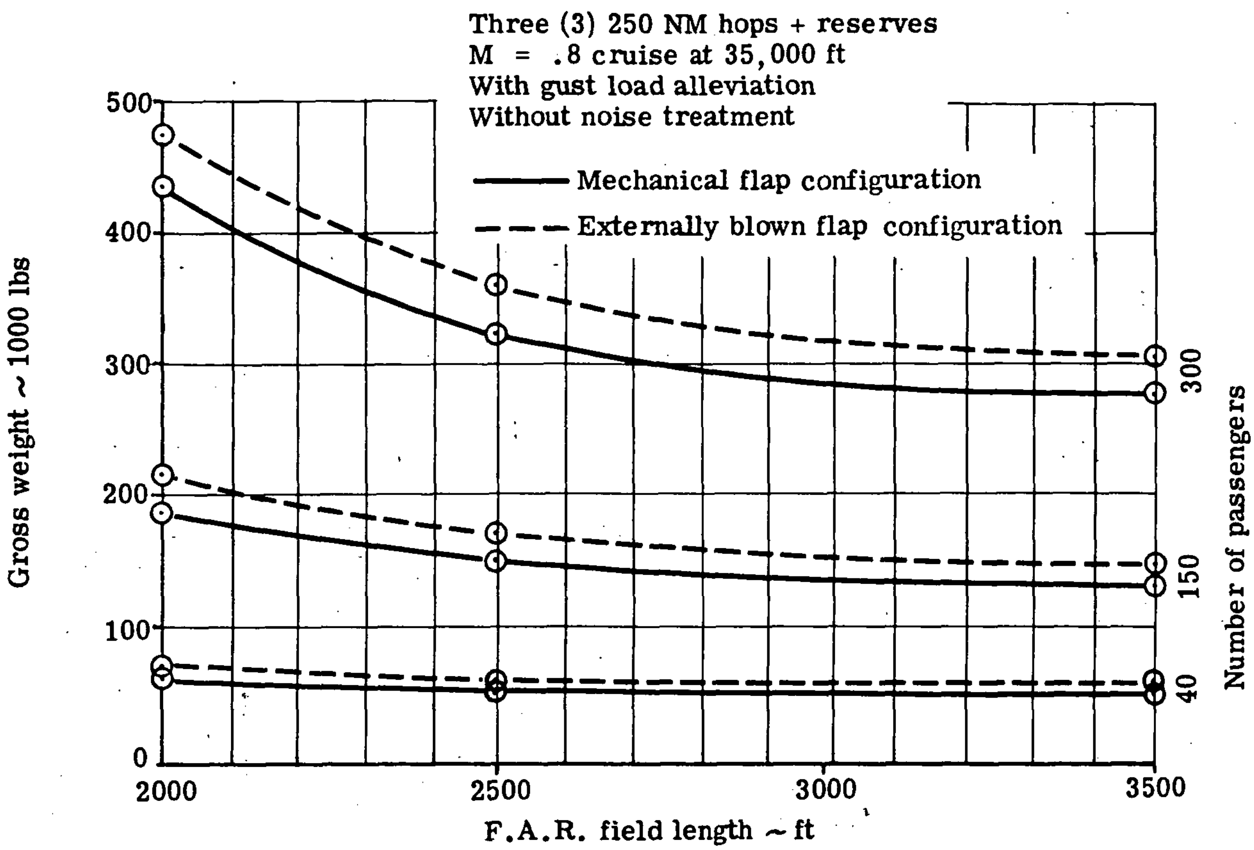

Figure 46 Stol transport-size comparison

	$\Delta\alpha$ All Engines	Engine Out Gradient	Configuration Change	Speed Change	Engine out Lateral Trim Drag
①	15°	0°	Yes	No	No
②	10°	-1°	Yes	Yes	No
③	Takeoff requirement				

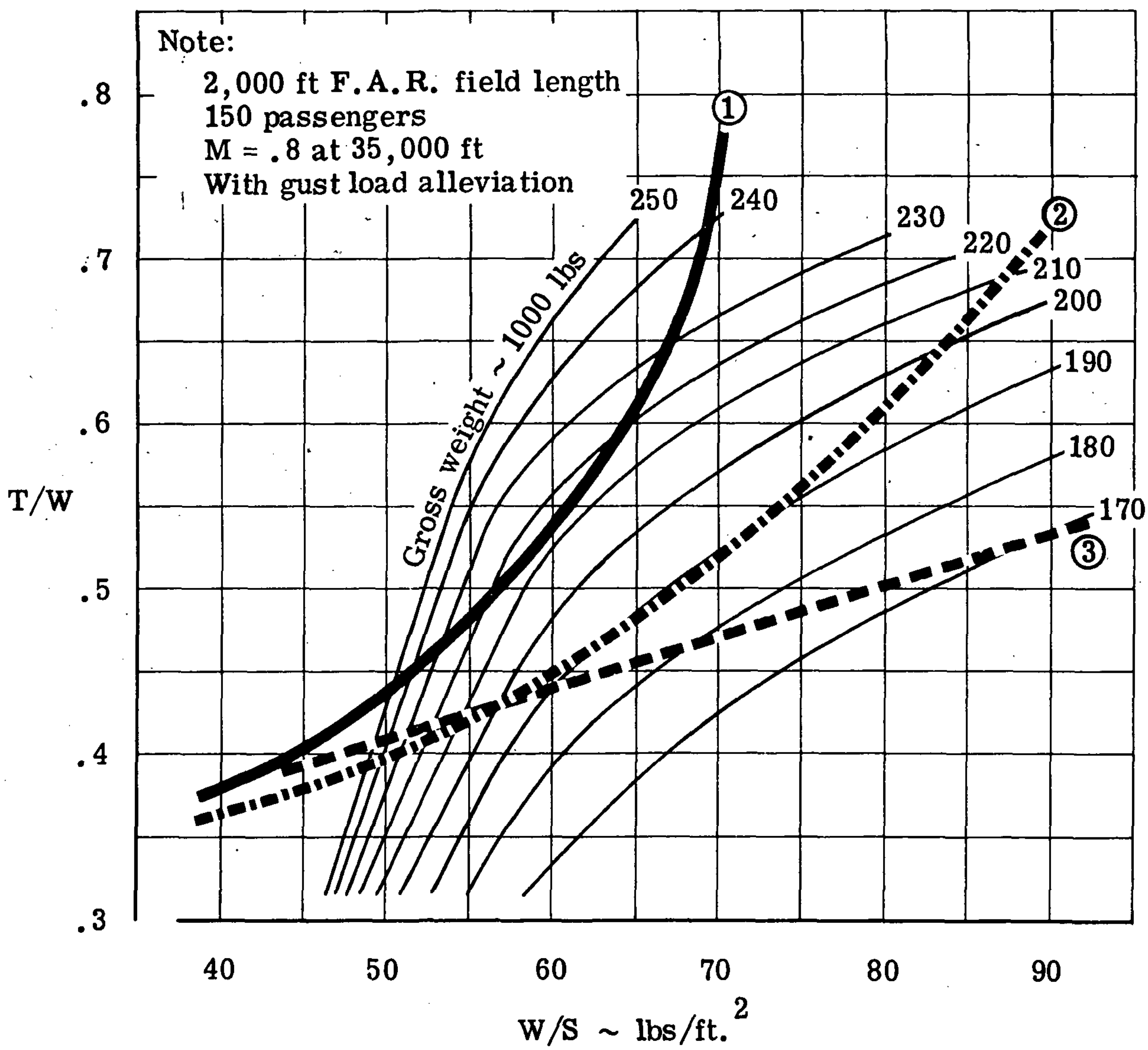

Figure 47 EBF configuration sensitivity to engine out go-around procedure

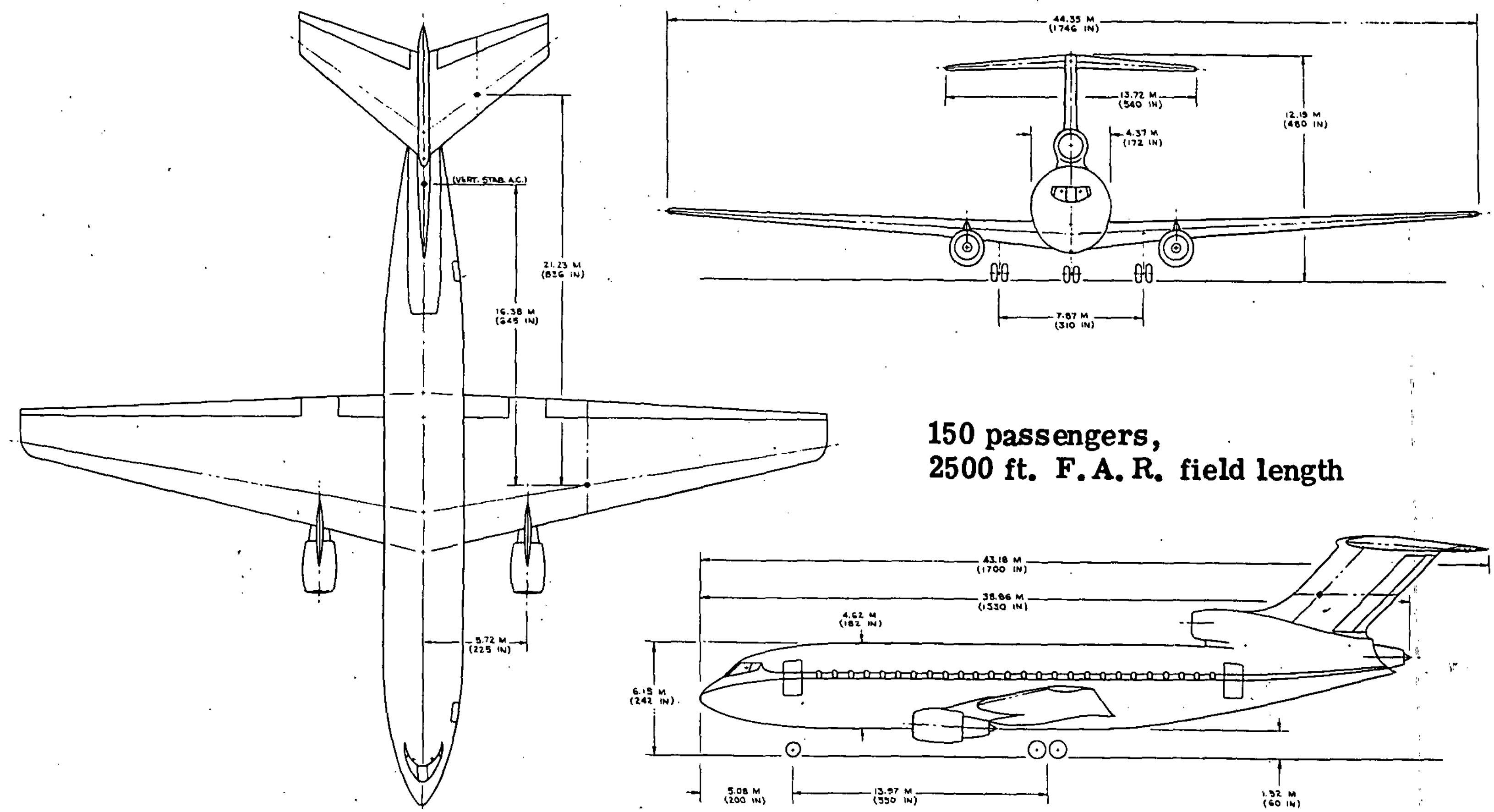

150 passengers,
2500 ft. F.A.R. field length

WING

AREA (AERODYNAMIC REFERENCE)	246.01 M²	2648 FT²
ASPECT RATIO	8.0	
TAPER RATIO	.275	
SWEEP @ C/4	9.3°	
DIHEDRAL	3.0°	
INCIDENCE (ROOT)	2.0°	
INCIDENCE (TIP)	0°	
MEAN AERODYNAMIC CHORD	6.13 M	241.5 IN
THICKNESS RATIO (ROOT)	.172	
THICKNESS RATIO (MAC)	.130	
THICKNESS RATIO (TIP)	.127	
ROOT CHORD	8.69 M	342.0 IN
TIP CHORD	2.39 M	94.0 IN

HORIZONTAL STABILIZER

AREA	54.63 M²	588 FT²
ASPECT RATIO	3.45	
TAPER RATIO	.40	
LEADING EDGE SWEEP	40.0°	
DIHEDRAL	-3.0°	
MEAN AERODYNAMIC CHORD	4.23 M	166.4 IN
THICKNESS RATIO (ROOT)	.10	
THICKNESS RATIO (TIP)	.10	
ROOT CHORD	5.69 M	224.0 IN
TIP CHORD	2.29 M	90.0 IN
VOLUME COEFFICIENT	.769	

VERTICAL STABILIZER

AREA	32.61 M²	351 FT²
ASPECT RATIO	1.0	
TAPER RATIO	1.0	
LEADING EDGE SWEEP	43.5°	
MEAN AERODYNAMIC CHORD	5.69 M	224.0 IN
THICKNESS RATIO	.10	
ROOT CHORD	5.69 M	224.0 IN
TIP CHORD	5.69 M	224.0 IN
VOLUME COEFFICIENT	.0490	

Figure 48 MF configuration STOL aircraft

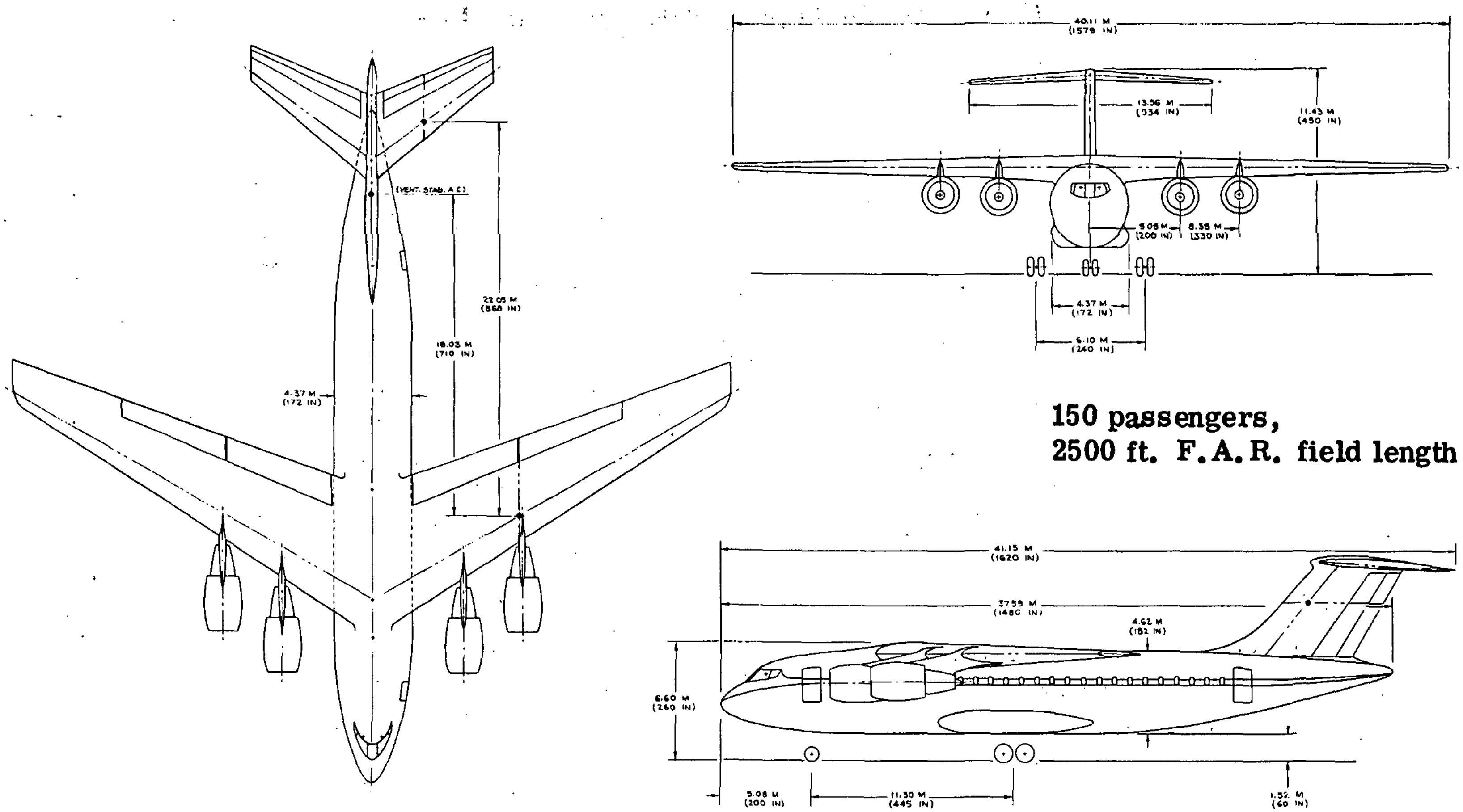

150 passengers,
2500 ft. F.A.R. field length

WING		
AREA (AERODYNAMIC REFERENCE)	214.98 M²	2314 FT²
ASPECT RATIO	7.48	
TAPER RATIO	.290	
SWEEP @ C/4	30.0°	
DIHEDRAL	0°	
INCIDENCE (ROOT)	2.0°	
INCIDENCE (TIP)	0°	
MEAN AERODYNAMIC CHORD	5.89 M	232.0 IN
THICKNESS RATIO (ROOT)	.208	
THICKNESS RATIO (MAC)	.157	
THICKNESS RATIO (TIP)	.152	
ROOT CHORD	8.31 M	327.0 IN
TIP CHORD	2.41 M	95.0 IN

HORIZONTAL STABILIZER		
AREA	45.99 M²	495 FT²
ASPECT RATIO	4.00	
TAPER RATIO	.40	
LEADING EDGE SWEEP	40.0°	
DIHEDRAL	-3.0°	
MEAN AERODYNAMIC CHORD	3.60 M	141.7 IN
THICKNESS RATIO (ROOT)	.10	
THICKNESS RATIO (TIP)	.10	
ROOT CHORD	4.84 M	190.7 IN
TIP CHORD	1.94 M	76.3 IN
VOLUME COEFFICIENT	.800	

VERTICAL STABILIZER		
AREA	31.77 M²	342 FT²
ASPECT RATIO	1.0	
TAPER RATIO	.75	
LEADING EDGE SWEEP	42.0°	
MEAN AERODYNAMIC CHORD	5.68 M	223.4 IN
THICKNESS RATIO	.10	
ROOT CHORD	6.44 M	253.6 IN
TIP CHORD	4.83 M	190.2 IN
VOLUME COEFFICIENT	.0665	

Figure 49 EBF configuration STOL aircraft

150 passengers, 2000 ft. F.A.R. field length

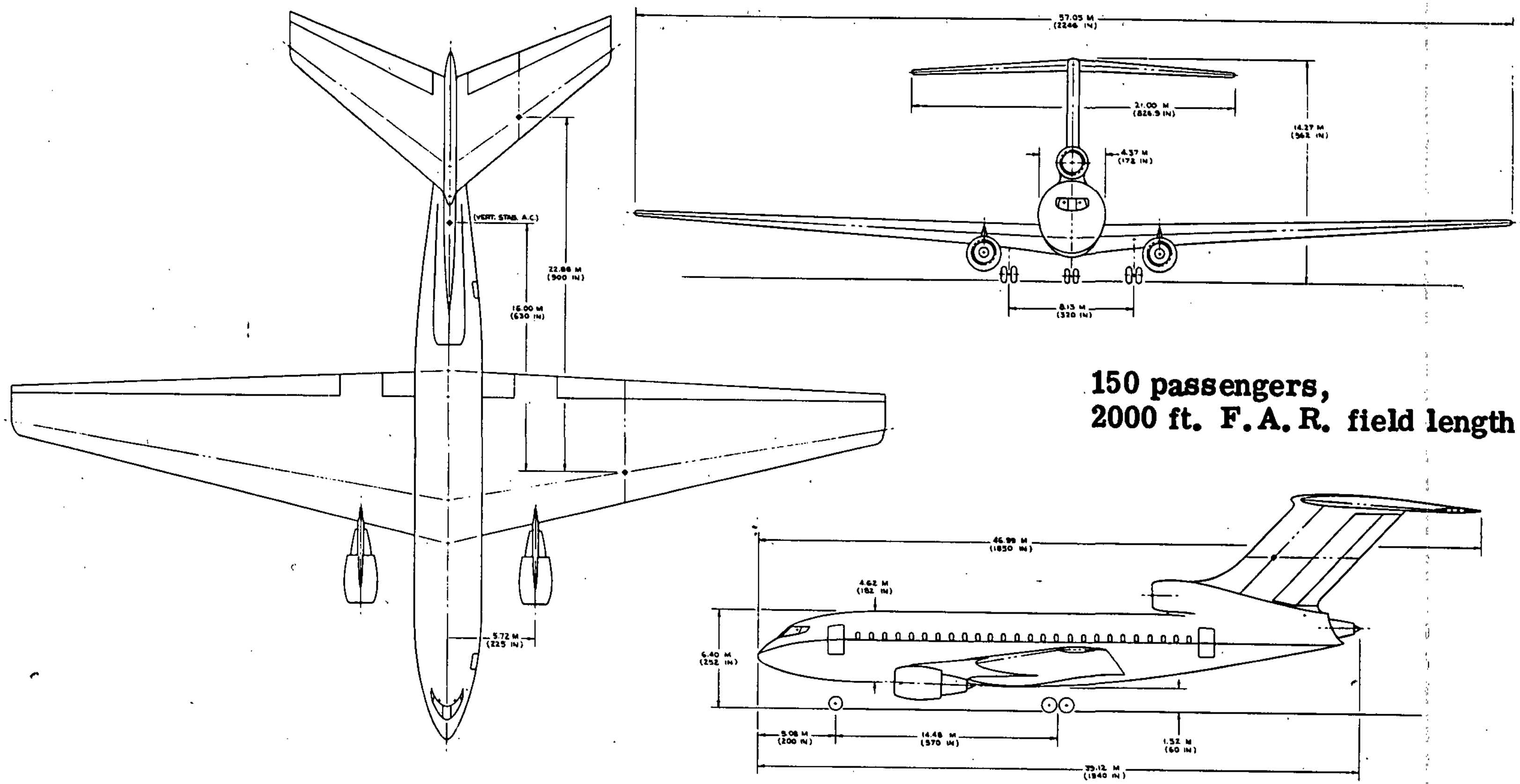

WING

AREA (AERODYNAMIC REFERENCE)	406.822 M^2	4379 FT^2
ASPECT RATIO	8.00	
TAPER RATIO	.275	
SWEEP @ C/4	9.68°	
DIHEDRAL	0°	
INCIDENCE (ROOT)	2.0°	
INCIDENCE (TIP)	0°	
MEAN AERODYNAMIC CHORD	7.900 M	311.0 IN
THICKNESS RATIO (ROOT)	.172	
THICKNESS RATIO (MAC)	.130	
THICKNESS RATIO (TIP)	.127	
ROOT CHORD	11.186 M	440.4 IN
TIP CHORD	3.076 M	121.1 IN

HORIZONTAL STABILIZER

AREA	110.276 M^2	1187 FT^2
ASPECT RATIO	4.00	
TAPER RATIO	.400	
LEADING EDGE SWEEP	40.0°	
DIHEDRAL	-3.0°	
MEAN AERODYNAMIC CHORD	5.572 M	219.4 IN
THICKNESS RATIO (ROOT)	.10	
THICKNESS RATIO (TIP)	.10	
ROOT CHORD	7.501 M	295.3 IN
TIP CHORD	3.000 M	118.1 IN
VOLUME COEFFICIENT	.784	

VERTICAL STABILIZER

AREA	55.370 M^2	596 FT^2
ASPECT RATIO	1.0	
TAPER RATIO	1.0	
LEADING EDGE SWEEP	43.5°	
MEAN AERODYNAMIC CHORD	7.441 M	293.0 IN
THICKNESS RATIO	.10	
ROOT CHORD	7.441 M	293.0 IN
TIP CHORD	7.441 M	293.0 IN
VOLUME COEFFICIENT	.0382	

Figure 50 MF configuration STOL aircraft

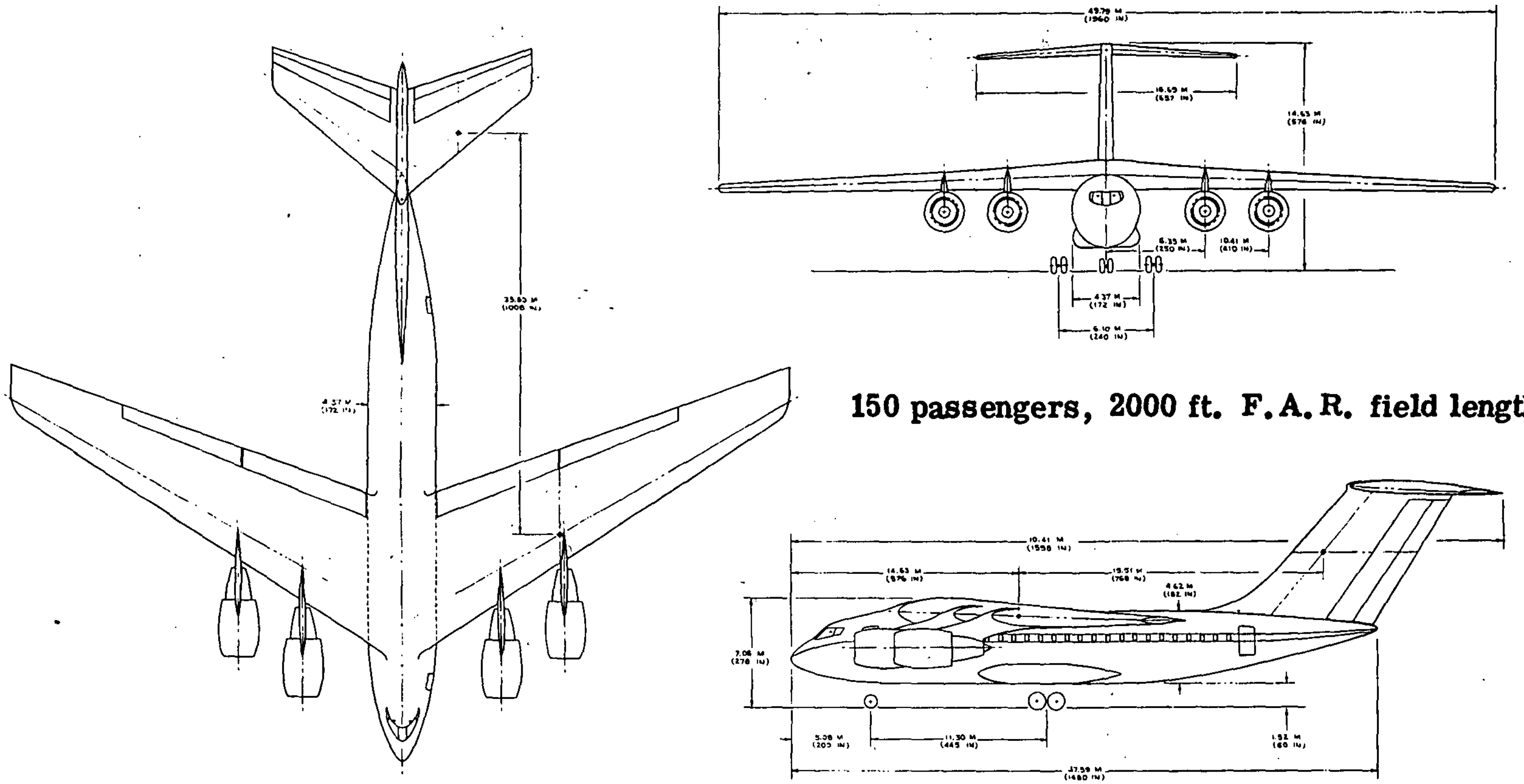

150 passengers, 2000 ft. F.A.R. field length

WING		
AREA (AERODYNAMIC REFERENCE)	331.478 M^2	3568 FT^2
ASPECT RATIO	7.48	
TAPER RATIO	.290	
SWEEP @ C/4	30.0°	
DIHEDRAL	0°	
INCIDENCE (ROOT)	2.0°	
INCIDENCE (TIP)	0°	
MEAN AERODYNAMIC CHORD	7.329 M	288.5 IN
THICKNESS RATIO (ROOT)	.208	
THICKNESS RATIO (MAC)	.157	
THICKNESS RATIO (TIP)	.152	
ROOT CHORD	10.321 M	406.3 IN
TIP CHORD	2.993 M	117.8 IN

HORIZONTAL STABILIZER		
AREA	80.826 M^2	870 FT^2
ASPECT RATIO	3.45	
TAPER RATIO	.400	
LEADING EDGE SWEEP	40.0°	
DIHEDRAL	-3.0°	
MEAN AERODYNAMIC CHORD	5.137 M	202.2 IN
THICKNESS RATIO (ROOT)	.10	
THICKNESS RATIO (TIP)	.10	
ROOT CHORD	6.915 M	272.2 IN
TIP CHORD	2.766 M	108.9 IN
VOLUME COEFFICIENT	.852	

VERTICAL STABILIZER		
AREA	65.404 M^2	704 FT^2
ASPECT RATIO	1.0	
TAPER RATIO	.750	
LEADING EDGE SWEEP	42.0°	
MEAN AERODYNAMIC CHORD	8.142 M	320.6 IN
THICKNESS RATIO	.10	
ROOT CHORD	9.243 M	363.9 IN
TIP CHORD	6.932 M	272.9 IN
VOLUME COEFFICIENT	.0772	

Figure 51 EBF configuration STOL aircraft

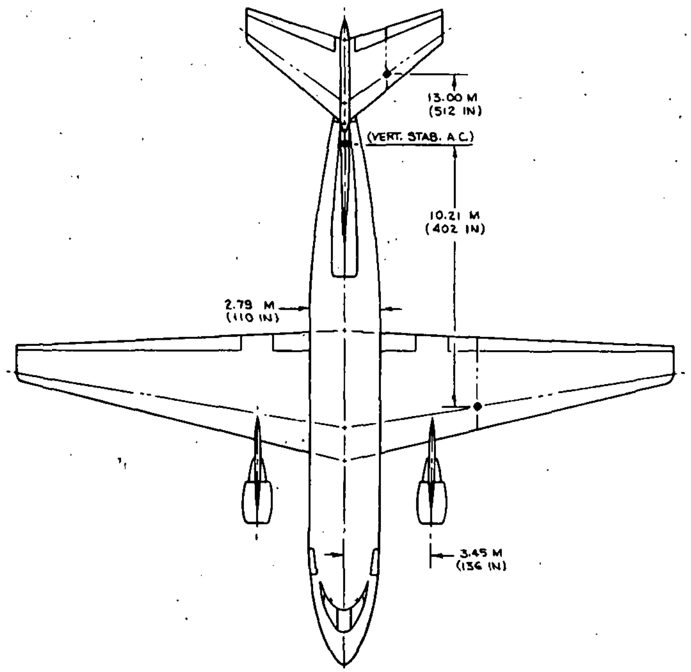

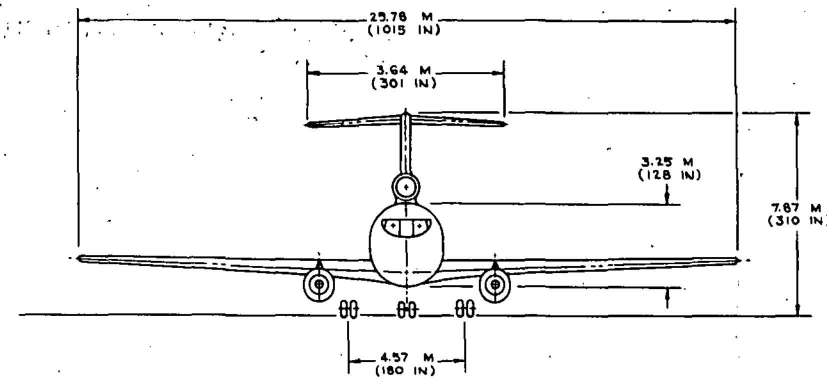

40 passengers, 2500 ft. F.A.R. field length

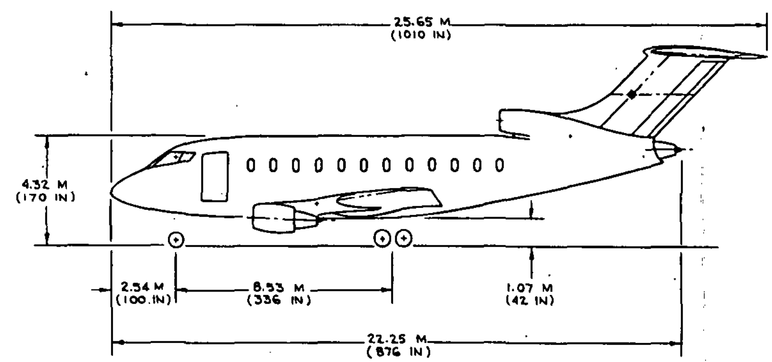

WING		
AREA (AERODYNAMIC REFERENCE)	83.148 M²	895 FT²
ASPECT RATIO	8.00	
TAPER RATIO	.275	
SWEEP @ C/4	9.68°	
DIHEDRAL	3.0°	
INCIDENCE (ROOT)	2.0°	
INCIDENCE (TIP)	0°	
MEAN AERODYNAMIC CHORD	3.571 M	140.6 IN
THICKNESS RATIO (ROOT)	.172	
THICKNESS RATIO (MAC)	.130	
THICKNESS RATIO (TIP)	.127	
ROOT CHORD	5.057 M	199.1 IN
TIP CHORD	1.391 M	54.8 IN

HORIZONTAL STABILIZER		
AREA	17.466 M²	188 FT²
ASPECT RATIO	3.35	
TAPER RATIO	.400	
LEADING EDGE SWEEP	40.0°	
DIHEDRAL	-3.0°	
MEAN AERODYNAMIC CHORD	2.423 M	95.4 IN
THICKNESS RATIO (ROOT)	.10	
THICKNESS RATIO (TIP)	.10	
ROOT CHORD	3.262 M	128.4 IN
TIP CHORD	1.305 M	51.4 IN
VOLUME COEFFICIENT	.795	

VERTICAL STABILIZER		
AREA	10.647 M²	114.6 FT²
ASPECT RATIO	1.0	
TAPER RATIO	1.0	
LEADING EDGE SWEEP	43.5°	
MEAN AERODYNAMIC CHORD	3.263 M	128.5 IN
THICKNESS RATIO	.10	
ROOT CHORD	3.263 M	128.5 IN
TIP CHORD	3.263 M	128.5 IN
VOLUME COEFFICIENT	.0507	

Figure 52 MF configuration STOL aircraft

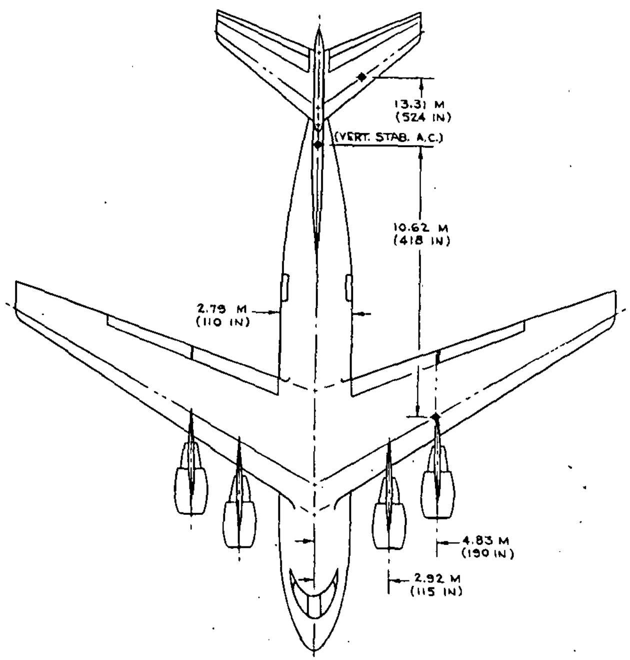

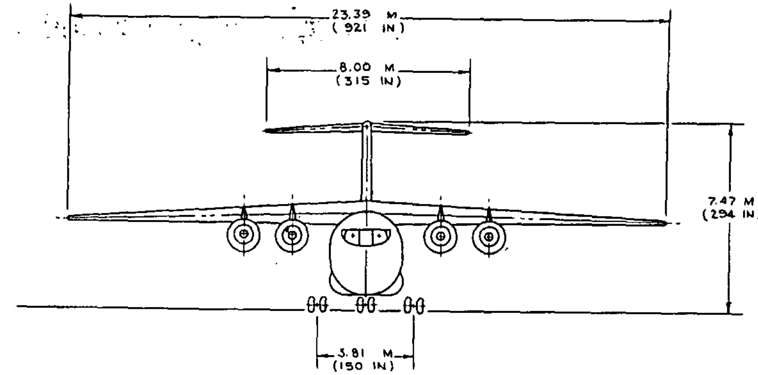

40 passengers, 2500 ft. F.A.R. field length

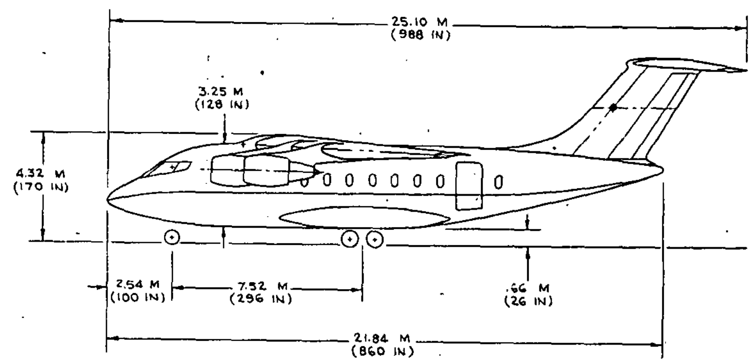

WING

AREA (AERODYNAMIC REFERENCE)	73.208 M²	788 FT²
ASPECT RATIO	7.48	
TAPER RATIO	.288	
SWEEP @ C/4	30.0°	
DIHEDRAL	0°	
INCIDENCE (ROOT)	2.0°	
INCIDENCE (TIP)	0°	
MEAN AERODYNAMIC CHORD	3.447 M	136.7 IN
THICKNESS RATIO (ROOT)	.208	
THICKNESS RATIO (MAC)	.157	
THICKNESS RATIO (TIP)	.152	
ROOT CHORD	4.858 M	191.3 IN
TIP CHORD	1.400 M	55.1 IN

HORIZONTAL STABILIZER

AREA	15.961 M²	171.8 FT²
ASPECT RATIO	4.00	
TAPER RATIO	.400	
LEADING EDGE SWEEP	40.0°	
DIHEDRAL	-3.0°	
MEAN AERODYNAMIC CHORD	2.120 M	83.5 IN
THICKNESS RATIO (ROOT)	.10	
THICKNESS RATIO (TIP)	.10	
ROOT CHORD	2.854 M	112.3 IN
TIP CHORD	1.141 M	44.9 IN
VOLUME COEFFICIENT	.836	

VERTICAL STABILIZER

AREA	10.981 M²	118.2 FT²
ASPECT RATIO	1.0	
TAPER RATIO	1.0	
LEADING EDGE SWEEP	42.0°	
MEAN AERODYNAMIC CHORD	3.336 M	131.4 IN
THICKNESS RATIO	.10	
ROOT CHORD	3.787 M	149.1 IN
TIP CHORD	2.840 M	111.8 IN
VOLUME COEFFICIENT	.0671	

Figure 53 EBF configuration STOL aircraft

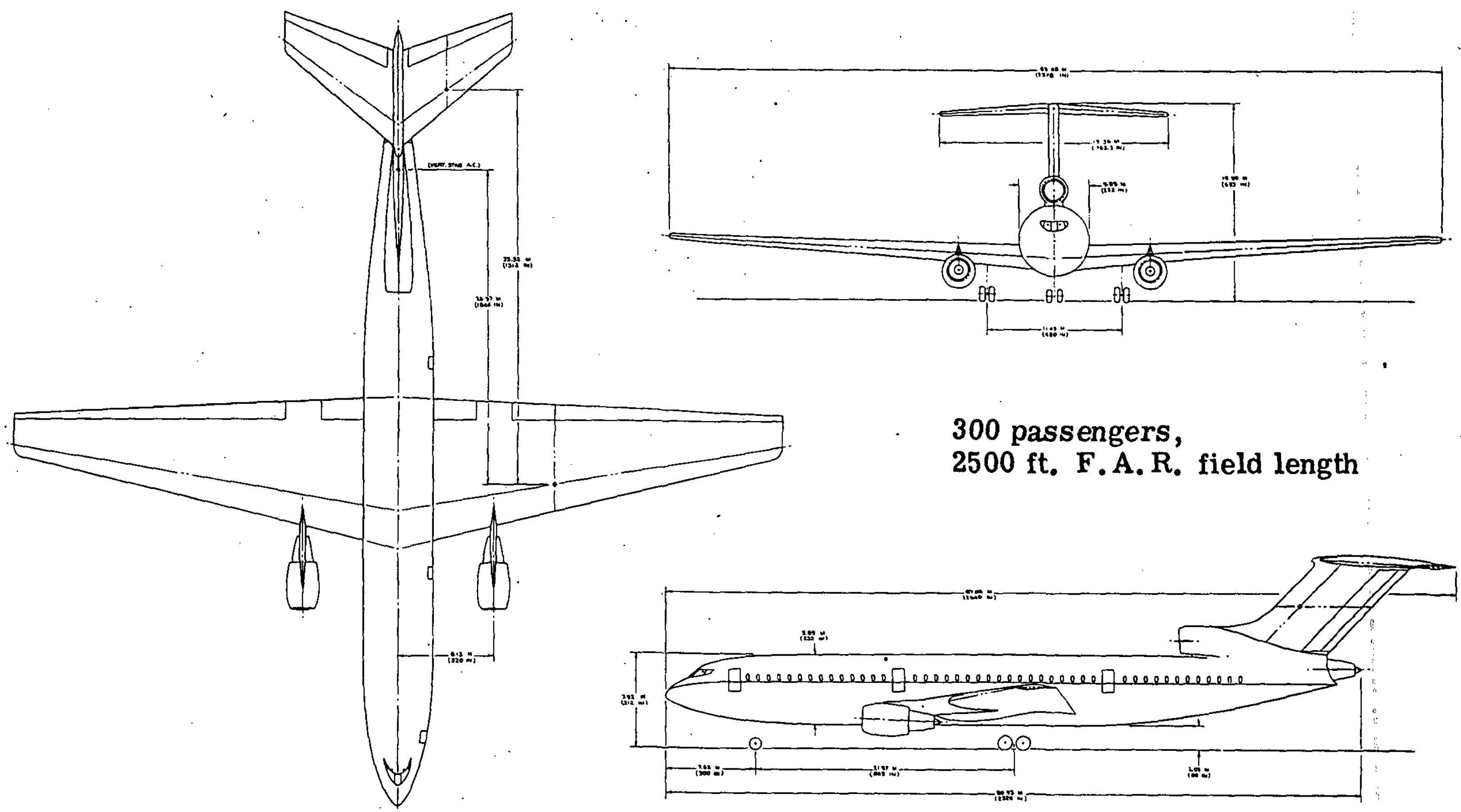

300 passengers,
2500 ft. F.A.R. field length

WING

AREA (AERODYNAMIC REFERENCE)	538.068 M²	5768 FT²
ASPECT RATIO	8.00	
TAPER RATIO	.278	
SWEEP @ C/4	9.68°	
DIHEDRAL	0°	
INCIDENCE (ROOT)	2.0°	
INCIDENCE (TIP)	0°	
MEAN AERODYNAMIC CHORD	9.068 M	356.9 IN
THICKNESS RATIO (ROOT)	.172	
THICKNESS RATIO (MAC)	.130	
THICKNESS RATIO (TIP)	.127	
ROOT CHORD	12.838 M	505.4 IN
TIP CHORD	3.531 M	139.0 IN

HORIZONTAL STABILIZER

AREA	110.926 M²	1194 FT²
ASPECT RATIO	3.30	
TAPER RATIO	.400	
LEADING EDGE SWEEP	40.0°	
DIHEDRAL	-3.0°	
MEAN AERODYNAMIC CHORD	6.076 M	239.4 IN
THICKNESS RATIO (ROOT)	.10	
THICKNESS RATIO (TIP)	.10	
ROOT CHORD	8.184 M	322.2 IN
TIP CHORD	3.274 M	128.9 IN
VOLUME COEFFICIENT	.761	

VERTICAL STABILIZER

AREA	66.983 M²	721 FT²
ASPECT RATIO	1.0	
TAPER RATIO	1.0	
LEADING EDGE SWEEP	43.5°	
MEAN AERODYNAMIC CHORD	8.184 M	322.2 IN
THICKNESS RATIO	.10	
ROOT CHORD	8.184 M	322.2 IN
TIP CHORD	8.184 M	322.2 IN
VOLUME COEFFICIENT	.0887	

Figure 54 MF configuration STOL aircraft

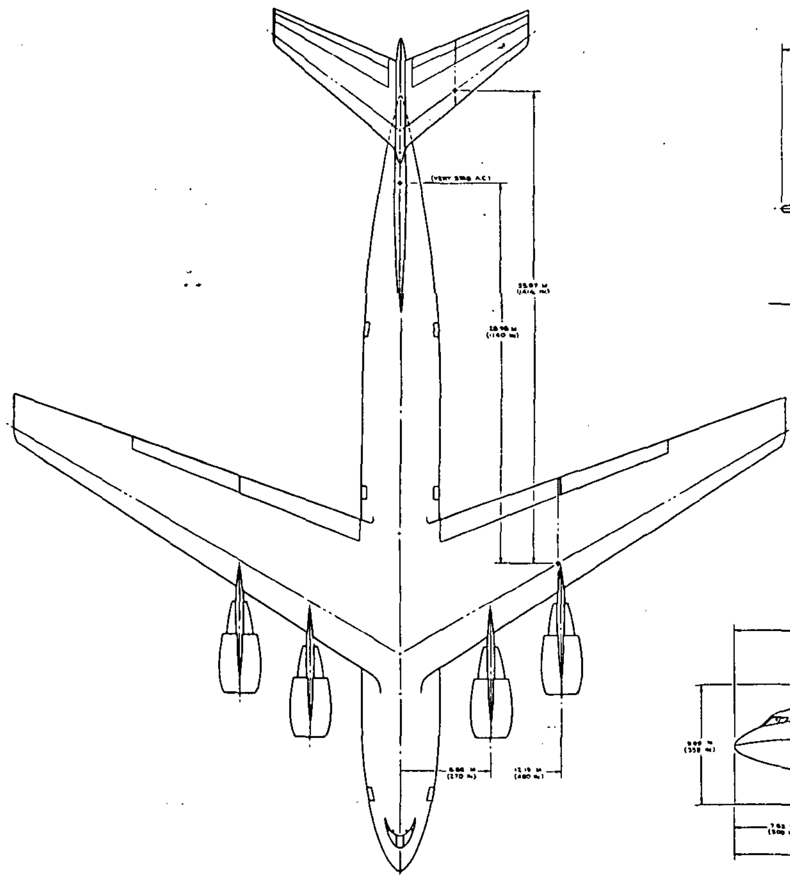

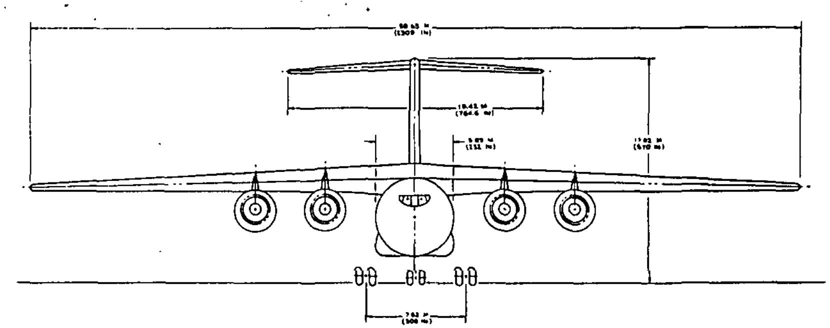

300 passengers,
2500 ft. F.A.R. field length

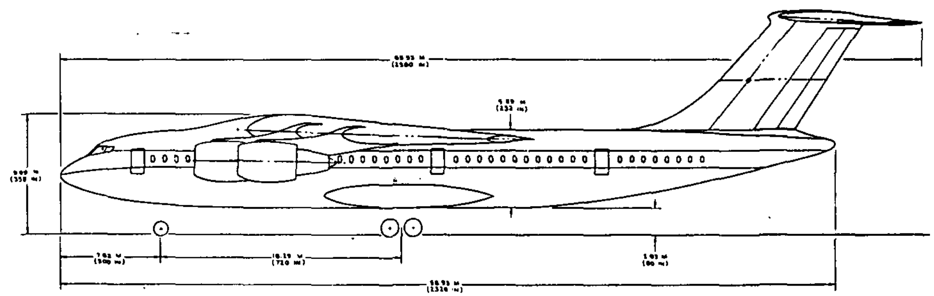

WING

AREA (AERODYNAMIC REFERENCE)	459.870 M²	4950 FT²
ASPECT RATIO	7.48	
TAPER RATIO	.290	
SWEEP @ C/4	30.0°	
DIHEDRAL	0°	
INCIDENCE (ROOT)	3.0°	
INCIDENCE (TIP)	0°	
MEAN AERODYNAMIC CHORD	8.633 M	339.9 IN
THICKNESS RATIO (ROOT)	.206	
THICKNESS RATIO (MAC)	.157	
THICKNESS RATIO (TIP)	.152	
ROOT CHORD	12.157 M	478.6 IN
TIP CHORD	3.525 M	138.8 IN

HORIZONTAL STABILIZER

AREA	82.459 M²	895 FT²
ASPECT RATIO	4.05	
TAPER RATIO	.400	
LEADING EDGE SWEEP	40.0°	
DIHEDRAL	-3.0°	
MEAN AERODYNAMIC CHORD	5.051 M	198.9 IN
THICKNESS RATIO (ROOT)	.10	
THICKNESS RATIO (TIP)	.10	
ROOT CHORD	6.800 M	267.7 IN
TIP CHORD	2.720 M	107.1 IN
VOLUME COEFFICIENT	.657	

VERTICAL STABILIZER

AREA	53.453 M²	563 FT²
ASPECT RATIO	1.0	
TAPER RATIO	.750	
LEADING EDGE SWEEP	45.0°	
MEAN AERODYNAMIC CHORD	8.018 M	315.7 IN
THICKNESS RATIO	.10	
ROOT CHORD	9.134 M	359.6 IN
TIP CHORD	4.068 M	160.0 IN
VOLUME COEFFICIENT	.0661	

Figure 55 EBF configuration STOL aircraft

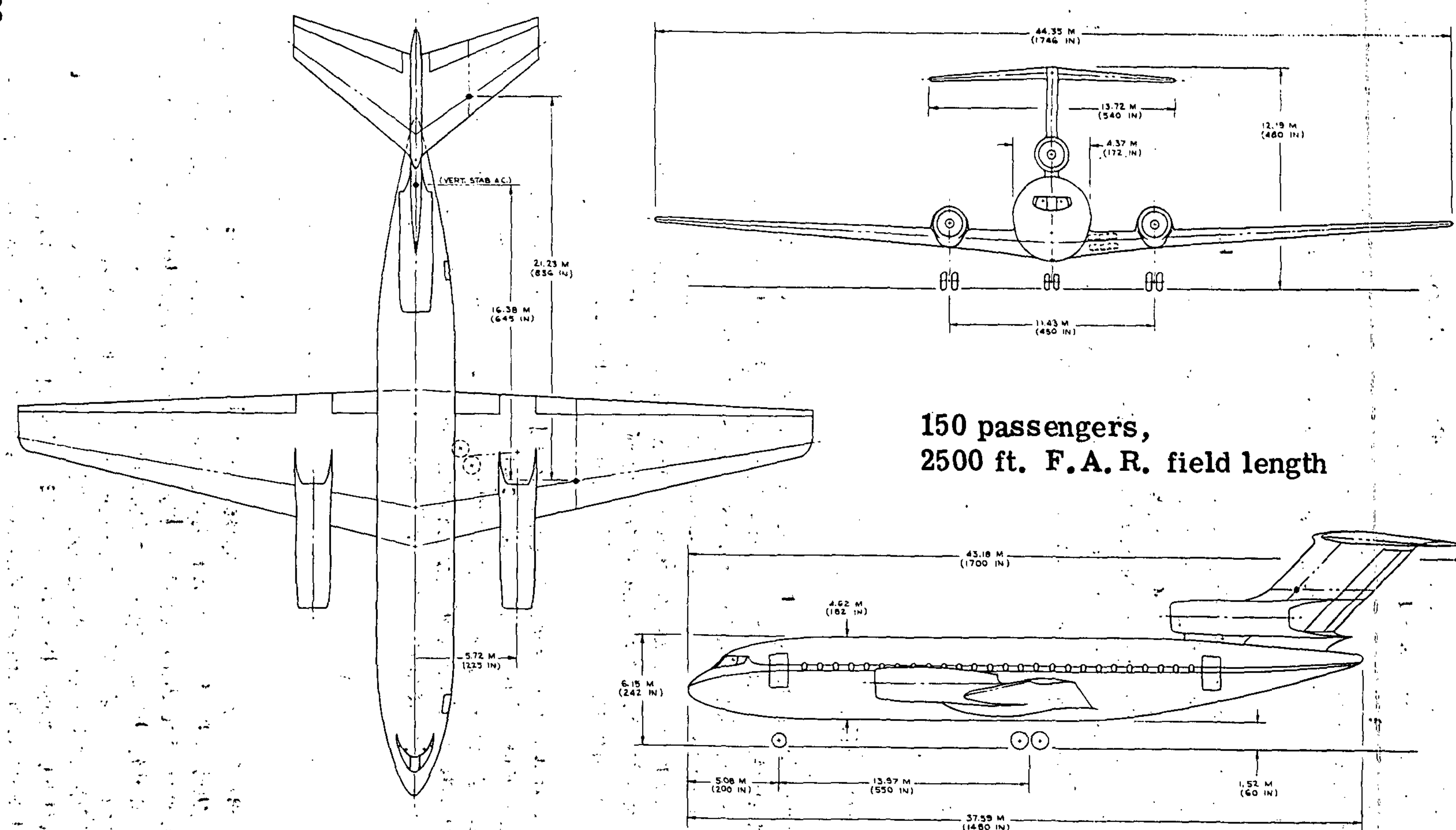

150 passengers,
2500 ft. F.A.R. field length

WING

AREA (AERODYNAMIC REFERENCE)	246.01 M²	2648 FT²
ASPECT RATIO	8.0	
TAPER RATIO	.275	
SWEEP @ C/4	9.3°	
DIHEDRAL	3.0°	
INCIDENCE (ROOT)	2.0°	
INCIDENCE (TIP)	0°	
MEAN AERODYNAMIC CHORD	6.13 M	241.5 IN
THICKNESS RATIO (ROOT)	.172	
THICKNESS RATIO (MAC)	.130	
THICKNESS RATIO (TIP)	.127	
ROOT CHORD	8.69 M	342.0 IN
TIP CHORD	2.39 M	94.0 IN

HORIZONTAL STABILIZER

AREA	54.63 M²	588 FT²
ASPECT RATIO	3.45	
TAPER RATIO	.40	
LEADING EDGE SWEEP	40.0°	
DIHEDRAL	-3.0°	
MEAN AERODYNAMIC CHORD	4.23 M	166.4 IN
THICKNESS RATIO (ROOT)	.10	
THICKNESS RATIO (TIP)	.10	
ROOT CHORD	5.69 M	224.0 IN
TIP CHORD	2.29 M	90.0 IN
VOLUME COEFFICIENT	.769	

VERTICAL STABILIZER

AREA	32.61 M²	351 FT²
ASPECT RATIO	1.0	
TAPER RATIO	1.0	
LEADING EDGE SWEEP	43.5°	
MEAN AERODYNAMIC CHORD	5.69 M	224.0 IN
THICKNESS RATIO	.10	
ROOT CHORD	5.69 M	224.0 IN
TIP CHORD	5.69 M	224.0 IN
VOLUME COEFFICIENT	.0490	

Figure 56 MF configuration STOL aircraft (overwing engine installation)

The 150 passenger, 2,500 foot MF alternate configuration of Figure 56 was not actually sized. The MF configuration on Figure 48 is representative of the geometry described to ASAMP for the purpose of drag and weight. The alternate configuration simply has the same general dimensions but the wing-mounted engines were moved over the wing (OTW). The major advantage of the alternate configuration lies in the possible noise reduction due to shielding of the engines by the wing. Recent studies by Boeing also indicate that lower drag and weight may be realized. This arrangement seems to have many interesting possibilities.

For every MF configuration 3-view there is an EBF configuration 3-view for the same field length and payload to allow a one-for-one size comparison. The payload series were drawn for the 2,500 foot F.A.R. field length to assure that the component parts would "fit" together reasonably. The 2,000 foot F.A.R. field length, 150 passenger airplanes were drawn for the same purpose with the additional objective to determine the engine clearance and position peculiarities as well as the tail sizes. The 3,500 foot F.A.R. field lengths were not drawn since they are similar to conventional airplanes.

8.7 SENSITIVITY STUDIES

8.7.1 GUST LOAD ALLEVIATION

Gross weight reductions to the 150 passenger airplanes provided by gust load alleviation (GLA) are shown on Figure 57. It is extremely advantageous to incorporate a GLA system on the MF airplanes capable of operation from F.A.R. field lengths less than about 2,500 feet. For the 2,000 foot F.A.R. field length the MF configuration is 43 percent lighter with GLA whereas the EBF configuration would only be about 11 percent lighter. A sensitivity to design without GLA is overlayed on the original gross weight comparison chart and shown on Figure 58. Without GLA the EBF configuration would be the lighter airplane for F.A.R. field lengths less than 2,400 feet.

Figure 59 illustrates the most critical requirements from the 18 percent chord full span trailing edge flap segment to alleviate gust loads. The lowest wing loading airplane is used, that is, the 150 passenger, 2,000 foot MF configuration ($W/S = 42$ lbs/ft^2). The figure indicates that at about 180 KEAS, flap deflection is required to offset load factors in excess of 2.5 g's. At 360 KEAS just over four degrees of flap is required to reduce the gust load factor from 4.7 g's to the design load factor of 2.5 g's.

8.7.2 ALTITUDE

A sensitivity to designing the 150 passenger airplanes for cruising at altitudes other than the nominal mission altitude (35,000 feet) is shown on Figure 60. As anticipated, the 2,000 foot MF configuration was quite sensitive to cruising at altitudes less than its optimum cruise altitude of 38,000 feet. However, the penalty for cruising at the 35,000 foot nominal altitude for the design mission was less than one percent. The 2,500 foot EBF configuration demonstrated a cruise altitude sensitivity similar to the 2,500 foot MF configuration indicating a penalty of about 11 percent for designing for cruise at 20,000 feet rather than 35,000 feet. The higher wing loading airplanes are much less sensitive to being designed to cruise at altitudes other than their optimum cruise altitude.

8.7.3 CRUISE MACH NUMBER

The sensitivity to designing the 150 passenger 2,500 foot airplanes for cruising at Mach numbers other than the nominal .8 Mach number is shown on Figure 61. The procedure used to solve for the average wing thickness ratio according to the level of supercritical wing technology assumed was also used in this analysis to determine the thickness required as a function of design cruise Mach number. Specifically, the thickness value used was that which would cause the wing to reach drag divergence at .01 Mach above the design cruise Mach number.

Figure 61 indicates that at about M = .86 the MF and EBF configurations have the same gross weight and for Mach numbers higher than this the EBF is the lighter airplane. Wing thickness causes the MF airplanes to be more sensitive to design Mach number, however, .8 Mach appears to be a very reasonable design Mach number for the study mission for both types of airplanes.

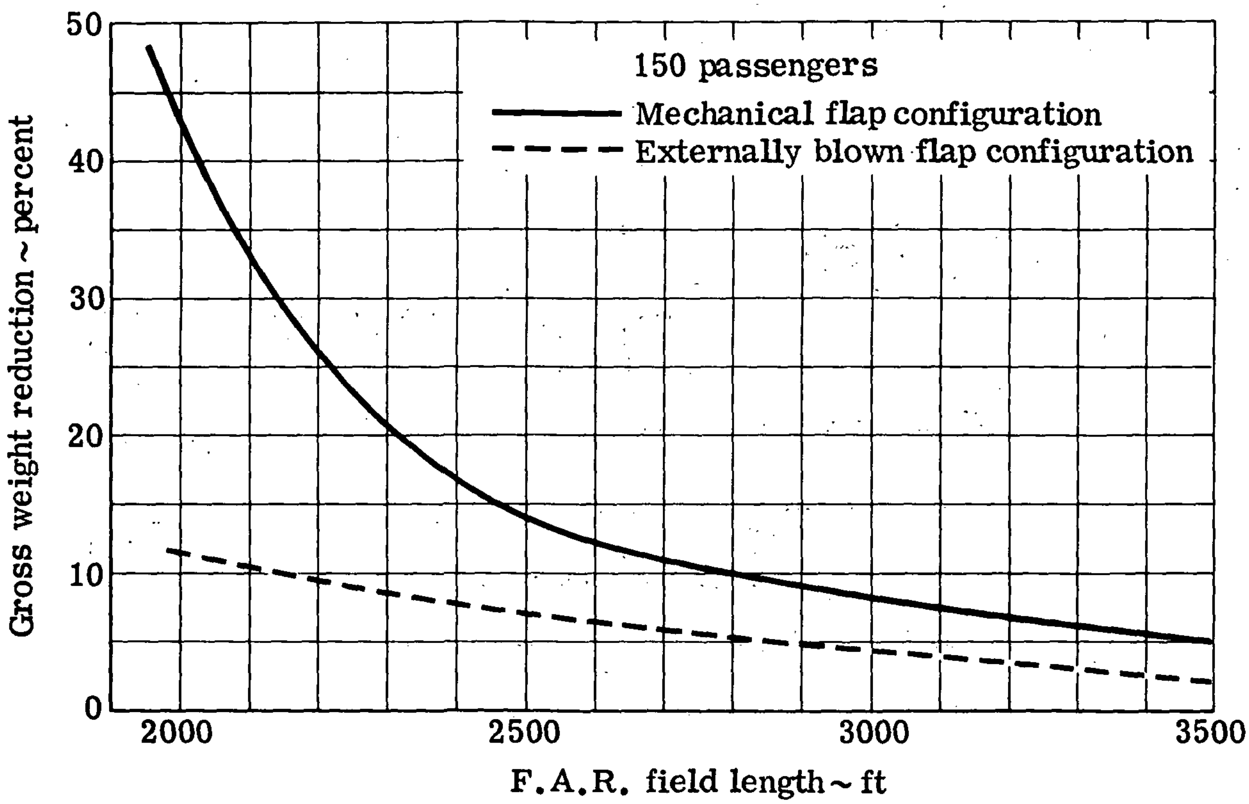

Figure 57 Gross weight reduction provided by gust load alleviation

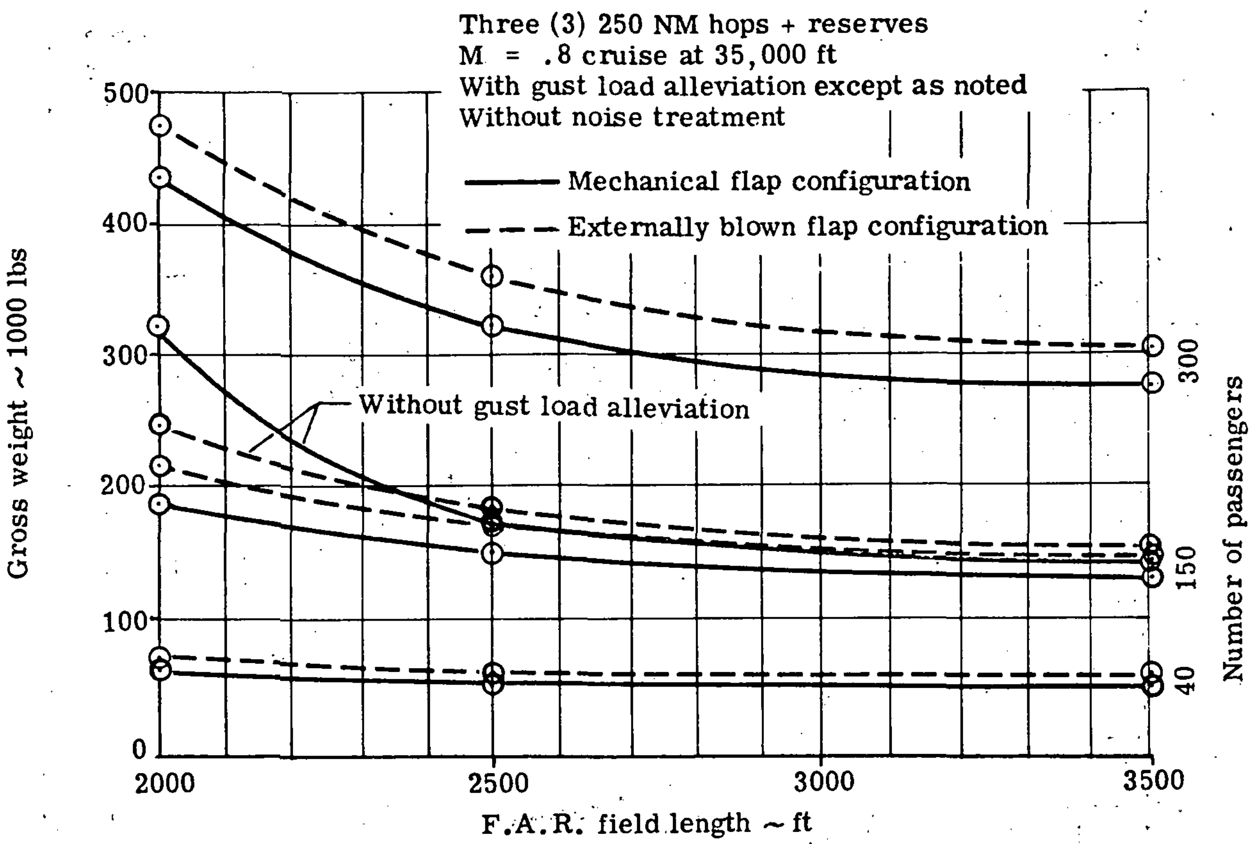

Figure 58 Stol transport-size comparison

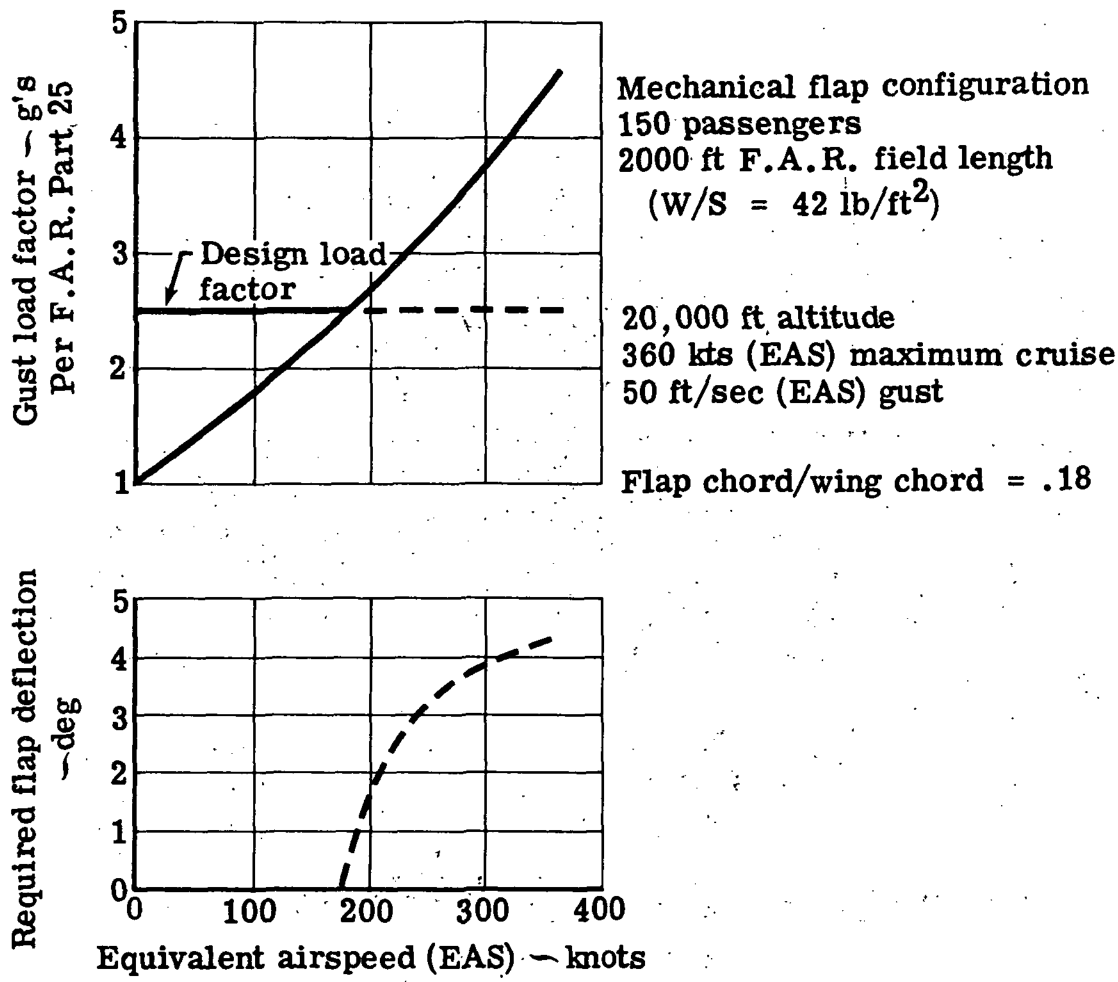

Figure 59 Gust load alleviation requirements

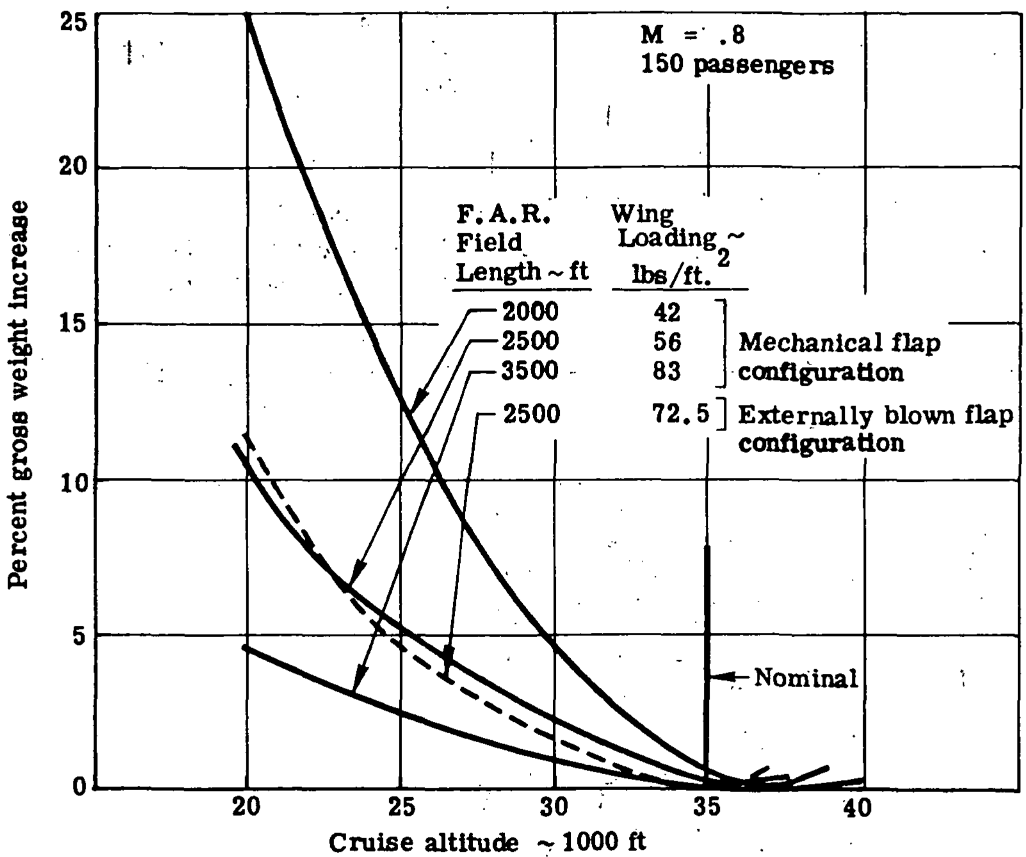

Figure 60 Gross weight sensitivity to cruise altitude

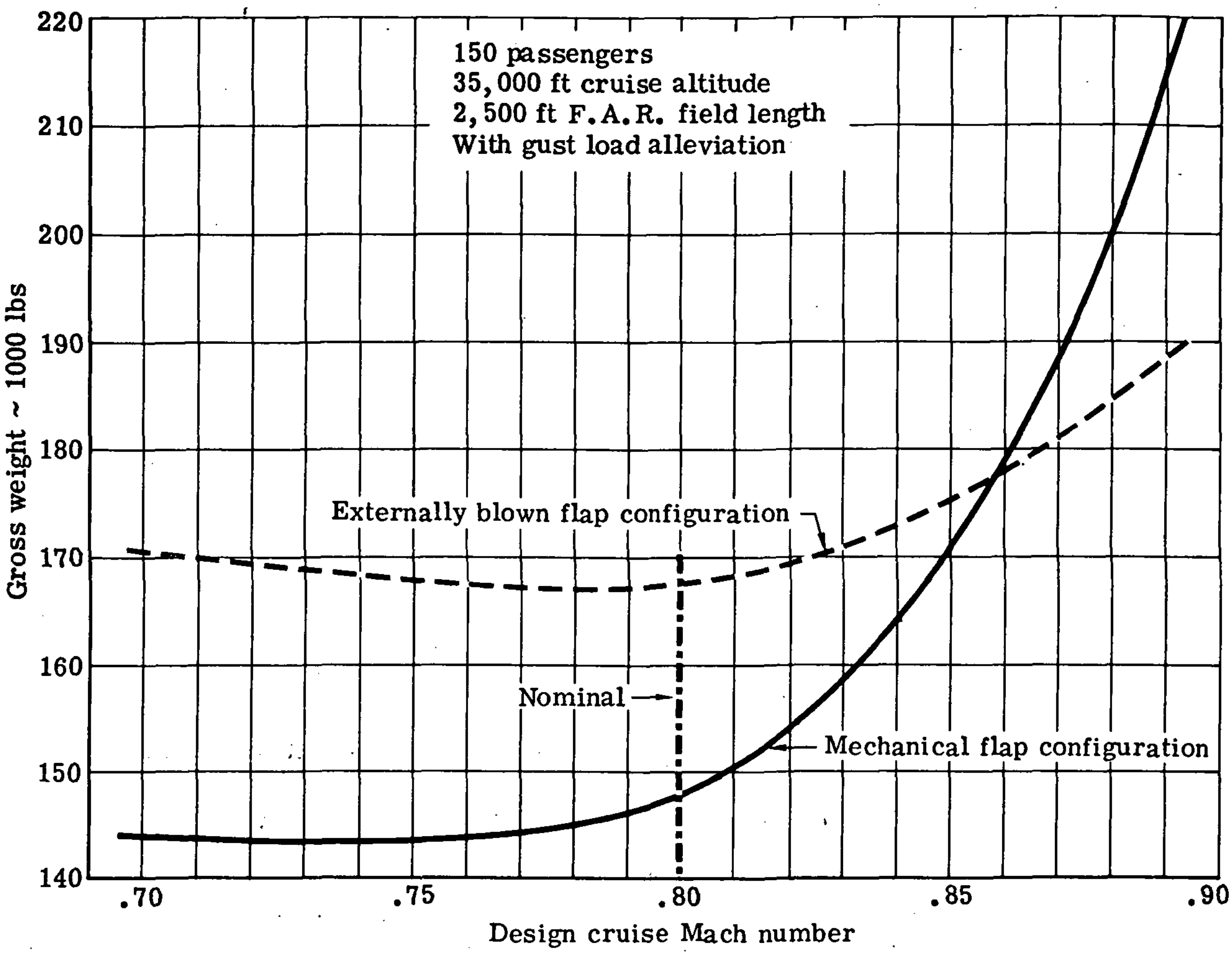

FIGURE 61 Gross weight sensitivity to cruise Mach number

9.0 NOISE

The acoustic analysis of the turbofan powered STOL transports was conducted based on the F.A.R. Part 36 (Reference 18) measuring station locations (See Figure 62). On approach, the noise measuring point is located underneath the flight path, 1 NM from the threshold. At takeoff, the measuring station is located 3.5 NM from brake release underneath the flight path. The maximum sideline noise is determined by finding the location where the EPNL value is a maximum with the measuring station located 500 feet to the side of the flight path.

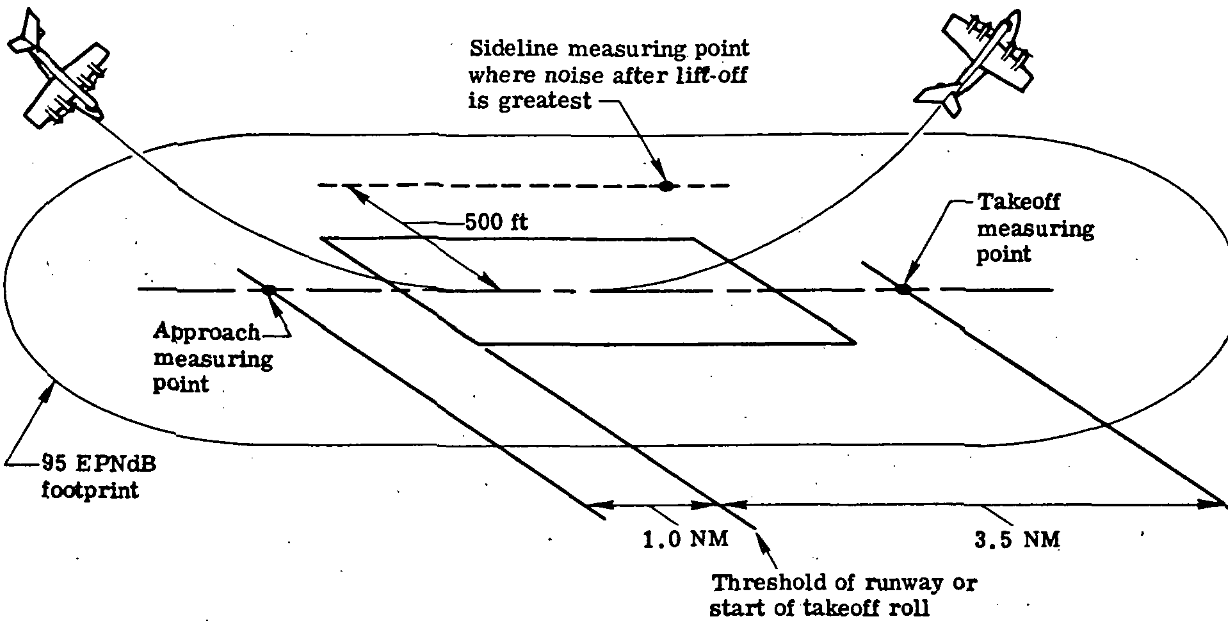

Figure 62 Noise measuring points and data requirement definitions

Additional information on community noise can be gained by developing equal noise contours or "footprints".

In predicting the acoustic characteristics of the engines, the scaling procedure used assumes that the fan tip speed remains constant and that the area and airflow sizing factors are proportional to the change in maximum thrust between the basic engine and the scaled version.

9.1 ESTIMATION METHODOLOGY

The acoustic characteristics of the turbofan engines were estimated using a noise prediction program. The program is designed to calcultate the noise by components. Engine shape factor maps and propulsion maps are used to estimate the subcomponents for the fan noise (i.e., discrete tones, broadband noise and buzz saw noise). The noise due to the jet flow is separated in a component due to the secondary air stream and primary jet. Other noise components are summed together to form core noise (such as turbine noise, combustion noise, etc.). The total noise spectra is the power sum of each of the individual components. The components are predicted at a 150 foot polar arc, at angles relative to the inlet from 10^{o} to 160^{o} at 10^{o} intervals.

The reduction in sound pressure level (SPL) of an acoustic spectrum is usually referred to as applying attenuation to a baseline component spectra. The amount of attenuation for each component should be representative of the attenuation which can be realized and, thus, provide the basis for a balanced design.

The acoustic noise spectrum and airplane flight characteristics are used to determine the perceived noise level by accounting for factors such as the propagation time, the varying distance, the atmospheric attenuation corrections, and directivity index.

The air attenuation corrections considered are atmospheric absorption as a function of distance, relative humidity and temperature, and the extra ground attenuation as a function of elevation angle and distance. The variations in distance are accounted for by the spherical divergence correction which takes the form of:

$$\Delta \mathrm{dB} = 20 \log_{10} \frac{\text{Distance corresponding to the input data}}{\text{Distance corresponding to the projected data}}$$

The corrections due to the doppler shift effect are taken from Reference 21.

The difference in the number of engines between the input and projected condition is corrected by using the relation

$$\Delta \mathrm{dB} = 10 \log_{10} \quad (\text{change in number of engines} + 1)$$

The relative jet velocity correction consists of a frequency shift and a change in SPL level. The frequency shift is calculated as

$$f_{v_1} = f_{v_0} \frac{(V_{jet} - V)_{v_1}}{(V_{jet} - V)_{v_0}}$$

The "0" subscript refers to the initial condition and the "1" subscript refers to the projected condition. The airplane velocity is denoted by "V".

The change in the SPL level is expressed as

$$\Delta \mathrm{dB}_{v_1} = 80 \log_{10} \frac{(V_{jet} - V)_{v_1}}{(V_{jet} - V)_{v_0}}$$

The correction is applied to the primary jet noise only.

The conversion from measured values to subjective units is performed by converting each SPL value to the subjective NOY unit.

The perceived noise levels (PNL) are calculated at each angle by using the relation

$$PNL = 40 + 33.3 \log_{10} NOY_{max} + .15 \left(NOY - NOY_{max} \right)$$

When tone irregularities are present, the PNL value is corrected to a tone corrected PNL by applying a technique which examines the adjacent bands of a SPL spectrum to determine the relative difference in sound pressure levels.

The effective perceived noise level (EPNL) is determined from a time history of the tone corrected PNL as outlined in Reference 18.

9.2 ATTENTUATION

A set of rules were established for describing the growth of airplanes for the penalties of noise attenuation. These rules reflect experience gained by Boeing-Wichita on recent programs. The scaling factors are:

Nacelle Weight Multiplier	=	2.0 (Doubles Nacelle Weight)
Fuel Flow Increase at Constant Thrust	=	4%
Uninstalled Thrust Required	=	4% Increase (airplane installed T/W maintained constant)

The 150 passenger airplanes were resized for noise treatment penalties. The gross weight increase data for noise treatment are shown in Figure 63.

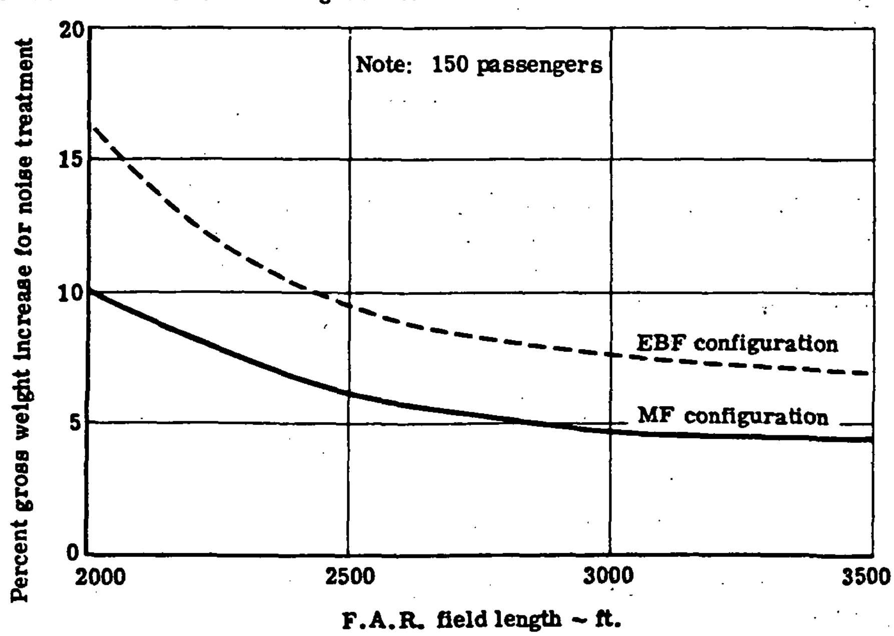

Figure 63 Noise treatment penalties

The pertinent flight path information for each configuration is listed in Table 8. The inlet and aft fan attenuation spectra, Figure 64, represent an increase of 5 dB over the currently available treatment (NASA Lewis Quiet Engine Nacelle) to account for 1975 technology. The jet treatment consists of a 5 dB attenuation, whereas the turbine noise has been attenuated by 10 dB. The noise level increase, due to the under wing blowing for the EBF configuration was estimated to be 10 dB.

TABLE 8 SUMMARY OF FLIGHT PATH DATA

CONFIGURATION	INSTALLED MAXIMUM THRUST PER ENGINE (LBS.)	T/O (AT 3.5 NM FROM B.R.)			APP. (AT 1 NM BEFORE T.D.)		
		ALTITUDE (FT.)	VELOCITY (FT/SEC)	CLIMB ANGLE (DEGREES)	ALTITUDE (FT.)	VELOCITY (FT/SEC)	DESCENT ANGLE (DEGREES)
MF 2000	20,270	3588	129.1	10.1	638	118.2	6.
MF 2500	15,330	2973	146.9	8.6	638	138.4	6.
MF 3500	13,430	2611	177.2	7.9	638	170.5	6.
EBF 2000	28,900	3386	129.1	9.5	638	118.2	6.
EBF 2500	19,930	2462	146.0	7.1	638	138.4	6.
EBF 3500	15,850	2115	179.0	6.4	638	170.5	6.

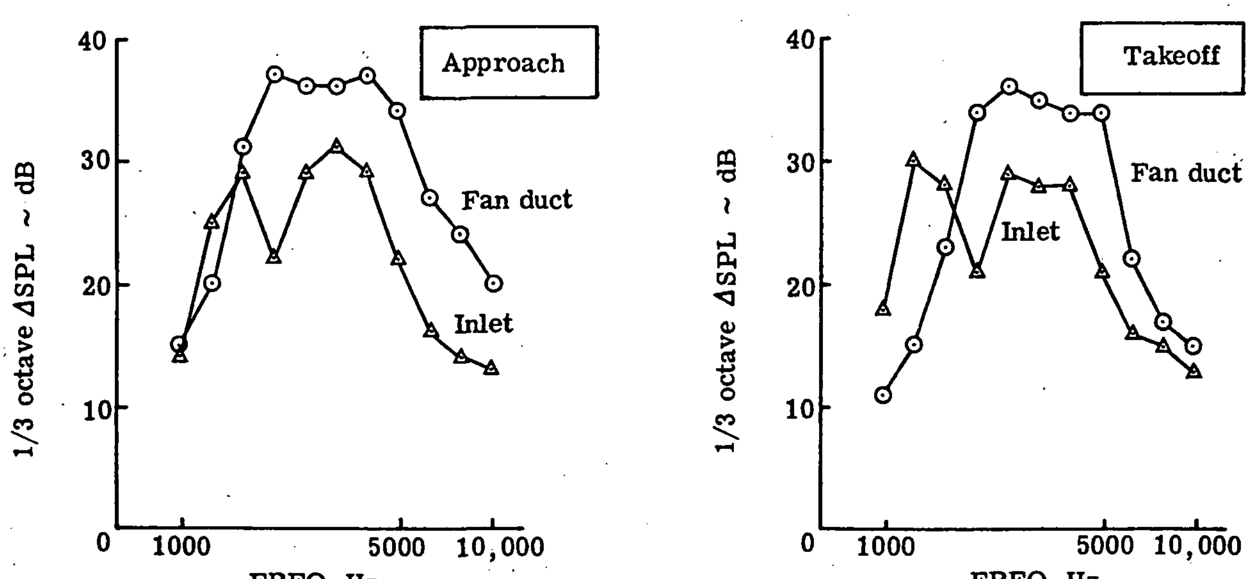

Figure 64
Attenuation spectra for approach and takeoff for the inlet and fan duct

The results are presented on Figure 65. Suppressed engine footprint plots are shown. Information in the table includes areas and 500 foot sideline noise levels for the airplanes before and after suppression. The baseline data before noise treatment are shown in parenthesis. Also shown for comparison are the noise levels at the F.A.R. Part 36 measuring points.

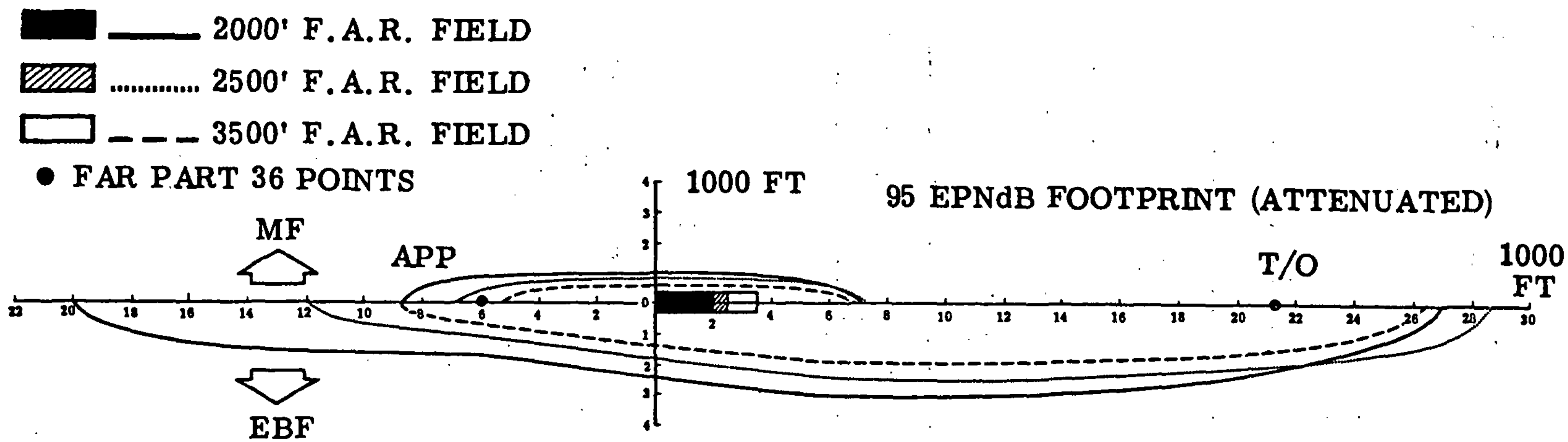

	F.A.R. field length	95 EPNdB footprint area ~ acres		500 ft maximum sideline ~EPNdB	FAA point ~EPNdB	
		App. & T/O	T/O only		Approach	Takeoff
150 passengers Mechanical flap configuration	2000	580 (2,680)*	250 (1,240)	101 (112)	99 (108)	82 (90)
	2500	380 (2,250)	190 (1,430)	99 (112)	96 (105)	83 (92)
	3500	220 (1,750)	140 (1,210)	97 (111)	94 (102)	83 (92)
150 passengers Externally blown flap configuration	2000	3,590 (19,470)	2,650 (10,860)	114 (126)	106 (124)	100 (110)
	2500	2,560 (15,180)	2,200 (9,580)	111 (126)	101 (121)	100 (110)
	3500	1,700 (16,580)	1,530 (12,110)	109 (127)	98 (118)	98 (112)

*Numbers in parenthesis refer to baseline conditions

Figure 65 Summary of acoustic analysis

10.0 DIRECT OPERATING COST

Direct operating costs (DOC) for selected point design airplanes from the set of 18 airplanes used for the sizing study are denoted in Table 9.

TABLE 9 STOL TRANSPORT DATA MATRIX

NUMBER OF PASSENGERS	MECHANICAL FLAP F.A.R. FIELD LENGTH (FT)			EXTERNALLY BLOWN FLAP F.A.R. FIELD LENGTH (FT)		
	2000	2500	3500	2000	2500	3500
40	BASIC	BASIC DOC	BASIC	BASIC	BASIC DOC	BASIC
150	BASIC NT DOC DOC (NT)	BASIC NT DOC DOC (NT)	BASIC NT DOC DOC (NT)	BASIC NT DOC DOC (NT)	BASIC NT DOC DOC (NT)	BASIC NT DOC DOC (NT)
300	BASIC	BASIC DOC	BASIC	BASIC	BASIC DOC	BASIC

BASIC = SIZED WITHOUT NOISE TREATMENT
NT = SIZED WITH NOISE TREATMENT
DOC = DOC'S CALCULATED FOR AIRPLANES WITHOUT NOISE TREATMENT
DOC (NT) = DOC'S CALCULATED FOR AIRPLANES WITH NOISE TREATMENT

The DOC's were calculated using modified ATA rules according to an agreement between NASA-Ames, Lockheed and McDonnell Douglas. These rules were used during the first phase of their studies entitled, "Study of Quiet Turbofan STOL Aircraft For Short-Haul Transportation". Table 10 is a listing of the adjustments to the 1967 ATA formula to account for STOL operation.

TABLE 10 D.O.C. FORMULA MODIFICATIONS

Adjustments To 1967 ATA Cost Formula Per 1972 NASA-Ames Modification For STOL

Crew pay (3-man subsonic jet)	40% increase
Fuel	11.5% increase
Maintenance labor rate	50% increase
Airframe maintenance - hourly	25% decrease
Airframe maintenance - cycle	25% decrease
Engine investment spares ratio	37.5% decrease
Utilization (hours/year)	2500

All other ATA rules and conservatisms remained the same except for reserves. Reserve fuel is available for a one-half hour loiter at 30,000 feet, plus a climb, cruise and descent to an alternate field 100 NM away. The alternate field cruise is at best range speed at 15,000 feet.

Airframe and engine prices vary according to the curves on Figures 66 and 67, respectively. The summation of the two, accounting for number of engines, is the total airplane price. The prices are indicative of an airplane that would be used at least 3,500 block hours per year.

Typical input information for the 150 passenger, 2,500 ft. STOL airplanes for a 500 NM non-stop trip is shown in Table 11. This set of data and all DOC curves to be presented are for cruise at M = .8 at 35,000 feet. Weight of one passenger and baggage was assumed to be 200 lbs. and the passenger load factor was 100 percent. For DOC estimation the agreed upon annual utilization value is 2,500 block hours per year; however, as noted above, the airplane prices were based on a utilization of about 3,500 block hours per year. DOC's are presented in 1972 dollars.

A variation of DOC with range for the airplanes described in Table 11 is shown on Figure 68(a). Sensitivity to number of passengers is shown on Figure 68(b) assuming 2,500 feet F.A.R. field length capability. The sensitivity to F.A.R. field length for 150 passenger airplanes is shown on Figure 68(c). The percent DOC increase for the same airplanes with noise treatment is shown on Figure 68(d).

These trades indicate that trip distances of at least 400 NM are desirable, that 150 passengers is near optimum and that field lengths longer than 2,500 feet are more economical especially when the noise treatment penalties are considered.

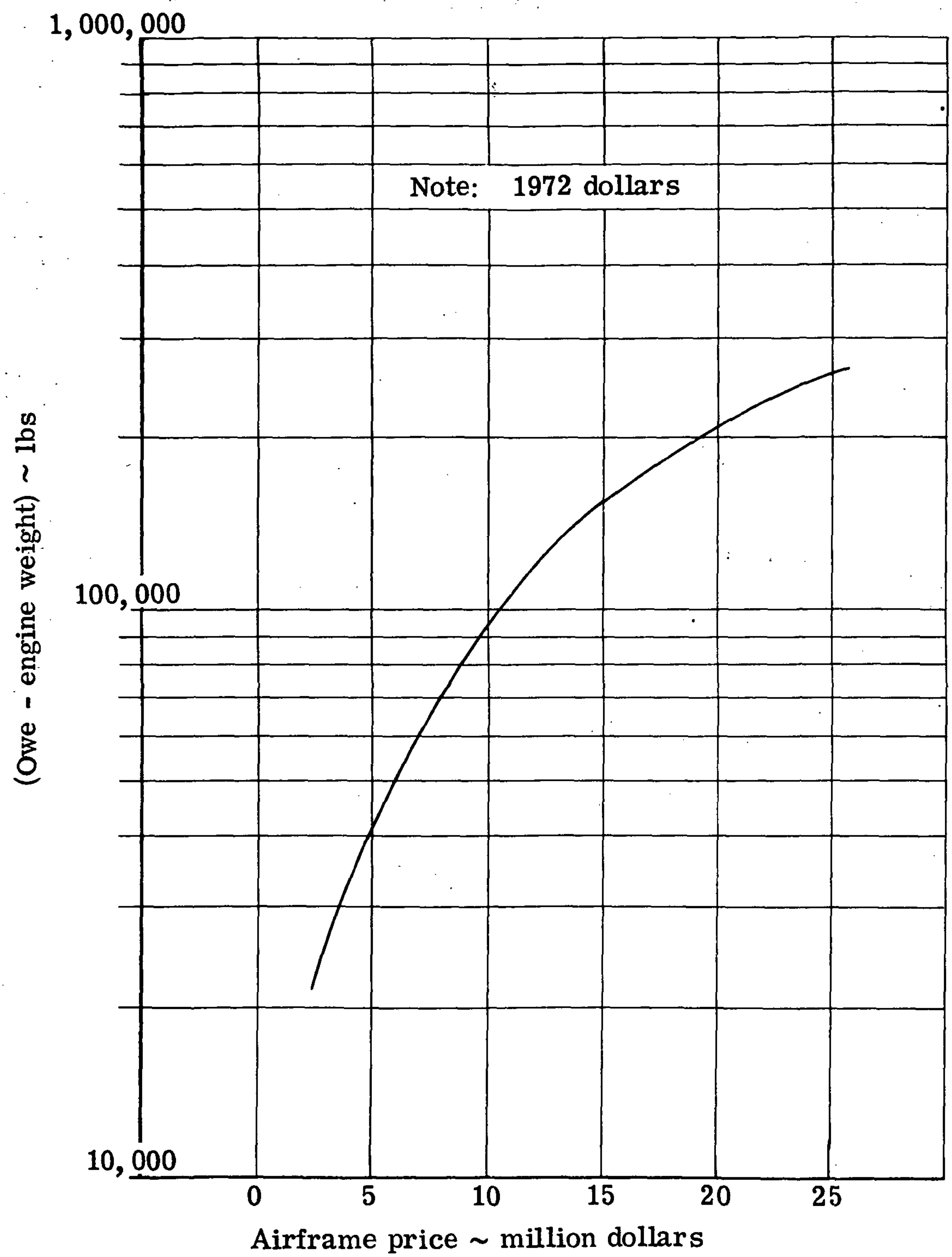

Figure 66 Airframe prices

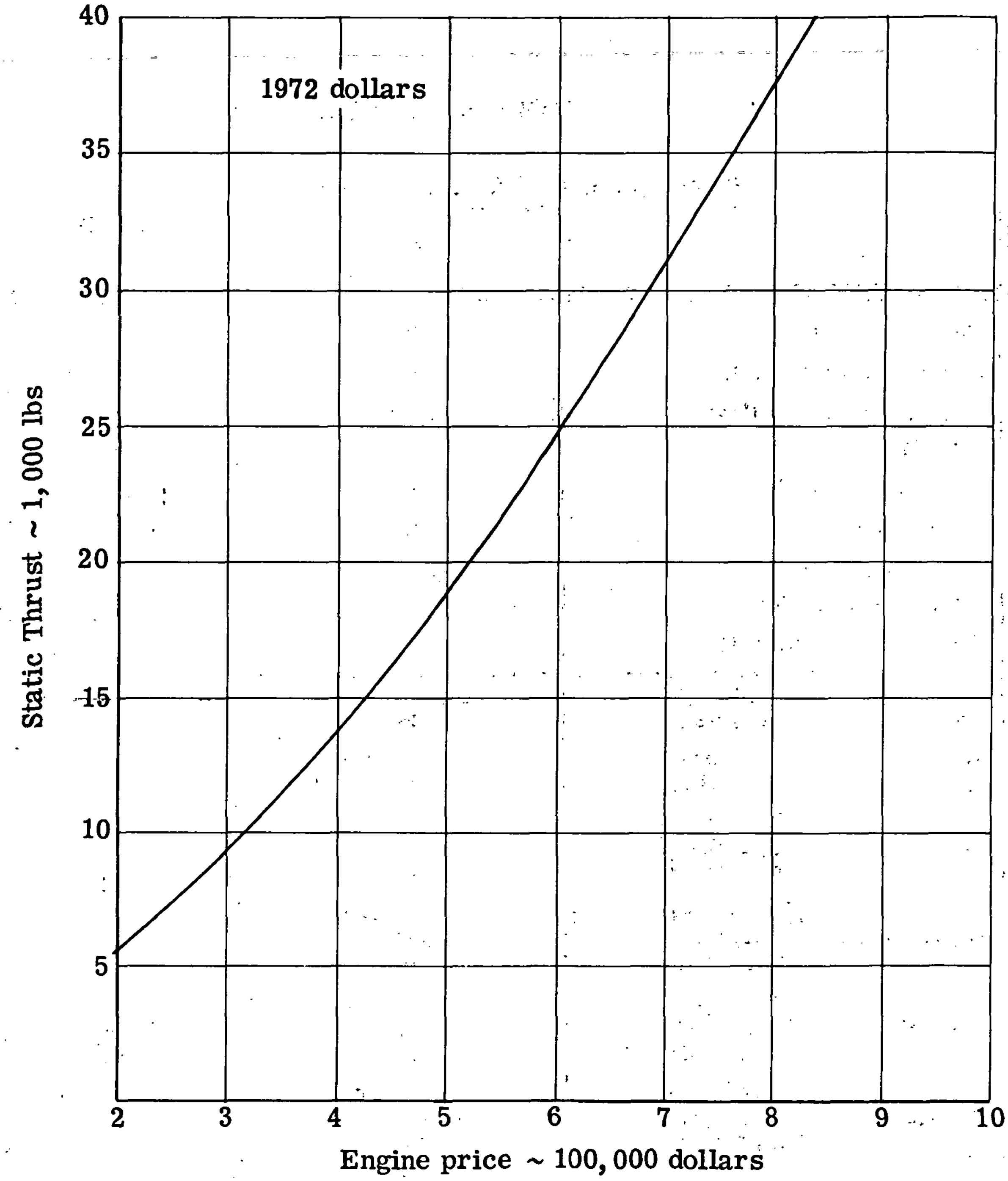

Figure 67 Engine prices

TABLE 11 DIRECT OPERATING COST INPUT

Trip Distance = 575 SM (500NM)

		Mechanical Flap Configuration	Externally Blown Flap Configuration
No. passengers		150	150
F.A.R. field length (ft)		2,500	2,500
Total gross weight (lbs)		148,300	167,800
OWE (lbs)		96,500	111,700
Fuel capacity (lbs)		21,800	26,000
Total engine weight (lbs)		7,000	12,100
Thrust/eng. (lbs)		15,350	19,900
Total A/P cost ($M)		11	12.4
Cost of one engine ($M)		.467	.500
Ground Maneuver	Time (hrs)	.100	.100
	Fuel (lbs)	120	225
Air Maneuver	Time (hrs)	.067	.067
	Fuel (lbs)	240	330
Climb	Time (hrs)	.285	.144
	Fuel (lbs)	2,740	2,560
	Dist (NM)	83	52
Acceleration	Time (hrs)	.100	.014
	Fuel (lbs)	600	155
	Dist (NM)	40	6
Descent	Time (hrs)	.117	.117
	Fuel (lbs)	330	390
	Dist (NM)	50	50
Cruise	Time* (hrs)	.776	.918
	Fuel* (lbs)	4,940	6,360
	Dist* (NM)	358	423
Block Time (hrs)		1.445	1.360
Block Fuel (lbs)		8,970	10,020

*Standard ATA airway distance increment and traffic allowance included

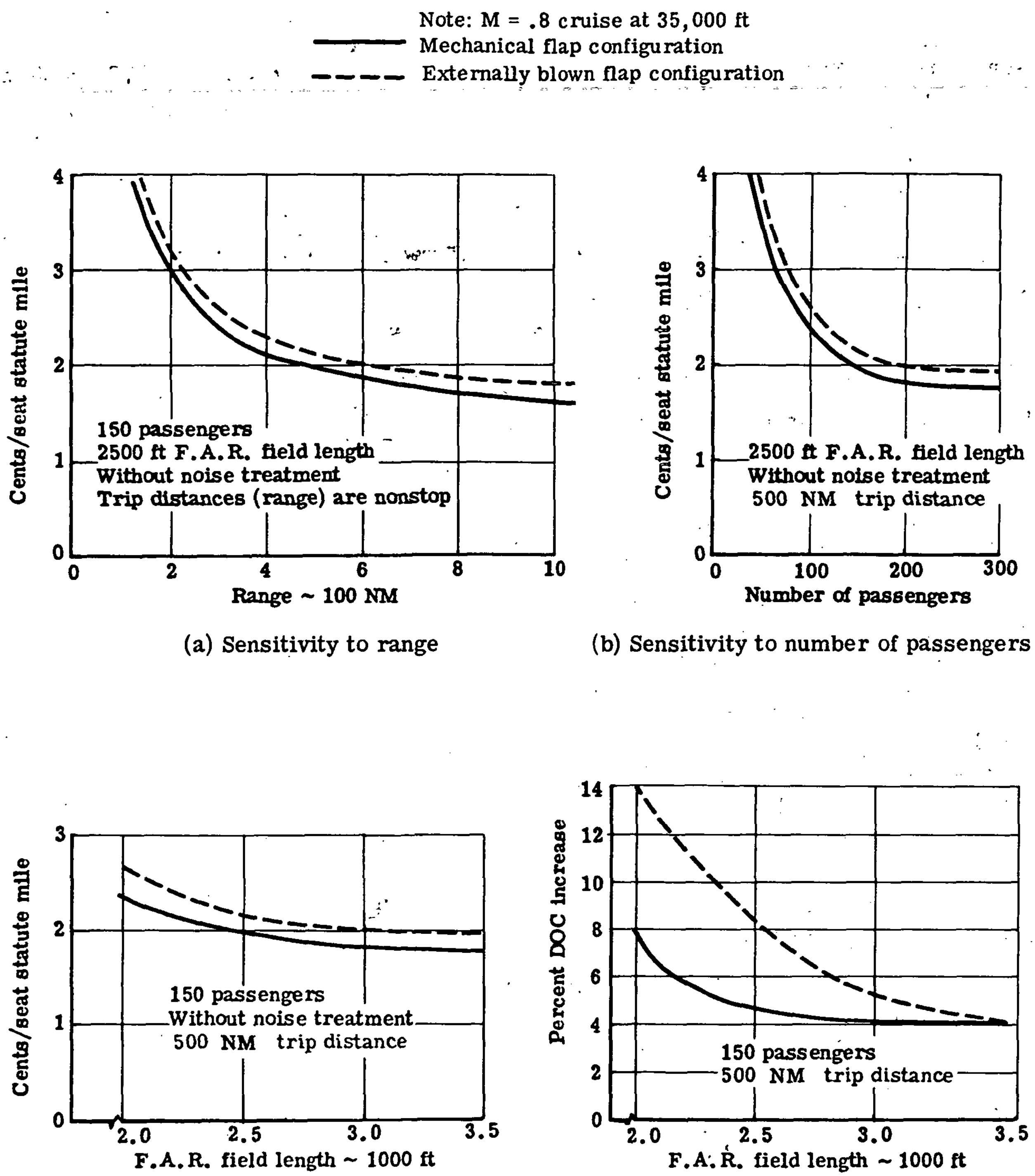

(a) Sensitivity to range

(b) Sensitivity to number of passengers

(c) Sensitivity to field length

(d) Sensitivity to noise treatment

Figure 68 D.O.C. trade study

11.0 CONCLUDING REMARKS

A conclusion of the feasibility study of Reference 1 was that through the use of modern control systems technology to provide ride smoothing, a low-wing-loading mechanical flap STOL airplane appears competitive with a high-wing-loading powered lift design (airplane Model 751 of Reference 1). Because powered lift was not relied upon, the resulting configuration offered advantages in system simplicity, reliability, and safety. A more significant conclusion of the present study is that through the use of an active control system for gust load alleviation, as well as for ride smoothing, and for the powered-lift airworthiness standards assumed, low-wing-loading mechanical flap airplanes are competitive with externally blown flap airplanes over a wide range of payloads and field lengths. Therefore, advantages in system simplicity, reliability, and safety can be realized regardless of the size of the airplane or the STOL field length.

For the range of field lengths and payloads investigated the MF configurations were lighter, quieter and more economical than the EBF configurations.

On the average the EBF airplanes were about 12 percent heavier than the MF airplanes for the same mission and field length.

Gust load alleviation provides a large gross weight reduction for airplanes with field lengths shorter than 2,500 feet. Without gust load alleviation the MF airplanes were heavier than the EBF airplanes for field lengths less than about 2,400 ft.

The EBF configurations are very sensitive to landing approach safety margins and go-around procedures. The EBF configuration approach speed was constrained by a requirement to have a $\Delta\alpha$ safety margin of 15 degrees for vertical gust protection at the approach power setting. Installed T/W was designed by a requirement to maintain level flight after loss of the most critical engine with the approach flap setting. As an example of the sensitivity consider a reduction of the $\Delta\alpha$ = 15 degree gust margin to 10 degrees which would offer less gust protection than today's CTOL airplanes; and allow a slight descent after engine failure. The EBF airplane could approach at a lower speed (have higher wing loading) and could possibly be designed with a lower installed T/W (depends on whether or not the required go-around climb gradient becomes critical). Preliminary analyses indicate that this combination would result in an 11 percent gross weight reduction.

The MF airplanes have a $1.3V_S$ approach speed which allows 16 degrees of margin for gust protection and they can meet the engine out climb gradients without a configuration change.

The EBF configurations require more complex vertical and horizontal tails to keep the surfaces from being excessively large.

The EBF airplane maximum sideline noise is about 12 EPNdB higher than the MF airplane at 500 feet. The 95 EPNdB footprint acreage of the EBF airplane is 11 times as large as the MF airplane for takeoff and a factor of 7 larger for the summation of approach and takeoff.

The EBF airplane DOC is about 10 percent higher than the MF airplane in terms of cents per seat statute miles versus range in nautical miles. This percentage remains fairly constant for the DOC sensitivity to payload and the DOC sensitivity to field length. In addition to the above comparison cost analyses for both the MF configuration and the EBF configuration show that: trip distances less than 400 NM begin to get expensive; a 150 passenger payload and 2,500 feet F.A.R. field length are reasonable design goals.

Page intentionally left blank

12.0 APPENDICES

12.1 APPENDIX A GROUP WEIGHT STATEMENTS

Final ASAMP predicted group weight statements are presented and the locations are noted in the following table:

Number of Passengers	F.A.R. Field Lendth					
	2000 Feet		2500 Feet		3500 Feet	
	MF	EBF	MF	EBF	MF	EBF
40	TABLE 12	TABLE 13	TABLE 14	TABLE 15	TABLE 16	TABLE 17
150	TABLE 18	TABLE 19	TABLE 20	TABLE 21	TABLE 22	TABLE 23
300	TABLE 24	TABLE 25	TABLE 26	TABLE 27	TABLE 28	TABLE 29

TABLE 12 GROUP WEIGHT STATEMENT
MF configuration, 40 passengers, 2000 ft. F.A.R. field length

ASAMP WEIGHTS

		WEIGHT		
PROPULSION GROUP				
	PRIMARY ENGINES	2970.	K5 =	1.00
	ENGINE ACCESSORIES	186.	K5 =	1.00
	ENGINE CONTROLS	150.	K3 =	1.00
	ENGINE STARTING SYSTEM	143.	K2 =	1.00
	THRUST REVERSERS	253.		
	FUEL SYSTEM	310.	K21=	1.00
	PROPULSION WEIGHT INCREMENT	0.		
TOTAL PROPULSION GROUP WEIGHT		4012.		
STRUCTURES GROUP				
	WING	9282.	K8 =	1.00
	HORIZONTAL TAIL	1179.	K9 =	1.00
	VERTICAL TAIL	1034.	K10=	1.00
	FUSELAGE	9425.	K11=	1.29
	LANDING GEAR	3628.	K12=	1.58
	ENGINE STRUTS	0.	K20=	1.00
	ENGINE NACELLES	435.	K14=	1.00
	ENGINE DUCT	372.		
	ENGINE MOUNT	33.		
	STRUCTURE WEIGHT INCREMENT	0.		
TOTAL STRUCTURE WEIGHT		25388.		
FIXED EQUIPMENT				
	INSTRUMENTS	582.	K4 =	1.00
	SURFACE CONTROLS	983.	K16=	1.04
	HYDRAULICS	805.	K17=	1.35
	PNEUMATICS	403.	K17=	1.35
	ELECTRICALS	780.	K6 =	1.00
	ELECTRONICS	983.	K7 =	1.28
	FLIGHT DECK ACCOMMODATIONS	676.	K15=	1.00
	PASSENGER ACCOMMODATIONS	1971.		
	CARGO ACCOMMODATION	235.	K13=	0.67
	EMMERGENCY EQUIPMENT	231.	K18=	1.12
	AIR CONDITIONING	466.		
	ANTI-ICING	261.		
	APU	769.		
	FIXED EQUIP. WEIGHT INCREMENT	0.		
TOTAL FIXED EQUIPMENT WEIGHT		9144.		
MANUFACTURERS EMPTY WEIGHT		38544.		
WEIGHT OF STANDARD AND OPERATIONAL ITEMS		1201.	K19=	1.00
OPERATIONAL EMPTY WEIGHT		39746.		
PAYLOAD		8000.		
FUEL		9652.		
GROSS WEIGHT		57398.		

TABLE 13 GROUP WEIGHT STATEMENT
EBF configuration, 40 passengers, 2000 ft. F.A.R. field length

ASAMP WEIGHTS			
PROPULSION GROUP	WEIGHT		
PRIMARY ENGINES	5556.	K5 =	1.00
~~ENGINE ACCESSORIES~~	272.	K5 =	1.00
ENGINE CONTROLS	150.	K3 =	1.00
~~ENGINE STARTING SYSTEM~~	208.	K2 =	1.00
THRUST REVERSERS	956.		
~~FUEL SYSTEM~~	379.	K21=	1.00
PROPULSION WEIGHT INCREMENT	0.		
TOTAL PROPULSION GROUP WEIGHT	7521.		
STRUCTURES GROUP			
WING	8797.	K8 =	1.00
~~HORIZONTAL TAIL~~	1859.	K9 =	1.00
VERTICAL TAIL	1544.	K10=	1.00
~~FUSELAGE~~	10972.	K11=	1.29
LANDING GEAR	4278.	K12=	1.58
~~ENGINE STRUTS~~	1352.	K20=	1.00
ENGINE NACELLES	814.	K14=	1.00
~~ENGINE DUCT~~	0.		
ENGINE MOUNT	0.		
~~STRUCTURE WEIGHT INCREMENT~~	0.		
~~TOTAL STRUCTURE WEIGHT~~	29616.		
~~FIXED EQUIPMENT~~			
~~INSTRUMENTS~~	589.	K4 =	1.00
SURFACE CONTROLS	1379.	K16=	1.02
~~HYDRAULICS~~	729.	K17=	1.18
PNEUMATICS	384.	K17=	1.18
~~ELECTRICALS~~	780.	K6 =	1.00
ELECTRONICS	918.	K7 =	1.14
~~FLIGHT DECK ACCOMMODATIONS~~	676.	K15=	1.00
PASSENGER ACCOMMODATIONS	1971.		
~~CARGO ACCOMMODATION~~	235.	K13=	0.67
EMMERGENCY EQUIPMENT	264.	K18=	1.12
~~AIR CONDITIONING~~	466.		
ANTI-ICING	264.		
~~APU~~	769.		
FIXED EQUIP. WEIGHT INCREMENT	0.		
TOTAL FIXED EQUIPMENT WEIGHT	9425.		
MANUFACTURERS EMPTY WEIGHT	46562.		
WEIGHT OF STANDARD AND OPERATIONAL ITEMS	1217.	K19=	1.00
OPERATIONAL EMPTY WEIGHT	47779.		
PAYLOAD	8000.		
FUEL	11906.		
GROSS WEIGHT	67686.		

TABLE 14 GROUP WEIGHT STATEMENT

MF configuration, 40 passengers, 2500 ft. F. A. R. field length

ASAMP WEIGHTS

PROPULSION GROUP	WEIGHT		
PRIMARY ENGINES	2419.	K5 =	1.00
ENGINE ACCESSORIES	164.	K5 =	1.00
ENGINE CONTROLS	150.	K3 =	1.00
ENGINE STARTING SYSTEM	143.	K2 =	1.00
THRUST REVERSERS	39.		
FUEL SYSTEM	269.	K21=	1.00
PROPULSION WEIGHT INCREMENT	0.		
TOTAL PROPULSION GROUP WEIGHT	3184.		
STRUCTURES GROUP			
WING	5856.	K8 =	1.00
HORIZONTAL TAIL	780.	K9 =	1.00
VERTICAL TAIL	734.	K10=	1.00
FUSELAGE	9273.	K11=	1.29
LANDING GEAR	3168.	K12=	1.58
ENGINE STRUTS	0.	K20=	1.00
ENGINE NACELLES	354.	K14=	1.00
ENGINE DUCT	336.		
ENGINE MOUNT	27.		
STRUCTURE WEIGHT INCREMENT	0.		
TOTAL STRUCTURE WEIGHT	20529.		
FIXED EQUIPMENT			
INSTRUMENTS	576.	K4 =	1.00
SURFACE CONTROLS	984.	K16=	1.03
HYDRAULICS	738.	K17=	1.27
PNEUMATICS	355.	K17=	1.27
ELECTRICALS	780.	K6 =	1.00
ELECTRONICS	898.	K7 =	1.21
FLIGHT DECK ACCOMMODATIONS	676.	K15=	1.00
PASSENGER ACCOMMODATIONS	1971.		
CARGO ACCOMMODATION	235.	K13=	0.67
EMMERGENCY EQUIPMENT	207.	K18=	1.12
AIR CONDITIONING	466.		
ANTI-ICING	233.		
APU	769.		
FIXED EQUIP. WEIGHT INCREMENT	0.		
TOTAL FIXED EQUIPMENT WEIGHT	8889.		
MANUFACTURERS EMPTY WEIGHT	32602.		
WEIGHT OF STANDARD AND OPERATIONAL ITEMS	1191.	K19=	1.00
OPERATIONAL EMPTY WEIGHT	33794.		
PAYLOAD	8000.		
FUEL	8331.		
GROSS WEIGHT	50124.		

TABLE 15 GROUP WEIGHT STATEMENT
EBF configuration, 40 passengers, 2500 ft. F.A.R. field length

ASAMP WEIGHTS			
PROPULSION GROUP	WEIGHT		
PRIMARY ENGINES	4123.	K5 =	1.00
ENGINE ACCESSORIES	227.	K5 =	1.00
ENGINE CONTROLS	150.	K3 =	1.00
ENGINE STARTING SYSTEM	208.	K2 =	1.00
THRUST REVERSERS	400.		
FUEL SYSTEM	315.	K21=	1.00
PROPULSION WEIGHT INCREMENT	0.		
TOTAL PROPULSION GROUP WEIGHT	5423.		
STRUCTURES GROUP			
WING	5938.	K8 =	1.00
HORIZONTAL TAIL	834.	K9 =	1.00
VERTICAL TAIL	778.	K10=	1.00
FUSELAGE	10721.	K11=	1.29
LANDING GEAR	3609.	K12=	1.58
ENGINE STRUTS	1057.	K20=	1.00
ENGINE NACELLES	604.	K14=	1.00
ENGINE DUCT	0.		
ENGINE MOUNT	0.		
STRUCTURE WEIGHT INCREMENT	0.		
TOTAL STRUCTURE WEIGHT	23540.		
FIXED EQUIPMENT			
INSTRUMENTS	582.	K4 =	1.00
SURFACE CONTROLS	1319.	K16=	1.02
HYDRAULICS	673.	K17=	1.13
PNEUMATICS	337.	K17=	1.13
ELECTRICALS	780.	K6 =	1.00
ELECTRONICS	844.	K7 =	1.10
FLIGHT DECK ACCOMMODATIONS	676.	K15=	1.00
PASSENGER ACCOMMODATIONS	1971.		
CARGO ACCOMMODATION	235.	K13=	0.67
EMMERGENCY EQUIPMENT	230.	K18=	1.12
AIR CONDITIONING	466.		
ANTI-ICING	236.		
APU	769.		
FIXED EQUIP. WEIGHT INCREMENT	0.		
TOTAL FIXED EQUIPMENT WEIGHT	9117.		
MANUFACTURERS EMPTY WEIGHT	38080.		
WEIGHT OF STANDARD AND OPERATIONAL ITEMS	1202.	K19=	1.00
OPERATIONAL EMPTY WEIGHT	39282.		
PAYLOAD	8000.		
FUEL	9817.		
GROSS WEIGHT	57099.		

TABLE 16 GROUP WEIGHT STATEMENT
MF configuration, 40 passengers, 3500 ft. F.A.R. field length

ASAMP WEIGHTS

	WEIGHT		
PROPULSION GROUP			
PRIMARY ENGINES	2184.	K5 =	1.00
ENGINE ACCESSORIES	154.	K5 =	1.00
ENGINE CONTROLS	150.	K3 =	1.00
ENGINE STARTING SYSTEM	143.	K2 =	1.00
THRUST REVERSERS	-52.		
FUEL SYSTEM	253.	K21=	1.00
PROPULSION WEIGHT INCREMENT	0.		
TOTAL PROPULSION GROUP WEIGHT	2831.		
STRUCTURES GROUP			
WING	3554.	K8 =	1.00
HORIZONTAL TAIL	545.	K9 =	1.00
VERTICAL TAIL	559.	K10=	1.00
FUSELAGE	9185.	K11=	1.29
LANDING GEAR	2900.	K12=	1.58
ENGINE STRUTS	0.	K20=	1.00
ENGINE NACELLES	320.	K14=	1.00
ENGINE DUCT	319.		
ENGINE MOUNT	24.		
STRUCTURE WEIGHT INCREMENT	0.		
TOTAL STRUCTURE WEIGHT	17406.		
FIXED EQUIPMENT			
INSTRUMENTS	573.	K4 =	1.00
SURFACE CONTROLS	1027.	K16=	1.02
HYDRAULICS	652.	K17=	1.14
PNEUMATICS	306.	K17=	1.14
ELECTRICALS	780.	K6 =	1.00
ELECTRONICS	807.	K7 =	1.11
FLIGHT DECK ACCOMMODATIONS	676.	K15=	1.00
PASSENGER ACCOMMODATIONS	1971.		
CARGO ACCOMMODATION	235.	K13=	0.67
EMMERGENCY EQUIPMENT	193.	K18=	1.12
AIR CONDITIONING	466.		
ANTI-ICING	210.		
APU	769.		
FIXED EQUIP. WEIGHT INCREMENT	0.		
TOTAL FIXED EQUIPMENT WEIGHT	8665.		
MANUFACTURERS EMPTY WEIGHT	28903.		
WEIGHT OF STANDARD AND OPERATIONAL ITEMS	1187.	K19=	1.00
OPERATIONAL EMPTY WEIGHT	30090.		
PAYLOAD	8000.		
FUEL	7799.		
GROSS WEIGHT	45889.		

TABLE 17 GROUP WEIGHT STATEMENT
EBF configuration, 40 passengers, 3500 ft. F.A.R. field length

ASAMP WEIGHTS			
PROPULSION GROUP	WEIGHT		
PRIMARY ENGINES	3410.	K5 =	1.00
ENGINE ACCESSORIES	202.	K5 =	1.00
ENGINE CONTROLS	150.	K3 =	1.00
ENGINE STARTING SYSTEM	208.	K2 =	1.00
THRUST REVERSERS	124.		
FUEL SYSTEM	289.	K21=	1.00
PROPULSION WEIGHT INCREMENT	0.		
TOTAL PROPULSION GROUP WEIGHT	4383.		
STRUCTURES GROUP			
WING	3826.	K8 =	1.00
HORIZONTAL TAIL	514.	K9 =	1.00
VERTICAL TAIL	535.	K10=	1.00
FUSELAGE	10590.	K11=	1.29
LANDING GEAR	3259.	K12=	1.56
ENGINE STRUTS	904.	K20=	1.00
ENGINE NACELLES	499.	K14=	1.00
ENGINE DUCT	0.		
ENGINE MOUNT	0.		
STRUCTURE WEIGHT INCREMENT	0.		
TOTAL STRUCTURE WEIGHT	20127.		
FIXED EQUIPMENT			
INSTRUMENTS	577.	K4 =	1.00
SURFACE CONTROLS	1329.	K16=	1.00
HYDRAULICS	602.	K17=	1.03
PNEUMATICS	292.	K17=	1.03
ELECTRICALS	780.	K6 =	1.00
ELECTRONICS	770.	K7 =	1.03
FLIGHT DECK ACCOMMODATIONS	676.	K15=	1.00
PASSENGER ACCOMMODATIONS	1971.		
CARGO ACCOMMODATION	235.	K13=	0.67
EMMERGENCY EQUIPMENT	212.	K18=	1.12
AIR CONDITIONING	466.		
ANTI-ICING	213.		
APU	769.		
FIXED EQUIP. WEIGHT INCREMENT	0.		
TOTAL FIXED EQUIPMENT WEIGHT	8892.		
MANUFACTURERS EMPTY WEIGHT	33402.		
WEIGHT OF STANDARD AND OPERATIONAL ITEMS	1196.	K19=	1.00
OPERATIONAL EMPTY WEIGHT	34598.		
PAYLOAD	8000.		
FUEL	8972.		
GROSS WEIGHT	51570.		

TABLE 18 GROUP WEIGHT STATEMENT
MF configuration, 150 passengers, 2000 ft. F.A.R. field length

ASAMP WEIGHTS

PROPULSION GROUP	WEIGHT		
PRIMARY ENGINES	9235.	K5 =	1.00
ENGINE ACCESSORIES	372.	K5 =	1.00
ENGINE CONTROLS	150.	K3 =	1.00
ENGINE STARTING SYSTEM	143.	K2 =	1.00
THRUST REVERSERS	2672.		
FUEL SYSTEM	811.	K21=	1.00
PROPULSION WEIGHT INCREMENT	0.		
TOTAL PROPULSION GROUP WEIGHT	13383.		
STRUCTURES GROUP			
WING	41104.	K8 =	1.00
HORIZONTAL TAIL	4206.	K9 =	1.00
VERTICAL TAIL	3344.	K10=	1.00
FUSELAGE	22602.	K11=	1.29
LANDING GEAR	11623.	K12=	1.58
ENGINE STRUTS	0.	K20=	1.00
ENGINE NACELLES	2564.	K14=	1.00
ENGINE DUCT	1301.		
ENGINE MOUNT	102.		
STRUCTURE WEIGHT INCREMENT	0.		
TOTAL STRUCTURE WEIGHT	86846.		
FIXED EQUIPMENT			
INSTRUMENTS	674.	K4 =	1.00
SURFACE CONTROLS	1966.	K16=	1.04
HYDRAULICS	1164.	K17=	1.35
PNEUMATICS	846.	K17=	1.35
ELECTRICALS	1560.	K6 =	1.00
ELECTRONICS	1571.	K7 =	1.28
FLIGHT DECK ACCOMMODATIONS	906.	K15=	1.00
PASSENGER ACCOMMODATIONS	9445.		
CARGO ACCOMMODATION	808.	K13=	0.67
EMMERGENCY EQUIPMENT	640.	K18=	1.12
AIR CONDITIONING	1862.		
ANTI-ICING	404.		
APU	988.		
FIXED EQUIP. WEIGHT INCREMENT	0.		
TOTAL FIXED EQUIPMENT WEIGHT	22834.		
MANUFACTURERS EMPTY WEIGHT	123062.		
WEIGHT OF STANDARD AND OPERATIONAL ITEMS	3409.	K19=	1.00
OPERATIONAL EMPTY WEIGHT	126471.		
PAYLOAD	30000.		
FUEL	27442.		
GROSS WEIGHT	183912.		

TABLE 19 GROUP WEIGHT STATEMENT
EBF configuration, 150 passengers, 2000 ft. F.A.R. field length

ASAMP WEIGHTS			
PROPULSION GROUP	WEIGHT		
PRIMARY ENGINES	17571.	K5 =	1.00
ENGINE ACCESSORIES	552.	K5 =	1.00
ENGINE CONTROLS	150.	K3 =	1.00
ENGINE STARTING SYSTEM	208.	K2 =	1.00
THRUST REVERSERS	5051.		
FUEL SYSTEM	980.	K21=	1.00
PROPULSION WEIGHT INCREMENT	0.		
TOTAL PROPULSION GROUP WEIGHT	24511.		
STRUCTURES GROUP			
WING	37793.	K8 =	1.00
HORIZONTAL TAIL	6253.	K9 =	1.00
VERTICAL TAIL	4896.	K10=	1.00
FUSELAGE	27444.	K11=	1.29
LANDING GEAR	13529.	K12=	1.58
ENGINE STRUTS	3497.	K20=	1.00
ENGINE NACELLES	4750.	K14=	1.00
ENGINE DUCT	0.		
ENGINE MOUNT	0.		
STRUCTURE WEIGHT INCREMENT	0.		
TOTAL STRUCTURE WEIGHT	98161.		
FIXED EQUIPMENT			
INSTRUMENTS	696.	K4 =	1.00
SURFACE CONTROLS	2738.	K16=	1.02
HYDRAULICS	1092.	K17=	1.18
PNEUMATICS	831.	K17=	1.18
ELECTRICALS	1560.	K6 =	1.00
ELECTRONICS	1524.	K7 =	1.14
FLIGHT DECK ACCOMMODATIONS	906.	K15=	1.00
PASSENGER ACCOMMODATIONS	9445.		
CARGO ACCOMMODATION	808.	K13=	0.67
EMMERGENCY EQUIPMENT	738.	K18=	1.12
AIR CONDITIONING	1862.		
ANTI-ICING	436.		
APU	988.		
FIXED EQUIP. WEIGHT INCREMENT	0.		
TOTAL FIXED EQUIPMENT WEIGHT	23623.		
MANUFACTURERS EMPTY WEIGHT	146295.		
WEIGHT OF STANDARD AND OPERATIONAL ITEMS	3446.	K19=	1.00
OPERATIONAL EMPTY WEIGHT	149741.		
PAYLOAD	30000.		
FUEL	34326.		
GROSS WEIGHT	214066.		

TABLE 20 GROUP WEIGHT STATEMENT
MF configuration, 150 passengers, 2500 ft. F.A.R. field length

ASAMP WEIGHTS

PROPULSION GROUP	WEIGHT		
PRIMARY ENGINES	6998.	K5 =	1.00
ENGINE ACCESSORIES	314.	K5 =	1.00
ENGINE CONTROLS	150.	K3 =	1.00
ENGINE STARTING SYSTEM	143.	K2 =	1.00
THRUST REVERSERS	1816.		
FUEL SYSTEM	662.	K21=	1.00
PROPULSION WEIGHT INCREMENT	0.		
TOTAL PROPULSION GROUP WEIGHT	10084.		
STRUCTURES GROUP			
WING	23325.	K8 =	1.00
HORIZONTAL TAIL	2578.	K9 =	1.00
VERTICAL TAIL	2106.	K10=	1.00
FUSELAGE	20820.	K11=	1.29
LANDING GEAR	9371.	K12=	1.58
ENGINE STRUTS	0.	K20=	1.00
ENGINE NACELLES	1623.	K14=	1.00
ENGINE DUCT	1088.		
ENGINE MOUNT	77.		
STRUCTURE WEIGHT INCREMENT	0.		
TOTAL STRUCTURE WEIGHT	60989.		
FIXED EQUIPMENT			
INSTRUMENTS	648.	K4 =	1.00
SURFACE CONTROLS	1942.	K16=	1.03
HYDRAULICS	1000.	K17=	1.27
PNEUMATICS	678.	K17=	1.27
ELECTRICALS	1560.	K6 =	1.00
ELECTRONICS	1329.	K7 =	1.21
FLIGHT DECK ACCOMMODATIONS	906.	K15=	1.00
PASSENGER ACCOMMODATIONS	9445.		
CARGO ACCOMMODATION	808.	K13=	0.67
EMMERGENCY EQUIPMENT	525.	K18=	1.12
AIR CONDITIONING	1862.		
ANTI-ICING	339.		
APU	988.		
FIXED EQUIP. WEIGHT INCREMENT	0.		
TOTAL FIXED EQUIPMENT WEIGHT	22029.		
MANUFACTURERS EMPTY WEIGHT	93102.		
WEIGHT OF STANDARD AND OPERATIONAL ITEMS	3375.	K19=	1.00
OPERATIONAL EMPTY WEIGHT	96477.		
PAYLOAD	30000.		
FUEL	21804.		
GROSS WEIGHT	148280.		

TABLE 21 GROUP WEIGHT STATEMENT
EBF configuration, 150 passengers, 2500 ft. F.A.R. field length

ASAMP WEIGHTS

PROPULSION GROUP	WEIGHT		
PRIMARY ENGINES	12112.	K5 =	1.00
ENGINE ACCESSORIES	439.	K5 =	1.00
ENGINE CONTROLS	150.	K3 =	1.00
ENGINE STARTING SYSTEM	208.	K2 =	1.00
THRUST REVERSERS	3501.		
FUEL SYSTEM	774.	K21=	1.00
PROPULSION WEIGHT INCREMENT	0.		
TOTAL PROPULSION GROUP WEIGHT	17184.		
STRUCTURES GROUP			
WING	23171.	K8 =	1.00
HORIZONTAL TAIL	2700.	K9 =	1.00
VERTICAL TAIL	2208.	K10=	1.00
FUSELAGE	24807.	K11=	1.29
LANDING GEAR	10602.	K12=	1.58
ENGINE STRUTS	2572.	K20=	1.00
ENGINE NACELLES	2454.	K14=	1.00
ENGINE DUCT	0.		
ENGINE MOUNT	0.		
STRUCTURE WEIGHT INCREMENT	0.		
TOTAL STRUCTURE WEIGHT	68515.		
FIXED EQUIPMENT			
INSTRUMENTS	662.	K4 =	1.00
SURFACE CONTROLS	2578.	K16=	1.02
HYDRAULICS	936.	K17=	1.13
PNEUMATICS	660.	K17=	1.13
ELECTRICALS	1560.	K6 =	1.00
ELECTRONICS	1286.	K7 =	1.10
FLIGHT DECK ACCOMMODATIONS	906.	K15=	1.00
PASSENGER ACCOMMODATIONS	9445.		
CARGO ACCOMMODATION	808.	K13=	0.67
EMMERGENCY EQUIPMENT	588.	K18=	1.12
AIR CONDITIONING	1862.		
ANTI-ICING	359.		
APU	988.		
FIXED EQUIP. WEIGHT INCREMENT	0.		
TOTAL FIXED EQUIPMENT WEIGHT	22637.		
MANUFACTURERS EMPTY WEIGHT	108336.		
WEIGHT OF STANDARD AND OPERATIONAL ITEMS	3400.	K19=	1.00
OPERATIONAL EMPTY WEIGHT	111736.		
PAYLOAD	30000.		
FUEL	26014.		
GROSS WEIGHT	167750.		

TABLE 22 GROUP WEIGHT STATEMENT
MF configuration, 150 passengers, 3500 ft. F.A.R. field length

ASAMP WEIGHTS

	WEIGHT		
PROPULSION GROUP			
PRIMARY ENGINES	6124.	K5 =	1.00
ENGINE ACCESSORIES	289.	K5 =	1.00
ENGINE CONTROLS	150.	K3 =	1.00
ENGINE STARTING SYSTEM	143.	K2 =	1.00
THRUST REVERSERS	1477.		
FUEL SYSTEM	603.	K21=	1.00
PROPULSION WEIGHT INCREMENT	0.		
TOTAL PROPULSION GROUP WEIGHT	8785.		
STRUCTURES GROUP			
WING	13479.	K8 =	1.00
HORIZONTAL TAIL	1795.	K9 =	1.00
VERTICAL TAIL	1514.	K10=	1.00
FUSELAGE	19940.	K11=	1.29
LANDING GEAR	8260.	K12=	1.58
ENGINE STRUTS	0.	K20=	1.00
ENGINE NACELLES	1256.	K14=	1.00
ENGINE DUCT	995.		
ENGINE MOUNT	67.		
STRUCTURE WEIGHT INCREMENT	0.		
TOTAL STRUCTURE WEIGHT	47306.		
FIXED EQUIPMENT			
INSTRUMENTS	635.	K4 =	1.00
SURFACE CONTROLS	2082.	K16=	1.02
HYDRAULICS	855.	K17=	1.14
PNEUMATICS	557.	K17=	1.14
ELECTRICALS	1560.	K6 =	1.00
ELECTRONICS	1148.	K7 =	1.11
FLIGHT DECK ACCOMMODATIONS	906.	K15=	1.00
PASSENGER ACCOMMODATIONS	9445.		
CARGO ACCOMMODATION	808.	K13=	0.67
EMMERGENCY EQUIPMENT	458.	K18=	1.12
AIR CONDITIONING	1862.		
ANTI-ICING	293.		
APU	988.		
FIXED EQUIP. WEIGHT INCREMENT	0.		
TOTAL FIXED EQUIPMENT WEIGHT	21607.		
MANUFACTURERS EMPTY WEIGHT	77698.		
WEIGHT OF STANDARD AND OPERATIONAL ITEMS	3361.	K19=	1.00
OPERATIONAL EMPTY WEIGHT	81059.		
PAYLOAD	30000.		
FUEL	19638.		
GROSS WEIGHT	130697.		

TABLE 23 GROUP WEIGHT STATEMENT
EBF configuration, 150 passengers, 3500 ft. F.A.R. field length

ASAMP WEIGHTS			
PROPULSION GROUP	WEIGHT		
PRIMARY ENGINES	9631.	K5 =	1.00
ENGINE ACCESSORIES	382.	K5 =	1.00
ENGINE CONTROLS	150.	K3 =	1.00
ENGINE STARTING SYSTEM	208.	K2 =	1.00
THRUST REVERSERS	2538.		
FUEL SYSTEM	692.	K21=	1.00
PROPULSION WEIGHT INCREMENT	0.		
TOTAL PROPULSION GROUP WEIGHT	13600.		
STRUCTURES GROUP			
WING	14219.	K8 =	1.00
HORIZONTAL TAIL	1688.	K9 =	1.00
VERTICAL TAIL	1431.	K10=	1.00
FUSELAGE	23549.	K11=	1.29
LANDING GEAR	9206.	K12=	1.58
ENGINE STRUTS	2129.	K20=	1.00
ENGINE NACELLES	1410.	K14=	1.00
ENGINE DUCT	0.		
ENGINE MOUNT	0.		
STRUCTURE WEIGHT INCREMENT	0.		
TOTAL STRUCTURE WEIGHT	53632.		
FIXED EQUIPMENT			
INSTRUMENTS	646.	K4 =	1.00
SURFACE CONTROLS	2642.	K16=	1.00
HYDRAULICS	805.	K17=	1.03
PNEUMATICS	543.	K17=	1.03
ELECTRICALS	1560.	K6 =	1.00
ELECTRONICS	1121.	K7 =	1.03
FLIGHT DECK ACCOMMODATIONS	906.	K15=	1.00
PASSENGER ACCOMMODATIONS	9445.		
CARGO ACCOMMODATION	808.	K13=	0.67
EMERGENCY EQUIPMENT	516.	K18=	1.12
AIR CONDITIONING	1862.		
ANTI-ICING	309.		
APU	988.		
FIXED EQUIP. WEIGHT INCREMENT	0.		
TOTAL FIXED EQUIPMENT WEIGHT	22151.		
MANUFACTURERS EMPTY WEIGHT	89383.		
WEIGHT OF STANDARD AND OPERATIONAL ITEMS	3382.	K19=	1.00
OPERATIONAL EMPTY WEIGHT	92765.		
PAYLOAD	30000.		
FUEL	22893.		
GROSS WEIGHT	145658.		

TABLE 24 GROUP WEIGHT STATEMENT
MF configuration, 300 passengers, 2000 ft. F.A.R. field length

ASAMP WEIGHTS

PROPULSION GROUP	WEIGHT		
PRIMARY ENGINES	21356.	K5 =	1.00
ENGINE ACCESSORIES	622.	K5 =	1.00
ENGINE CONTROLS	150.	K3 =	1.00
ENGINE STARTING SYSTEM	143.	K2 =	1.00
THRUST REVERSERS	4757.		
FUEL SYSTEM	1521.	K21=	1.00
PROPULSION WEIGHT INCREMENT	0.		
TOTAL PROPULSION GROUP WEIGHT	28550.		
STRUCTURES GROUP			
WING	126486.	K8 =	1.00
HORIZONTAL TAIL	9994.	K9 =	1.00
VERTICAL TAIL	7775.	K10=	1.00
FUSELAGE	51140.	K11=	1.29
LANDING GEAR	27482.	K12=	1.58
ENGINE STRUTS	0.	K20=	1.00
ENGINE NACELLES	7662.	K14=	1.00
ENGINE DUCT	3472.		
ENGINE MOUNT	235.		
STRUCTURE WEIGHT INCREMENT	0.		
TOTAL STRUCTURE WEIGHT	234246.		
FIXED EQUIPMENT			
INSTRUMENTS	856.	K4 =	1.00
SURFACE CONTROLS	3165.	K16=	1.04
HYDRAULICS	1875.	K17=	1.35
PNEUMATICS	1723.	K17=	1.35
ELECTRICALS	2984.	K6 =	1.00
ELECTRONICS	2737.	K7 =	1.28
FLIGHT DECK ACCOMMODATIONS	1154.	K15=	1.00
PASSENGER ACCOMMODATIONS	20576.		
CARGO ACCOMMODATION	2041.	K13=	0.67
EMMERGENCY EQUIPMENT	1452.	K18=	1.12
AIR CONDITIONING	3011.		
ANTI-ICING	611.		
APU	1426.		
FIXED EQUIP. WEIGHT INCREMENT	0.		
TOTAL FIXED EQUIPMENT WEIGHT	43611.		
MANUFACTURERS EMPTY WEIGHT	306407.		
WEIGHT OF STANDARD AND OPERATIONAL ITEMS	6346.	K19=	1.00
OPERATIONAL EMPTY WEIGHT	312753.		
PAYLOAD	60000.		
FUEL	62097.		
GROSS WEIGHT	434850.		

TABLE 25 GROUP WEIGHT STATEMENT
EBF configuration, 300 passengers, 2000 ft. F.A.R. field length

ASAMP WEIGHTS			
PROPULSION GROUP	WEIGHT		
PRIMARY ENGINES	39008.	K5 =	1.00
ENGINE ACCESSORIES	900.	K5 =	1.00
ENGINE CONTROLS	150.	K3 =	1.00
ENGINE STARTING SYSTEM	208.	K2 =	1.00
THRUST REVERSERS	7313.		
FUEL SYSTEM	1685.	K21=	1.00
PROPULSION WEIGHT INCREMENT	0.		
TOTAL PROPULSION GROUP WEIGHT	49263.		
STRUCTURES GROUP			
WING	106473.	K8 =	1.00
HORIZONTAL TAIL	13384.	K9 =	1.00
VERTICAL TAIL	10357.	K10=	1.00
FUSELAGE	60275.	K11=	1.29
LANDING GEAR	30035.	K12=	1.58
ENGINE STRUTS	6751.	K20=	1.00
ENGINE NACELLES	13766.	K14=	1.00
ENGINE DUCT	0.		
ENGINE MOUNT	0.		
STRUCTURE WEIGHT INCREMENT	0.		
TOTAL STRUCTURE WEIGHT	241042.		
FIXED EQUIPMENT			
INSTRUMENTS	885.	K4 =	1.00
SURFACE CONTROLS	4260.	K16=	1.02
HYDRAULICS	1739.	K17=	1.18
PNEUMATICS	1629.	K17=	1.18
ELECTRICALS	2984.	K6 =	1.00
ELECTRONICS	2605.	K7 =	1.14
FLIGHT DECK ACCOMMODATIONS	1154.	K15=	1.00
PASSENGER ACCOMMODATIONS	20576.		
CARGO ACCOMMODATION	2041.	K13=	0.67
EMMERGENCY EQUIPMENT	1583.	K18=	1.12
AIR CONDITIONING	3011.		
ANTI-ICING	686.		
APU	1426.		
FIXED EQUIP. WEIGHT INCREMENT	0.		
TOTAL FIXED EQUIPMENT WEIGHT	44579.		
MANUFACTURERS EMPTY WEIGHT	334884.		
WEIGHT OF STANDARD AND OPERATIONAL ITEMS	6370.	K19=	1.00
OPERATIONAL EMPTY WEIGHT	341254.		
PAYLOAD	60000.		
FUEL	73985.		
GROSS WEIGHT	475239.		

TABLE 26 GROUP WEIGHT STATEMENT
MF configuration, 300 passengers, 2500 ft. F.A.R. field length

ASAMP WEIGHTS

	WEIGHT		
PROPULSION GROUP			
PRIMARY ENGINES	15070.	K5 =	1.00
ENGINE ACCESSORIES	502.	K5 =	1.00
ENGINE CONTROLS	150.	K3 =	1.00
ENGINE STARTING SYSTEM	143.	K2 =	1.00
THRUST REVERSERS	4095.		
FUEL SYSTEM	1234.	K21=	1.00
PROPULSION WEIGHT INCREMENT	0.		
TOTAL PROPULSION GROUP WEIGHT	21194.		
STRUCTURES GROUP			
WING	64099.	K8 =	1.00
HORIZONTAL TAIL	5484.	K9 =	1.00
VERTICAL TAIL	4331.	K10=	1.00
FUSELAGE	45839.	K11=	1.29
LANDING GEAR	20415.	K12=	1.58
ENGINE STRUTS	0.	K20=	1.00
ENGINE NACELLES	5018.	K14=	1.00
ENGINE DUCT	2827.		
ENGINE MOUNT	166.		
STRUCTURE WEIGHT INCREMENT	0.		
TOTAL STRUCTURE WEIGHT	148179.		
FIXED EQUIPMENT			
INSTRUMENTS	775.	K4 =	1.00
SURFACE CONTROLS	3031.	K16=	1.03
HYDRAULICS	1466.	K17=	1.27
PNEUMATICS	1253.	K17=	1.27
ELECTRICALS	2984.	K6 =	1.00
ELECTRONICS	2096.	K7 =	1.21
FLIGHT DECK ACCOMMODATIONS	1154.	K15=	1.00
PASSENGER ACCOMMODATIONS	20576.		
CARGO ACCOMMODATION	2041.	K13=	0.67
EMMERGENCY EQUIPMENT	1090.	K18=	1.12
AIR CONDITIONING	3011.		
ANTI-ICING	479.		
APU	1426.		
FIXED EQUIP. WEIGHT INCREMENT	0.		
TOTAL FIXED EQUIPMENT WEIGHT	41383.		
MANUFACTURERS EMPTY WEIGHT	210755.		
WEIGHT OF STANDARD AND OPERATIONAL ITEMS	6292.	K19=	1.00
OPERATIONAL EMPTY WEIGHT	217048.		
PAYLOAD	60000.		
FUEL	45971.		
GROSS WEIGHT	323018.		

TABLE 27 GROUP WEIGHT STATEMENT
EBF configuration, 300 passengers, 2500 ft. F.A.R. field length

ASAMP WEIGHTS			
PROPULSION GROUP	**WEIGHT**		
PRIMARY ENGINES	25910.	K5 =	1.00
ENGINE ACCESSORIES	700.	K5 =	1.00
ENGINE CONTROLS	150.	K3 =	1.00
ENGINE STARTING SYSTEM	208.	K2 =	1.00
THRUST REVERSERS	6106.		
FUEL SYSTEM	1386.	K21=	1.00
PROPULSION WEIGHT INCREMENT	0.		
TOTAL PROPULSION GROUP WEIGHT	34461.		
STRUCTURES GROUP			
WING	61841.	K8 =	1.00
HORIZONTAL TAIL	5575.	K9 =	1.00
VERTICAL TAIL	4419.	K10=	1.00
FUSELAGE	54137.	K11=	1.29
LANDING GEAR	22680.	K12=	1.58
ENGINE STRUTS	4317.	K20=	1.00
ENGINE NACELLES	8257.	K14=	1.00
ENGINE DUCT	0.		
ENGINE MOUNT	0.		
STRUCTURE WEIGHT INCREMENT	0.		
TOTAL STRUCTURE WEIGHT	161725.		
FIXED EQUIPMENT			
INSTRUMENTS	801.	K4 =	1.00
SURFACE CONTROLS	3976.	K16=	1.02
HYDRAULICS	1389.	K17=	1.13
PNEUMATICS	1220.	K17=	1.13
ELECTRICALS	2984.	K6 =	1.00
ELECTRONICS	2049.	K7 =	1.10
FLIGHT DECK ACCOMMODATIONS	1154.	K15=	1.00
PASSENGER ACCOMMODATIONS	20576.		
CARGO ACCOMMODATION	2041.	K13=	0.67
EMMERGENCY EQUIPMENT	1206.	K18=	1.12
AIR CONDITIONING	3011.		
ANTI-ICING	531.		
APU	1426.		
FIXED EQUIP. WEIGHT INCREMENT	0.		
TOTAL FIXED EQUIPMENT WEIGHT	42364.		
MANUFACTURERS EMPTY WEIGHT	238549.		
WEIGHT OF STANDARD AND OPERATIONAL ITEMS	6322.	K19=	1.00
OPERATIONAL EMPTY WEIGHT	244871.		
PAYLOAD	60000.		
FUEL	53989.		
GROSS WEIGHT	359860.		

TABLE 28 GROUP WEIGHT STATEMENT
MF configuration, 300 passengers, 3500 ft. F.A.R. field length

ASAMP WEIGHTS

	WEIGHT		
PROPULSION GROUP			
PRIMARY ENGINES	12828.	K5 =	1.00
ENGINE ACCESSORIES	455.	K5 =	1.00
ENGINE CONTROLS	150.	K3 =	1.00
ENGINE STARTING SYSTEM	143.	K2 =	1.00
THRUST REVERSERS	3639.		
FUEL SYSTEM	1102.	K21=	1.00
PROPULSION WEIGHT INCREMENT	0.		
TOTAL PROPULSION GROUP WEIGHT	18367.		
STRUCTURES GROUP			
WING	35218.	K8 =	1.00
HORIZONTAL TAIL	3657.	K9 =	1.00
VERTICAL TAIL	2940.	K10=	1.00
FUSELAGE	43475.	K11=	1.29
LANDING GEAR	17325.	K12=	1.58
ENGINE STRUTS	0.	K20=	1.00
ENGINE NACELLES	4075.	K14=	1.00
ENGINE DUCT	2566.		
ENGINE MOUNT	141.		
STRUCTURE WEIGHT INCREMENT	0.		
TOTAL STRUCTURE WEIGHT	109396.		
FIXED EQUIPMENT			
INSTRUMENTS	739.	K4 =	1.00
SURFACE CONTROLS	3243.	K16=	1.02
HYDRAULICS	1199.	K17=	1.14
PNEUMATICS	980.	K17=	1.14
ELECTRICALS	2984.	K6 =	1.00
ELECTRONICS	1726.	K7 =	1.11
FLIGHT DECK ACCOMMODATIONS	1154.	K15=	1.00
PASSENGER ACCOMMODATIONS	20576.		
CARGO ACCOMMODATION	2041.	K13=	0.67
EMMERGENCY EQUIPMENT	932.	K18=	1.12
AIR CONDITIONING	3011.		
ANTI-ICING	401.		
APU	1426.		
FIXED EQUIP. WEIGHT INCREMENT	0.		
TOTAL FIXED EQUIPMENT WEIGHT	40412.		
MANUFACTURERS EMPTY WEIGHT	168175.		
WEIGHT OF STANDARD AND OPERATIONAL ITEMS	6265.	K19=	1.00
OPERATIONAL EMPTY WEIGHT	174440.		
PAYLOAD	60000.		
FUEL	39688.		
GROSS WEIGHT	274128.		

TABLE 29 GROUP WEIGHT STATEMENT
EBF configuration, 300 passengers, 3500 ft. F.A.R. field length

ASAMP WEIGHTS

PROPULSION GROUP	WEIGHT		
PRIMARY ENGINES	20202.	K5 =	1.00
ENGINE ACCESSORIES	601.	K5 =	1.00
ENGINE CONTROLS	150.	K3 =	1.00
ENGINE STARTING SYSTEM	208.	K2 =	1.00
THRUST REVERSERS	5472.		
FUEL SYSTEM	1246.	K21=	1.00
PROPULSION WEIGHT INCREMENT	0.		
TOTAL PROPULSION GROUP WEIGHT	27880.		
STRUCTURES GROUP			
WING	36874.	K8 =	1.00
HORIZONTAL TAIL	3449.	K9 =	1.00
VERTICAL TAIL	2781.	K10=	1.00
FUSELAGE	51221.	K11=	1.29
LANDING GEAR	19310.	K12=	1.58
ENGINE STRUTS	3923.	K20=	1.00
ENGINE NACELLES	5857.	K14=	1.00
ENGINE DUCT	0.		
ENGINE MOUNT	0.		
STRUCTURE WEIGHT INCREMENT	0.		
TOTAL STRUCTURE WEIGHT	123414.		
FIXED EQUIPMENT			
INSTRUMENTS	762.	K4 =	1.00
SURFACE CONTROLS	4096.	K16=	1.00
HYDRAULICS	1151.	K17=	1.03
PNEUMATICS	970.	K17=	1.03
ELECTRICALS	2984.	K6 =	1.00
ELECTRONICS	1719.	K7 =	1.03
FLIGHT DECK ACCOMMODATIONS	1154.	K15=	1.00
PASSENGER ACCOMMODATIONS	20576.		
CARGO ACCOMMODATION	2041.	K13=	0.67
EMMERGENCY EQUIPMENT	1034.	K18=	1.12
AIR CONDITIONING	3011.		
ANTI-ICING	440.		
APU	1426.		
FIXED EQUIP. WEIGHT INCREMENT	0.		
TOTAL FIXED EQUIPMENT WEIGHT	41363.		
MANUFACTURERS EMPTY WEIGHT	192657.		
WEIGHT OF STANDARD AND OPERATIONAL ITEMS	6295.	K19=	1.00
OPERATIONAL EMPTY WEIGHT	198952.		
PAYLOAD	60000.		
FUEL	46583.		
GROSS WEIGHT	305535.		

12.2 APPENDIX B HIGH SPEED DRAG POLARS

Final ASAMP predicted high speed drag polars are presented and the locations are noted in the following table:

Number of Passengers	F.A.R. Field Length					
	2000 Feet		2500 Feet		3500 Feet	
	MF	EBF	MF	EBF	MF	EBF
40	FIGURE 69	FIGURE 70	FIGURE 71	FIGURE 72	FIGURE 73	FIGURE 74
150	FIGURE 75	FIGURE 76	FIGURE 77	FIGURE 78	FIGURE 79	FIGURE 80
300	FIGURE 81	FIGURE 82	FIGURE 83	FIGURE 84	FIGURE 85	FIGURE 86

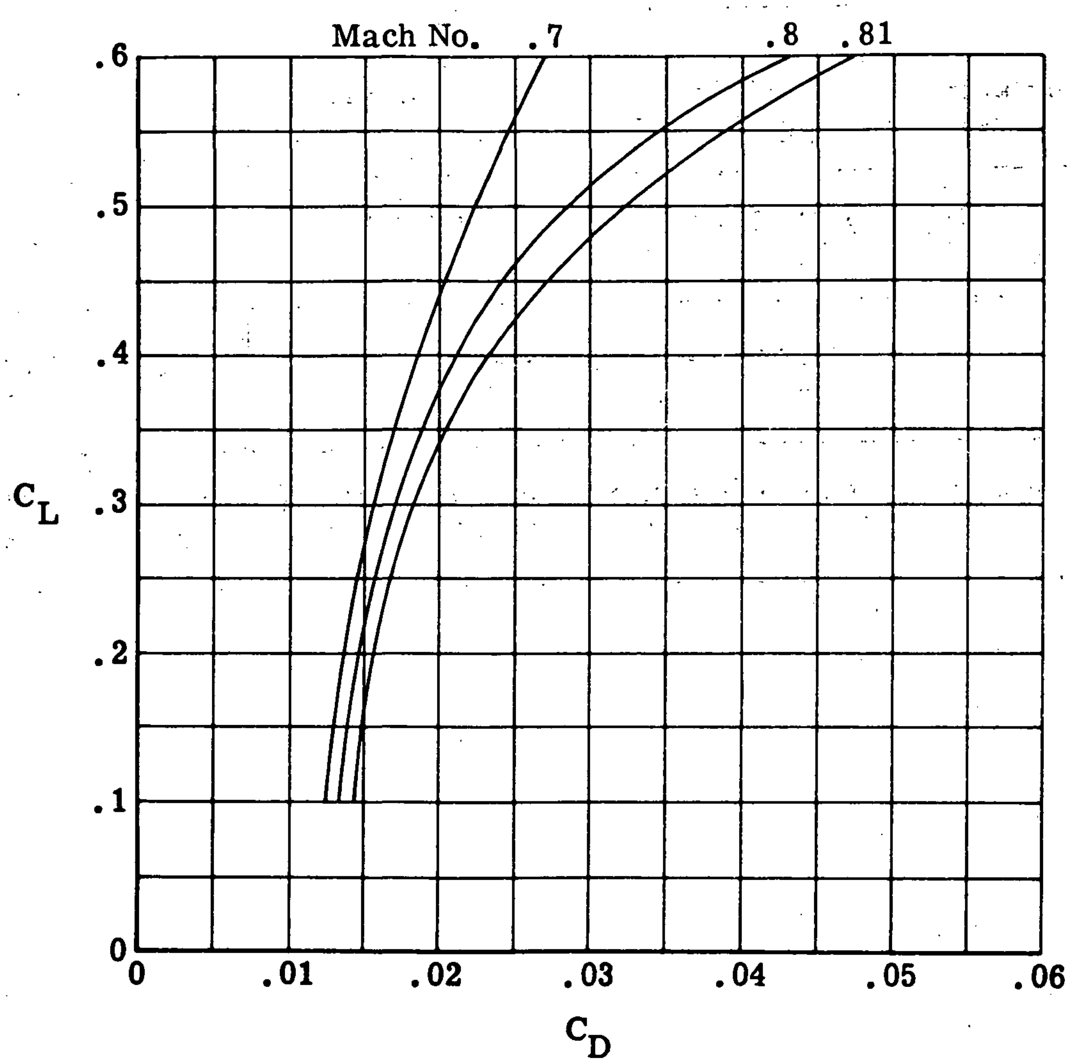

Figure 69 High speed drag polar
MF configuration, 40 passengers, 2000 ft. F.A.R. field length

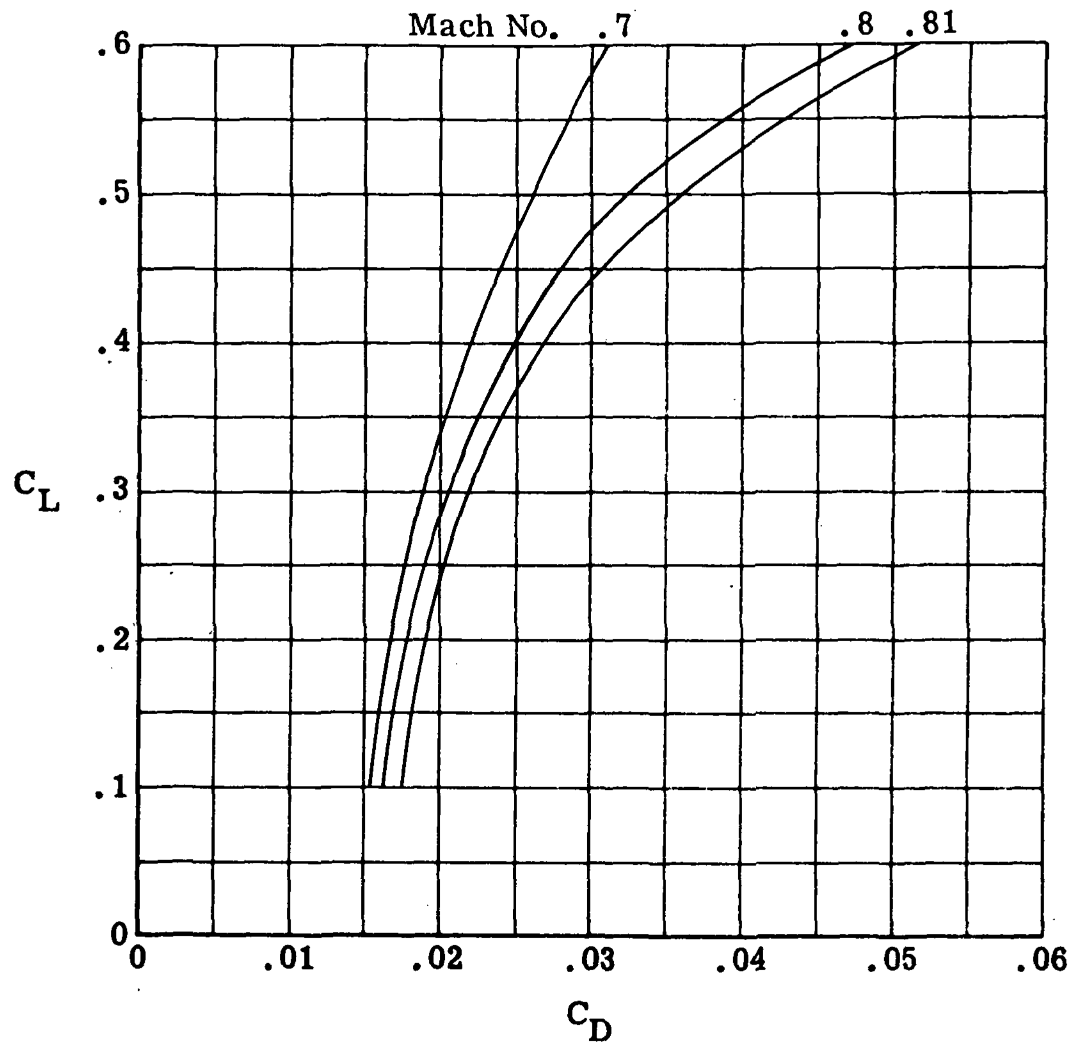

Figure 70 High speed drag polar
EBF configuration, 40 passengers, 2000 ft. F.A.R. field length

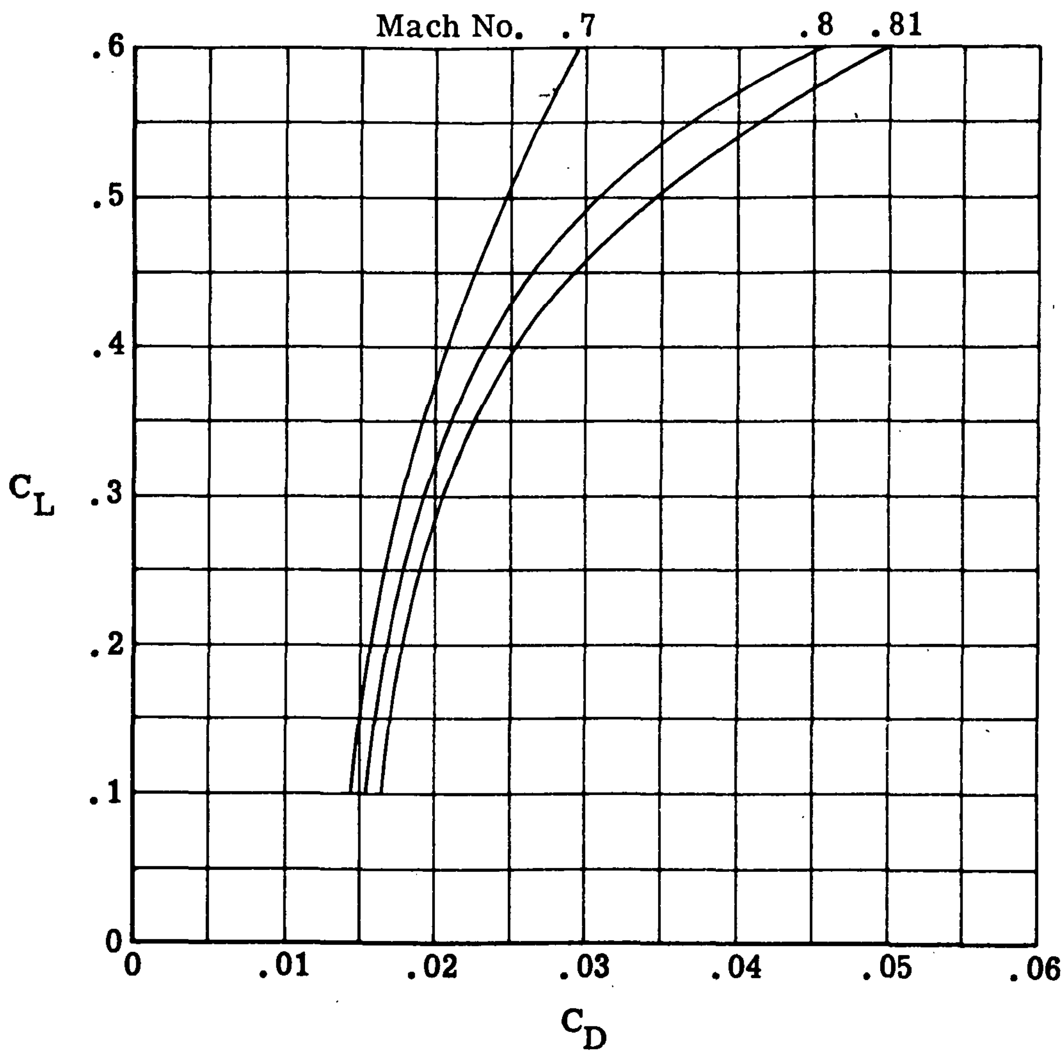

Figure 71 High speed drag polar
MF configuration, 40 passengers, 2500 ft. F.A.R. field length

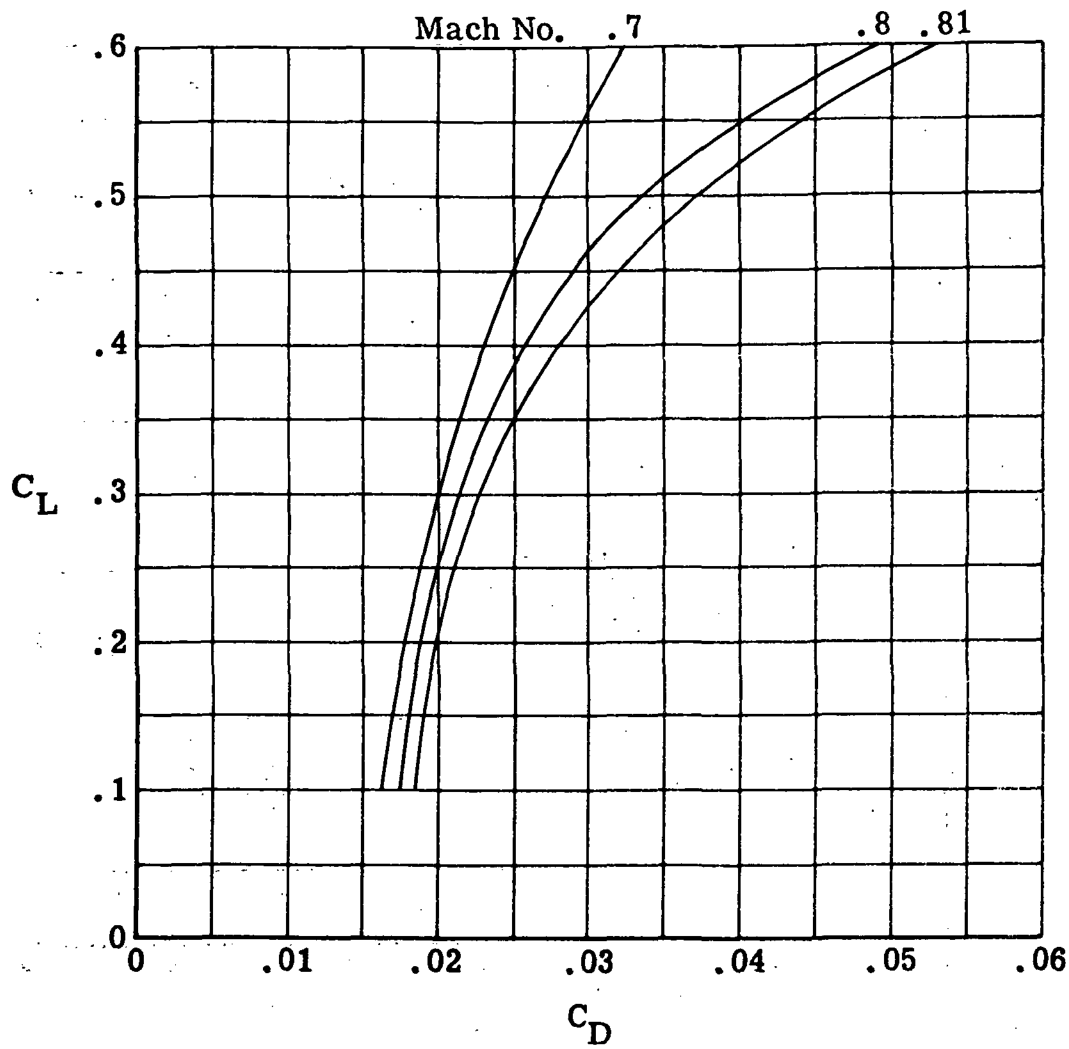

Figure 72 High speed drag polar
EBF configuration, 40 passengers, 2500 ft. F.A.R. field length

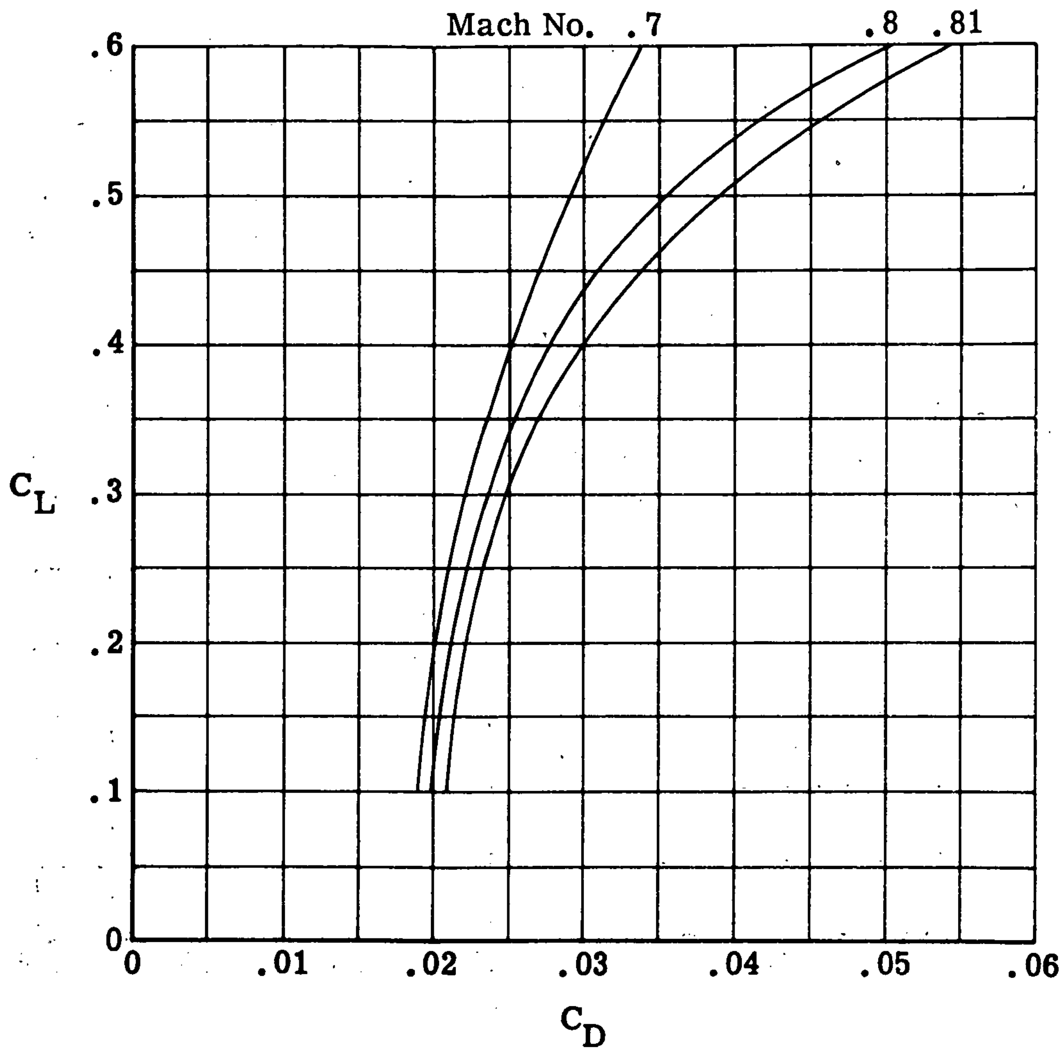

Figure 73 High speed drag polar
MF configuration, 40 passengers, 3500 ft. F.A.R. field length

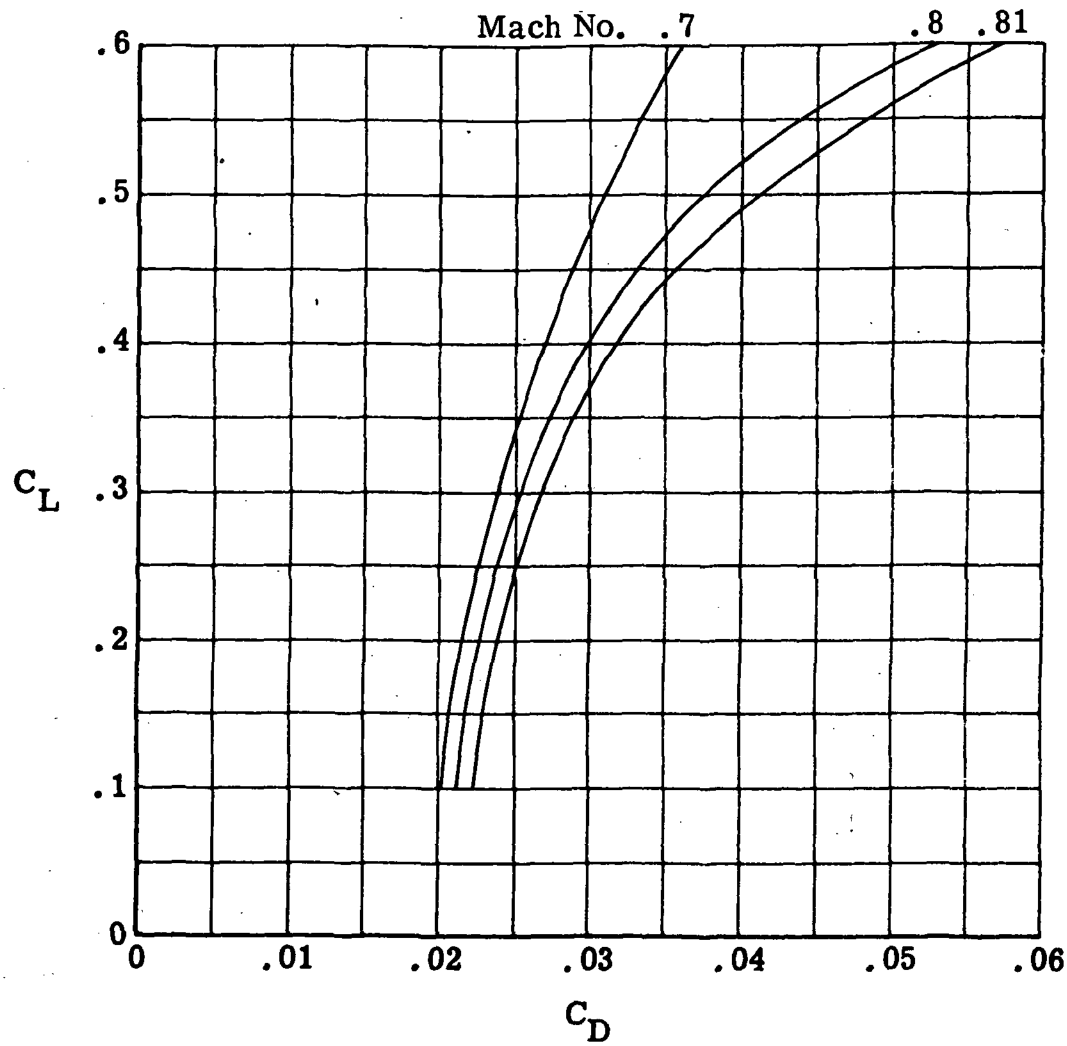

Figure 74 High speed drag polar
EBF configuration, 40 passengers, 3500 ft. F.A.R. field length

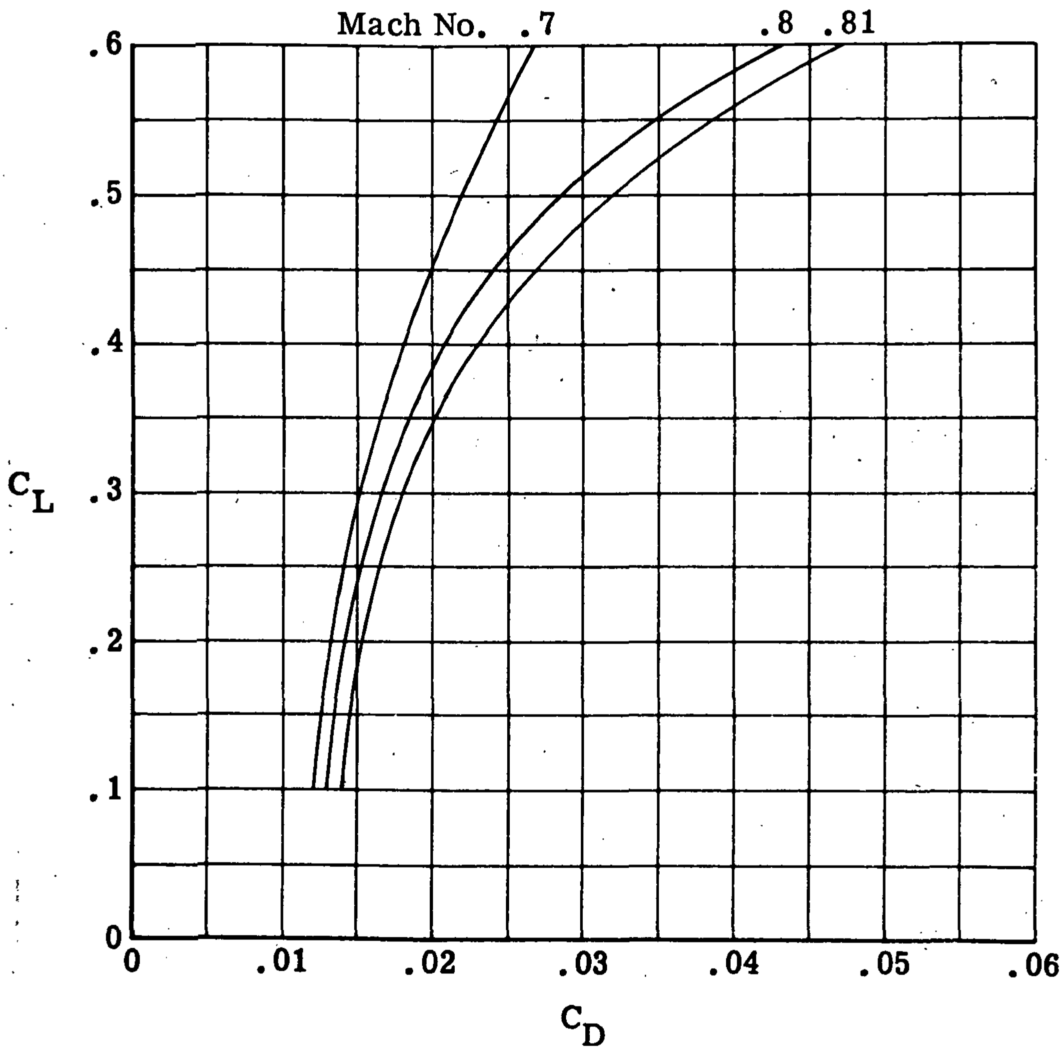

Figure 75 High speed drag polar
MF configuration, 150 passengers, 2000 ft. F.A.R. field length

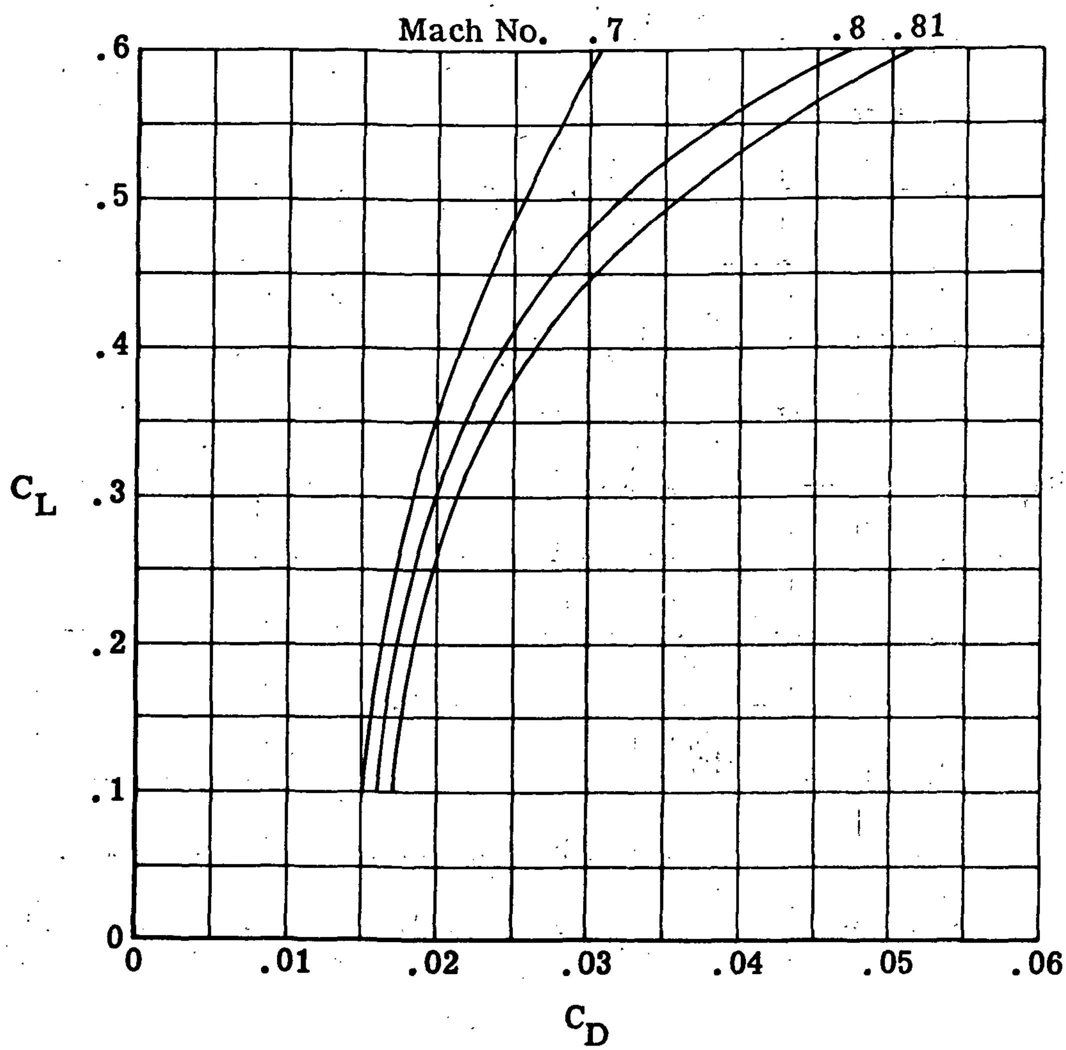

Figure 76 High speed drag polar
EBF configuration, 150 passengers, 2000 ft. F.A.R. field length

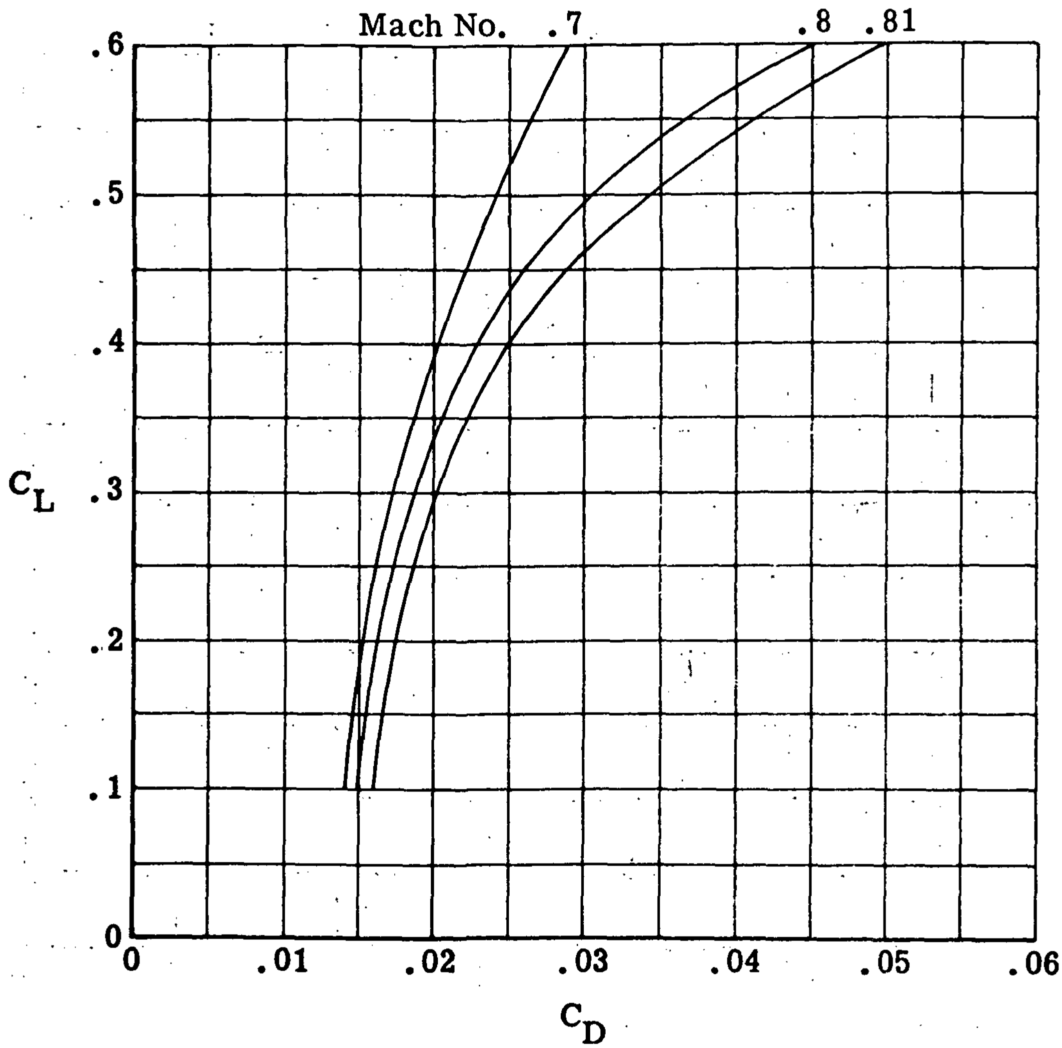

Figure 77 High speed drag polar
MF configuration, 150 passengers, 2500 ft. F.A.R. field length

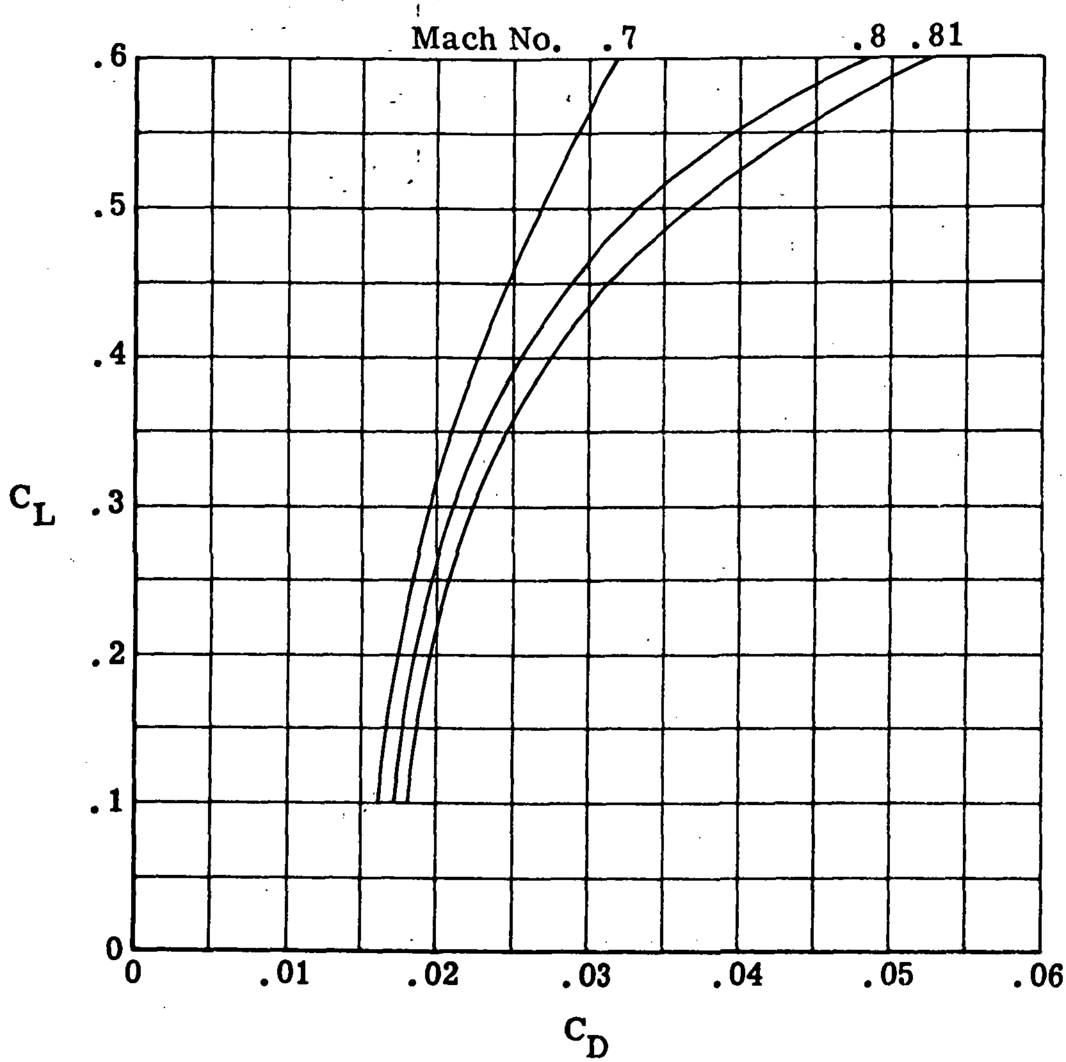

Figure 78 High speed drag polar
EBF configuration, 150 passengers, 2500 ft. F.A.R. field length

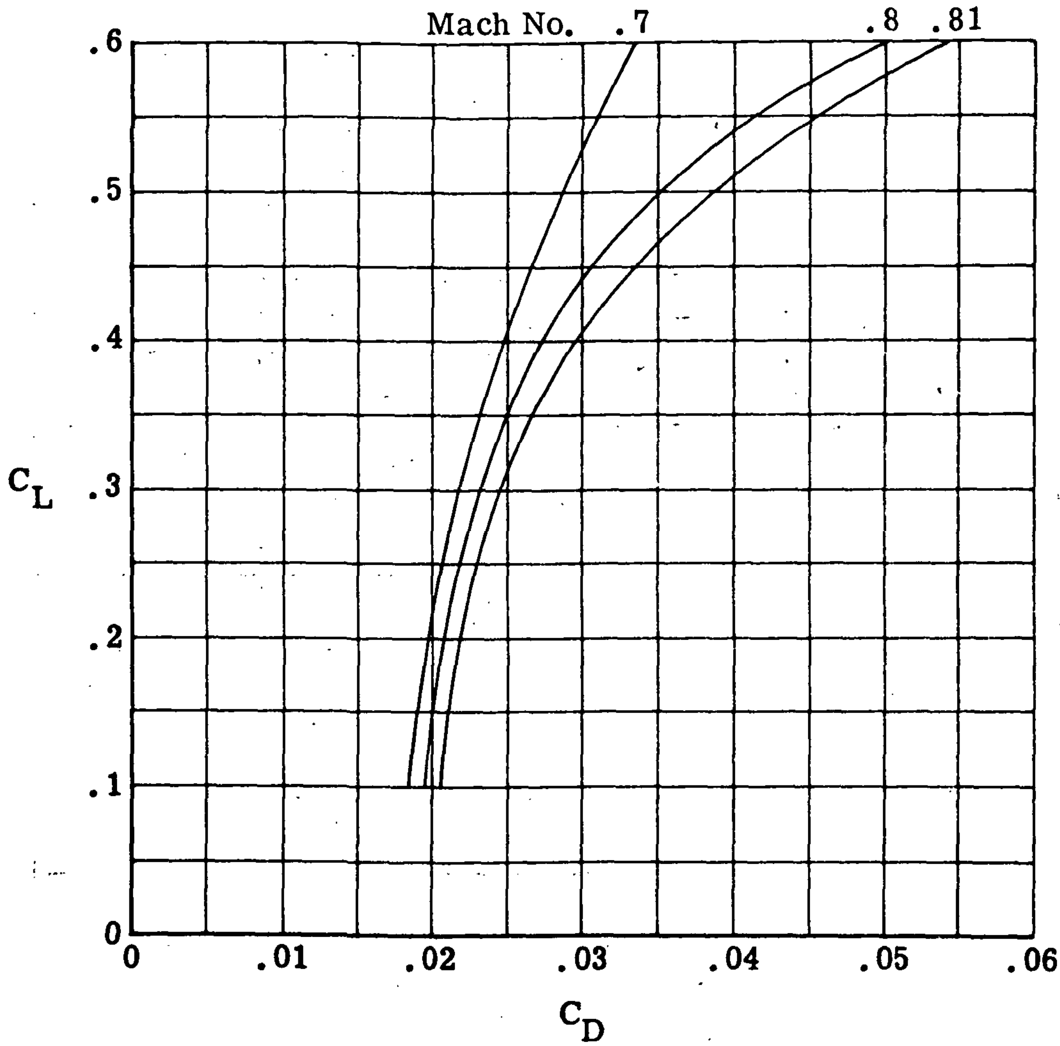

Figure 79 High speed drag polar
MF configuration, 150 passengers, 3500 ft. F.A.R. field length

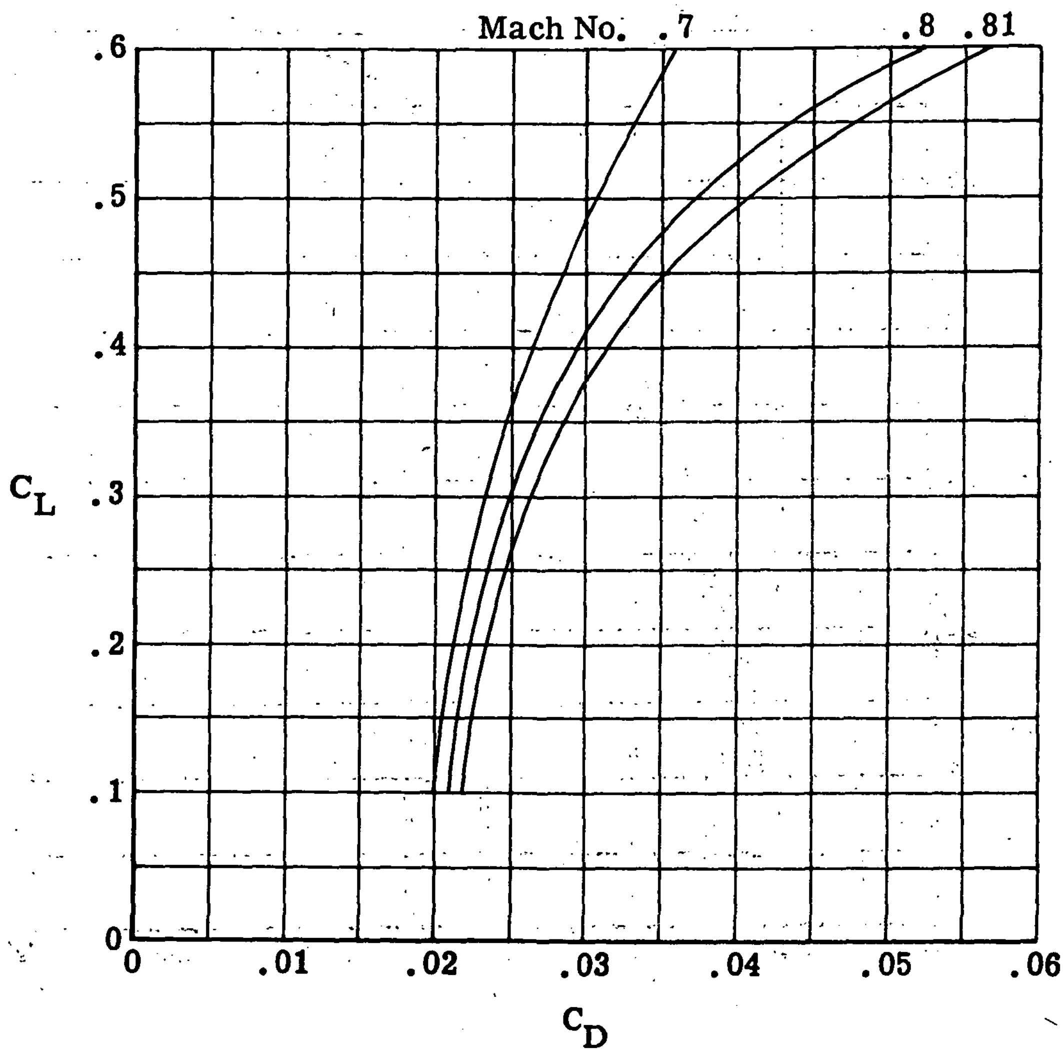

Figure 80 High speed drag polar
EBF configuration, 150 passengers, 3500 ft. F.A.R. field length

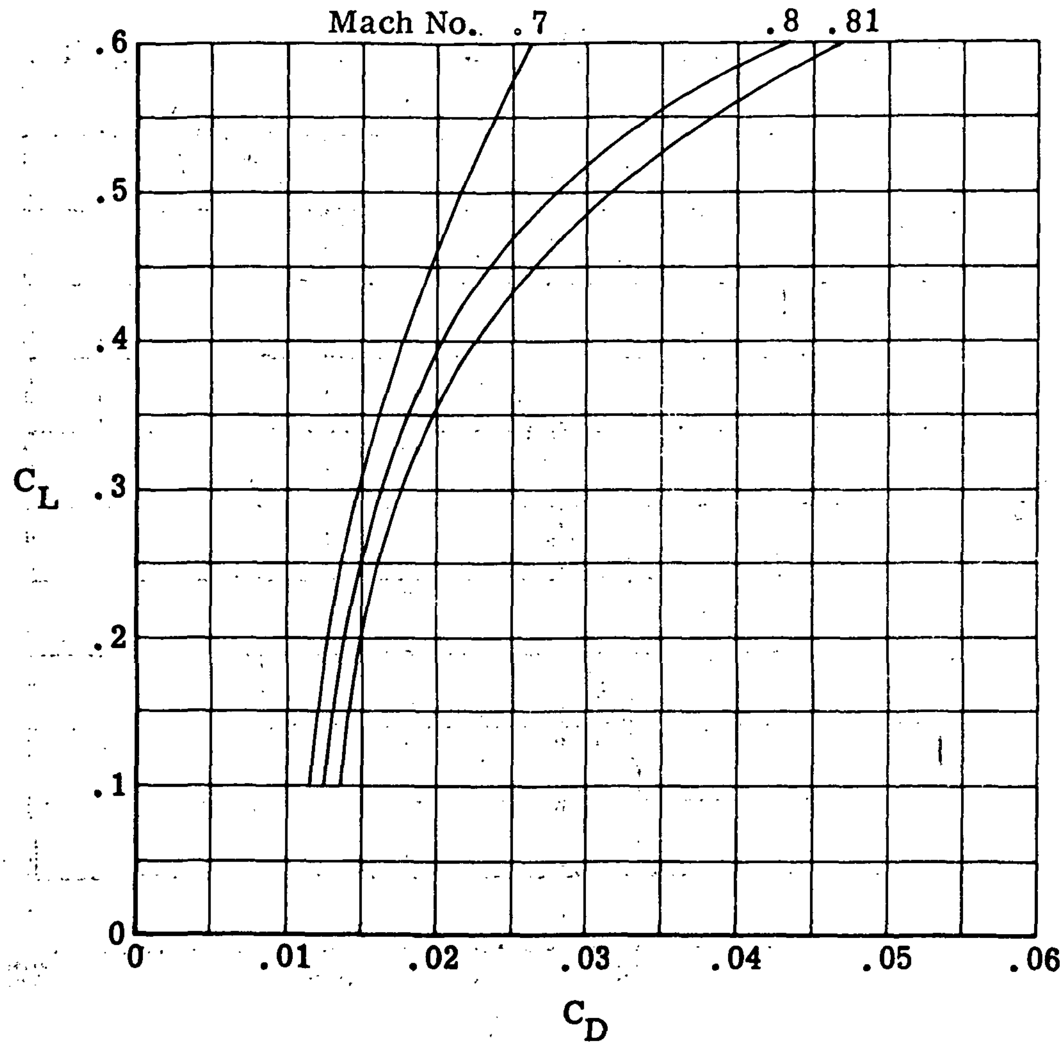

Figure 81 High speed drag polar
MF configuration, 300 passengers, 2000 ft. F.A.R. field length

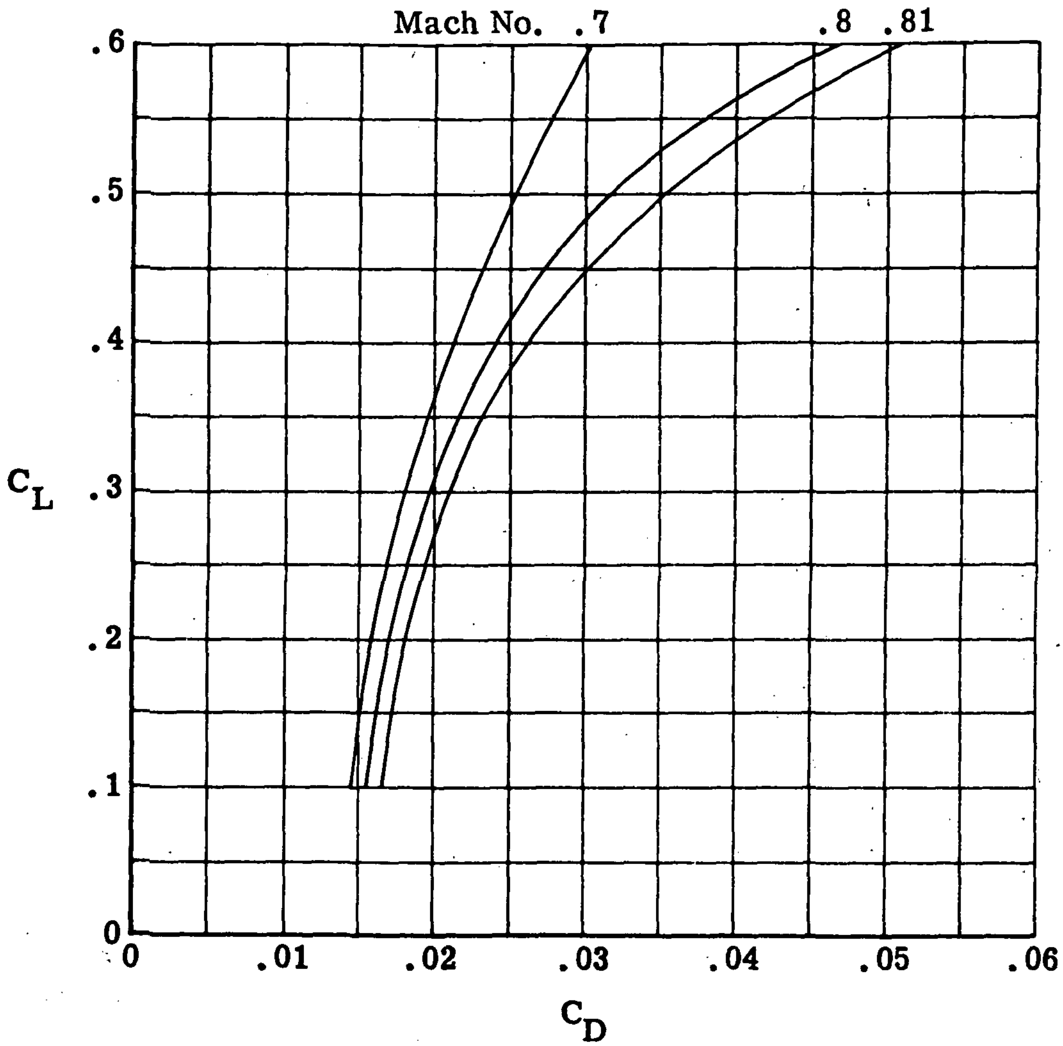

Figure 82 High speed drag polar
EBF configuration, 300 passengers, 2000 ft. F.A.R. field length

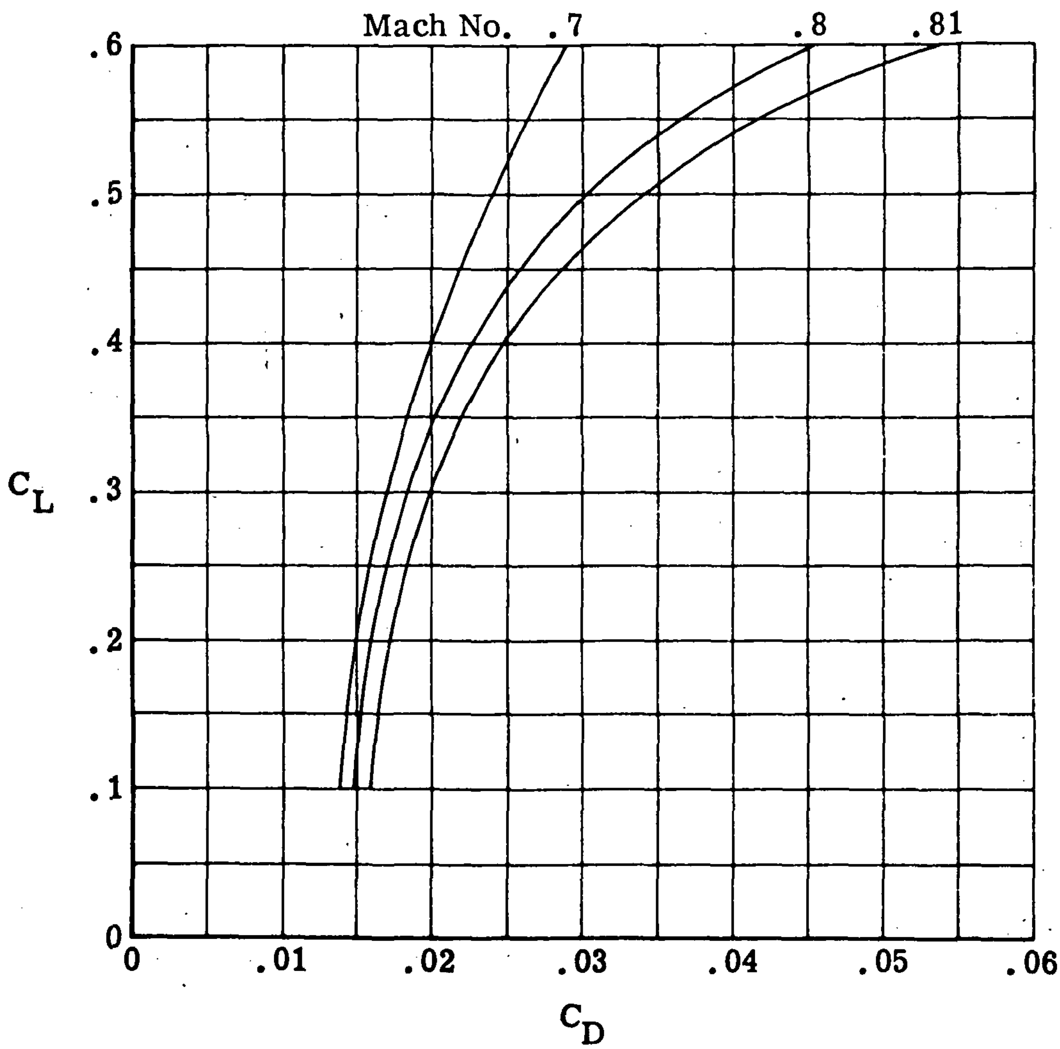

Figure 83 High speed drag polar
MF configuration, 300 passengers, 2500 ft. F.A.R. field length

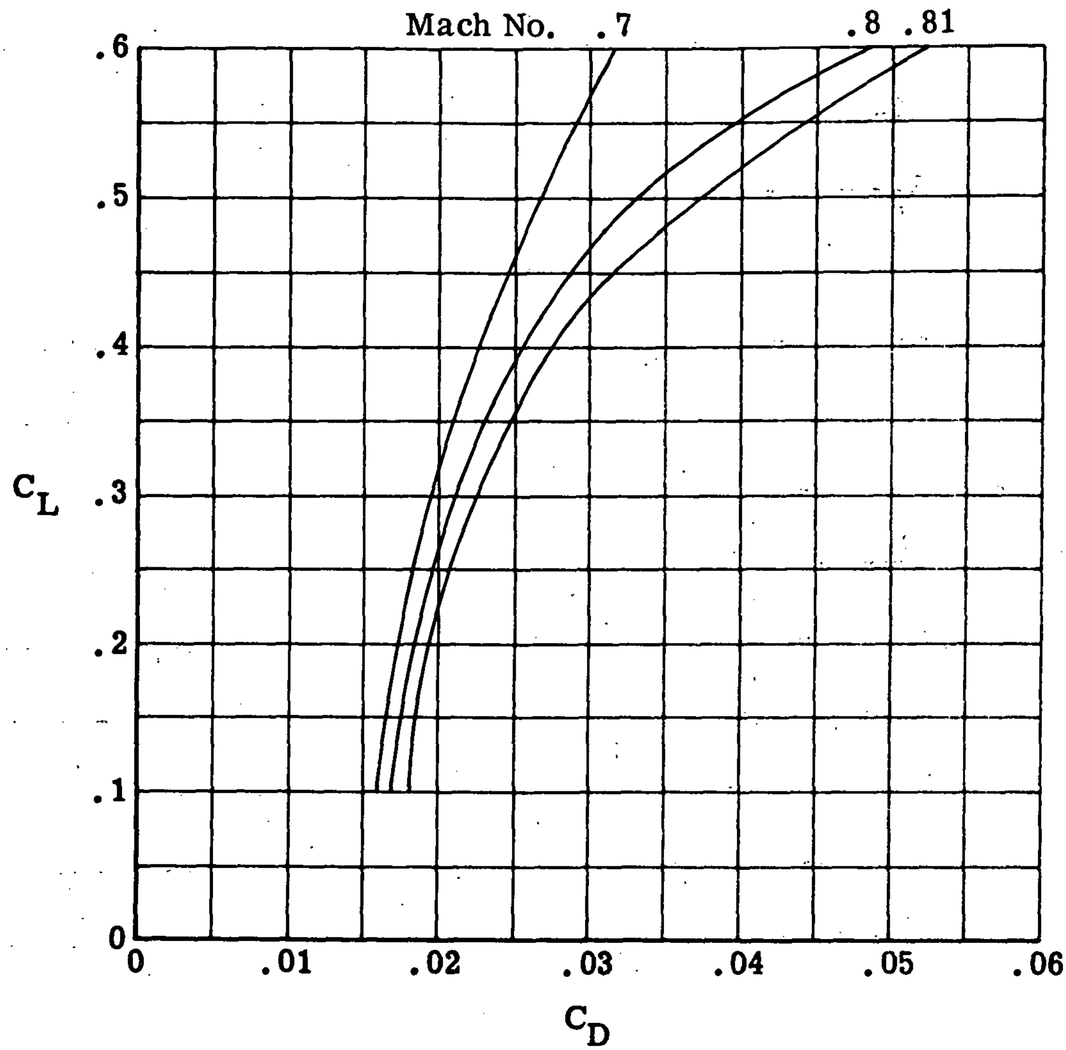

Figure 84 High speed drag polar
EBF configuration, 300 passengers, 2500 ft. F.A.R. field length

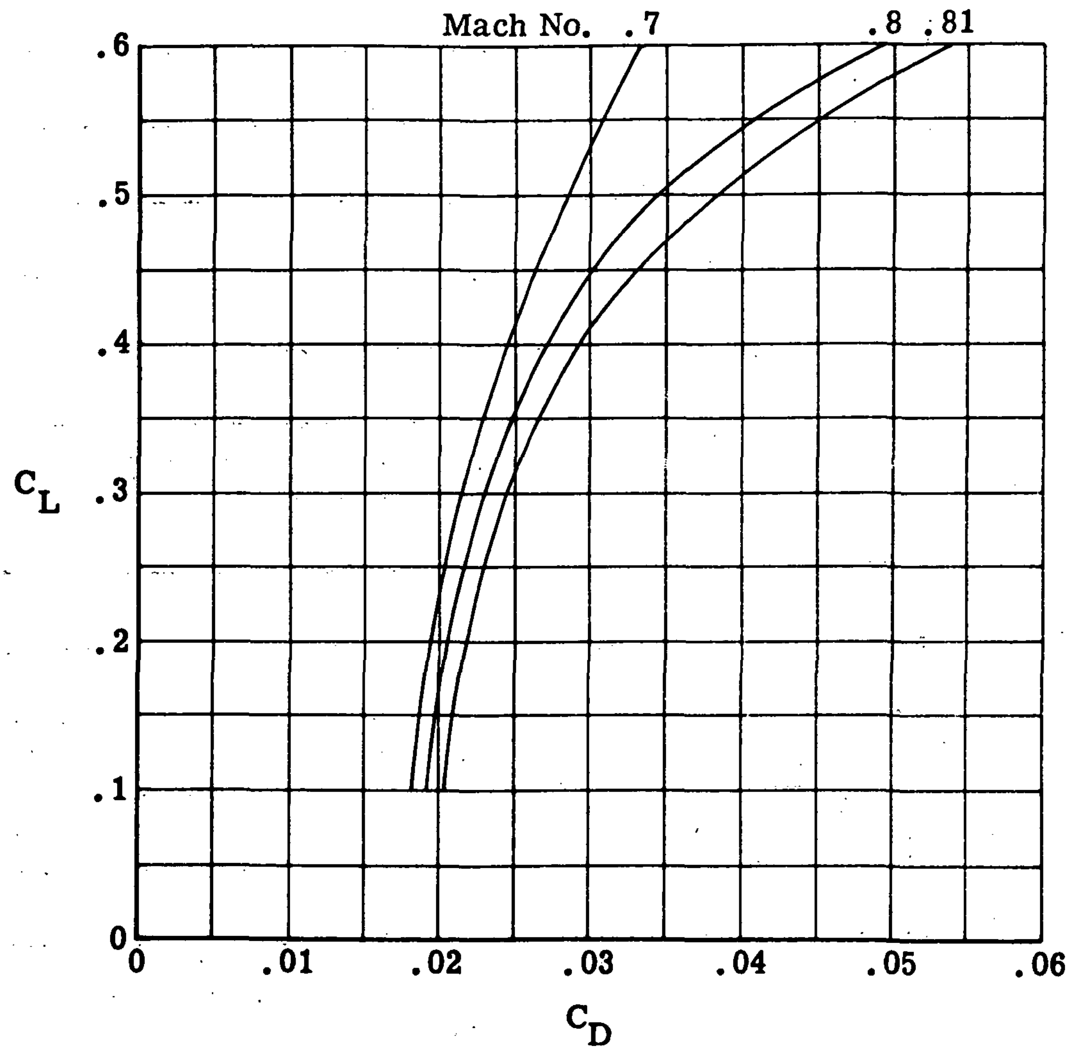

Figure 85 High speed drag polar
MF configuration, 300 passengers, 3500 ft. F.A.R. field length

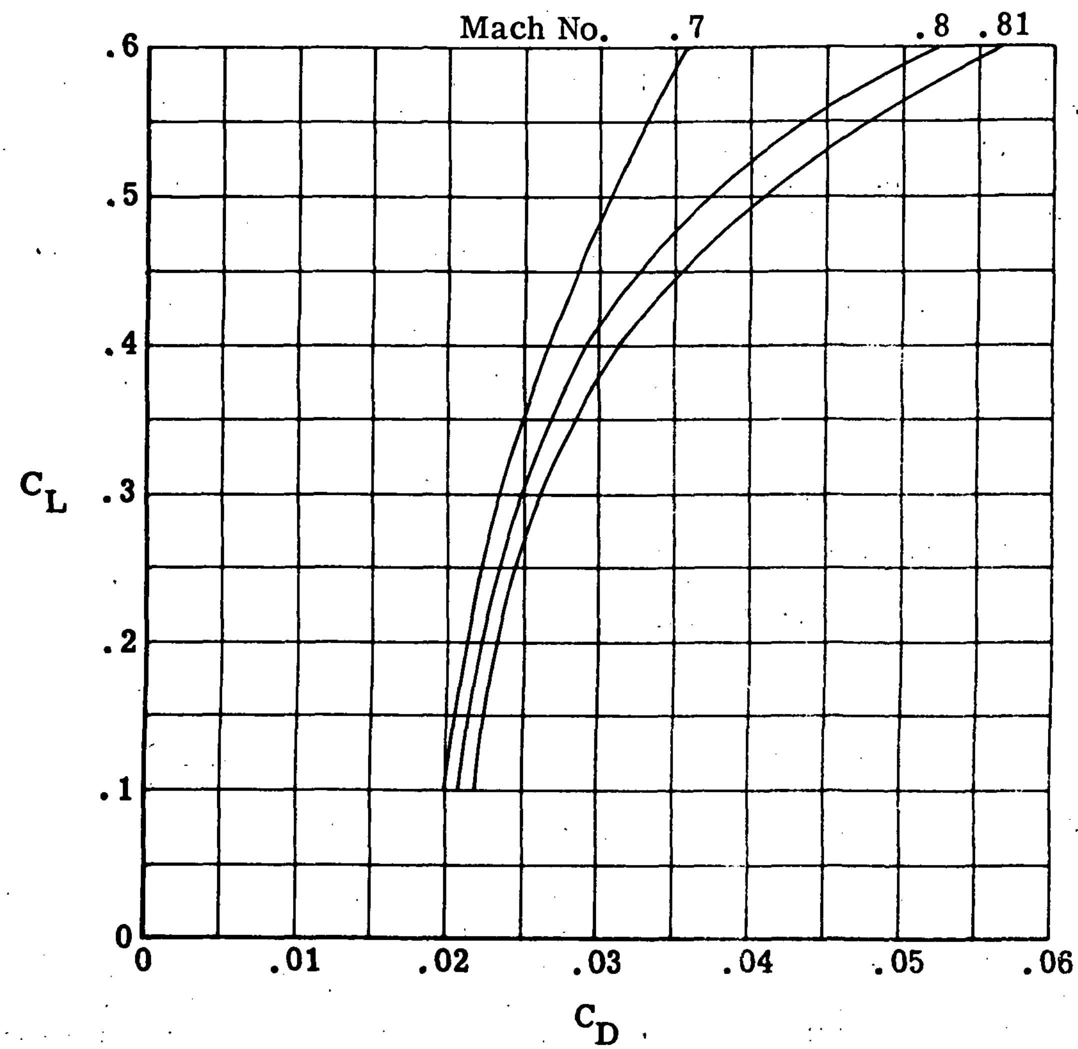

Figure 86 High speed drag polar
EBF configuration, 300 passengers, 3500 ft. F.A.R. field length

12.3 APPENDIX C DETERMINATION OF EBF WING LOADING AND THRUST TO WEIGHT

The step by step determination of the optimum wing loading (W/S) and thrust to weight ratios (T/W) for landing and approach for a given field length airplane is outlined in the following Section.

The rules in terms of landing gradients and margins are presented in Section 5.2. This Section will present the actual numbers and plots for the baseline EBF configurations. As discussed in Section 4.3.4 the low speed aerodynamic data for the EBF configuration with and without an engine out were defined for flap settings of 15°, 25°, 35° and 45°. These aerodynamic data with the appropriate engine data were input to the gradient and margin computer program. Output from this program is presented by Figure 87(a) through 87(d) for flap settings of 15°, 25°, 35° and 45°, respectively. The all engine data are presented on the left portion of the figures and the engine out data on the right portion of each figure. Examination of these data in light of the rules presented in Paragraph 5.2 reveal that at $\Delta\alpha$ = 15° the all engine approach power setting is the limiting (maximum) usable approach lift coefficient for all approach flap settings. For a given W/S, the approach speed is thus defined, $V_{APP} = \sqrt{\frac{W/S}{2\rho C_{L_{APP}}}}$ for each flap setting. Figure 18 presents the F.A.R. landing field length as a function of V_{APP}. Utilizing these data, the F.A.R. field length for each flap setting and W/S is defined.

Definition of the required design T/W for each approach flap setting is the greater of:

$$\left.\begin{array}{ll} \bullet\ \text{All engine climb gradient} & = .032 \\ \bullet\ \text{Engine out climb gradient} & = 0 \end{array}\right\} \text{approach flap setting}$$

or

$$\bullet\ \text{Engine out climb gradient} = .027 \ \} \ \text{go-around flap setting}$$

See Section 5.2 for discussion of configuration change for go-around.

Based on these criteria a go-around flap setting was determined by allowing the approach flap setting to be reduced until the required engine out T/W for a climb gradient of .027 at the approach lift coefficient was equal to or less than the T/W required to maintain a level flight path (γ = 0°) at the approach flap setting, while maintaining all other margins. This allows the sink rate to be arrested while the flaps are retracted to the go-around setting at constant airspeed. Determination of the go-around flap setting and required minimum T/W is a search process and requires cross plotting. The results are summarized in Table 30 for each assumed approach flap setting (Reference Figures 87(a) through 87(d)).

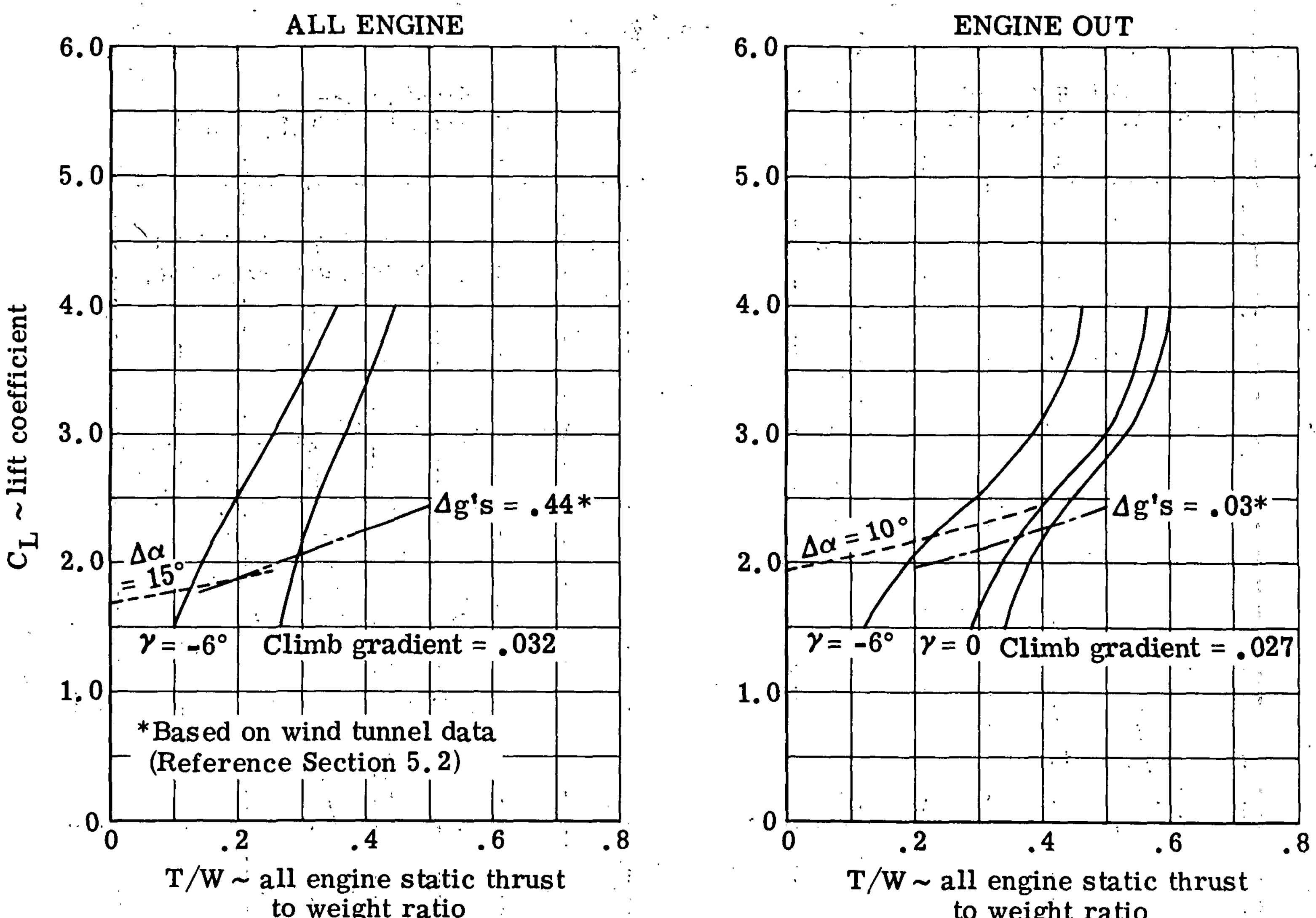

(a) $\delta_F = 15°$

Figure 87 EBF configuration approach margins and gradients

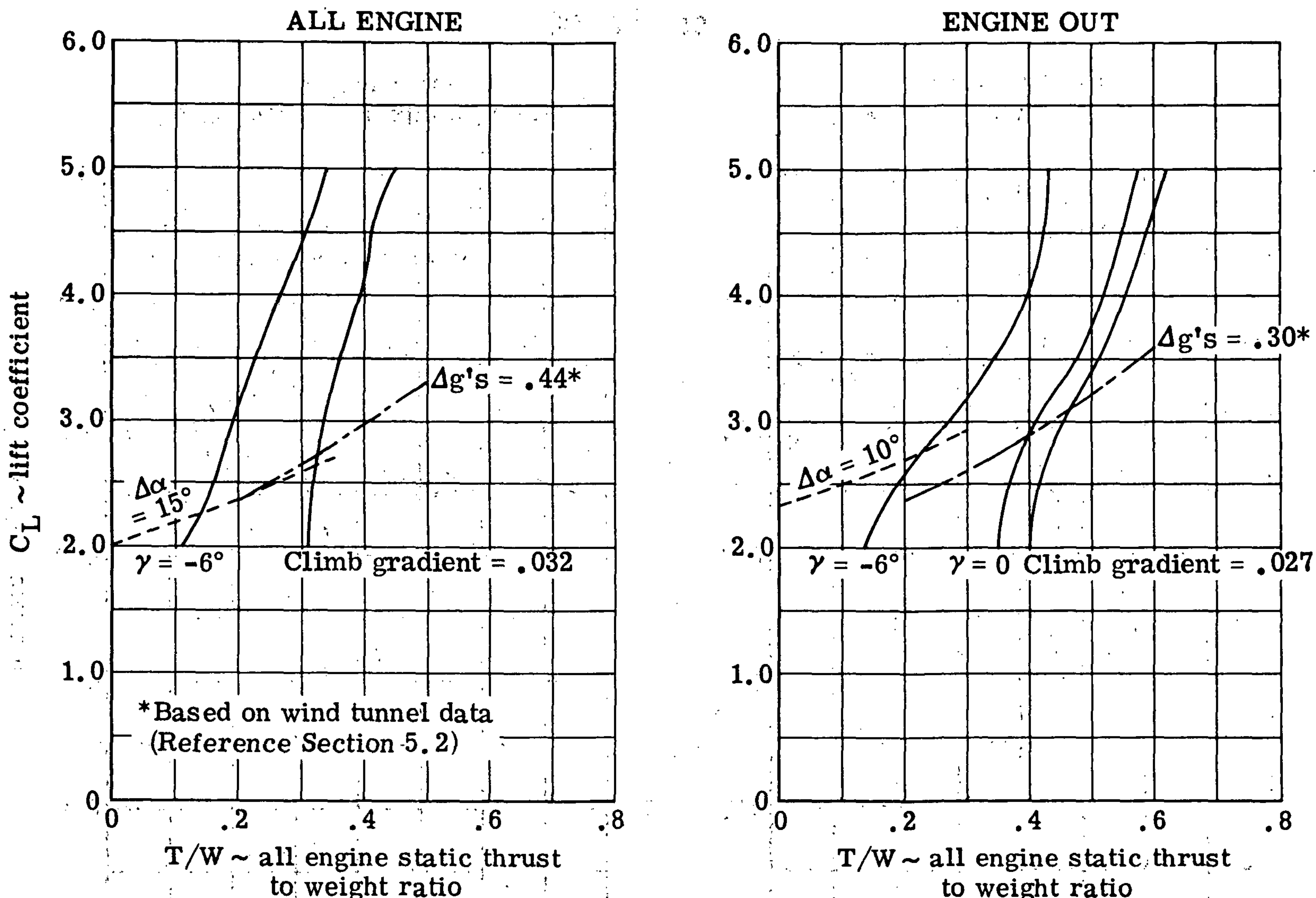

(b) $\delta_F = 25°$

Figure 87 (continued)

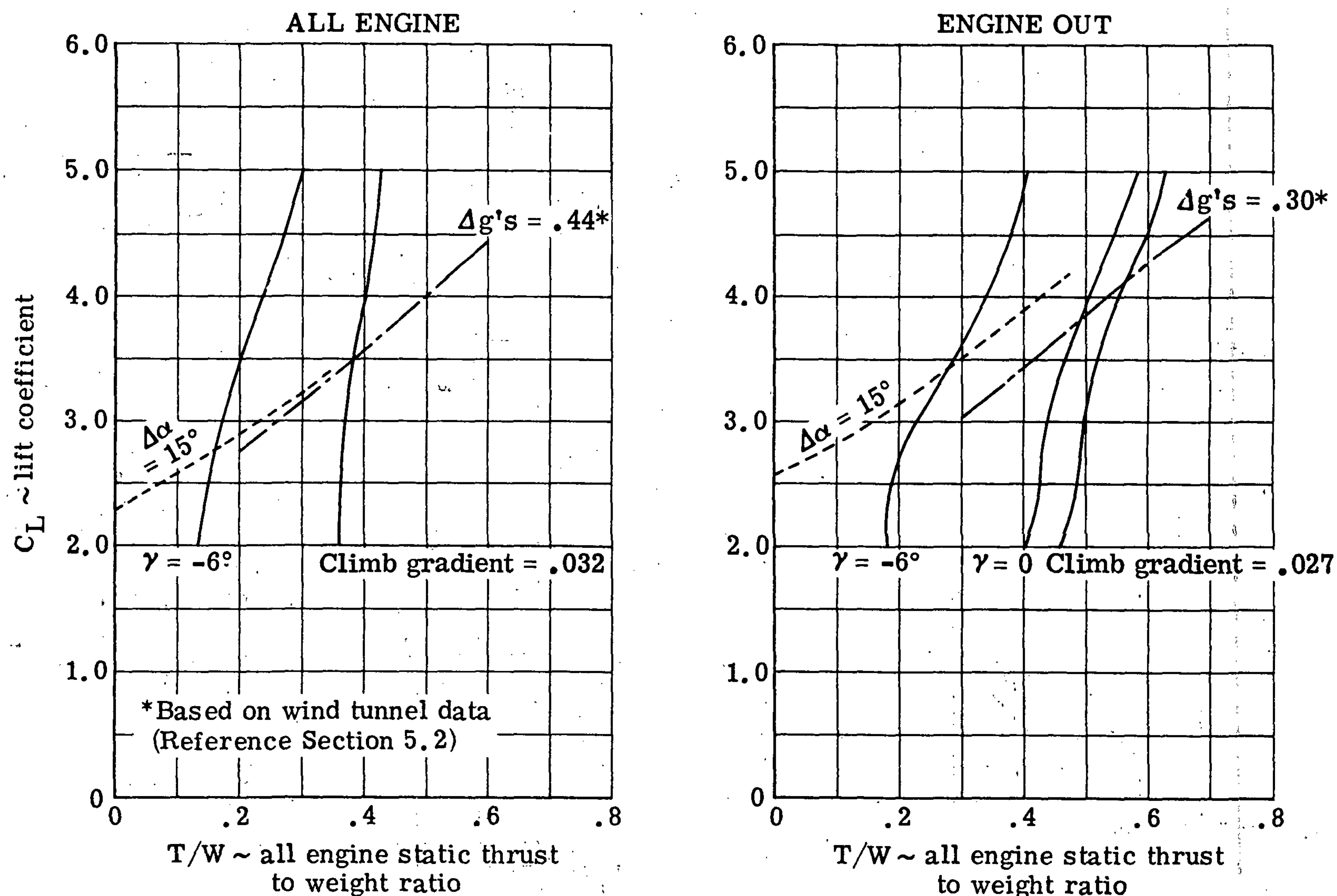

(c) $\delta_F = 35°$

Figure 87 (continued)

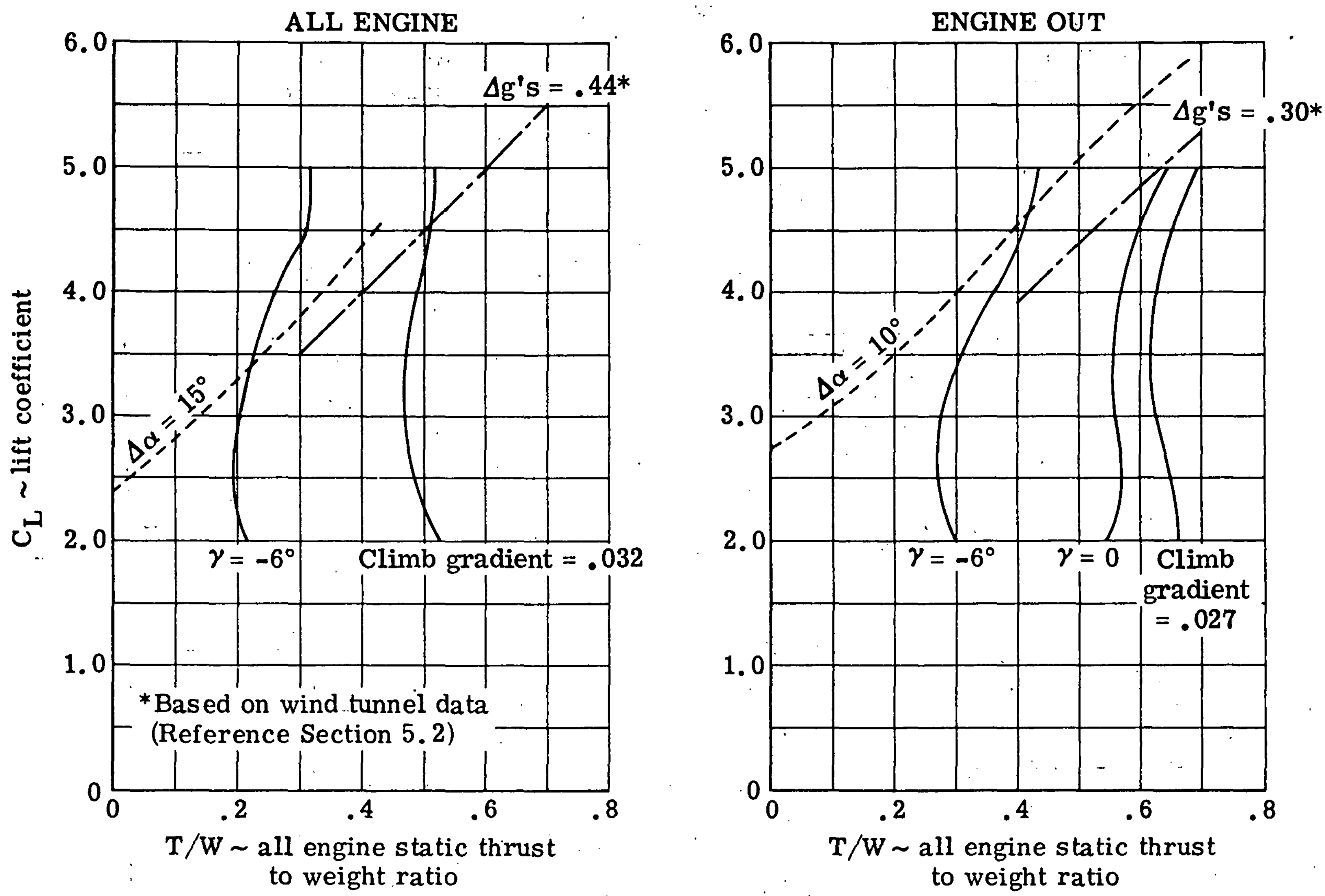

(d) $\delta_F = 45°$

Figure 87 (concluded)

TABLE 30 EBF CONFIGURATION LIFT AND THRUST CONSTRAINTS

(δ_F) APPROACH	$C_{L_{APPROACH}}$	$(T/W)^1$	$(TW)^2$	(δ_F) GO-AROUND	$(T/W)^3$
15°	1.78	.315	.355	15°	.355
25°	2.26	.350	.400	20°	.380
35°	2.78	.430	.490	31°	.430
45°	3.45	.555	.620	40°	.555

$(T/W)^1$ — Engine out T/W required for $\gamma = 0°$ at the approach flap setting

$(T/W)^2$ — Engine out T/W required for climb gradient = .027 at approach flap setting (no configuration change allowed for engine out go-around)

$(T/W)^3$ — Engine out T/W required for climb gradient = .027 at go-around flap setting

Based on these data the FAR field length as a function of design T/W (approach flap setting) can be presented as in Figure 88. From these data the various combinations of W/S and corresponding T/W for given field lengths can be determined. These data are presented on Figure 89 for field lengths of 2,000, 2,500, and 3,500 feet. For a given field length many different combinations of W/S and T/W are possible. Thus to achieve a given field length, there exists a trade off between W/S and T/W (flap setting). For a given field length the optimum configuration was defined as the lightest gross weight configuration to perform the design mission.

Pertinent approach and go-around data for the EBF configurations are presented on Figure 90. The go-around thrust coefficient is referenced to the all engine gross thrust.

12.4 APPENDIX D WEIGHT AND BALANCE

Weight and balance CG determinations for the 150 passenger, 2,500 foot field length MF and EBF aircraft are shown in Tables 31 and 32 respectively.

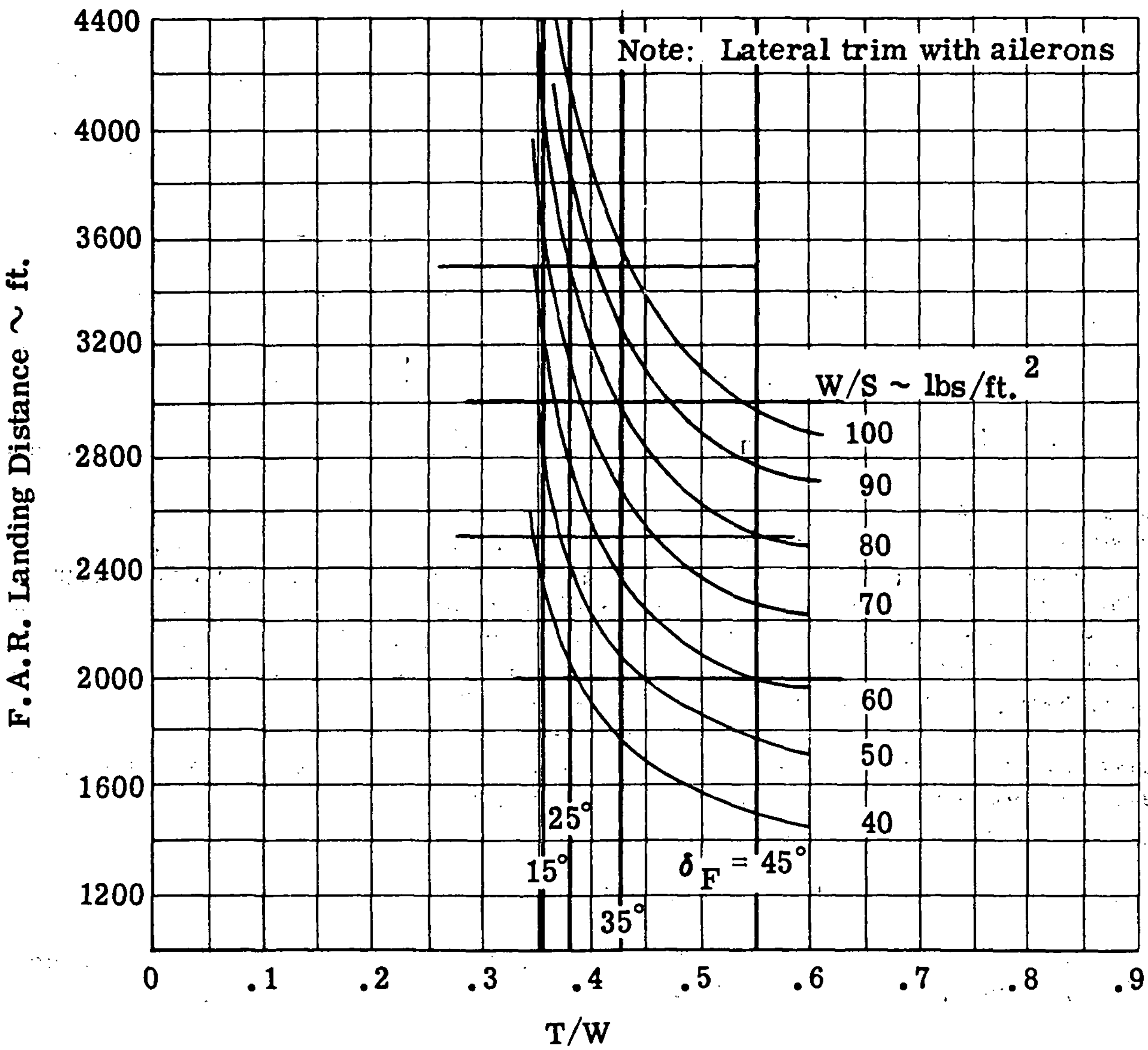

Figure 88 EBF configuration landing design chart

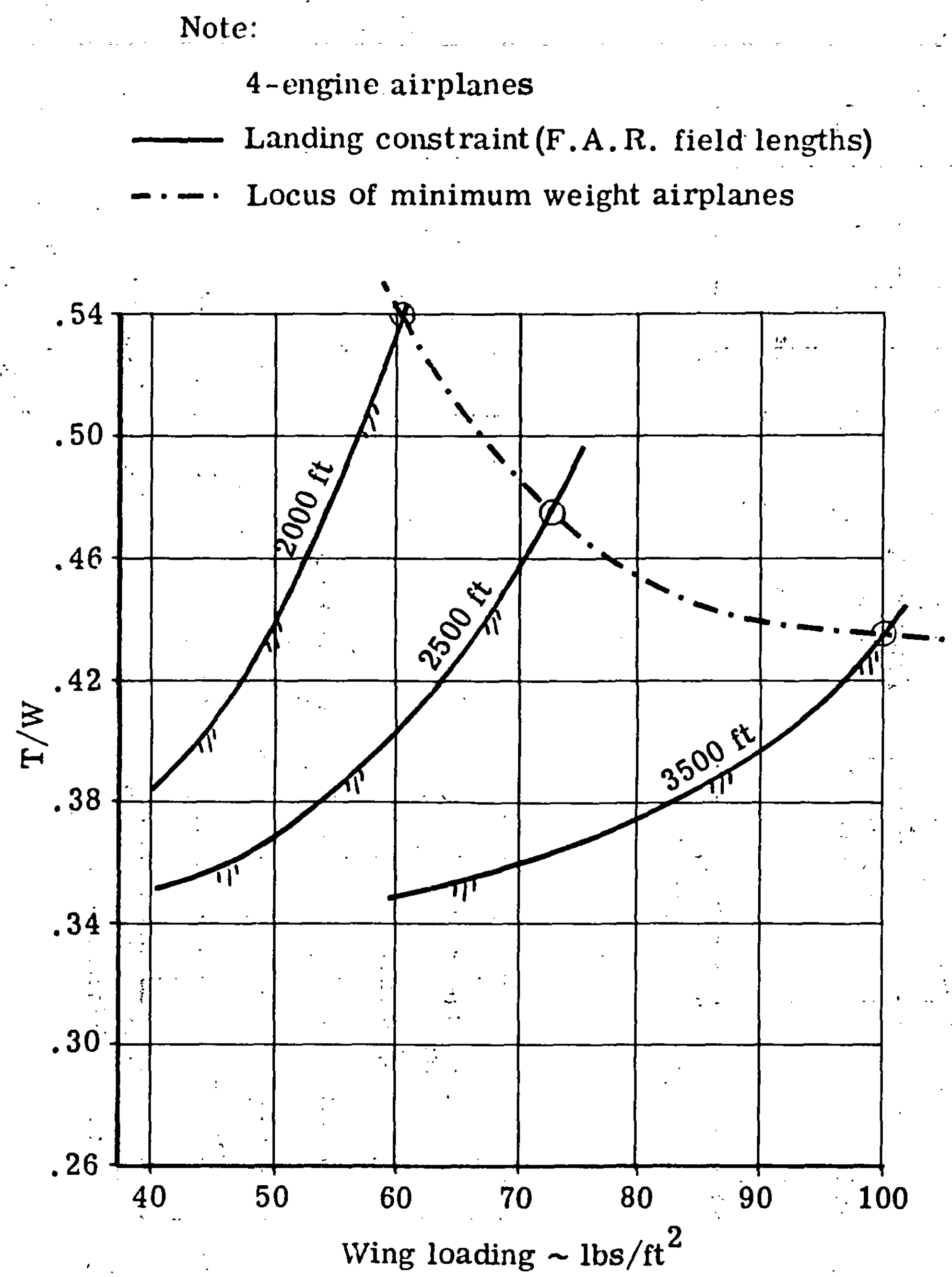

Figure 89 EBF Configuration landing design constraints

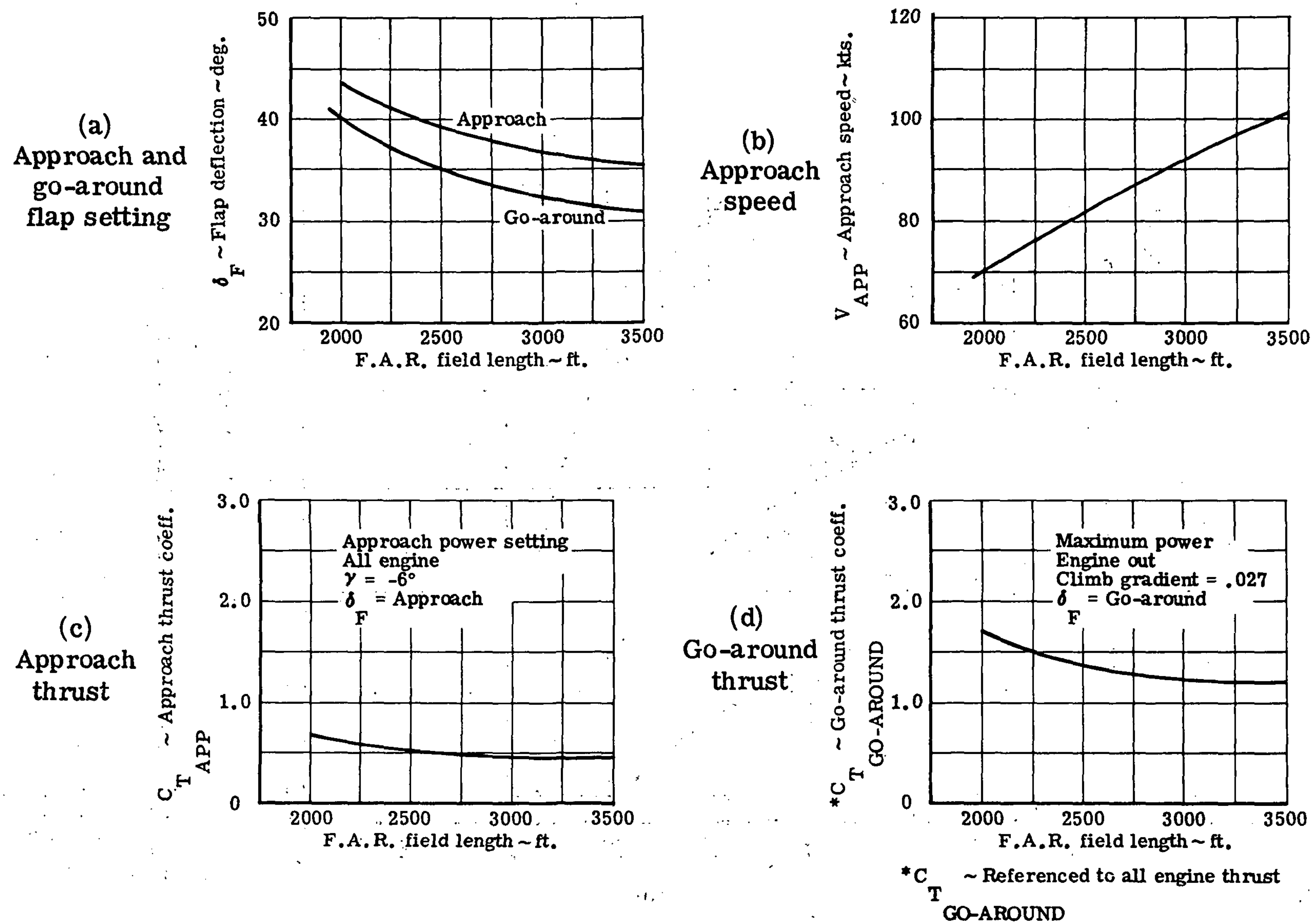

Figure 90 EBF configuration approach and landing characteristics

TABLE 31
MF CONFIGURATION CG DETERMINATION
150 PASSENGERS,
2500 FT. FIELD LENGTH

Component	Weight (lb)	Arm (in)	Moment (in-lb)	% MAC
Wing Engines	8,345	673	5,616,185	
Tail Engine	4,527	1,325	5,998,275	
Wing	23,325	738	17,213,850	
Horiz. Tail	2,578	1,504	3,877,312	
Vert. Tail	2,106	1,337	2,815,722	
Fuselage	20,820	640	13,324,800	
Land. Gear	9,371	586	5,491,406	
Instruments	648	293	189,864	
Surface Controls	1,942	800	1,553,600	
Hydraulics	1,000	681	681,000	
Pneumatics	678	547	370,000	
Electricals	1,560	371	578,760	
Electronics	1,329	347	461,163	
F.D. Accomo	906	106	96,036	
Pass. Accomo	9,445	662	6,252,590	
Cargo	808	441	356,328	
Emerg. Equip.	525	512	268,800	
A/C	1,862	744	1,385,328	
Anti-ice	339	398	134,922	
APU	988	598	590,824	
Manufacturers Empty Weight	93,102	(722)	67,257,631	38.9
Standard & OP Items	3,375	566	1,910,250	
O.W.E.	96,477	(717)	69,167,881	36.5
Payload	30,000	658	19,740,000	
Fuel	21,804	723	15,764,292	
Max. Gross	148,281	(706)	104,672,173	32.0

TABLE 32
EBF CONFIGURATION CG DETERMINATION
150 PASSENGERS,
2500 FT. FIELD LENGTH

Component	Weight (lb)	Arm (in)	Moment (in-lb)	% MAC
I.B. Engines	11,105	331	3,675,755	
O.B. Engines	11,105	411	4,564,155	
Wing	23,171	601	13,925,771	
Horiz. Tail	2,700	1,490	4,023,000	
Vert. Tail	2,208	1,330	2,936,640	
Fuselage	24,807	637	15,802,059	
Land. Gear	10,602	448	4,749,696	
Instruments	662	293	193,966	
Surface Controls	2,578	800	2,062,400	
Hydraulics	936	681	637,416	
Pneumatics	660	547	361,020	
Electricals	1,560	371	578,760	
Electronics	1,286	347	446,242	
F.D. Accomo.	906	106	96,036	
Pass. Accomo.	9,445	662	6,252,590	
Cargo Accomo.	808	441	356,328	
Emerg. Eq.	588	512	301,056	
A/C	1,862	744	1,385,328	
Anti-ice	359	398	142,882	
APU	988	598	590,824	
Manufacturers Empty Weight	108,336	(582)	63,081,924	33.2
Standard & OP Items	3,400	566	1,924,400	
O.W.E.	111,736	(582)	65,006,324	33.0
Payload	30,000	658	19,740,000	
Fuel	26,014	581	15,114,134	
Max. Gross	167,750	(595)	99,860,458	38.7

Page intentionally left blank

13.0 REFERENCES

1. Boeing Document: Low-Wing-Loading STOL Transport Ride Smoothing Feasibility Study. D3-8514-2, 1971.

2. Holloway, R. B.; Thompson, G. O.; Rohling, W. J.: Prospects for Low-Wing-Loading STOL Transports with Ride Smoothing. Journal of Aircraft, August 1972.

3. Boeing Document: User's Manual for ASAMP, Aircraft Sizing and Mission Performance Program. D3-7949, 1968.

4. Boeing Document: Weight Prediction Manual — Class I. D6-23201TN, 1968.

5. Boeing Document: Parametric/Statistical Weight Estimating Methods (Class I). D6-15095TN, Revision C, 1972.

6. Technical Report: Control Configured Vehicles Advanced Tanker Study. ASD/XRL-72-44, 1972.

7. Boeing Document: Compatibility of Maneuver Load Control and Relaxed Static Stability. D3-8766, 1972.

8. Boeing Document: B-52 Weight and Balance Data Retrofit and Modification Kits and Technical Order. D3-1407, 1970.

9. Boeing Document: Theoretical Analyses for Transonic Airplane Model Designs. D6-9341.

10. Boeing Document: A Simple Method for Rapid Hand Calculation of the Span Loading and Induced Drag for Arbitrary Wings. D6-24204 TN.

11. De Young, J. L. and Harper, C. W.: Theoretical Symmetric Span Loading at Subsonic Speeds for Wings Having Arbitrary Planform. NACA Report 921, 1948.

12. Hoak, D. E. and Finck, R. D.: USAF Stability and Control Datcom. 1972 Revision.

13. Anon: Data Sheets. Royal Aeronautical Society, 1972 Revision

14. Boeing Document: Low Speed Aerodynamic Prediction Method. D6-26011 TN, 1970.

15. Department of Transportation, Federal Aviation Administration: Federal Aviation Regulations. Volume III, Part 25 Airworthiness Standards: Transport Category Airplanes.

16. Department of Transportation, Federal Aviation Administration: Tentative Airworthiness Standards For Powered Lift Transport Category Aircraft. Part XX, 1970.

17. Hammond, Alexander D. and Johnson, William G., Jr.: Development of Wing-Tunnel Test Techniques for Propulsion System Simulations For Use in Small-Scale V/STOL Models. Presented at ASME Conference in San Francisco, March 1972.

18. Department of Transportation, Federal Aviation Administration: Federal Aviation Regulations. Volume III, Part 36 Noise Standards: Aircraft Type Certification.

19. The Boeing Company: Phase I Final Report for Quiet Experimental STOL Transport Research Airplane. PDR 612-1, 1972.

20. Rohling, Walter J.: Flying Qualities: An Integral Part of a Stability Augmentation System. J. Aircraft, Vol. 6, No. 6, Nov.-Dec. 1969, pp. 510-515.

21. Boeing Document: Doppler Effect Correction for Motions of Source, Observer, and Fluid. D6-17095 TN, 1966.

☆U.S. GOVERNMENT PRINTING OFFICE: 1973-739-155/65